# 16th International Symposium on Electrets


4 – 8 September 2017

KU Leuven, Belgium

# Final Program

# &

# Book of Abstracts

# Book of Abstracts

Editing and layout:
Peter Cornelis, Tristan Putzeys, Michael Wübbenhorst

Laboratory for Soft Matter and Biophysics
Department of Physics and Astronomy
KU Leuven
Belgium

Leuven, August 28, 2017



ISBN 978-90-8649-798-0

D/2017/10.705/1

## Content

## Welcome to the ISE16

On behalf of the local organizing committee, the KU Leuven and the city of Leuven, it is our pleasure to welcome you to the 16th International Symposium on Electrets (ISE16), which takes place from September 4th till September 8th, 2017.

This year, ISE16 celebrates the 50th anniversary of a continuous series of successful international meetings dedicated to research on Electret science that started in Chicago in October 1967. Electrets and related phenomena continue to receive much interest from both fundamental and applied points of view. Charge storage in insulators is crucial for many applications, it involves a wide range of materials (organic, inorganic, hybrid, powder, thin & thick films, bulk, porous, …) and, hence, is at the frontier of many scientific domains.

The venue of the ISE16 will be the *Promotiezaal*, a spacious auditorium that combines architectural heritage (dating back to 1317) with state-of-the-art audio-visual facilities. This scenery will be the stage for 54 plenary lectures, which are complemented by two extensive poster sessions nearby.

Following the symposium, a tutorial based workshop “Ferroelectric polymers for flexible electronics” will be held from Sept. 7, 4:00 pm till Sept. 8, 12:30 pm. The program comprises four tutorial lectures given by well-known experts in the field.

We are happy to announce the 5th Bernhard Gross Memorial Lecturer, an award that was introduced at the ISE12 in Brazil. Professor Reimund Gerhard has been elected by the Scientific Advisory Committee of the ISE16 and will receive the award as appreciation for his excellent contributions to the field of electrets, ferroelectrets and electromechanically active polymers. Following the tradition of the recent ISE-meetings, he will deliver the opening lecture on 4 September.

In addition to the BGML, the Dilip Das-Gupta awards for the best oral and poster presentation of a young scientist will be awarded during the symposium.

We take the opportunity to thank the members of the International Scientific Advisory Committee, our colleagues from the Local Committee and all participants for their contributions to the organization and scientific quality of this symposium.

Michael Wübbenhorst, Jan van Turnhout, Siegfried Bauer

Leuven, August 2017

## History of the International Symposium on Electrets

- Electrical & Related Electrostatic Charge Storage Phenomena
  15 – 20 October 1967, Chicago, USA
- Electrets, Charge, Storage & Transport in Dielectrics
  08 – 13 October 1972, Miami, USA
- International Symposium on Electrets and Dielectrics
  01 – 06 September 1975, São Carlos, Brazil
- Charge, Storage, Charge Transport and Electrostatics with Applications
  08 – 12 October 1978, Tokyo, Japan
- 5th International Symposium on Electrets (ISE 5)
  04 – 06 September 1985, Heidelberg, Germany
- 6th International Symposium on Electrets (ISE 6)
  01 – 03 September 1988, Oxford, United Kingdom
- 7th International Symposium on Electrets (ISE 7)
  25 – 27 September 1991, Berlin, Germany
- 8th International Symposium on Electrets (ISE 8)
  07 – 09 September 1994, Paris, France
- 9th International Symposium on Electrets (ISE 9)
  25 – 30 September 1996, Shanghai, China
- 10th International Symposium on Electrets (ISE 10)
  22 – 24 September 1999, Delphi, Greece
- 11th International Symposium on Electrets (ISE 11)
  01 – 03 October 2002, Melbourne, Australia
- 12th International Symposium on Electrets (ISE 12)
  11 – 14 September 2005, Salvador, Brazil
- 13th International Symposium on Electrets (ISE 13)
  15 – 17 September 2008, Tokyo, Japan
- 14th International Symposium on Electrets (ISE 14)
  27 – 31 August 2011, Montpellier, France
- 15th International Symposium on Electrets (ISE 15)
  10 – 13 August 2014, Baltimore, Maryland, USA
- 16th International Symposium on Electrets (ISE 16)
  4 – 8 September 2017, Leuven, Belgium

## Bernhard Gross Memorial Awardees

| | | | |
|---|---|---|---|
| 2005 | Gerhard Sessler | (ISE-12, | Salvador) |
| 2008 | Jacques Lewiner | (ISE-13, | Tokyo) |
| 2011 | Jan van Turnhout | (ISE-14, | Montpellier) |
| 2014 | James West | (ISE-15, | Baltimore) |
| 2017 | Reimund Gerhard | (ISE-16, | Leuven) |

## Local Organizing Committee

| | | |
|---|---|---|
| Michael Wübbenhorst | (KU Leuven) | General Chair |
| Jan van Turnhout | (TU-Delft) | General Vice Chair, Publication Chair |
| Prof. Siegfried Bauer | (Univ. Linz) | Technical Program Chair |
| Tristan Putzeys | (KU Leuven) | Financial Chair |
| Danielle Verachtert | (KU Leuven) | Logistics, Administration |
| Peter Cornelis | (KU Leuven) | IT, Website |
| Jan Genoe | (IMEC) | Exhibition Chair |

## Scientific Advisory Committee

| | | | |
|---|---|---|---|
| Siegfried Bauer | (Linz, Austria) | Cheolmin Park | (Seoul, South-Korea) |
| Roberto M Faria | (Sao Carlos, Brazil) | Heinz von Seggern | (Darmstadt, Germany) |
| Robert Fleming | (Melbourne, Australia) | Gerhard Sessler | (Darmstadt, Germany) |
| Eiichi Fukada | (Tokyo, Japan) | Syed Tofail | (Limerick, Ireland) |
| Takeo Furukawa | (Tokyo, Japan) | Jan van Turnhout | (Delft, The Netherlands) |
| Reimund Gerhard | (Potsdam, Germany) | Jim West | (Baltimore, USA) |
| Reuben Hackam | (Windsor, Canada) | Michael Wübbenhorst | (Leuven, Belgium) |
| Francois Henn | (Montpellier, France) | Qiming Zhang | (Pennsylvania, USA) |
| Apostolos Kyritsis | (Athens, Greece) | Xiaoqing Zhang | (Shanghai, China) |
| Sydney Lang | (Beer Shevaa, Israel) | Yuji Suzuki | (Tokyo, Japan) |
| Jacques Lewiner | (Paris, France) | Peng Fang | (Shenzhen, China) |
| Axel Mellinger | (Mount Pleasant, USA) | Carmo Lanca | (Lisboa, Portugal) |
| Preston Murphy | (Singapore) | Davide Fabiani | (Bologna, Italy) |
| Rameshwar Nath | (Sagar, India) | | |

## Sponsors

The International Symposium on Electrets is traditionally sponsored by the IEEE Dielectrics and Electrical Insulation Society. This 16th edition co-sponsored to equal parts by the IEEE-DEIS and the KU Leuven.

IEEE Advancing Technology for Humanity

DEIS

KU LEUVEN

## Exhibitors

- Novocontrol Technologies GmbH & Co. KG
- Princeton Applied Research and Solartron Analytical (parts of AMETEK AMT)

Princeton Applied Research

solartron analytical

novocontrol Technologies

## The program of ISE16 includes the following topics:

- Charge related phenomena in dielectrics (injection, storage, transport, trapping, measurements)
- Dielectric and space charge relaxations in polymers and organics
- Dielectric and electrical responses of dielectrics to high electric fields
- Dielectric relaxation spectroscopy
- Energy storage in dielectrics and ionic materials
- Thermally stimulated phenomena
- Electrets for energy harvesting: principle, design, characterization and applications
- Piezo-, pyro- and ferroelectrets
- Electrocaloric and pyroelectric materials
- Piezo-electric phenomena in polymers and organics/biomaterials
- Applications of organic and polymer based piezo-electric materials
- Electrets and functional polymers in organic electronics
- Optical effects, photoelectrets
- Electrostatic and dielectric phenomena in life sciences - bioelectrets
- Soft transducers: sensors and actuators, including dielectric elastomers
- Nanoscale electrostatic, dielectric and electret materials
- Electret and dielectric phenomena in nanoscale structures
- Other related and emerging topics

# Timetable

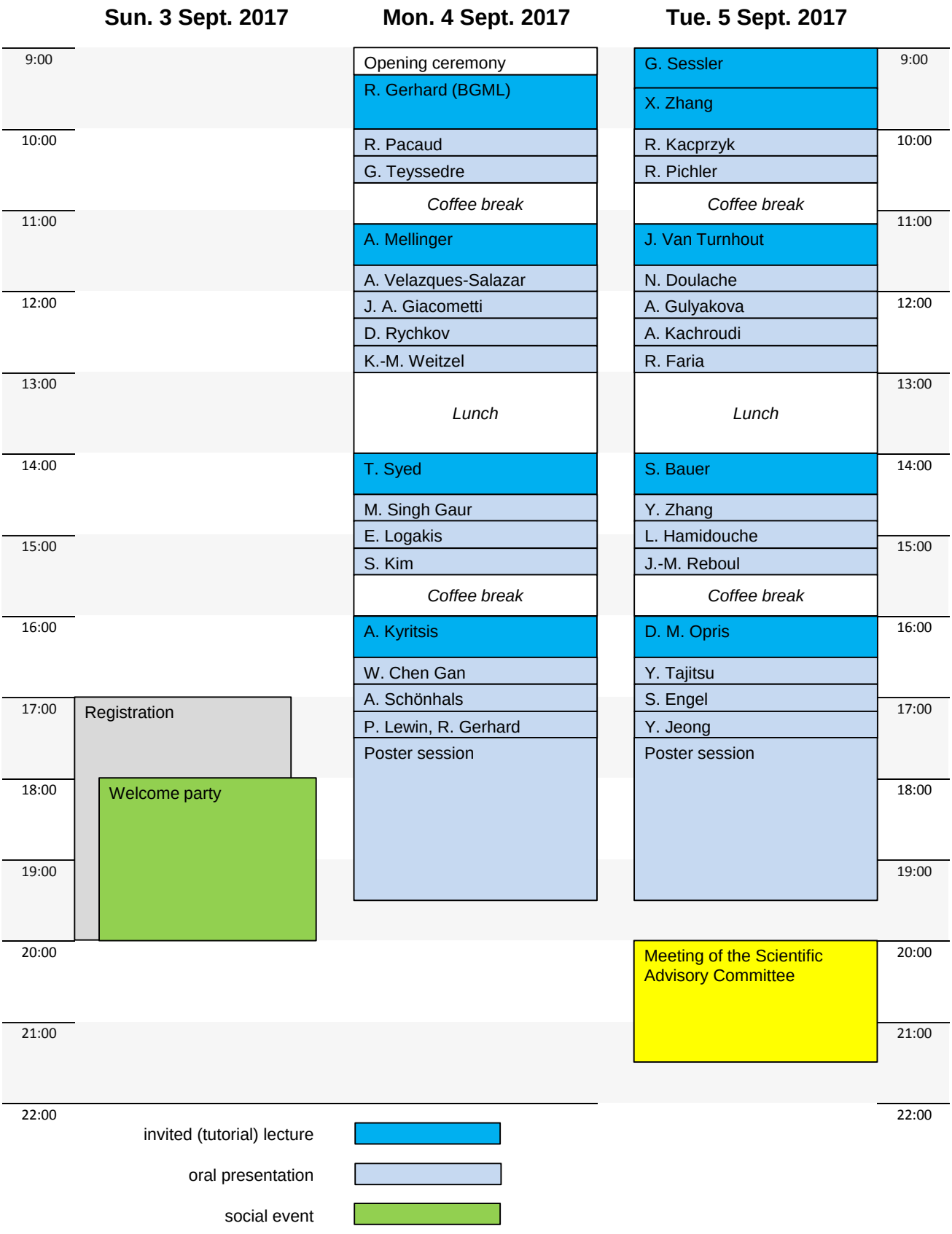
Sun. 3 Sept. 2017
Mon. 4 Sept. 2017
Tue. 5 Sept. 2017
9:00
10:00
11:00
12:00
13:00
14:00
15:00
16:00
17:00
18:00
19:00
20:00
21:00
22:00
Opening ceremony
R. Gerhard (BGML)
R. Pacaud
G. Teyssedre
Coffee break
A. Mellinger
A. Velazques-Salazar
J. A. Giacometti
D. Rychkov
K.-M. Weitzel
Lunch
T. Syed
M. Singh Gaur
E. Logakis
S. Kim
Coffee break
A. Kyritsis
W. Chen Gan
A. Schönhals
P. Lewin, R. Gerhard
Poster session
G. Sessler
X. Zhang
R. Kacprzyk
R. Pichler
Coffee break
J. Van Turnhout
N. Doulache
A. Gulyakova
A. Kachroudi
R. Faria
Lunch
S. Bauer
Y. Zhang
L. Hamidouche
J.-M. Reboul
Coffee break
D. M. Opris
Y. Tajitsu
S. Engel
Y. Jeong
Poster session
Registration
Welcome party
Meeting of the Scientific Advisory Committee
invited (tutorial) lecture
oral presentation
social event

# Timetable

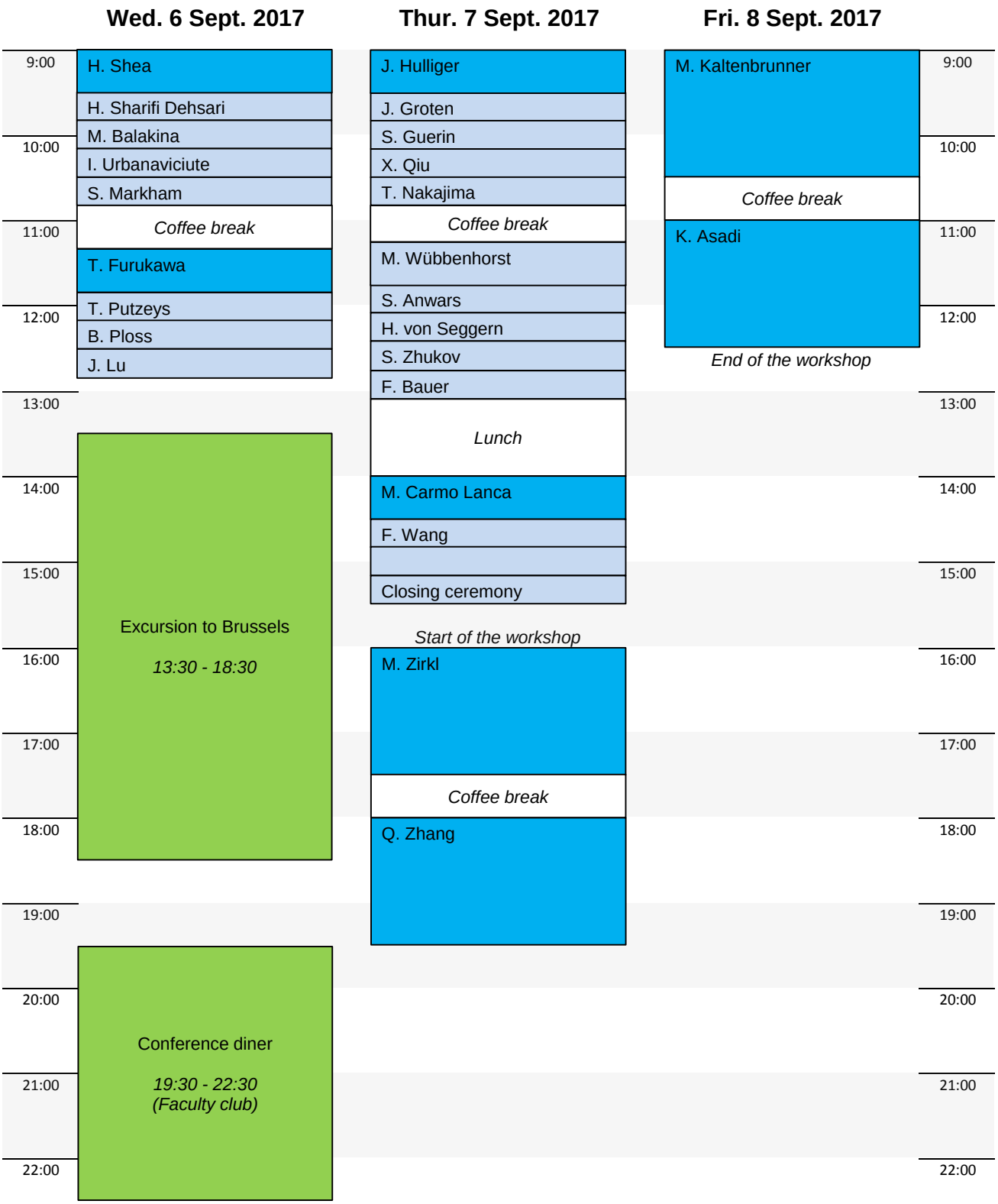
Wed. 6 Sept. 2017
Thur. 7 Sept. 2017
Fri. 8 Sept. 2017
9:00
10:00
11:00
12:00
13:00
14:00
15:00
16:00
17:00
18:00
19:00
20:00
21:00
22:00
H. Shea
H. Sharifi Dehsari
M. Balakina
I. Urbanaviciute
S. Markham
Coffee break
T. Furukawa
T. Putzeys
B. Ploss
J. Lu
Excursion to Brussels
13:30 - 18:30
Conference diner
19:30 - 22:30
(Faculty club)
J. Hulliger
J. Groten
S. Guerin
X. Qiu
T. Nakajima
Coffee break
M. Wübbenhorst
S. Anwars
H. von Seggern
S. Zhukov
F. Bauer
Lunch
M. Carmo Lanca
F. Wang
Closing ceremony
Start of the workshop
M. Zirkl
Coffee break
Q. Zhang
M. Kaltenbrunner
Coffee break
K. Asadi
End of the workshop

# Event schedule and oral presentations

## Monday, September 4, 2017

### Opening Session: charge related phenomena (09:00 – 10:40)

*Chairperson: Gerhard Sessler*

09:00 Opening ceremony

09:20 But They Do Move: Electret Charges on Dielectrics Enable Electromechanical Transduction (Bernhard Gross Memorial lecture)
GERHARD, Reimund (Potsdam, Germany)

10:00 1-D Physical Model for the Description of Charge Transport in Dielectric Materials under Representative Space Radiations
PACAUD, Rémi (Toulouse, France)

10:20 Field and charge distribution at semicon/polyethylene interfaces from combinations of probe force microscopy measurements
TEYSSEDRE, Gilbert (Toulouse, France)

Coffee Break (10:40 – 11:10)

### Session 1: charge related phenomena II (11:10 – 13:00)

*Chairperson: Jacques Lewiner*

11:10 Finite Element Analysis of LIMM Space Charge Deposition Measurements in Tubular Channel Ferroelectrets (invited)
MELLINGER, Axel (Mount Pleasant, USA)

11:40 Optimization of the thermal calibration process in (F)LIMM under electrical DC field
VELAZQUEZ-SALAZAR, Amanda (Toulouse, France)

12:00 Corona charging with constant current to investigate the electric properties of thin dielectric films
GIACOMETTI, Jose Alberto (São Carlos, Brazil)

12:20 Trap-energy spectrum in corona-charged polytetrafluoroethylene (PTFE) electret films with modified surfaces
RYCHKOV, Dmitry (Potsdam, Germany)

12:40 Charge Attachment Induced Ion Transport – Electro-diffusion, chemical diffusion and grain boundary diffusion
WEITZEL, Karl-Michael (Marburg, Germany)

Lunch (13:00 – 14:00)

**Session 2: bio-electrets/charge related phenomena (14:00 – 15:30)**
*Chairperson: Carmo Lança*

14:00 Bioelectrets: A tool to understand electrically mediated interactions in biology (invited)
SYED, Tofail (Limerick, Ireland)

14:30 Bioelectret biosensor for detection of TSH in human blood
GAUR, Mulayam Singh (Farah, Mathura, India)

14:50 Field dependence of dielectric properties in low density polyethylene insulation as studied by high voltage dielectric spectroscopy
LOGAKIS, Emmanuel (Baden-Daettwil, Switzerland)

15:10 Quantum Chemical Study of Charge Trap in Amorphous Perfluoro Polymer Electret
KIM, Seonwoo (Tokyo, Japan)

Coffee Break (15:30 – 16:00)

**Session 3: dielectric relaxation spectroscopy (16:00 – 17:30)**
*Chairperson: Takeo Furukawa*

16:00 Dielectric studies on interfacial effects in polymer nanocomposites (invited)
KYRITSIS, Apostolos (Athens, Greece)

16:30 Molecular dynamic and polarization switching of solvent-cast poly(vinylidene fluoride)
GAN, Wee Chen (Sepang, Malaysia)

16:50 Dielectric Relaxation of Discotic Liquid Crystals
SCHOENHALS, Andreas (Berlin, Germany)

17:10 The IEEE Future Directions initiative "Smart Materials" led by the DEIS
Plenary discussion led by Paul LEWIN (Southampton, UK), President of the DEIS; Reimund GERHARD (Potsdam, Germany), Administrative Vice President of the DEIS

**Poster session (17:30 – 19:30)**

## Tuesday, September 5, 2017

### Session 4: energy harvesting (09:00 – 10:40)

*Chairperson: Reimund Gerhard*

09:00 Vibrational energy harvester based on transverse piezoelectric effect in piezoelectrets (invited)
SESSLER, Gerhard (Darmstadt, Germany)

09:30 Broad Bandwidth Vibration Energy Harvesters based on Wavy Fluoro ethylene propylene Electret Films (invited)
ZHANG, Xiaoqing (Shanghai, China)

10:00 Piezo-tube
KACPRZYK, Ryszard (Wroclaw, Poland)

10:20 Electret-Like Elastomer Membrane for Large Scale Energy Harvesting of Low Density Energy Sources
PICHLER, Robert (Linz, Austria)

Coffee Break (10:40 – 11:10)

### Session 5: thermally stimulated phenomena (11:10 – 13:00)

*Chairperson: Gilbert Teyssedre*

11:10 Computational tools for a refined multi-model analysis of TSD spectra (invited)
VAN TURNHOUT, Jan (Delft, The Netherlands)

11:40 TSDC study of electrical aging of polybutylene terephtalate (PBT)
DOULACHE, Naima (Algiers, Algeria)

12:00 Investigation of relaxation processes in P(VDF-TrFE-CFE) terpolymer films by means of thermally stimulated depolarization and dielectric relaxation spectroscopy
GULYAKOVA, Anna (St. Petersburg, Russian Federation)

12:20 Post-annealing effect on the parylene C electret thermal stability
KACHROUDI, Achraf (Grenoble, France)

12:40 Space charge generation at ITO/organic semiconductor interface and oxygen effects
FARIA, Roberto (São Carlos, Brazil)

Lunch (13:00 – 14:00)

**Session 6: Special session dedicated to Wolfgang Eisenmenger (14:00 – 15:30)**
*Chairperson: Sidney Lang*

14:00 A tribute to Wolfgang Eisenmenger: From phonon spectroscopy to piezoelectrically generated pressure steps (invited)
BAUER, Siegfried (Linz, Austria)

14:30 Surface Fluorinated Semiconductive Electrodes for Space Charge Injection of Polyethylene under DC High Voltage
ZHANG, Yewen (Shanghai, China)

14:50 Measurement of space charge in thin films with high spatial resolution using Electro-Acoustic Reflectometry (EAR)
HAMIDOUCHE, Louiza (Paris, France)

15:10 A double method for the electric field recovery in the electrets
REBOUL, Jean-Michel (Cherbourg, France)

Coffee Break (15:30 – 16:00)

**Session 7: soft transducers & optical effects (16:00 – 17:30)**
*Chairperson: Gangjin Chen*

16:00 Thin functional dielectric elastomers: synthesis and applications (invited)
OPRIS, Dorina Maria (Dübendorf, Switzerland)

16:30 A new wearable sensor in the shape of a braided cord (Kumihimo)
TAJITSU, Yoshiro (Osaka, Japan)

16:50 Influence of photoexcitation on the ferroelectric behaviour of ferroelectric-semiconductor-composites
ENGEL, Sebastian (Jena, Germany)

17:10 pMUT device compatible with large-area display technology
JEONG, Yongbin (Leuven, Belgium)

**Poster session (17:30 – 19:30)**

Meeting of the Scientific Advisory Committee (20:00 – 21:30)

## Wednesday, September 6, 2017

### Session 8: organic electronics (09:00 – 10:50)

*Chairperson: Siegfried Bauer*

09:00 Miniaturized Elastomer-Based Actuators: enabling complex smart soft machines (invited)
SHEA, Herbert (Neuchatel, Switzerland)

09:30 Ambient Processing of P(VDF-TrFE) Ferroelectric Thin-Films for Application in non-Volatile Memory Devices
SHARIFI DEHSARI, Hamed (Mainz, Germany)

09:50 Polymer Electrets with quadratic Nonlinear-optical activity
BALAKINA, Marina (Kazan, Russian Federation)

10:10 Record performance of organic ferroelectric liquid crystal BTA
URBANAVICIUTE, Indre (Linköping, Sweden)

10:30 Piezoelectricity in screen-printed hydroxyapatite
MARKHAM, Sarah (Limerick, Ireland)

Coffee Break (10:50 – 11:15)

### Session 9: piezo, pyro, ferro-electrets (11:15 – 13:00)

*Chairperson: Peng Fang*

11:15 Toward comprehensive understanding of piezoelectricity and its relaxation in VDF-based ferroelectric polymers (invited)
FURUKAWA, Takeo (Tokyo, Japan)

11:45 Ferroelectric properties and detection of charge injection/trapping in liquid crystals via Laser Intensity Modulation Method (LIMM) and Dielectric Relaxation Spectroscopy (DRS)
PUTZEYS, Tristan (Leuven, Belgium)

12:05 Change in the ferroelectric to paraelectric phase transition order in P(VDF-TrFE) copolymer ultra-thin films
PLOSS, Bernd (Jena, Germany)

12:25 Soft-X-ray-charged Piezoelectret with Embedded Electrodes
LU, Jia (Tokyo, Japan)

Excursion (13:30 – 18:30)

Conference dinner (19:30 – 22:30)

## Thursday 07 September 2017

### Session 10: piezoelectric phenomena (09:00 – 10:50)

*Chairperson: Axel Mellinger*

09:00 On the generation of polarity: A property being not allowed for a stationary state (invited)
HULLIGER, Jürg (Berne, Switzerland)

09:30 Screen printed PVDF-TrFE-co-PbTiO3 nanocomposite for selective piezo- or pyroelectric sensing
GROTEN, Jonas (Weiz, Austria)

09:50 First Principles Design of Organic Piezoelectric Devices
GUERIN, Sarah (Limerick, Ireland)

10:10 Influence of elevated temperature and humidity on the electrical-insulation behaviour of cellular polypropylene (PP) foams
QIU, Xunlin (Potsdam, Germany)

10:30 Structure and piezoelectric properties of self-polarized ferroelectric polymer thin film
NAKAJIMA, Takashi (Tokyo, Japan)

Coffee Break (10:50-11:15)

### Session 11: piezo, pyro, ferro-electrets (11:15 – 13:05)

*Chairperson: Bernd Ploss*

11:15 Dielectric relaxations and ferroelectric behaviour of thin films of trialkylbenzene-1,3,5-tricarboxamide (BTA)
WÜBBENHORST, Michael (Leuven, Belgium)

11:45 Revisiting Ferroelectricity in Nylons
ANWARS, Saleem (Mainz, Germany)

12:05 Polarized tubular fluoropolymer arrays with high piezoelectric response
VON SEGGERN, Heinz (Darmstadt, Germany)

12:25 Polarization switching dynamics in ferroelectric polymers by Inhomogeneous Field Mechanism
ZHUKOV, Sergey (Darmstadt, Germany)

12:45 PVDF: a strong candidate for pressure gauge for blast loading measurements. Changes in shape of the hysteresis loop of a relaxor terpolymer with CFE under uniaxial stress
BAUER, Francois (Saint-Louis, France)

Lunch (13:05 – 14:00)

**Closing Session (14:00 – 15:30)**
*Chairperson: Dorina Opris*

14:00 Electrical polarization of chitosan and hydroxyapatite for tissue engineering
LANÇA, M Carmo (Lisboa, Portugal)

14:30 Influence of corona charging on transformer-oil filtration of fluorinated nonwoven polypropylene films
WANG, Feipeng (Chongqing, China)

15:10 Closing ceremony

15:30 End of the symposium

**Workshop: Ferroelectric polymers for flexible electronics, part I (16:00-19:30)**

16:00 Screen Printing as a powerful tool to add multiple functionality to flexible substrates (invited tutorial lecture)
ZIRKL, Martin (Graz, Austria)

Coffee Break (17:30 – 18:00)

18:00 Beyond PVDF-Based Normal Ferroelectric Polymers: Advances, Opportunities, and Outlooks (invited tutorial lecture)
ZHANG, Qiming (University Parc, USA)

## Friday 08 September 2017

### Workshop: Ferroelectric polymers for flexible electronics, part II (09:00 – 12:30)

09:00 Soft Electronics and Machines with Tough Hydrogels (invited tutorial lecture)
KALTENBRUNNER, Martin (Linz, Austria)

Coffee Break (10:30 – 11:00)

11:00 Polymeric ferroelectric diodes for non-volatile memory applications in flexible electronics (invited tutorial lecture)
ASADI, Kamal (Mainz, Germany)

12:30 End of the workshop

# Poster presentations

## Monday 04 & Tuesday 05 September 2017

### Poster Sessions (17:30 – 19:30)

P1 Influence of foreign chemical structures from nitric acid treatment on electret and electrical-insulation properties of polypropylene
WANG, Jingwen

P2 Comparative study on charge storage capacity of mesomorphic and α crystalline polypropylene melt-blown electret fabric
CHEN, Gangjin

P3 Piezoelectrically generated Pressure Steps (PPS) for studying charge distributions on corona-charged Polypropylene (PP) films
NGUYEN, Quyet D.

P4 Space Charge Measurement System for High Hydrostatic Pressure Based on PIPWP Method
ZHANG, Yewen

P5 Swift optimization and prediction of the beneficial effect of physical aging on electrets
VAN TURNHOUT, Jan

P6 Air-stable reconfigurable memory diodes based on ferroelectric semiconductor blends
KUMAR, Manasvi

P7 Capacitive-electret sensor for measuring high-voltage discharges
ALTAFIM, Ruy Alberto C.; ALTAFIM, Ruy Alberto P.

P8 Studying the electrical polarization of coatings of hydroxyapatite and bioglass deposited by plasma-spray and CoBlast techniques
LANÇA, M Carmo

P9 Influence of surface fluorination on space charge characteristics of oil-impregnated Nomex paper
WANG, Feipeng; ZHANG, Tao

P10 Numerical model for calculating the space charge around defects inside polymer films
MULLA, Awat

P11 Molecular mobility studies on the amorphous part of poly(vinylidene fluoride) (PVDF)/silica nanocomposites
KYRITSIS, Apostolos

P12 Ferroelectret Behavior in De-Lignified Wood
KIERZEWSKI, Iain

P13 In situ measurement of electrical field distribution in thin films from double sides by thermal pulse method
ZHENG, Feihu; ZHANG, Yewen

P14 Lifetime estimation for electrical breakdown on PVC sheath
LAIFAOUI, Abdelkrim; REBOUL, Jean-Michel

P15 Study of electret state in epoxyamine polymers by dielectric spectroscopy
GALIKHANOV, Eduard

P16 Cell detection by surface imprinting polymers (SIPs) – a study of the sensor surface by optical and dielectric relaxation spectroscopy
GENNARO, Alessia

P17 New interdigitated comb electrode (IDE) design for detecting cells
GENNARO, Alessia

P18 Study of Dielectric Parameters of $\gamma$-irradiated atactic Polymethyl methacrylate (PMMA) by the Thermostimulated Depolarisation Currents (TSDC) Method
KHEMICI, Mohammed Wafik

P19 Study of thermally stimulated discharge current and optical band-gap of ZnO filled polysulfone polymer nanocomposites
SINGH, Pramod Kumar

P20 New ways of TSD sampling for a high-resolution activation energy analysis
VAN TURNHOUT, Jan

P21 TSDC study of polyvinyl chloride/polymethyl methacrylate (PVC/PMMA) blends
DOULACHE, Naima

P22 Trusty conversion of TSD data into ultralow frequency $\varepsilon'$, $\varepsilon''$ and $d\varepsilon'/d\ln\omega$ spectra
VAN TURNHOUT, Jan

P23 New avenues for calculating the distribution function from TSD spectra
VAN TURNHOUT, Jan

P24 Low cost electrostatic energy harvester based on negatively charged polypropylene cellular films with a folded structure
ZHANG, Xiaoqing

P25 Polarisation profiles in VDF-TrFE copolymer bilayers of molar ratio 70/30 and 56/44
SMYKALLA, David

P26 Acoustic energy harvesting using ferroelectret film attached Helmholtz resonators
ZHANG, Xiaoqing

P27 Piezoelectric resonance and electro-mechanical relaxation in uniaxially-drawn and poled of polyvinylidene fluoride
KODAMA, Hidekazu

P28 Effect of rare-earth ions on the properties of modified Sr0.47Ba0.53Nb2O6 ceramics
VELAYUTHAM, Thamil Selvi

P29 Pyroelectric Properties of hybrid nanocomposites system
GAUR, Mulayam Singh gaur

P30 Pressure dependence of the piezoelectric d33 coefficient and the cellular-foam structure in polypropylene ferro- and piezoelectrets
WIRGES, Werner; QIU, Xunlin

P31 Nonlinear Capacitance Dilatometry in Laminated Ferroelectrets
MELLINGER, Axel

P32 Synthesis and study of bone like hydroxyapatite from cuttlefish bones and its piezoelectric properties
MARKHAM, Sarah

P33 Pyroelectricity in polycrystalline aggregates of globular protein lysozyme
SYED, Tofail

P34 Calcite crystals show weak, measurable piezoelectricity
GUERIN, Sarah

P35 Printed flexible sensors based on P(VDF:TrFE) for spatially resolved monitoring of impact forces
SCHÄFFNER, Philipp

P36 Intermediate polarization states in organic ferroelectrics
CORNELISSEN, Tim

P37 Electrical polarization of chitosan and hydroxyapatite for tissue engineering
LANÇA, M Carmo

P38 Charge Stability of Water Submerged Dielectric Elastomers for Ocean Wave Energy Harvesting
PICHLER, Robert

P39 Design of a combined-structural piezoelectret system for sensing force signals in both normal and tangential directions
FANG, Peng

P40 Preparation and electromechanical properties of P(VDF-TrFE-CFE) relaxor-ferroelectric terpolymer films
RAMAN VENKATESAN, Thulasinath

P41 Controlling Dielectric Loss and Ionic Conductivity through Film Processing – Optimization of Fluorinated Electrostrictive Polymers
PEDROLI, Francesco

P42 Chitosan/Casein Multilayers on Corona Charged Polylactic Acid Substrates
YOVCHEVA, Temenuzhka

# Abstracts

# Invited and oral presentations

# But They Do Move: Electret Charges on Dielectrics Enable Electromechanical Transduction

Reimund Gerhard[1]

Author's e-mail addresses: reimund.gerhard@uni-potsdam.de or reimund@ieee.org

[1]Applied Condensed-Matter Physics, Institute of Physics and Astronomy, Faculty of Science, University of Potsdam, Karl-Liebknecht-Strasse 24-25, 14476 Potsdam-Golm, Germany

**Abstract:** Electrets have a long history starting more 2600 years ago and a bright future in the areas of soft transducers, plastic electronics, etc. From the beginning, the similarities, the differences, and the combinations of dielectric and magnetic materials, of positive and negative "electricities", of internal hetero-charges and external homo-charges, etc. have been puzzling natural philosophers and scientists, but have at the same time led to slow, but continuous progress in the understanding and the application of electrets. Recently, the essential role of charges in the piezoelectricity of ferroelectric polymers and polymer ferroelectrets led not only to new electret-based materials and devices, but also to new approaches for understanding the diversity of electrets.

**Keywords:** Electret history, homo-charge, hetero-charge, charge-dipole interaction, ferro- and piezoelectricity, ferroelectrets (cavity-containing polymers), electro-electrets (dielectric elastomers), charge-spring model

## Introduction

The mutual attraction and repulsion between pieces of amber (ἤλεκτρον) was already known to Thales of Miletus and his disciples after 600 B.C.E. In the 17th and 18th centuries, phenomenological studies and systematic inventions yielded not only devices such as Leiden jars and electrophores, but also early theories about electrical phenomena. During the 19th century, the experimental and theoretical development of electrostatics and electrodynamics culminated not only in Maxwell's equations, but also in the suggestion of the name "electret" [1]. Over the last century, the original wax and resin electrets were replaced by a variety of special polymers which allowed for the optimization of specific properties and the development of a range of very successful device applications.

## Results and Discussion

Starting from the systematic classification of homo- and hetero-charge [2] and various combinations of charges and dipoles, crucial experiments on the quasi-ferroelectricity of ferroelectrets, on charge-dipole interactions in polar polymers and on the stabilization of ferroelectric polarization in semi-crystalline fluoropolymers with useful piezo- and pyroelectricity are reviewed and discussed in order to illustrate the complexity of electret phenomena in polymers and their relation to the morphology and structure of the respective materials.

In order to better understand, explain and predict the piezoelectrical response of electro-mechanically active polymers, a quite recently introduced charge-spring model [3] will be discussed, and its results will be compared to selected experimental data on ferroelectrets, ferroelectric polymers and ceramics from the literature. It will be shown that even well-known inorganic piezoelectric crystals such as barium titanate and lead zirconate titanate can be modelled with the charge-spring concept if the spring lengths in the tetragonal unit cells of the perovskites are properly taken into consideration.

## Conclusion

Clearly, the movement of "electro**static**" charges that are fixed to the electret material may be achieved either by mechanical stresses on the material or by electrical stresses on the charges – direct or inverse piezoelectricity, respectively.

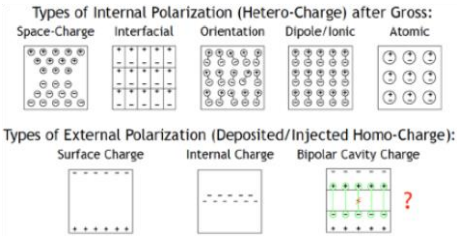


*Figure 1: Categories of hetero- and homo-charge in dielectrics (adapted and amended after [2]).*

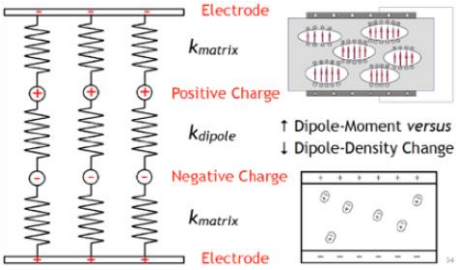


*Fig. 2: Charges and Springs for modelling primary and secondary piezoelectricity in electrets [3].*

## References

[1] O. Heaviside, *The Electrician* **1885**, Section XII, pp. 230 - 231 (August 7, 1885).

[2] B. Gross, *Endeavour (ICI)* **1971**, Vol. *30*, No. *111*, pp. 115 - 119, doi: 10.1016/0160-9327(71)90036-6.

[3] R. Gerhard, in: *Electromechanically Active Polymers. A Concise Reference (F.Carpi, ed.),* **2016**, pp. 489 – 507, doi: 10.1007/978-3-319-31767-0_21-1.

# 1-D Physical Model for the Description of Charge Transport in Dielectric Materials under Representative Space Radiations

Rémi PACAUD [1], Thierry PAULMIER[2], Pierre SARRAILH[3]

Remi.Pacaud@onera.fr Thierry.Paulmier@onera.fr Pierre.Sarrailh@onera.fr

[1, 2, 3]ONERA – The French Aerospace Lab, F-31055 Toulouse, France

**Abstract:** This paper describes a 1-D physical model, developed at ONERA, for the description of charge distribution, charge transport and ionization processes in dielectric materials under representative space electron radiation. This model extends the previous circuit model [1] which relies on solid-state physics. The 1-D model aims at predicting charging behaviours of space used dielectric materials such as Teflon® FEP or Kapton® HN in representative multi-energetic electron irradiation. Physical validations of the model have been performed using experimental facilities that enable crossed comparisons between experimental and numerical results.

**Keywords:** Charge transport, conductivity, dielectrics, polymers, electrostatic discharges, radiations, spacecraft.

## Introduction

In space, dielectrics and especially polymers are commonly used on spacecraft for their electrical, mechanical and thermal properties. Under space radiations, their charging behaviour changes over time as incident particles get implanted in the material bulk. This leads to potential differences between materials which may trigger electrical discharges, electromagnetic disturbances and malfunctioning in satellite equipment. Incident high energy particles can also ionize the polymer which modifies the material electric bulk conductivity. This effect is known as radiation induced conductivity (RIC) and has already been described in previous papers [1] and [2].

The previous circuit model was not realistic enough to describe charge transport under complex irradiation conditions as it was dimensionless. Interfaces and bulk phenomena were not taken into account. Therefore, we extended it to a 1-D model. In this new approach, the electron deposition profile and the generation rate of electron-hole pairs in the material are depth-dependant and nonuniform which allows us to work under multienergetic electron irradiation.

## Results and Discussion

We compared Teflon® FEP and Kapton® HN surface potential measurements with numerical results of our 1-D model. In order to reproduce space environment spectra, the sample (127-µm) is irradiated with a low energetic beam *[20 keV, 250 pA/cm²]* used to charge the material and a high energetic beam *[400 keV, 50 pA/cm²]* used to induce conductivity through ionization processes. For Teflon® FEP, the results showed a very specific charging profile with three distinct phases that we were able to explain with use of the 1-D model. In the first phase the surface potential increases with irradiation time because of electron implantation. In the second phase, it decreases because of free holes that reach the surface sample through convection currents. In the third phase, it increases because of trapping phenomena and recombination processes, preventing free holes from reaching the surface sample. For Kapton® HN, the results also showed a specific charging profile, but different from Teflon® FEP. We observed only two phases. In the first phase the surface potential drastically increases because of electron implantation and in the second phase it slowly decreases because of hole de-trapping processes. Free holes continuously drift towards the sample surface under the electric field influence.

## Conclusions

Charge transport in Teflon® FEP is mainly steered by hole convection currents, trapping phenomena and recombination processes while in Kapton® HN it is mainly steered by hole de-trapping processes.

The numerical results from our 1-D model were in good agreement with the experimental data, which shows that the model is quite well representative of charge transport. However, the model can still be improved. For instance, we are currently working on taking into account the temperature and the electric field dependence on charge transport. For the electric field, further investigations will be made in order to know whether its influence on charge transport is Poole-Frenkel related or not.

## References

[1] R. Hanna *et al.*, "Radiation induced conductivity in teflon FEP irradiated with multienergetic electron beam", *IEEE Trans. Plasma Sci*, vol. 41, no. 12, pp. 3520-3525, Dec. 2013.

[2] G. M. Sessler, *et al.*, "Models of charge transport in electron-beam irradiated insulators", *IEEE Trans. Dielectr. Electr. Insul.*, vol. 11, no. 2, pp. 192-202, Apr. 2004.

## Acknowledgements

Our acknowledgements go to the region Occitanie and the CNES for their financial support.

# Field and charge distribution at semicon/polyethylene interfaces from combinations of probe force microscopy measurements

F. Gullo[1], T. Christen[2], C. Villeneuve-Faure[1], H. Hillborg[3], C. Laurent[1], S. Le Roy[1], G. Teyssedre[1]

gullo@laplace.univ-tlse.fr

[1] LAPLACE, Université de Toulouse, CNRS, INPT, UPS, France
[2] ABB Corporate Research, Baden, Switzerland
[3] ABB Corporate Research, Vasteras, Sweden

**Abstract:** Two modes of Atomic Force Microscopy, namely the Peak Force – Quantitative Nano Mechanics and the Kelvin Probe Force Microscopy, are used for the nanoscale characterization of semicon(SC)-polyethylene(PE) interfaces in a SC-PE-SC-sandwich. A combination of the two methods provides physical (local geometry, roughness) and electrical (electric field, space charge) properties.

**Keywords:** HVDC insulation, space charge, semicon-contact, AFM, KPFM, polyethylene

## Introduction

To understand electrical conduction mechanisms in polymer insulation is crucial for high voltage direct current (HVDC) applications, particularly for the prediction and control of the field distribution. Dielectric polymers exhibit properties which aggravate a sound physical understanding of bulk conductivity: amorphous or semi-crystalline structure, small intrinsic carrier density, low-mobility states and carrier traps, charge carrier injection etc.. In this contribution, we focus on the electrode contact, which is relevant because (1) the contact properties can strongly determine the electrical conductance behaviour of the insulation, e.g. due to injection of majority carriers in combination with the smallness of intrinsic carrier density, and (2) the calculation of electric fields based on drift-diffusion models requires realistic boundary conditions at the contacts [1]. In this work, we consider a typical prototype interface, as ubiquitous in HV equipment, between a carbon black (CB) filled host polymer ('semicon', SC) and the insulating pure host polymer (polyethylene, PE). The fundamental processes which govern the contact physics and their dependence on the microstructure properties in such systems are still poorly understood [2]. We report on results on the application of Peak Force - Quantitative Nano Mechanics (PF-QNM) and Kelvin Probe Force Microscopy (KPFM) techniques [3] to the SC/PE interface in a SC/PE/SC sandwich structure.

## Results and Discussion

The geometrical interface was characterized by measuring the adhesion force with PF-QNM. This parameter shows a contrast between CB dots and the PE matrix, and provides the CB-induced interface roughness. Electrical properties were characterized by measuring the surface potential with KPFM. The determination of the charge distribution requires the solution of Poisson's equation, $\varepsilon_0 \Delta V = -\rho_{free} - \rho_{pol}$, where the free and polarization charges need to be considered with special care on the nanoscale in this strongly nonuniform and anisotropic system. Also the spatial derivatives on experimental and thus noisy data needs a special treatment. We use the Savitzky-Golay method which fits locally a polynomial function such that the derivatives can be performed analytically. In figure 1, resulting E-field (first derivatives) and space charge (second derivatives) distributions are shown for a specific case. Charges appear close to the SC/PE interface (few microns) with negative charge in PE and positive charge in SC.

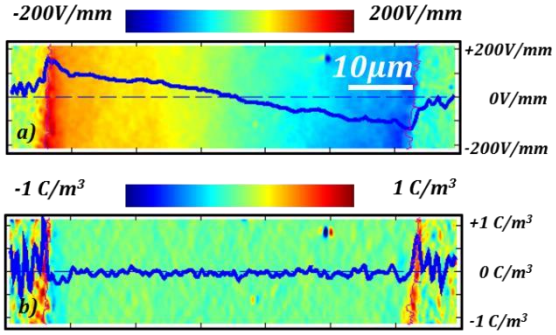


*Figure 1: a) Electric field and b) charge density for a 50µm thick SC/PE/SC structure. Blue curve: profile along the dotted line.*

## Conclusions

KPFM and PF-QNM measurements allows us to characterize the SC/PE interface roughness and the contact charge density. Our approach will allow to determine the boundary conditions for field simulations and to gain new insight into physical phenomena at the electrode interface.

## References

[1] T. Christen, *IEEE Trans. Dielectr. Electr. Insul.* **2015**, *22*, 35; (ibid) **2016**, 23, 3712.

[2] G. Teyssedre, C. Laurent, *IEEE Trans. Dielectr. Electr. Insul.* **2005**, *12*, 857.

[3] M. Nonnenmacher *Appl. Phys. Lett.* **1991**, *58*, 2921.

# Finite Element Analysis of LIMM Space Charge Deposition Measurements in Tubular Channel Ferroelectrets

Neerajan Nepal[1], Axel Mellinger[1], and Ruy Alberto Pisani Altafim[2]

axel.mellinger@cmich.edu (Corresponding e-mail address)

[1]Central Michigan University, Department of Physics, Mount Pleasant, MI 48859, USA
[1]Department of Computer Systems, Federal University of Paraíba, João Pessoa PB, Brazil

**Abstract:** Space charge deposition in tubular-channel ferroelectrets has been investigated using the LaserIntensity Modulation Method (LIMM) and low-level fluorescence light imaging. Distinctive features of the LIMM spectra, such as thermomechanical resonances and polarity changes between samples were successfully modeled and explained using finite element analysis (FEA). This demonstrates the great potential of the combined LIMM/FEA approach for mapping space charge distributions in inhomogeneous materials.

**Keywords:** LIMM, ferroelectrets, piezoelectrets, finite element analysis, space charge

## Introduction

The study of space charge deposition and retention in ferro- or piezoelectrets is an active research topic in the quest for materials with large piezoelectric $d_{33}$ coefficients. Thermal-wave or -pulse techniques, such as the Laser Intensity Modulation Method (LIMM), are well-known for their ability to non-destructively map space charge in one, two and three dimensions [1]. However, analysis of LIMM signals has largely relied on one-dimensional analytical solutions of the heat conduction equation. This approach fails to take into account the inhomogeneous morphology of ferroelectrets, which typically consist of box- or lentil-shaped voids embedded in a host polymer. The present work demonstrates that LIMM spectra in tubular channel ferroelectrets can be analyzed and understood using finite element analysis (FEA).

## Results and Discussion

The tubular channel ferroelectrets [2] were charged by applying 20 cycles of a sinusoidal high voltage waveform. Low-level light emission measurements helped to detect the onset of dielectric barrier discharges [3]. In addition, the deposition of space charge was independently confirmed with LIMM. Both techniques yielded the same threshold voltage for charge deposition; however, the LIMM spectra exhibited strong oscillations above 10 kHz, as well as inconsistent polarity between samples.

To explain these results, the thermo-electromechanical response of a ferroelectret sample to surface heating with a laser pulse or wave was studied using FEA. The calculations revealed strong thermoelastic resonances 50 µs after the initial heating (Fig. 1), in good agreement with the observed oscillations in the frequency domain. Samples with an initial downward bending of the upper barrier layer were found to produce a LIMM signal with the opposite polarity compared to samples with a flat barrier.

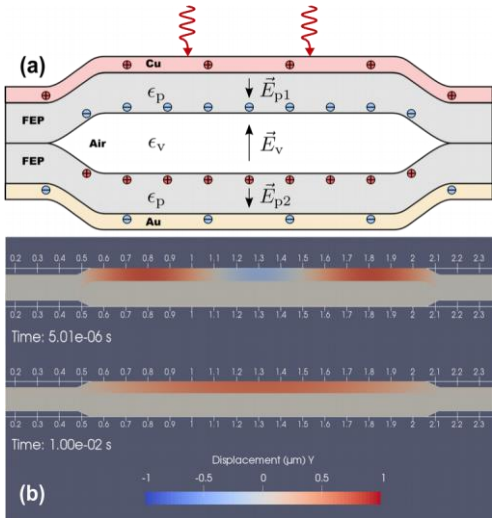


*Figure 1: (a) Schematic view of a charged tubular channel ferroelectret with FEP barriers; (b) FEA modeling of vertical displacement in the top barrier after heating with a 1 µs laser pulse at the top electrode. Note the spatial oscillations at* 50 µs.

## Conclusions

Finite element analysis of the thermo-electromechanical response has been shown to be an indispensable tool in the analysis of thermal-wave or -pulse studies of space charge and polarization.

## References

[1] A. Mellinger and R. Singh, "*Polarization and Space Charge Profiling with Laser-Based Thermal Techniques*", in: Nanomaterials; Processing and Characterization with Lasers, ed. by S.C. Singh, H.B. Zeng, C. Guo and W. Cai, WILEY-VCH, Germany, 2012.

[2] R. A. P. Altafim, X. Qiu, W. Wirges, R. Gerhard, R. A. C. Altafim, H. C. Basso, W. Jenninger, and J. Wagner, J. Appl. Phys. **106**, 014106 (2009).

[3] N. Nepal, A. Mellinger and R. A. Pisani Altafim, 2016 IEEE Conf. on El. Insul. and Dielectr. Phenom., Toronto, ON, Canada, Oct. 2016, pp 388-391.

# Optimization of the thermal calibration process in (F)LIMM under electrical DC field

Amanda Velazquez-Salazar, Laurent Berquez, Didier Marty-Dessus

velazquez@laplace.univ-tlse.fr

LAPLACE, Université de Toulouse, CNRS, INPT, UPS, France

**Abstract:** Dielectric materials widely used for their insulating properties generally undergo high stresses in industrial environments. When they are submitted to strong external electric fields, the space charge creation and/or behaviour can induce a premature ageing of these insulations. The (F)LIMM technique devoted to space charge studies has recently evolved to "on-line" measurements. Now, space charge evolutions may be registered simultaneously with a DC voltage application. However, a thermal calibration prior to any charge recording is compulsory. In this paper, this calibration procedure is detailed and experimental results obtained are discussed.

**Keywords:** dielectrics, space charge, (F)LIMM, thermal diffusion simulation, thermal calibration

## Introduction

The (F)LIMM technique [1-2] has recently evolved towards a new "on-line" set-up allowing the measurement of space charge simultaneously with the application of an external electric DC field [3]. In this configuration, a new term appears in the fundamental mathematical equation that describes the FLIMM currents evolutions versus frequency. This one is directly linked to the thermal gradient produced by the heating laser source and to the external voltage applied. In some specific configurations of study, by recording the experimental FLIMM current resulting from an external DC voltage application, a direct experimental evaluation of the thermal gradient becomes possible. Then, by comparing the experimental results with a thermal theoretical model describing the heat diffusion in the measurement cell, an absolute calibration of the thermal diffusion model can be realized. In this study, simulated currents were compared to experimental ones showing that a calibration procedure was possible and efficient.

## Results and Discussion

The calibration tests were carried out on virgin polymer layers of two different thicknesses: 25 µm (PEN, PET, PE, FEP) and 12 µm (PEN). A top gold electrode (150nm) was sputtered on each sample. An identical experimental protocol based on successive positive and negative external DC voltage applications was used for all samples, all voltage levels remaining low enough to avoid charge injection. For each voltage applied, the (F)LIMM currents versus frequency were recorded (real and imaginary parts). In parallel, a 1-D-sixlayers thermal model describing the real thermal environment of the sample in its measurement cell was used in order to simulate the (F)LIMM expected currents in each case of experiment. Then, by comparing simulations and experiments, a thermal calibration coefficient can be calculated to get a best fit between the two. For all samples, a good agreement between experimental and simulated curves was obtained on a broad range of frequencies (up to $10^4$ Hz) allowing a thermal coefficient of calibration to be evaluated for each situation. But beyond this frequency, it appeared necessary to improve the process of calibration considering the differences between calculated and experimental data. This was carried out by the development of an optimization procedure based on a Levenberg-Marquardt algorithm. By using this additional step of calibration, a proper correction of some physical parameters that were not really controlled in our experiments became possible (sample thickness, actual power of diode for instance) with a final good match between experimental and simulated currents over the whole range of frequencies used.

## Conclusions

The possibility of a thermal calibration in (F)LIMM experiment is of primary importance as it improves the accuracy of absolute charge levels in space charge profiles. The newly developed (F)LIMM "on-line" set-up showed its ability in calibrating the thermal diffusion process at the basis of interactions with these charges.

## References

[1] Lang S. B.; and Das-Gupta D. K.; *Ferroelectrics* **1981**, doi:10.1080/00150198108219626

[2] Marty-Dessus D.; Berquez L.; Petre A.; Franceschi J. L.; *J. Phys. Appl. Phys.* **2002**, doi: 10.1088/0022-3727/35/24/316

[3] Velazquez-Salazar, A.; Berquez, L.; Marty-Dessus, D. *IEEE International Conference on Dielectrics (ICD)*, **2016**, doi: 10.1109/ICD.2016.7547585

# Corona charging with constant current to investigate the electric properties of thin dielectric films

José A. Giacometti

giacometti@ifsc.usp.br

Instituto de Física de São Carlos, Universidade de São Paulo, Av. Trabalhador São-carlense, 400, 13566-590, São Carlos, SP, Brazil.

**Abstract:** We present a new version of the corona triode with constant current to investigate electric properties of thin dielectric films with thicknesses of circa of few hundred nanometers. Poly(methyl methacrylate) polymeric thin films were employed to show the capabilities of the technique and the electric characterization of such thin films was performed.

**Keywords:** corona charging, thin dielectric films, constant current charging, organic electronics

## Introduction

In the past, we developed a corona triode setup allowing charging a dielectric film with a constant current and simultaneously measuring its surface potential. The technique was applied to investigate dielectric films as electrets, ferroelectric and azodye polymeric films [1,2]. Nowadays there is a strong interest in the characterization of thin dielectric films for organic electronics, with thicknesses of the order of few hundred nanometers. Because of the high electric capacitances, up to 10 nF/cm$^2$, the application of the corona technique requires much larger charging current densities than used before, up to 100 nA/cm$^2$, making the construction of the corona triode a challenge.

We describe the new version corona triode setup and the results obtained with thin dielectric films of poly(methyl methacrylate), PMMA, ~400 nm thick, deposited by the spin coating technique, showing the capabilities of the technique.

## Results and Discussion

The corona triode consists of the corona discharge chamber above the metallic grid and the thin film holder below the grid. The electric circuit used in the setup consists of DC power supplies, an electrometer to measure the charging current and a control circuit that acts on the grid voltage supply to have a constant current for the charging process.

The surface potential, $V(t)$, of the thin film and the grid voltage, $V_g(t)$, fulfil the equation:

$$V_g(t) = V(t) + V_{ga}$$

were $V_{ga}$ is the potential drop in the air gap between the grid and the film surface to drive ions across the air gap. Measurements showed that $V_{ga}$ is constant under a given value of the charging current density, $J_0$, allowing the surface potential determination. Worth to mention is that in the past the quantity $V_{ga}$ was neglected compared to the measured surface potential since the charging current densities were very small, less than 0.5 nA/cm$^2$. It is also possible to follow the surface potential decay setting the control circuit to run using a negligible charging current. The electric capacitance of the film per area unit can be obtained directly by the variation of the grid voltage at the beginning of the charging process by the equation:

$$C = J_0/(dV_g/dt)_{t \to 0}$$

and values obtained are in good agreement with measurements performed with an impedance analyzer.

Exemplary results obtained with PMMA thin films showed that the surface potential increase cannot be explained by considering an ohmic conduction process in agreement with the fact the measured of characteristic curves of the current versus the stationary surface potential is not linear.

## Conclusions

It is shown that the corona triode with constant current can be applied to characterize thin dielectric films. Further measurements are under way to investigate the electric properties of thin films employed in organic field effect transistors.

## References

[1] Giacometti, J.A.; Oliveira Jr, O.N. *IEEE Trans. Elec. Insul.* **1992**, 27, 924-943

[2] Giacometti, J.A.; Fedosov, S.N.; Costa, M.M. Braz. Journal Physics, **1999**, *29*, 269-280.

## Acknowledgements

Acknowledgments to the project Institute of Organic Electronics (INEO) and to CNPq for the financial support.

# Trap-energy spectrum in corona-charged polytetrafluoro-ethylene (PTFE) electret films with modified surfaces

Dmitry Rychkov[1], Reimund Gerhard[1], Alexey Kuznetsov[2] and Andrey Rychkov[2]

rychkov@uni-potsdam.de

[1]Applied Condensed-Matter Physics, Institute of Physics and Astronomy, University of Potsdam, Karl-Liebknecht-Str. 24-25, 14476 Potsdam, Germany
[2]Department of Industrial and Designer Technologies, Herzen State Pedagogical University of Russia, Moika emb. 48, 191186 St-Petersburg, Russia

**Abstract:** Chemical modification is an effective method for enhancing (or decreasing) the charge-storage properties of polymer-electret materials. Here, we report how the combined treatment of polymer surfaces in the high-frequency (HF) plasma of a glow discharge and subsequently in titanium-tetrachloride vapor modifies the energy spectrum of surface traps on positively charged polytetrafluoroethylene (PTFE) films.

**Keywords:** polytetrafluoroethylene (PTFE), space-charge electret, trap-energy distribution, charge storage and transport, surface modification, plasma treatment, chemical surface modification

## Introduction

As shown previously [1,2], the stability of electret charges on corona-charged polytetrafluoroethylene (PTFE) films can be substantially enhanced by means of suitable surface modifications. In particular, we achieved very high thermal stability of the positive homocharge on PTFE films (comparable with the excellent thermal stability of negative charge on PTFE) [3]. To this end, we had first treated (activated) the PTFE-film surfaces by means of a HF glow-discharge plasma in a water-vapor atmosphere and then chemically modified them in titanium-tetrachloride ($TiCl_4$) vapor.
In the present work, we determine the energy spectrum of the surface traps on PTFE films that underwent such a two-stage treatment.

## Results and Discussion

Our samples were 13 µm thick oriented PTFE films manufactured by AO "Plastpolymer", St-Peterburg. The films were metallized with aluminium on their rear side in order to provide good electrical contact for charge-decay measurements. After the two-stage modification as described in [3], the films were charged in a positive corona discharge up to an initial surface potential of $V_0$ = +150 V. Then, temperature-dependent charge-decay curves were obtained, and the surface-trap parameters were determined with the procedure described in [2].
The results shown in Figure 1 indicate that surface modification either in a glow discharge (2) or with $TiCl_4$ vapor (3) leads to the formation of additional and energetically deeper surface traps. The effect of a $TiCl_4$-vapor treatment is more pronounced, but by far the deepest traps are found after the combined treatment (curve 4, blue trace). In this case, it has been shown [3] that the atomic concentration of titanium on the surface is increased to 4 atom% as opposed to only 2.8 atom% for the $TiCl_4$-vapor treatment without the earlier HF-plasma exposure.

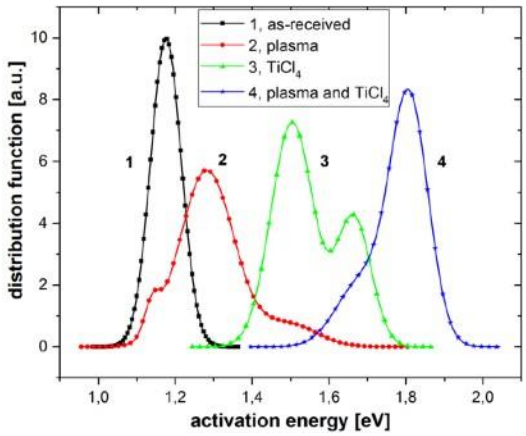


*Figure 1: Energy spectra of the surface traps on positively charged PTFE electrets.*

Our calculations also show that the frequency factors of the surface traps are improved as well, in this case from 70 THz for the as-received films to 6 THz for films that received the combined glow-discharge + chemical-vapor treatment.

## Conclusions

We have demonstrated that both plasma and chemical treatment of PTFE surfaces results in the formation of traps that are considerably deeper than those on as-received material. The results may be useful for electret-device applications where the thermal stability of positive charge is essential.

## References

1. D. Rychkov and R. Gerhard, *Appl. Phys. Lett.* **2011**, Vol. 98, paper 122901, doi: 10.1063/1.3565166
2. D. Rychkov, R. Gerhard, V. Ivanov, A. Kuznetsov, and A. Rychkov, *Annu. Rep. CEIDP* **2015**, pp. 87-89, doi: 10.1109/CEIDP.2015.7352080
3. N. Efimov, A. Malygin, and A. Rychkov, *Russ. J. Appl. Chem*. **2016**, Vol. 89, No. 5, pp. 930-936.

# Charge Attachment Induced Ion Transport – Electro-diffusion, chemical diffusion and grain boundary diffusion

Karl-Michael Weitzel [1]

weitzel@chemie.uni-marburg.de

[1] Chemistry Department, Philipps Universität Marburg, Hans Meerwein Str. 4, 35043 Marburg, Germany

**Abstract:** A new experimental approach for studying the transport of cations in solid state samples will be described. The approach is based on attaching charged species at the surface of a sample of interest. Ultimately the new technique provides quantitative information on many kinds of transport aspects, e.g. electro-diffusion chemical diffusion and grain boundary diffusion.

**Keywords:** ionic conductivity, concentration profiles, transport theory

## Introduction

The charge attachment induced transport (CAIT) is a recently developed technique for investigating ion transport in the solid state. It is based on attaching ions to the surface of a solid sample in contact with a single metal electrode. This causes gradients of the electrical potential and/or the particle density across the sample and consequently transport of particles towards the backside electrode. If ions of different chemical identity are involved concentrations profiles will evolve. These concentration profiles can be measured quantitatively by means of ToF-SIMS and modelled quantitatively by means of Nernst-Planck-Poisson theory providing unique access to position and concentration dependent transport coefficients.

## Results and Discussion

Three major examples will be discussed.

- The competition between $Na^+$ and $K^+$ in a mixed Na-K-borosilicate glass has been investigated by charging the sample surface with $Cs^+$ ions. Analysis of the Cs, K, and Na profiles arising allows the derivation of concentration dependent diffusion coefficients in particular for the native $Na^+$ and $K^+$ in the glass [1].

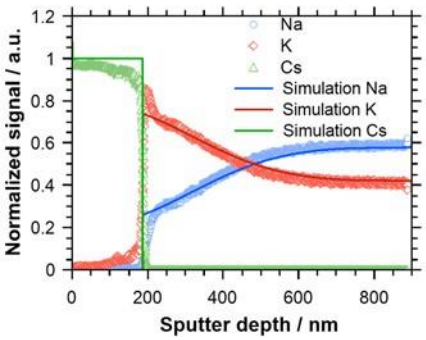


*Figure 1: Concentration profiles of Cs, K, and Na in a borosilicate glas after foreign ion bombardment.*

- The mobility of $Na^+$ and $Ca^{++}$ in a bioactive Na-Ca-phosphate glass has been investigated by charging the sample with $K^+$ ions. The concentration profiles arising demonstrate the depletion of Na and Ca by means of electro-diffusion. On a much longer time scale these concentration profiles are demonstrated to evolve further by chemical diffusion- leading to a partial refilling of the former depletion zone. Theoretical analysis demonstrates that for chemical back diffusion D(Ca) > D(Na) [2].

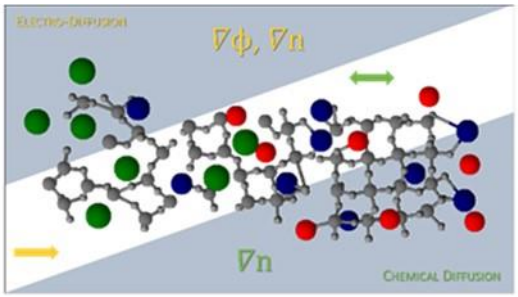


*Figure 2: Sketch of electro-diffusion of $K^+$, $Na^+$ and $Ca^{++}$ in forward direction and consecutive chemical diffusion in forward and backward direction.*

- In a thin film sample of $PrMnO_3$ the electronical conductivity is so high that the surface is not charged, but alkali metal is deposited at the front of the sample. In this case concentration driven diffusion of the alkali metal into the perovskite is observed. Theoretical analysis clearly reveals a competition between bulk and grain boundary diffusion, which is also supported by high resolution FIB-TEM [3].

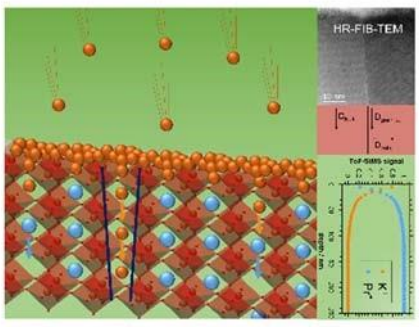


*Figure 3: Sketch of charge attachment induced ion transport in a perowskite. Shown on the right are*

*concentration profiles as well a high resolution FIBTEM image of a grain boundary.*

## Conclusions

The charge attachment induced transport (CAIT) technique is a universal, new method for analyzing ion transport in solid matter. The technique allows studying the mobility and also the immobility of charge carriers in solid matter.

Most of the information currently available for ionic conductivity is derived from impedance spectroscopy. However, impedance spectroscopy is in general not capable of distinguishing the contribution from two different cationic charge carriers. As we demonstrate, our CAIT can easily solve this problem.

Most of the information currently available for chemical diffusion of ions in solid matter and on the mixed alkali effect is derived from tracer diffusion experiments, where you need to prepare one sample for each composition. Since our technique looks at all different compositions in the concentration profile simultaneously, the CAIT is much more efficient than tracer diffusion experiments. Under conditions, where one would expect that concentration profiles written into a solid material are time independent, we demonstrate that concentration profiles evolve on a longer time scale.

The thinner a sample of interest is, the more important are nano-scale processes for transport and other dielectric properties. We demonstrate that grain boundary diffusion and chemical diffusion can easily be distinguished in a thin perovskite film.

For the future, we expect that the technique could also be applied to study e.g. unipolar space charge zones and dielectric breakdown in solid matter.

## References


[1] J. Martin, S. Mehrwald, M. Schäfer, T. Kramer, C. Jooss, K.-M. Weitzel, Electrochimica Acta, 191, 616–623, (2016).

[2] A. Hein, J. Martin, M. Schäfer, K.-M. Weitzel, J. Phys. Chem. C, 121, 3203 - 3211 (2017)

[3] J. Martin, M. Gräf, T. Kramer, C. Jooss, M.-J. Choe, K. Thornton, K.-M. Weitzel, Phys. Chem. Chem. Phys., 19, 9762 - 9769, (2017)


## Acknowledgements


Financial support of this work by the Deutsche Forschungsgemeinschaft (DFG We 1330/17-1) is gratefully acknowledged.

# Bioelectrets: A tool to understand electrically mediated interactions in biology

Syed A. M. Tofail[1] tofail.syed@ul.ie

[1]Department of Physics and Bernal Institute, University of Limerick, National Technological Park, V94 T9PX, Limerick, Ireland

**Abstract:** The abstract should be no longer than 6 lines words and written in a clear and appealing style. Even colleagues, who are not really a specialist in your field, will find it worthwhile to listen to your lecture and to visit your poster and have an informal talk with you while drinking a cup of tea or coffee together.

**Keywords:** relaxation spectroscopy, ionic materials, ferroelectrets

## Introduction

The term bioelectret has been coined by Sergio Mascarenhas [1] to describe the ability of a permanent storage of electrical charge and/or polarisation storage by materials of biological importance. The separation of charges and the alignment of dipoles are capable of creating permanent electrical polarisation in insulators as well as semiconductors. Biological building blocks such as amino acids, proteins and enzymes, deoxyribonucleic acids (DNA), ribonucleic acids possess chirality and low symmetry. This, together with an essential and ubiquitous presence of water, both in the bound state and in the surrounding, allows charge separation and dipole orientation. Thus biological building blocks can be inherently in electret states in their native molecular organisation, hierarchical organisation (e.g. in organelles, cells, tissues and organs) as well as in their synthetic crystalline forms. As electrets, such materials exhibit piezoelectricity, pyroelectricity, thermal depolari-sation and relaxation, streaming potentials and even switchable polarisation e.g. ferroelectricity. Since the pioneering work of piezoelectricity in wood [2] and bone [3] there has been significant effort in the understanding of the phenomenology and physiological relevance of bioelectrets. The effort in understanding of the solid state dielectric behaviour of tissues such as bone dominated the field with a view to accelerate calcification. This approach has still remained in the mainstream albeit with an emphasis on nanoscale manifestation of electret properties. We will provide a brief overview of the developments in the field of bioelectrets especially in the last two decades. We will then highlight the potentials of bioelectrets to be used as a biophysical tool to understand electrically mediated interactions in biology.

## Results and Discussion

Nanocrystalline hydroxyapatite (HA), the synthetic bone mineral used in medical implants and coatings, shows piezoelectricity, pyroelectricity and ferro-electricity [4]. We have used its electret forms to provide a convenient tool for understanding electrical interactions of biological species. The premises within which electrically mediated interactions are to be understood however pose real challenges in implementation. We overcame some of these challenges using thin films of nanocrystalline HA electrets. These thin films have been modified by electron beam poling to have a controlled localised polarisation [5,6]. The interactions of model protein and cellular systems on these electrostatic domains showed that coulombic attraction/repulsion dominated the interfacial binding between biological species and the charged electrets *ceteris paribus*.

## Conclusions

Bioelectrets can be a convenient tool for investigating electrically mediated biological interactions. Physiological impact of bioelectrets are poorly understood. The methodology and examples presented here can provide real means to understand biological interfaces with medical devices, therapeutic drugs as well as pathogenesis and growth. The significance of bioelectrets can thus be far more extended beyond the current trend in the understanding of solid state behaviours only.

## References

[1] Mascarenhas, S. In *Electrets* (ed. G.M. Sessler) Springer Verlag: Berlin, 1987.
[2] V.A. Bazhenov, V.P. Konstantinova, *Doklody Akad. Nauk. SSSR, Chem. Abst.* **1951**, *45*, 2747.
[3] E. Fukada, I. Yasuda, *J. Phys. Soc. Jpn.* **1957**, *12*, 1158-1162.
[4] S.B. Lang et al. *Sci. Report* **2013,** *3*, 2215- 2219.
[5] S. Robin et al. *Langmuir*, **2011**, *27*, 14968-14974.
[6] Salazar-Alarez, M. et al. In *Electrically Active Materials for Medical Devices* (eds. S.A.M. Tofail, J. Bauer), Imperial College Press: London, 2016.

## Acknowledgements

European Commission FP7 project BioElectricSurface (Grant no: EC-NMP4-SL-2008-212533).

# Bioelectret biosensor for detection of TSH in human blood

Mulayam Singh Gaur[1], Dayal Saran

mulayamgaur@rediffmail.com (Corresponding e-mail address)

[1]Interdisciplinary Research laboratory, Hindustan College of Science and Technology, Farah, Mathura, UP 281122, India Affiliated to Dr. A. P. J. Abdul Kalam Technical University, Lucknow ( U P ), India

**Abstract:** The bioelectret state in human blood is being analyzed by thermally stimulated current (TSC). The heating of sample after application of 100 volt DC field and subsequently record of current as a function of temperature(TSC). It is observed that the position of TSC peak is different for deferent level of TSH. The activation energy, charge released and peak current were observed to be decreases with TSH nonpolar salt in human blood. It is noted that TSC can be suitable diagnostics of thyroid-stimulating hormone (TSH) in human blood.

**Keywords:** bioelectret, TSC, TSH, polarization

## Introduction

The bioelectret effect in organic objects has been studied, and its role in the detection of biological species like TSH is being analyzed. The electret state is not only the injection of charges, fixation of rotations of dipoles etc. In a series of investigations are evidence that the electrets state are general properties of biological material such as poly-peptides (proteins), polynucleotides (including DNA) and polysaccharides, cellulose and chitin of various biological origins.

The electrets state in bio material is used to emphasize the implicated characteristics of bio-electret state [1-3]. The aim of present work is develop simple method based on principle of bio-electret thermal analysis followed by TSC measurement to distinguish different level of TSH.

## Results and Discussion

The TSC characteristics of fresh human blood with normal TSH and abnormal TSH are shown in figure 1. The blood sample are characterized by single negative peak with continuous heating. The acti-vation energy of this peak is varies from 0.25eV to 1.5eV. The possible deviation of activation energy can be due to a different contribution from excited states, mainly vibration. If the temperature is high enough, and the contribution of excited states is important. Higher value of activation energy is corresponding to large number of excited state due to ionic polarization in blood samples. However, decrease in this value is corresponding to interfacial polarization. It is due to small interface formed between blood and Teflon ring. Human blood is known to be multicomponant system consisting of a water solution of mineral salts amino acids, proteins, steroid, enzyme etc (i.e. plasma). The H ions of the acid or OH ions of the alkali were adsorbed by the blood cells in preference to the other ions on account of their greater rapidity of migration. It is necessary to account for the fact that cell membranes become positively charged in the presence of acid and negatively charged in the presence of alkali. The electrical charges of the colloidal solution (i.e. blood serum) are apparently diminished during heating or destroyed by the salt on the assumption of a preferential adsorption of one of the ions of TSH salt. The important consequence of this is that long range interactions are possible between hydrophobic solute molecules, and they can be detected by means of TSC peak [21].

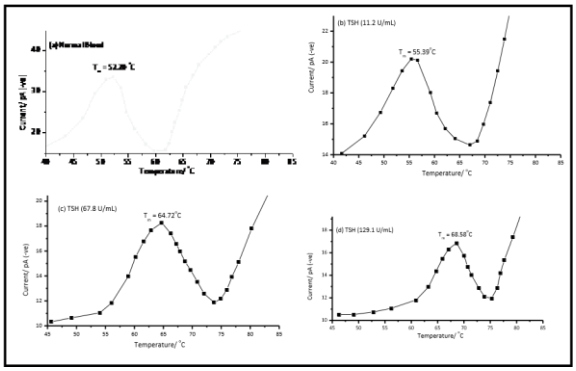


*Figure 1:*

## Conclusions

TSC shows significantly better analytical sensi-tivities and reproducibility at the level of lower TSH concentrations as compared to the advance method.

## References

[1] Pinchuk, L.S.; Goldade, V.A; Sessler, G.M.; Kravtsov, A.G.; Zotov,S.V.; Tsvetkova, E.A. *Med. Eng. & Phy.2002*, 24, 361–364

[2] Mascarenhas, S.; *J. of Electrostatics 1975*, 1, 141146

[3] Pinchuk, L.S.; Kravtsov, A. G.; Zotov, S. V.; *Tech. Phys. 2001*,46, 620-624

[4] Jain, D.; Nath, R.; Sharath Chandra, L. S.; Ganesan, V.; *J. of Instrm. Soc. of India 2009*,1.39,35-37

# Field dependence of dielectric properties in low density polyethylene insulation as studied by high voltage dielectric spectroscopy

Emmanuel Logakis[1], Thomas Christen[1]

emmanuel.logakis@ch.abb.com (Corresponding e-mail address)

[1]ABB Corporate Research, Segelhofstrasse 1K, 5405 Baden-Daettwil, Switzerland

**Abstract:** This work discusses dielectric spectroscopy results on low density polyethylene films at high voltages (AC and AC/DC fields up to 10 kV/mm). A sharp increase in the dielectric losses, at AC fields exceeding 7 kV/mm, was observed and interpreted in terms of the "flat" loss model, proposed by Jonscher.

**Keywords:** high voltage dielectric spectroscopy, polymer insulation, low density polyethylene, flat response

## Introduction

Dielectric spectroscopy measurements are widely utilised in the electric power industry, since they provide valuable information during the selection or development of new materials, as well as to improve the insulation design, processing, quality, and control of a product. The determination of the dielectric properties is typically done under low voltages, usually only few volts, associated with far lower electric fields (at most a few V/mm) compared to the ones the material will be exposed to during service (kV/mm range). This contribution discusses high voltage dielectric spectroscopy measurements (HVDS) on low density polyethylene (LDPE) films. LDPE was chosen as a model system for this study (low density of impurities).

## Results and Discussion

Thin films (≈ 100μm thick) were produced by compression molding of clean, non-stabilized LDPE granules. The granules were pressed between polyethylene terephthalate films in order to reduce surface oxidation as well as humidity absorption and conta-mination. A Polystat 300S laboratory press was used. The material was molten in the press at 140°C followed by pressing at 285 bar for 6 min and additional 9 min at 80°C. Afterwards the samples were cooled at room temperature.

Round electrodes (Au over Cr), 30 mm in diameter, were deposited on both sides of the films to ensure good electrical contacts for the measurements.

Measurements were conducted in a broad frequency band ($10^{-2}$ to $10^{4}$ Hz), and in large temperature (-150 to 70°C) and field ranges ($10^{4}$ to $10^{7}$ V/m), both AC and AC with superimposed DC bias, using a Novocontrol Alpha Analyzer with HVB 4000 interface.

Characteristic examples of such measurements are provided in Figure 1, where the dielectric losses (ε") as a function of frequency are shown for various AC levels at 70°C. The low frequency-dependent region (region I) is dominated by conductivity contributions. The field dependence of the conductivity "tail" is also apparent. The most interesting finding is on the middle frequency region (region II), where a jump in ε" is observed at high fields (threshold between 7 and 8 kV/mm AC fields). The aforementioned results will be discussed in terms of the "flat" loss model proposed by Jonscher [1]. This "flat" response masks the characteristic loss peaks of dipolar nature of LDPE, which are only apparent in regions II and III, at fields below 7 kV/mm.

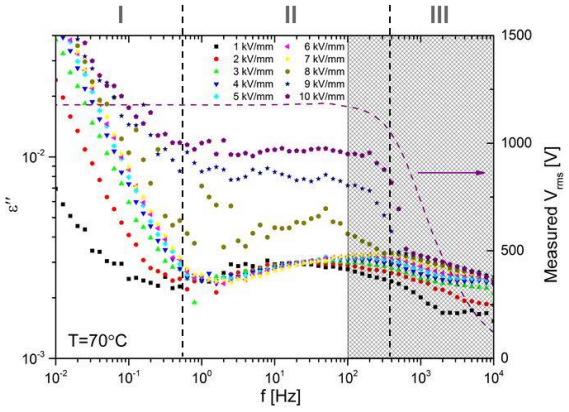


*Figure 1: Dielectric losses (ε") as a function of frequency for various AC amplitudes (dashed region denotes the area where the applied voltage is limited by the output impedance of the HV interface for safety reasons).*

## Conclusions

The appearance of the "flat" loss in the medium frequency region (region II) can be explained by: 1. accepting a sum of many Debye-like loss peaks (distribution of dipolar relaxation times), which however lacks of physical meaning, or 2. by charge carrier hopping between localized sites, thus distribution of hopping times (understood in terms of a wide distribution of distances and relative energy differences) [1].

## References

[1] Jonscher, A. K.;, Nature **1974**, 250, 191-193.

# Quantum Chemical Study of Charge Trap in Amorphous Perfluoro Polymer Electret

Seonwoo Kim [1], Yuji Suzuki [1]

skim@mesl.t.u-tokyo.ac.jp

[1] Dept. of Mechanical Engineering, The University of Tokyo, Hongo, Bunkyo-ku, Tokyo 113-8656, Japan

**Abstract:** Charge trap in a high-performance amorphous perfluoropolymer electret CYTOP is investigated with the aid of quantum chemical analysis. The charge concentration and electron trap depth of CYTOP oligomer with different end-group is examined using density-functional theory (DFT).

**Keywords:** polymer electret, density functional theory, CYTOP

## Introduction

CYTOP, an amorphous perfluoro polymer electret is known as a high-performance polymer electret, which gives the surface charge density up to 2 mC/m$^2$ for 15 μm-thick film [1,2]. Among different end groups, the amidosilyl end group gives highest sur-face charge density. However, the features deter-mining charge trapping remain unclear. In this study, the effect of the end-group of CYTOP on the charge trap is examined using quantum chemical analysis [3].

## Results and Discussion

Three systems of CYTOP oligomer with a different end group (i.e. Trifluoromethyl (CTL-S), Carboxyl (CTL-A) and Amidosilyl (CTL-M)) are studied. Among them, CTL-M gives the highest charge density [1]. Geometry of the systems is firstly determined by molecular dynamic optimization (MMFF94 force field, 300 K condition). Then, quantum chemical geometry optimization is em-ployed to ensure chemical equilibrium state. Opti-mized geometries of negatively charged system (-1) are prepared. Finally, quantum chemical energy computation is performed using density-functional theory(DFT) implemented in NWChem [4]. LCBLYP functional and 6-31G* basis sets are used to properly analyse polarization of fluorine-rich poly-mer system [5]. Fig. 1 shows optimized geometry of CTL-M and localized trapped electron distribution. The trapped electron is distinctly localized near the end group, while it is dispersed through the whole system for CTL-S. Fig. 2 displays orbital energy of trapped electrons. Bars with arrow show energy level of trapped electron. The electron trapped in CTL-M is the most stable, which is in accordance with the experimental findings [1]

## Conclusions

Quantum chemical analysis on CYTOP oligomer systems was performed. It is found that CTL-M gives the lowest orbital energy, which is in accordance with the experimental result [1]. This result implies applicability of the present method for developing new high-performance polymer electret.

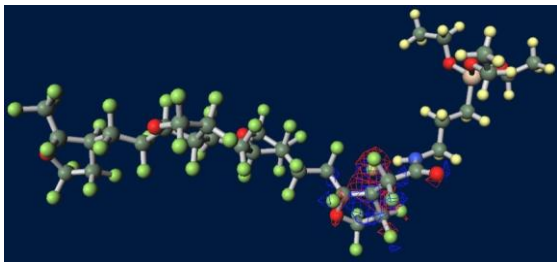

*Fig. 1. CTL-M oligomer system (Green: fluorine, Blue: nitrogen Red: oxygen, Khaki: carbon, Yellow: hydrogen Pink: silicon) and distribution of localized trapped electron (Red and Blue meshes).*

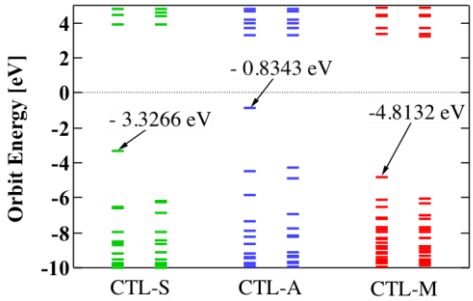


*Fig. 2. Orbital energy level of negatively charged CYTOP systems.*

## References

[1] Y. Sakane, et al., *J. Micromech. Microeng.* **2008**, *18*, 104011(6pp).

[2] K. Kashiwagi, et al., *J. Micromech. Microeng.* **2011**, *21*, 125016(8pp).

[3] M. Meunier, N. Quirke., *J., J. Chem. Phys*, **2001**, 115, 2876-2881.

[4] M. Valiev, et al., *Comput. Phys. Commun*. **2010**, *181*, 1477.

[5] S. Maekawa, K. Moorthi., *J. Phys. Chem. B*, **2016**, *120*, 2507−2516.

## Acknowledgements

This work is partially supported by JST CREST. The computation in this work has been done using the facilities of the Supercomputer Center, the Institute for Solid State Physics, the University of Tokyo. SK is supported through the Leading Graduates School Program, "Global Leader Program for Social Design and Management" by MEXT.

# Dielectric studies on interfacial effects in polymer nanocomposites

Kyritsis A., Klonos P., Pissis P.

akyrits@central.ntua.gr (Corresponding e-mail address)

Department of Physics, National Technical University of Athens, Zografou Campus, 15780, Athens, Greece

**Abstract:** The molecular mobility of poly(dimethylsiloxane) (PDMS) and poly(vinylidene fluoride) (PVDF) macromolecules in nanocomposites with silica or titania nanoparticles (PNCs) is investigated by means of dielectric spectroscopy. Glass transition and segmental dynamics of the polymers are found to be sensitive tools for studying interfacial effects in PNCs. Our results suggest that the strength of polymer-filler interactions, the porosity of the nanoparticles and the length of the polymer chains (in core-shell type PNCs) affect significantly the segmental mobility and the degree of crystallization of both polymers. Furthermore, the results are discussed in terms of interfacial characteristics, in particular polymer fraction in the interfacial layer and thickness of the interfacial layer.

**Keywords:** Dielectric spectroscopy, polymer nanocomposites, segmental relaxation, interfacial layer

## Introduction

Polymer nanocomposites (PNCs) are increasingly attracting interest in the scientific community and the industry, owing to significant improvement often observed for several properties of the polymer matrix (thermal, mechanical, barrier), as well as to new properties (electrical, magnetic, optical) added by the filler. It is generally accepted that interfacial effects, defined as changes in structure/organization, dynamics and properties of the polymer at the interface with the filler, play a significant role for the improvement of properties of PNCs. This work deals with the experimental investigation of interfacial effects in PNCs by means of dielectric spectroscopy (DS) focusing mainly on polymer segmental dynamics. DS is frequently employed to study polymer dynamics in polymer-based materials. The extremely broad frequency range of isothermal DS measurements of more than 12 decades in combination with temperature variation enables to follow on the same sample molecular motion in wide ranges of time and spatial scale, from tenths of nm to mm. By combining DS with calorimetry, we focus on structure/organization, thermal transitions and dynamics of the polymer in the polymer-filler interfacial layer, determined to be a few nm thick [1]. Two types of PNCs are investigated, in the first one silica or titania nanoparticles are dispersed within the polymer matrix whereas in the second type polymer chains are physically adsorbed onto spherical-like fumed silica or titania nanoparticles (core-shell type of PNCs).

## Results and Discussion

The basic system taken as example is poly(dimethylsiloxane) (PDMS)/(silica or titania) nanocomposites, in wide ranges of composition. The strength of polymer-filler interactions, the porosity of the nanoparticles and the length of the polymer chains (in core-shell type PNCs) have found to affect significantly the segmental mobility of PDMS and its crystallization (Figure 1) [1]. Dielectric studies allow for the investigation of the features of the interfacial

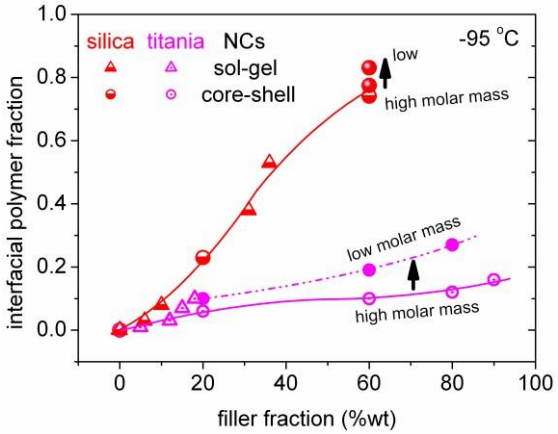


*Figure 1: Interfacial polymer fraction in PDMS based PNCs as a function of silica or titania nanoparticles fraction.*

layer, which has been found to exhibit its own molecular mobility. Poly(vinylidene fluoride) (PVDF)/silica NCs were also studied by employing similar experimental methodology and the results are critically discussed in comparison with those obtained on PDMS based NCs.

## Conclusions

DS reveals that in PDMS and PVDF NCs the segmental mobility in the vicinity of the nanoparticles is selectively activated depending on the constraints imposed by the nanoparticles.

## References

[1] Klonos P., Kyritsis A., Pissis P. Interfacial effects in polymer nanocomposites studied by thermal and dielectric techniques, Chapter 6 in Interface/ interphase in polymer nanocomposites, A.N. Netravali, K.L. Mittal (Eds.), WILEY - Scrivener Publishing LLC, **2016**, pp 191-248.

# Molecular dynamic and polarization switching of solvent-cast poly(vinylidene fluoride)

W.C.Gan [1], H. Kodama[2], T. Furukawa[2] wcgan@xmu.edu.my

[1]School of Engineering, Xiamen University Malaysia, Bandar SunSuria, 43900 Sepang, Selangor, Malaysia
[2]Piezoelectric Physics and Devices Laboratory, Kobayasi Institute of Physical Research, 3-20-41 Higashimotomachi, Kokubunji, Tokyo, Japan

**Abstract:** An overview of ferroelectric poly(vinylidene fluoride) (PVDF) is presented based on our recent work on molecular and polarization switching dynamics. The fundamental understanding on the extraordinary electrical responses of PVDF induced by electric field will be provided. It is shown that the ferroelectric, pyroelectric and dielectric properties of PVDF are depending on the hierarchical structures and molecular crystalline orientation. The structures and ferroelectric properties of solvent-cast PVDF are discussed in term of the simultaneous observation of polarization reversal and dielectric relaxation associated with two orthogonal directions (*a*- and *c*axis) of crystallites. A comprehensive picture of the dynamic features of PVDF-based ferroelectric polymers in relation to thermally-induced and electrical-field-induced molecular motions will be presented.

**Keywords:** dielectric relaxation, ferroelectric polarization switching

## Introduction

Poly(vinylidene fluoride) (PVDF) exhibits at least four crystalline polymorphs; Forms I, II, III, and IV ($\beta$, $\alpha$, $\gamma$, and $\delta$ phases). Solvent casting has attracted much interest recently because of more effective control of crystallinity, orientation and polymorphs. Here, the ferroelectric polarization switching of solvent-cast PVDF are discussed in term of the hierarchical structures and molecular crystalline orientation.

## Results and Discussion

Figure 1 shows the frequency spectra of complex permittivity for the samples cast from DMF (A), CHN (B) and acetone (C) as well as melt-crystallized (MC). We observe two distinct relaxation processes; $\alpha$ near 1 Hz and $\beta$ near 1 MHz which are attributed to the translational motion in Form II crystal and the rotational motion in Form I and/or non-crystalline regions. The MC sample exhibits equally strong $\alpha$ and $\beta$ processes that are consistent with its structure consisting of 50% crystallinity with Form II. Solvent-cast samples exhibit a weak $\beta$ process that is an indication of high crystallinity. The very strong $\alpha$ process in sample B ($\Delta\varepsilon \approx 30$) is consistent with the chain-axis orientation of Form II crystal in the thickness direction. The weak α-relaxation in sample C ($\Delta\varepsilon \approx 4$) suggests is the chain-axis orientation almost parallel to the glass substrate.

Figure 2 shows the *D-E* hysteresis loops for solvent-cast and ultra-drawn PVDF. The maximum value of remanent polarization $P_r$ exceeding 100mC/m$^2$ was obtained for ultra-drawn PVDF. Sample A showed a large $P_r$ of 85mC/m$^2$ that is attributable to the polarization switching in Form I. Sample B showed essentially no hysteresis because of perpendicular orientation of TGT$\bar{G}$ chains. In contrast, sample C exhibited large hysteresis loop when an extremely high electric field was applied. The x-ray result suggests that a phase transformation from Form II to IV after poling.

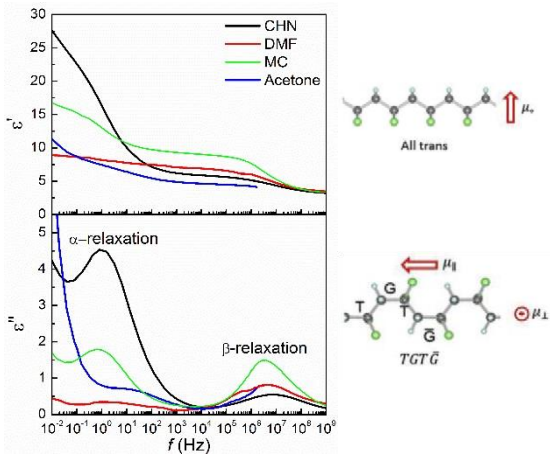


*Figure 1: Dielectric frequency spectra of PVDF at 30°C*

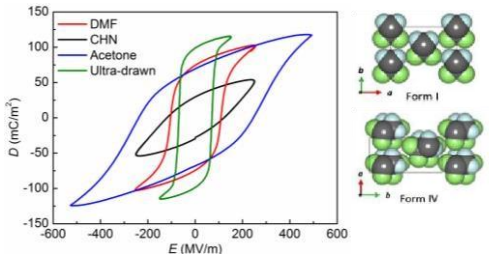


*Figure 2: D-E hysteresis loops for solvent-cast PVDF*

## Conclusions

We have shown that highly polar solvents favor the formation of Form I PVDF, whereas less polar solvents promote Form II. Resulting polymorphs were supported by dielectric relaxation and *D-E* hysteresis. Spin-casting from acetone yielded a unique thin film suggesting polarization switching in Form IV.

# Dielectric Relaxation of Discotic Liquid Crystals

Arda Yildirim, Christina Krause, Andreas Schönhals

Andreas.Schoenhals@bam.de

Bundesanstalt für Materialforschung und –prüfung, Unter den Eichen 87, 12205 Berlin, Germany

**Abstract:** The molecular dynamics of the discotic liquid crystals like pyrene-1,3,6,8-tetracarboxylic tetra(2ethylhexyl) ester is studied by dielectric relaxation spectroscopy. Dielectric spectroscopy shows 3 processes: a b-relaxation at low temperatures and an a-relaxation in the temperature range of the mesophases followed by conductivity. The dielectric a-relaxation is assigned to a restricted glassy dynamics in the plastic crystal as well as in the liquid crystalline phase.

**Keywords:** Broadband dielectric relaxation spectroscopy, Discotic liquid crystals, Plastic crystals

## Introduction

Discotic liquid crystals are unique materials which exhibit aspects both of a conventional fluid and a solid crystal. Usually they consist of a stiff disk-like core surrounded by flexible alkyl side chains. Whereas the former induces π-stacking, the latter leads to an increase of the solubility. Both of them result in a rich thermotropic behavior. At low temperature discotic liquid crystals have a crystalline or plastic crystal phase, followed by a hexagonal columnar mesophase at higher temperatures. At even higher temperatures they undergo a phase transition to a more or less isotropic liquid. The length and specific structure of the side chains determine the isotropization temperature and the temperature range of the hexagonal columnar mesophase.

Because of the highly ordered columnar structures these soft materials outperform many photo-conductive polymers (e. g. in terms of charge transport or short-lived excitonic response). Therefore, they have a high potential in molecular electronic devices and are promising to fulfill the need for effective, low-cost, portable and disposable elements such as tunable organic light-emitting diodes, thin film field-effect transistors or photo-voltaic chips.

Here broadband dielectric spectroscopy is applied to investigated the molecular mobility of model systems of discotic liquid crystals like pyrenes and triphenylen derivatives.

## Results and Discussion

Figure 1 presents the dielectric loss of pyrene1,3,6,8-tetracarboxylic tetra(2-ethylhexyl) ester (Py4CEH in) dependence on frequency and temperature in a 3D representation. Two relaxation processes can be identified as peaks in the dielectric loss. At low temperatures (or high frequencies) a so called β-relaxation takes place. At higher temperatures (or lower frequencies) a further process is observed which will further be called α-relaxation. This relaxation process takes place in both the plastic crystalline and the columnar liquid crystalline phase. At the phase transition the relaxation process changes in its temperature dependence.

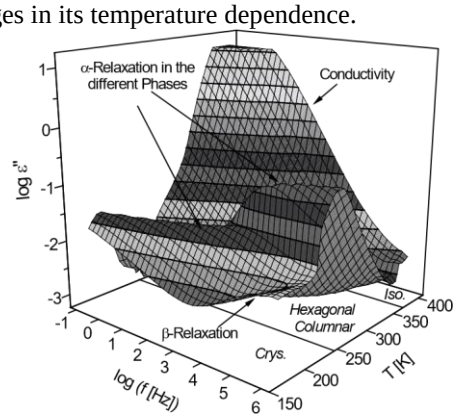


*Figure 1: Dielectric loss of Py4CEH in dependence on frequency and temperature during the cooling in a 3D representation [1].*

All processes are analysed in detail and discussed.

## Conclusions

The process observed at lower were assigned to localized fluctuations. Its temperatures dependence follows the Arrhenius equation. The process at higher temperatures follows the Vogel/Fulcher/Tammann law and was related to a α-relaxation. Its assignment is in agreement with results obtained by specific heat spectroscopy.

## References

[1] C. Krause et al. Soft Matter **2012**, 8, 11115.

## Acknowledgements

The financial support of DFG is highly acknowledged.

# Vibrational energy harvester based on transverse piezoelectric effect in piezoelectrets

G. M. Sessler[1] and X. Zhang[2]

g.sessler@nt.tu-darmstadt.de

[1]Institute for Telecommunications, Technische Universität Darmstadt, Merckstr. 25, 64283 Darmstadt, Germany [2]School of Physics Science and Technology, Tongji University,Siping Road 1239, Shanghai 200092, China

**Abstract:** Vibrational energy harvesters utilizing the transverse piezoelectric effect in piezoelectrets have been miniaturized and improved. These harvesters are based on parallel-tunnel piezoelectrets consisting of fused fluoroethylene propylene (FEP) films. Typically, with a total volume of 0.8 cm$^3$, a seismic mass of 0.3 g, a harvester resonance at 58 Hz, and a vibrational acceleration of 1 *g* (9.81 m/s$^2$), a peak output power at resonance of about 100 µW has been achieved.

**Keywords:** Piezoelectrets, energy harvesting, FEP, vibration-based

## Introduction

Energy harvesting with piezoelectret devices depending on the transverse ($d_{31}$) piezoelectric effect has only recently been demonstrated [1]. The reason is that the common piezoelectret material, charged polypropylene (PP), while having a large longitudinal piezoelectric coefficient $d_{33}$, exhibits only a very small transverse activity. This changed with the development of layered FEP ferroelectrets with parallel-tunnel structure [2]. Such films can be designed to have large $d_{31}$ activity. Their use and performance in energy harvesters of improved and miniaturized design will be discussed in the following.

## Results and Discussion

The new harvesters are similar to a device used before [1] and shown in Fig. 1. They differ mainly by miniaturized dimensions (1×1×0.8 cm$^3$ instead of 5×1×1 cm$^3$) and reduced angle α.

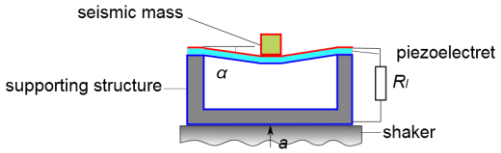


*Figure 1: Schematic view of energy harvester and shaker. The piezo- or ferroelectret is fixed on a support structure and deflected by the seismic mass due to the vibrations of the shaker* [1].

The optimal power output $P_{opt}$ into a load resistance $R_l$ at resonance $\omega_0$, due to an acceleration *a*, is given by [1]

$$\frac{P_{opt}}{a^2} = \frac{L^2\left(\frac{d_{31}}{t}\right)^2\sqrt{\frac{Ytwm^3}{L}}}{2\varsigma_\perp^2 C \sin^3\alpha}, \qquad (1)$$

where *L*, *w*, *t*, *Y*, $d_{31}$, $\varsigma_\perp$ and *C* are the length, width, thickness, Young's modulus, piezoelectric coefficient, damping coefficient, and capacitance, respectively, of the piezoelectret and *m* is the seismic mass. In Eq.(1), $R_l = 1/(C\,\omega_0)$ is assumed.

Experimental results obtained with this energy harvester using a seismic mass of 0.3 g are shown in Fig. 2. The power of 109 µW at resonance corresponds to the normalized value of the power $P_{opt}$ in Eq. (1).

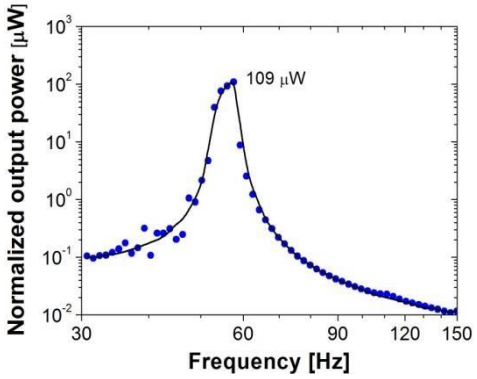


*Figure 2: Normalized power $P_n = (g/a)^2P$, where P is measured in response to an acceleration a, and g is 9.81m/s$^2$.*

## Conclusions

This power of about 100 µW with *m* = 0.3 g may be compared with the 200 µW obtained with 2 g for the previous device [1]. Considering the scaling with $m^{3/2}$ (see Eq.(1)), the new harvester exceeds the older one in performance by a factor of nine.

## References

[1] X. Zhang, P. Pondrom, L. Wu, and G. M. Sessler, *Appl. Phys. Lett.***108**, (2016) 193903.

[2] X. Zhang and Y. Wang, Proc. *IEEE 15th Inernat. Sympos. on Electrets*, Baltimore 2015, paper 2.2.

## Acknowledgements

The authors gratefully acknowledge financial support from the German DFG and the Chinese NSFC.

# Broad Bandwidth Vibration Energy Harvesters based on Wavy Fluoroethylenepropylene Electret Films

Xiaoqing Zhang [1, 2], Gerhard M. Sessler [2], Xingchen Ma [1], Yuan Xue[1], Liming Wu[1]

x.zhang@tongji.edu.cn

[1]School of Physics Science and Technology, Tongji University, Siping Road 1239, Shanghai 200092, China

[2]Institute for Telecommunications Technology, Technische Universität Darmstadt, Merckstr. 25, 64283 Darmstadt, Germany

**Abstract:** Thermally stable wavy fluoroethylene propylene (FEP) electret films were prepared by a patterning method followed by a corona charging process. A vibration energy harvester with a very simple sandwich structure, consisting of a central wavy FEP electret film and two metal electrodes, was designed and its performance was investigated. The results show that for an energy harvester with an area of 4 cm$^2$ and a seismic mass of 80g, the output power referred to 1 *g* (*g* is the gravity of the earth), resonance frequency, and 3 dB bandwidth are 1.85 mW, 90 Hz, and 24 Hz, respectively.

**Keywords:** energy harvesting, electret, wavy FEP, vibration

## Introduction

The large number of wireless communicating sensors used in the Internet of Things (IoT) makes the replacement of batteries impossible or very expensive as they are located in remote areas or harsh environments. A promising solution is to power the electronic devices by harvesting various ambient resources and converting their energy into useful electrical energy. Here, we report on vibration energy harvesting with wavy FEP electrets films.

## Results and Discussion

Negatively charged FEP films with wave-shape geometry were prepared by a patterning step followed by corona charging. Then, vibration energy harvesters with a very simple sandwich structure, as shown in Figure 1, were fabricated. One side of the wavy FEP film was metalized with an Al electrode by vacuum evaporation. A flat or wave-shaped counter electrode, facing the charged surface, was placed on top of the FEP film. The optimum output power is obtained at the resonance frequency $\omega_0$ with a matching load resistance of $R_{opt} = \frac{1}{\omega_0 C}$. It is given by the relation [1]

$$P_{out} = R_{opt} I^2 = R_{opt} \omega_0^2 Q_{rms}^2 \qquad (1)$$

where $I$ and $Q_{\mathrm{rms}}$ are the current and charge through the load resistor, respectively. As customary, $P_{out}$ is referred to an acceleration of $g$=9.81 m/s$^2$, the gravity of earth. The normalized value $P_n$ is then given by $P_n = P_{out}(^g/_a)^2$, where $a$ is the actual RMS acceleration.

Results on the normalized output power as a function of vibration frequency for the energy harvesters with flat and wave-shape counter electrode, working at matching load resistance, are shown in Figure 2. As seen in the figure, the maximum normalized output power of 1.85 mW is obtained from the energy harvester with a wave-shaped counter electrode. This energy harvester has a resonance frequency of 90 Hz and a relatively broad 3 dB bandwidth of 24 Hz.

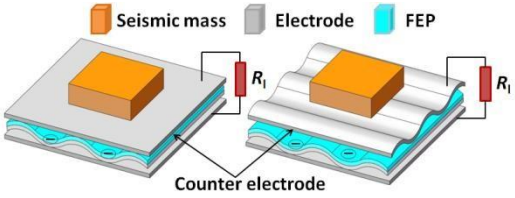


*Figure 1: Schematic of the energy harvesters based on wavy FEP electret films.*

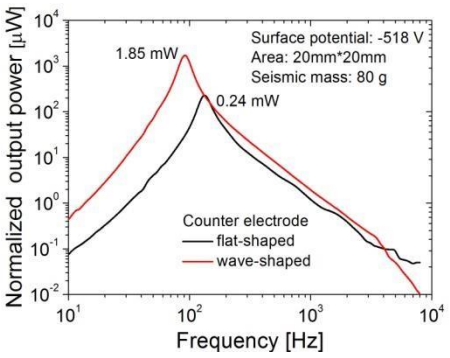


*Figure 2: Normalized output power as a function of frequency.*

## Conclusions

Compared with the energy harvesters with a flat counter electrode, the devices based on wavy FEP electret films with a wave-shaped counter electrode can generate more power. This could be due to the larger deformation of the structure under force. The output power of few mW from the energy harvester is sufficient to power some electronic devices.

## References

[1] P. Pondrom, J. Hillenbrand, G. M. Sessler, J. Bös, and T. Melz, *Appl. Phys. Lett*. **104**, (2014)172901.

## Acknowledgements

The authors gratefully acknowledge financial support from the Natural Science Foundation of China (NSFC) and the Deutsche Forschungsgemeinschaft (DFG).

# Piezo-Tubes

Ryszard Kacprzyk[1], Agnieszka Grygorcewicz

ryszard.kacprzyk@pwr.edu.pl

[1]Wroclaw University of Science and Technology, Wyb. Wyspianskiego 27, 50-370 Wroclaw, Poland

**Abstract:** The piezoelectric effect in PTFE tubes submitted to PD charging in dc electric field was described. The piezoelectric coefficient $d_{33}$ measured in static conditions was found to be on the level of 40±10 pC/N. The fabric made of PTFE tubes and submitted to PD charging exhibit similar piezoelectric properties like the individual tube. Time stability of the piezo-coefficient $d_{33}$ was also examined and confirmed its technical utility.

**Keywords:**, piezoelectric effect, PTFE tubes, PTFE fabric.

## Introduction

Non-uniform dielectric structures with built-in space charge exhibit piezoelectric properties [1-4]. The "hard"-"soft"-"hard" layers sandwich structure can be realized in the form of elastic dielectric tube – see Fig. 1. The "hard" layers are made of the basic polymer and are created by the walls of the tube R.

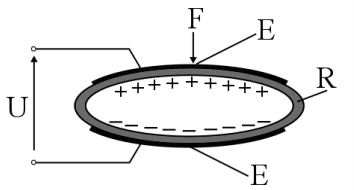


*Figure 1. Model of a piezo-tube transducer*

The "soft" layer is realized as the air gap limited by the bent part of the tube wall [5]. After bipolar charge (+) and (-) deposition (piezo-activation), the tube equipped with electrodes E converts the applied force F into output voltage U. Such a tube may be used as an elementary piezo-transducer or processed into structures like fabrics.

## Samples, Measurements and Results

The commercial PTFE tubes, with external diameter 2.0±0.2 mm and wall thickness 300±50 μm were flattened to get finally the tube with cross-section shown in Fig. 2. The samples-tubes were

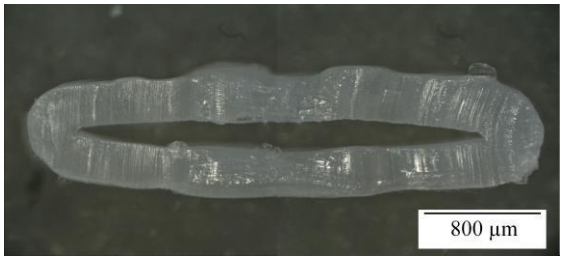


*Figure 2: Cross-section of the flattened PTFE tube.*

equipped with metallic electrodes (on both sides), placed in the flat electrode system immersed in transformer oil and polarized (voltage 0 - 20±1 kV/30±5 s). The piezoelectric coefficient $d_{33}$ was measured using static method [4]. The applied sampling pressure was equal 50 kPa. The equivalent voltage, measured across the inner surface of the activated tube (after catting and straightening the tube), was on the level of $U$ = (±) 1000±500 V and confirmed bipolar distribution of the charge deposited during PD discharges in the air gap (like that shown in Fig. 1).

Using the PTFE tubes as a yarn the fabric was prepared and submitted to piezo-activation process in the same system and in conditions like that used for the tubes. The average value of the $d_{33}$ coefficient for the fabric was found to be on the same level, i.e. 40±10 pC/N - like the measured for individual tubes. The $d_{33}$ value decreases (about 30%) within the first 10 days, when the samples were stored in ambient conditions. After that no any following changes were observed.

## Conclusions

Elastic dielectric tubes with bipolar charge distributed on their inner surface exhibit piezo-electric effect. The simplicity and the new shape of the piezoelectric transducer (tube-like) offers new space for application of the phenomenon (e.g. textronics) as well as new processing abilities for some of polymers exhibiting satisfactory electret properties.

## References

[1] Hilczer B., Małecki J. Electrets. Amsterdam: Elsevier, **1986**.

[2] Hillenbrand J., Sessler G M., *IEEE Trans. Diel. Electric. Insulat.* **2000**, 7, 537-542.

[3] Gerhard-Multhaupt R. *IEEE Trans. Diel. Electric. Insulat.* **2002**, 9, 850-859.

[4] Kacprzyk R., Kisiel A. *J. Electrostatics.* **2013**, 71, 400-402.

[5] Kacprzyk R, Grygorcewicz A., Patent pending (31.03.2017)

## Acknowledgements

This work was carried out as a statutory project supported by the Ministry of Science and Higher Education, Warsaw, Poland.

# Electret-Like Elastomer Membrane for Large Scale Energy Harvesting of Low Density Energy Sources

Daniela Wirthl, Robert Pichler, Siegfried Bauer, Reinhard Schwödiauer

daniela.wirthl@jku.at

Department of Soft Matter Physics, Johannes Kepler University Linz, Altenbergerstraße 69, 4040 Linz, Austria Altenbergerstrasse 69, 4040 Linz, Austria

**Abstract:** Ambient energy sources with low energy densities could be converted into electricity with large scale special purpose converter systems. This work presents a simple concept for a suitable electret-based electrostatic converter. The converter is a capacitive charge pump and it uses a charged electret-like elastomer membrane which enables operation without an initial bias voltage supply. The converter is capable of working at low frequencies (≤ 1 Hz) with a very low mechanical input energy of about 9 µJ/cm². The conversion efficiency is 63 % per conversion cycle.

**Keywords:** dielectric elastomer, electret, dielectric elastomer generator, energy harvesting

## Introduction

Besides wind and solar energy, many other ambient energy sources are readily available in various forms, e.g. with small temperature or pressure gradients, gentle movements of air or water, or small mechanical deformations, etc.; but these energy sources are at present largely unused. With this work, we propose and demonstrate an electrostatic energy converter (EEC) with an acryl elastomer membrane suitable for an efficient largescale mechanical to electrical energy conversion of ambient low density energy sources. Our simple not optimized EEC system, illustrated in Fig. 1(a-c).

## Results and Discussion

The relaxed elastomer membrane which is covered with a carbon grease electrode, was electrically stressed by applying a dc-voltage of -950 V for approx. 10 min. The high voltage across the 36 µm thin elastomer causes a space charge injection into the membrane surface from the inner metal electrode. After the dc-voltage had been switched off a surface charge density in the order of $\sigma \approx 10^{-8}$ C/cm² could be observed. A low pressure increase of about 100 Pa lifts the membrane and increases the voltage of the capacitive EEC system. The voltage difference drives the charge on the electrodes into a reservoir capacitor. This reservoir capacitor is connected and disconnected to the EEC via high voltage relays. The consecutive inflation and deflation of the surface charged electret-like elastomer membrane pumps further charges into the reservoir capacitor. This results in a successive increase of the reservoir voltage as shown in Fig. 1(d). A maximal output energy of ca. 280 µJ was converted after 15 sec of operation. At this time, a reservoir voltage of 354 V and a total charge of 7.6 µC has been accumulated, which gives a total energy of 1.35 mJ.

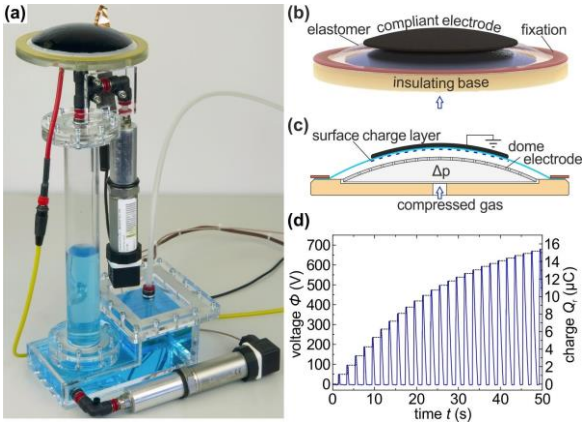


*Figure 1: The EEC mounted to a custom-made water-column volumeter used for pV - measurements. (a) Electrostatic elastomer converter in an actuated state of operation. (b) Cross-sectional view of the EEC showing a surface charge layer on the inner side of the elastomer membrane. (c) Transient diagram of the electrode voltage, $\phi$, (continuous blue), and the reservoir voltage (dashed black), together with the reservoir charge, $Q_r$. (d)*

## Conclusions

Our demonstration system is capable of converting low mechanical input energy with a remarkable high efficiency (> 60 %) into electrical energy. We expect a fully optimized system to deliver an electrical energy of more than 10 µJ/cm² per conversion cycle with a conversion efficiency beyond 80 %.

## Acknowledgement

The authors are grateful for the support of this work by the ERC within the Advanced Investigators Grant 'Soft-Map', by the Horizon 2020 project 641334-WETFEET, and by the FWF (P22912-N20).

# Computational tools for a refined multi-model analysis of TSD spectra

J. van Turnhout

j.vanturnhout@tudelft.nl

Dept. Materials Science and Engineering, Delft University of Technology,
Mekelweg 2, 2628CD Delft, The Netherlands

**Abstract:** Four options will be discussed. First, all sort of models from the ω and t domain have been converted. The conversion of operational permittivities is likewise possible. Spectral functions can be recruited as well. The methods can be applied for the analysis of all kind of thermally stimulated phenomena.

**Keywords:** modelling TSP, ω and t-conversion, spectral analysis, discharge kinetics

## Introduction

TSD measurements provide essential information about the charge storing behaviour of a material. The data are obtained easily and in a short time. This makes TSD attractive. However, it is a non-isothermal technique and so its spectra can be analysed less simply than those of DRS. We will show that the analysis can be facilitated a lot by invoking special mathematical tools. We have studied 4 options, cf. Fig.1.

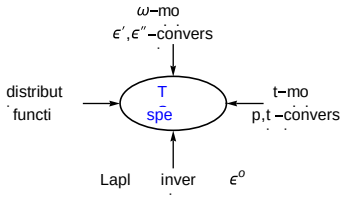


*Fig.1: All 4 routes to model TSD data can be done with one-liners and are easy to implement.*

## Results and Discussion

Fig. 1 shows the modelling of the thermally stimulated charge decay by conversion of the 2 parameter t-response of Dissado-Hill (see e.g. [1]). The lower the shape factors m and n, the broader the underlying distribution. Such distributions contain therefore many slowly reacting dipoles and/or slowly moving charges, which will be retained up to high temperatures.

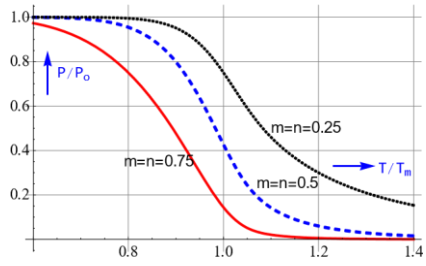


*Fig.2: TSD charge spectra for the DH-model.*

Fig.2 depicts the current spectra for KWW and CC for the same shape factor a=0.5. The KWW current drops earlier, because the KWW distribution contains less slow dipoles and/or charges. The CC spectra were obtained by use of the Mittag-Leffler function. This spectrum can also be acquired by the Laplace transform inversion of the operational permittivity $\varepsilon^0$ of Cole-Cole.

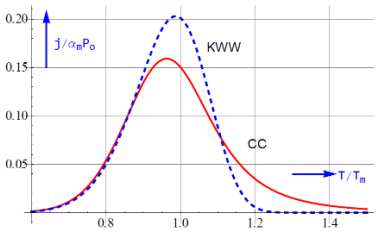


*Fig.3: Difference between the TSD of KWW and CC.*

Fig.4 gives 3 current spectra for the Gaussian log-normal distribution. This distribution becomes sharper if the shape factor b grows. This results in a narrower peak if b increases.

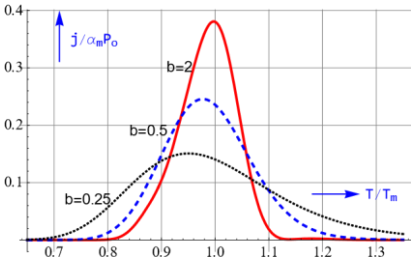


*Fig.4: Current spectra of Gauss' distribution.*

## Conclusions

TSD spectra are vital for assessing whether a material can store charges for a long time. We have extended the analysis to all sorts of response functions. In this way TSD spectra can be fitted to the most appropriate model. The modelling becomes more reliable by applying all-in-1 fitting [2]. By doing this for TSD spectra from 2 or more heating rates the mean activation energy can also be recovered more precisely.

## References

[1] F. Kremer, A. Schönhals, eds.: Broadband dielectric spectroscopy, Springer: Berlin 2003.

[2] J. van Turnhout, *Front. Chem.* **2016**, doi: 10.3389 /fchem.2016.00022.

## Acknowledgements

The author likes to thank Prof. J. Sietsma and Prof. I. M. Richardson for allowing him a stay in the Dept. of Materials Science and Engineering at the TU-Delft.

# TSDC study of electrical aging of polybutylene terephtalate (PBT)

Doulacha Naima[1], Souilem Souad[1], Khemici Mohammed Wafik[1,2], Azeddine Gourari.[1]

nkhemicidoulache@gmail.com

[1] University of Sciences and Technology Houari Boumediene (USTHB)
BP 32, El-Alia, Bab Ezzouar 16111, Algeria
[2] Department of Physics, Faculty of Sciences,
University of M'Hamed Bougara, Boumerdes, 35000, Algeria

**Abstract:** The aging notion describes one or more modifications of a polymer when it is submitted to stresses. In this work, we are particularly interested to the electrical aging of polybutylene terephthalate (PBT) by the thermally stimulated depolarization currents (TSDC) method. This study consists in submitting our sample to different electric fields $E_{ea}$, with intensities lower than the breakdown field of the material during different times

$\Delta t_{ea}$. The obtained results revealed a decrease in the molecular mobility of the material, its activation energy and its fragility index. Also, the effect of aging increases with $E_{ea}$ when the duration of the aging is constant.

**Keywords:** TSDC technique, PBT, Breakdown, aging

## Introduction

In view of its multiple uses, PBT occupied an essential place in the polymer industry (electronics, communi-cations, fiber optics etc…), which requires a good knowledge of its properties and their evolutions during the aging of the material [1,2]. It is in this perspective that we propose, in this frame work, to study by the TSDC technique the aging of PBT under the effect of an electrical stress of different intensities during different durations.

## Results and Discussion

PBT is a semi-crystalline thermoplastic of the aroma-tic polyester family. The samples of PBT in the form of thin films with 0.3mm thickness, were electrically aged according to the following protocol: Placed between the plates of a plane capacitor, the sample, was submitted to an electric field $E = 4 \times 10\ V/m$ for durations varying from 0 to 3 hours. For each dura-tion, the TSDC spectrum was recorded as well as its decomposition into elementary spectra by the thermal sampling method [3]. In a second step, we fixed the aging duration $\Delta t_{ea}$= 90min, then we varied the inten-sity of the applied electrical field $E_{ea}$.

Once the sample was aged, the TSDC spectra were recorded.

We represent as example, in figure 1, the TSDC spec-tra obtained for a field $E = 4 \times 10\ V/m$ applied during different times. The maximum intensity of the TSDC peak decreases when $\Delta t_{ea}$ increases (inset: upper right corner of figure 1). On the other hand, the temperature position of the peaks is not affected by this aging. This evolution reveals a decrease in the molecular mobility which is directly linked to the polarization which is none other than the area under the TSDC peak.

The decomposition into elementary spectra, revealed a decrease into the activation energy, which varies from the value of 2.3eV for the non-aged PBT to 1.7eV for an aging time of 2 hours (inset: lower right corner of figure 1); a reduction in the fragility index m of the material is also observed.

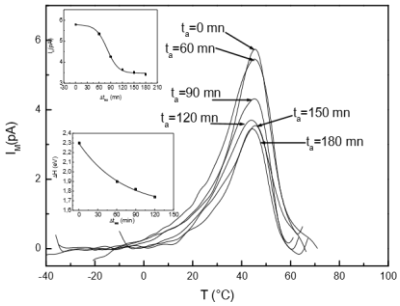


*Figure 1: TSDC spectra of aged PBT under an electrical filed of* $4 \times 10^6$ V/m *during different times. (insets: maximal currents end activation energy versus the aging times* $\Delta t_{ea}$ *).*

## Conclusions

We have been able to highlight the effect of electrical aging of PBT by the TSDC technique. This study shows a decrease in the molecular mobility due to a decrease in the free volume. The study of the fine structure of peaks revealed a decrease in the activation energy and the fragility index of the material when the aging time increases

## References

[1] Souilem, S ; Doulache, N ; Khemici, M.W ;Gourari, A, Int. J. Polym. Anal. Charact 2014, 14(2), 175– 188.
[2] Lahoud, N. Phd diss, 2009. Paul sabatier University, Toulouse, France.
[3] Khemici, M.W;Gourari. A; Doulache, N, Int. J. Polym. Anal. Charact 2009, 14, 322-335.

# Investigation of relaxation processes in P(VDF-TrFE-CFE) terpolymer films by means of thermally stimulated depolarization and dielectric relaxation spectroscopy

Anna A. Gulyakova[1], Yuri A. Gorokhovatsky[1], Thulasinath Raman Venkatesan[2], Peter Frübing[2], Reimund Gerhard[2]

Anne_Rut@mail.ru

[1]Department of General and Experimental Physics, Herzen State Pedagogical University, Moika River Embankment 48, 191186 St. Petersburg, Russia

[2]Department of Physics and Astronomy, Faculty of Science, University of Potsdam, Karl-Liebknecht-Strasse 24-25, 14476 Potsdam, Germany

**Abstract:** Relaxation processes in films of a relaxor-ferroelectric poly(vinylidene fluoride-trifluoroethylene-chlorofluoroethylene) (P(VDF-TrFE-CFE)) terpolymer with a monomer (VDF/TrFE/CFE) ratio of 55.4/37.2/7.3 (mol%) are investigated. By means of dielectric relaxation spectroscopy (DRS) and thermally stimulated depolarization current (TSDC) measurements it is shown that the dominant relaxation process which causes the strong increase of permittivity compared to PVDF is of dipolar origin and shows Vogel-Fulcher-Tammann behaviour, indicating a close relation to the α relaxation in PVDF.

**Keywords:** terpolymers, ferroelectric relaxor polymers, vinylidene fluoride, trifluoroethylene, chlorofluoro-ethylene, dielectric relaxation spectroscopy, thermoactivational spectroscopy.

## Introduction

Considerable attention is attracted currently to the investigation of ferroelectric polymers due to their possible application for electromechanical devices. Flexibility, easy processability and conformation to various shapes constitute important advantages compared to inorganic ferroelectrics.

Polyvinylidene fluoride (PVDF) and its copolymer with trifluoroethylene P(VDF-TrFE) exhibit relatively low dielectric constants, small field-induced strain, and large polarization-versus-field hysteresis. However, P(VDF-TrFE) can be converted into a ferroelectric relaxor by introduction of chemical defects such as chlorofluoroethylene (CFE). The resulting terpolymer P(VDF-TrFE-CFE) shows significant enhancement of the electromechanical response and the dielectric constant as well as vanishing hysteresis effect [1-3].

## Results and Discussion

Free-standing terpolymer films with the composition VDF/TrFE/CFE 55.4/37.2/7.3 mol% and a thickness of 60 μm have been prepared via drop-casting on glass substrates from a solution in acetone. The DRS measurements ($10^{-1}$ to $10^{7}$ Hz, -60 to 100 °C) exhibit the typical ferroelectric-relaxor behaviour of the dielectric constant: a huge permittivity step with a local maximum of the real permittivity ε' of about 50 (at 26 °C, 1 kHz) is observed after passing the glass transition of PVDF at about –40 °C. Its position shifts progressively towards higher temperature with increasing frequency. However, the corresponding dielectric-loss peak is not uniform. Two processes are visible in the loss-versus-temperature plot which merge at higher frequencies. They were separated by application of Havriliak-Negami fits to the loss-versus-frequency dependence. The high-temperature (HT) process below 1/T= 0.004 $K^{-1}$ (–23 °C) shows Vogel-Fulcher-Tammann (VFT) behaviour. The VFT fit yields a glass-transition temperature of –43.0 °C which represents the glass transition of the PVDF component. Above 1/T = 0.004 $K^{-1}$ another relaxation with Arrhenius behaviour (activation energy 0.45 eV) of still unknown origin appears.

The TSDC curves (after poling at 60 °C for 10 min with 3.33 to 16.7 MV/m, heating rate 4 K/min) show a peak at about 0 °C which corresponds to the HT process in DRS. The linear dependence of the peak height on the poling field indicates a dipolar origin. Two further TSDC peaks around 40 and 60 °C are probably caused by space charges.

## Conclusions

The P(VDF-TrFE-CFE) terpolymer exhibits a strong dielectric relaxation. Its dipolar origin and its co-operative character are verified by DRS and TSDC mea-surements. However, the additional relaxation processes are not yet fully understood and thus require further investigation.

## References

[1] F. Bauer *et al.*, IEEE Trans. Diel. El. Ins., **13**, 1149-1154 (2006).
[2] F. Bauer, Appl. Phys. A, **107**, 567-573 (2012).
[3] S. Zhang *et al.*, J. Appl. Phys., **99**, 044107 (2006).

## Acknowledgements

The authors are indebted to Piezotech Arkema for kindly providing the P(VDF-TrFE-CFE) terpolymer. A. A. G. is indebted to the Russian Ministry of Education and Science and the German Academic Exchange Service (DAAD) for granting a joint research fellowship.

# Post-annealing effect on the parylene C electret thermal stability

Achraf Kachroudi, Clara Lagomarsini and Alain Sylvestre

achraf.kachroudi@g2elab.grenoble-inp.fr

Univ. Grenoble Alpes, CNRS, Grenoble INP*, G2Elab, F-38000 Grenoble, France

**Abstract:** Post-annealing effect on the charge retention and thermal stability of electrets based on parylene C is investigated. Parameters allowing assessment of electrets in terms of technical applications are the charge lifetime and its equivalent surface potential. Using surface potential decay and thermally stimulated potential decay methods, post-annealing applied to parylene C allow revisiting capabilities of such materials like electrets at high temperature.

**Keywords:** Parylene C, electret, thermal stability, surface potential decay, polymer.

## Introduction

For some applications, polymer based electrets from implantation of electric charges by corona discharge should present a high thermal stability. Parylene C polymers are popular polymers now used in various fields of applications. This polymer was already proposed as electret but its performances don't appear as satisfactory particularly at high temperature when they reach their glass transition $T_g$ [1]. In this work, a post-annealing process on parylene C was proposed that appears as a simple method for the electret stability enhancement versus temperature changes.

## Results and Discussion

The *6µm* parylene C films were grown by chemical vapor deposition on aluminum plates. Annealing of parylene C was carried out during *6* hours at *60°C*, *90°C* (at $T_g$) and *150°C* respectively. After annealing, the samples were cooled down to *25°C* (cooling rate of *1°C/min*). Then, ions were injected by corona discharge with an imposed surface potential of *-1000V* following recommendations of Genter *et al* [1]. Afterwards, samples were stored during three weeks up to obtain a stable value of surface potential decay (SPD). After that, the surface potential decay was measured during a heating rate of *2°C/min* up to *200°C*. Figure 1 presents the normalized surface potential of the samples $V_S/V_0$ where $V_S$ is the surface potential at the temperature of measurement and $V_0$ is the initial value (e.g. at *25°C*). As observed, the range of stability for SPD is widened at higher annealing temperatures. In previous experiments (unpublished), crystallinity ratio and crystallites size increase both with the increase of annealing temperature. The decrease of thermally stimulated discharge (TSD) is in the vicinity of $T_g$ and the mobility of long chains of polymer are thus favourable for the ionic conduction. For higher annealing temperatures, long chains are more restricted by crystallites thus explaining a shift to higher temperatures of TSD. A singular decrease is observed from *110°C* for the as-deposited and *150°C* annealed samples. Complementary experiments are in progress to understand this result. More-over, the full disappearance of TSD is observed for the *150°C* annealing sample while *20%* of charges are always present for other samples at high temperature.

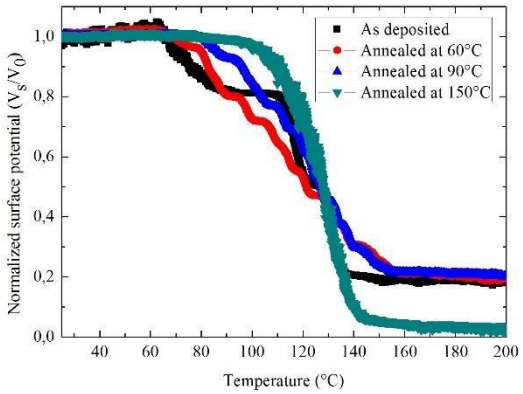


*Figure 1: Normalized thermally stimulated potential decay from 25°C to 200°C with a heating rate of 2°C/min for as-deposited and annealed parylene C electrets.*

## Conclusions

Post-annealing process carried out on parylene C films contributes clearly to the enhancement of the electret thermal stability. This is a promising result for the optimization of energy harvesting devices based on electret parylene C [2].

## References

[1] S. Genter, O. Paul, *PowerMems*, **2012**, Atlanta, GA, USA, December 2-5.

[2] C. Lagomarsini, A. Sylvestre, C. Jean-Mistral, S. Monfray in: *IEEE Intern. Conf. on Dielectrics*, Montpellier, **2016**, 16251064.

## Acknowledgements

The authors acknowledge the financial support of the ANR SEASEA and Région Rhône-Alpes (France), in the framework of the program "Communautés de Recherche Académique (ARC)" (grant No. 04, year 2014).

# Space charge generation at ITO/organic semiconductor interface and oxygen effects

R. M. Faria[1], D. J. Coutinho[2], G. C. Faria[1], and H. von Seggern[3]

faria@ifsc.usp.br

[1]São Carlos Institute of Physics, University of São Paulo, Av. do Trabalhador São-carlense 400, 13560-970, São Carlos, Brazil

[2]Federal University of Technology - Paraná, Rua Cristo Rei 19, 85902-490, Toledo, Brazil.

[3]Institute of Materials Science, Technische Universität Darmstadt, Alarich-Weiss-Straße 2, 64287, Darmstadt , Germany

**Abstract:** The alignment between the Fermi level of a film of poly(3-hexylthiophene) and the work function of ITO electrode generates an interfacial space charge of holes in an ITO/P3HT/Ag device immersed in inert atmosphere. The electrostatic attraction at the interface is overcome by a growing electric field and is swept out of the P3HT film, resulting in a electric current peak during CELIV measurements. This effect is erased when the device is exposed to oxygen atmosphere, but the action of the oxygen leaves the P3HT p-doped, generating a different CELIV peak. A quantitative analysis related with the dynamics of both peaks is carried out.

**Keywords:** Poly(3-hexylthiophene), dark-CELIV, space-charge, build-up time, oxygen doping.

## Introduction

Space-charge built-up at the ITO/P3HT interface has been investigated, under nitrogen and air atmospheres, using the charge extraction by linearly increasing voltage (CELIV) technique in the dark. It is demonstrated that this space-charge is extracted during the initial CELIV ramp When exposed to oxygen, this interfacial space charge is destroyed, and concomitantly the P3HT is positively doped due to electrons transfer from the phenyl rings to oxygen molecules[1].

## Results and Discussion

Fig. 1 shows CELIV transient measured from an ITO/P3HT/Ag device, in which the first measurement shown in Fig. 1a was carried out under a nitrogen atmosphere (peak N)[2]. Figures 1b to 1d are recorded at different exposure times to air (peak O). Peak N differs from a standard CELIV because it initiates only when the voltage reaches a value of approximately 0.6 V. Such a result is due to the built-in potential originated at the P3HT/ITO interface. CELIV measurements carried out under reverse voltage did not show any current extraction ($\Delta j$). When the device is exposed to air (or dry oxygen) peak N decreases continuously in time until its complete extinction. Concomitantly a new CELIV peak arises (peak O), whose current maximum is centered at $t_{max}$ = 7 µs (Figs. 1b to 1d). The amount of charge of peak N decreases and disappears after a few hours of air exposure, while the amount of charge from peak O continues to grow and saturates at ~ 0.4 nC after 1200 minutes.

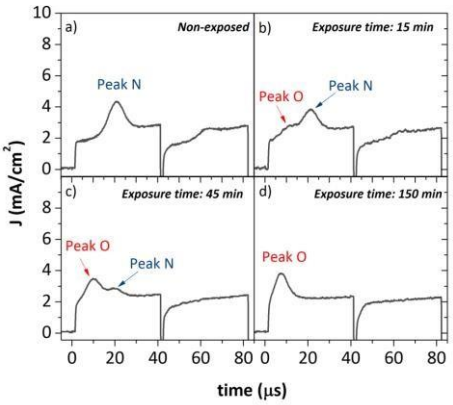


*Figure 1: a) CELIV measurements carried out under nitrogen; b), c), and d) evolution of CELIV response when the device is under air atmosphere.*

## Conclusions

We conclude that peak N is caused by the interfacial space charge, which disappears under the action of oxygen, and that peak O is due to the extraction of holes from the doped P3HT. The recovery time of both peaks are investigated.

## References

[1] M. S. A. Abdou, F. P. Orfino, Y. Son, and S. Holdcroft, J. Am. Chem. Soc.119, 4518-4524 (1997).

[2] Douglas J. Coutinho, Gregório C. Faria, Roberto M. Faria, Heinz von Seggern, Organic Electronics 26 (2015) 408–414.

## Acknowledgements

The authors are grateful to the agencies FAPESP, CNPq and MCT/INEO for funding.

# A tribute to Wolfgang Eisenmenger: From phonon spectroscopy to piezoelectrically generated pressure pulses

Siegfried Bauer [1], Reimund Gerhard [2]

Author's e-mail addresses: sbauer@jku.at and reimund.gerhard@uni-potsdam.de

[1]Soft Matter Physics, Johannes Kepler University Linz, Altenbergerstrasse 69, A-4040 Linz, Austria
[2]Applied Condensed-Matter Physics, Institute of Physics and Astronomy, Faculty of Science, University of Potsdam, Karl-Liebknecht-Strasse 24-25, 14476 Potsdam-Golm, Germany

**Abstract:** In 1982, Eisenmenger and Haardt proposed piezoelectrically generated pressure step (PPS) waves for probing charge and polarization distributions in space-charge and dipole electrets. Over the last 35 years, the PPS method has been successfully employed to measure e.g. charge-induced polarization zones in piezoelectric polymers, spread-out space charge in fluoropolymer electrets or charge-induced depolarization zones near the electrodes of poled polymers. The operating principle and several older and newer examples of PPS experiments and results, as well as conclusions drawn from them, will be briefly described and discussed.

**Keywords:** non-destructive probing, space-charge profiles, dipole-polarization zones, electric-field distributions

## Introduction

Wolfgang Eisenmenger was a pioneer in phonon spectroscopy, high frequency ultrasound and shock wave generation. Based on his deep knowledge in high frequency ultrasound he invented pressure wave propagation methods in the 1980s to probe space-charge and dipole-polarization distributions in thin polymer film electrets with µm resolution [1]. His timely research fitted well to the rapid development of several new techniques for investigating electric field and polarization profiles in thin film electrets (reviewed and compared in [2]). Main applications were in the analysis of polarization profiles and space-charge compensation of polarization zones in ferroelectric polymers such polyvinylidene fluoride (PVDF) and some of its copolymers.

## Results and Discussion

Here we will show that piezoelectrically generated pressure step (PPS) waves are still a highly useful alternative to Laser-Induced Pressure Pulses (LIPPs), pulsed electro-acoustic (PEA) methods and thermal probing techniques. The original setup for the PPS method [2] is shown in the top part of Figure 1: A high-voltage electrical square-wave pulse is used to drive an x-cut quartz plate. In order to avoid cross-talk, the step wave launched by the second acoustic pulse upon re-expansion of the quartz crystal is employed for probing (bottom part of Figure 1). Older and newer PPS measurements and results are reviewed and compared with acoustical and thermal high-resolution probing experiments on thin polymers [3,4]. It is shown that PPS waves are particularly useful for

- directly probing dipole-polarization profiles
- detecting broad or uniform charge distributions,
- achieving high signal-to-noise ratios, and
- *in-situ* probing during high-field poling.

PPS experiments are in excellent agreement with other charge and polarization profiling techniques. Verifying optical second harmonic generation experiments on partially poled ferroelectric polymers demonstrated the wide usefulness well beyond electret research [5].

## Conclusions

Together with advanced data-handling devices and piezoelectric pressure-step or -pulse generators, the PPS method still provides unique opportunities for the high-resolution probing of polarization zones and charge distributions during and after poling.

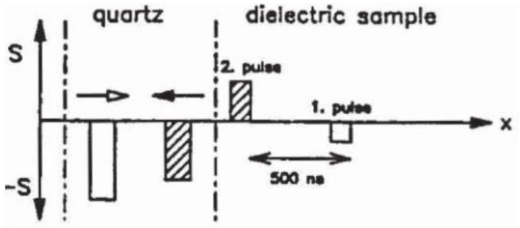


*Figure 1: Schematic drawing of the PPS method with a proposed scheme for selecting the most suitable pressure step from the piezoelectrically generated acoustic waves; original diagram from Reference [1].*

## References

[1] W. Eisenmenger and M. Haardt, *Solid State Communications* **1982**, Vol. *41*, pp. 917 – 920
[2] R. Gerhard(-Multhaupt), *IEEE Trans. Electr. Insul.* **1987**, Vol. *EI-22*, pp. 531 – 554
[3] S. Bauer-Gogonea and S. Bauer. *IEEE Trans. Diel. Electr. Insul.* **2003**, Vol. *10*, pp. 883-902
[4] R. Gerhard(-Multhaupt), M. Haardt, W. Eisenmenger, G. M. Sessler, *J. Phys. D: Appl. Phys.* **1983**, Vol. *16*, 2247 – 2256
[5] S. Bauer, G. Eberle, W. Eisenmenger, and H. Schlaich, *Opt. Lett.* **1993**, Vol. **18**, pp. 16-18

# Surface Fluorinated Semiconductive Electrodes for Space Charge Injection of Polyethylene under DC High Voltage

Mingshu Lv[1], Yewen Zhang[1,2*], Zhenlian An[1], Feihu Zheng[1]

*Email: yewen.zhang@tongji.edu.cn

[1]Department of Electrical Engineering, TongJi University, Shanghai 201804, China
[2]Shanghai Key Laboratory of Special Artificial Microstructure Materials and Technology, Department of Physics, TongJi University, Shanghai 200092, China

**Abstract:** Polyethylene（PE) has been widely used as insulating material in high voltage direct current（HVDC) power transmission systems. However, in the process of long-standing operation under the working voltage, space charge will gradually accumulate in the insulation and cause severe field distortion, which may finally result in dielectric breakdown. Therefore, study on restraining space charge injection from the electrode is of great significance. Considering that properties of electrode dielectric interface play a significant role in the injection, accumulation, and migration of space charge. In this paper, a novel method is proposed that we fluorinate the surface of electrode to restrain the injection of space charge.

**Keywords:** space charge, semi-conductive electrode, direct fluorination, polyethylene

## Introduction

Polyethylene insulation material has been widely used in the field of high-voltage power transmission system. However, space charge will gradually accumulate in the polymeric insulation under high DC electric field, which is generally claimed to be the main factor accelerating degradation of the polymeric insulation due to local electric field enhancement [1-2]. In this paper, a tentative method by modifying the properties of semiconducting electrodes is proposed for suppressing space charge injection.

## Results and Discussion

The semiconducting electrodes are attached to the PE plate by hot-pressing whose thickness is 0.8mm. There are two kinds of semiconducting electrodes. One kind of electrode is non-fluorinated (original, as a reference). The other kind of electrodes is surface fluorinated in a laboratory vessel using the fluorine concentration of 12.5% F2/N2 mixture at different temperatures and 0.1 MPa for 30 minutes at 28°C. Figure 1 shows the space charge distribution in the sample attached with original electrodes and fluorinated electrodes under 32 kV high voltage at 40 °C. It can be found that the electrode fluorination will increase the same polarity charge injection of the polyethylene.

Then, we conducted the attenuated total reflection infrared spectroscopy (ATR-IR) analysis of the electrodes and polyethylene before and after fluorination as shown in Figure 2. It can be observed that a clear fluorinated layer was formed on the electrode surface after the electrode fluorination, which blocking the impurities of electrode and polyethylene surface inject to the polyethylene inside.

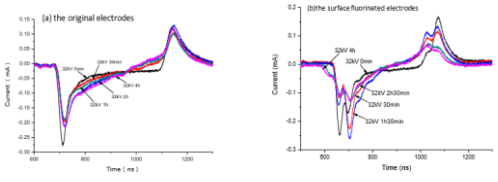


*Figure 1: Space charge distributions in samples with (a) the original electrodes and (b)the surface fluorinated electrodes.*

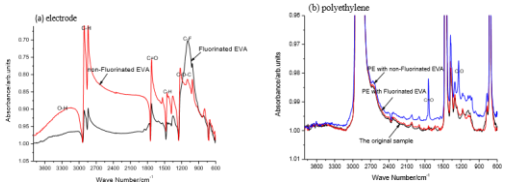


*Figure 2: ATR-IR spectra of the samples of (a) electrodes and (b) polyethylene before and after fluorination.*

## Conclusions

The impurities produce heterocharge. Reduction of heterocharge inside the polyethylene leads to the decrease of neutral with homocharge. Therefore, the injection of homocharge increases largely from the distribution of space charge by using the PWP method.

## References

[1] Y. Zhang, F. Zheng, Z. An, et al, IEEE. Electr. Insul., pp.14-25, 2012.
[2] Z. An, J. Cang, X. Chen, et al, IEEE Trans. Electr. Insul., pp.339-336, 2013.

## Acknowledgements

This work was supported by the National Natural Science Foundation of China (Grant No. 51477118).

# Measurement of space charge in thin films with high spatial resolution using Electro-Acoustic Reflectometry (EAR)

L. Hamidouche, E. Géron and S. Holé

louiza.hamidouche@espci.fr

LPEM – CNRS – PSL Research University, ESPCI-Paris – Sorbonne Universités, UPMC – Paris – France

**Abstract:** Non-destructive methods for space charge measurement have reached their limits in terms of spatial resolution. The Electro-Acoustic Reflectometry is a new method based on microwave principles and electro-elastic coupling. Excitation and measurement signals are both of electrical nature. The test on a PVDF material yields promising results. In order to apply this method on very thin insulating materials, an impedance matching-like system has first to be developed. In this talk, we expose the results so far obtained.

**Keywords:** Space charge, electro-elastic reflectometry, microwave, matching.

## Introduction

The continuous tendency towards miniaturization requires to reduce the thickness of films used in many electronic devices. Space charge distribution within films is a crucial aspect to determine their performance but the available non-destructive methods cannot be applied because they do not provide the necessary spatial resolution [1]. We recently proposed a new method called Electro-Acoustic Reflectometry (EAR) [2, 3]. It is an all electrical method based on applying various sinusoidal excitations on the sample and measuring the reflected electric signals on which the elastic resonances can be seen. The measured signal indeed depends on the electro-elastic coupling taking place inside the sample and on the dielectric losses which are due to the intrinsic capacitance of the sample. Since the capacitance along with the measurement system terminal impedance behaves like a filter (see Figure 1a), resonances above the cutoff frequency cannot be detected. Detecting resonance at high frequencies is necessary for reaching very high spatial resolution. Thus, we have first to design a system that can eliminate or at least minimize the sample capacitance effect. Generally, a variable inductor would do this task but since high frequencies are involved it is more convenient to use a variable length stub (see Figure 1b).

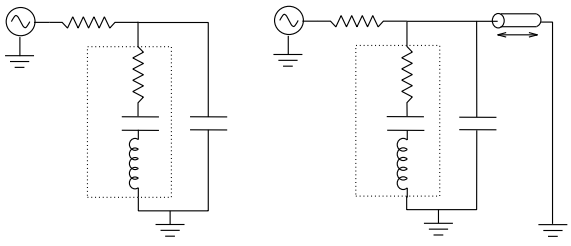

*Figure 1: Equivalent circuit of the sample. (a) The sample can be represented by a motion-branch in parallel with an intrinsic capacitance. (b) A short-circuit stub is inserted in parallel with the sample to eliminate the impedance of the capacitance.*

## Results and discussion

A test was conducted on a 9µm thick PVDF sample. Figures 2 shows the reflection coefficient amplitude $|S_{11}|$ measured with a network analyzer. We can see in Figure 2a, with the configuration of Figure 1a, that higher harmonics above the 3rd harmonic (around 390MHz) are not detected. A stub is inserted in parallel with the sample (configuration of Figure 1b) and measurements are taken for different stub lengths. The 9th harmonic (around 1.15GHz), for example, can now be well detected by varying the stub length as can be seen in Figure 2b in the range from 1 GHz to 1.25 GHz.

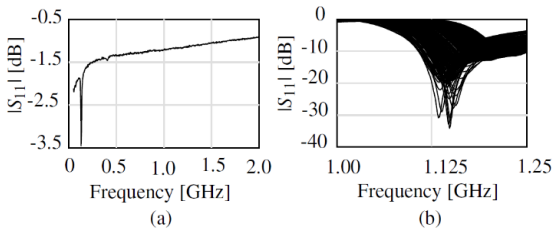


*Figure 2: Amplitude of the reflection coefficient $S_{11}$. (a) The measured raw signal before adding a stub. (b) The superposition of the measured signals with different stub lengths.*

## Conclusion

It is shown that high frequency measurements can be obtained using the matching capabilities of the EAR method. The results show the possibility to detect higher order harmonics with the means of a variable length stub. This will allow to go higher in frequency and thus be able to measure space charge within very thin samples.

## References

[1] G. Dagher , S. Holé , J. Lewiner, *in 12th International Symposium on Electrets*, pp. 204–207, 2005.

[2] L. Hamidouche, E. Géron, and S. Holé, *in 1st International Conference on Dielectrics*, pp. 46–48, 2016.

[3] L. Hamidouche, E. Géron, and S. Holé, *Dielectric and Electrical Insulation Magazine*, Accepted for publication, 2017.

# A double method for the electric field recovery in the electrets

Jean-Michel REBOUL [1], Abderezzak CHERIFI [2]

jean-michel.reboul@unicaen.fr

[1]Université de Caen Normandie, 50130 Cherbourg en Cotentin, France
[2]Université de Versailles St Quentin en Yvelines, 78200 Mantes-la-Jolie, France

**Abstract:** We present a double thermal method to measure the polarization electric field in the electrets. A temperature ramp and low frequency thermal waves are successively applied to the sample. All of these thermal excitations are sequentially produced with a controlled thermoelectric module. Two methods for retrieving the electric field from measurements are compared. The first one works in the time domain and is dedicated to the ramp heating measurements. It is a novel mathematical procedure. The second one uses the well-known frequency technique for the thermal waves measurements. The results show a good compliance of both techniques in the electric field recovery.

**Keywords:** thermal step method, LIMM, electric field recovery, electret, polarization.

## Introduction

The different thermal techniques for polarization measurement in electrets are classified by their own thermal profile excitations produced with their own specific device. For example, the sudden thermal step is usually realized with an hydraulic exchanger in the Thermal Step Method (TSM) [1]. A modulated laser produces the thermal waves of the Laser Induced Modulation Method (LIMM) [2]. The present work deals with the setting up of a procedure coupling the main advantages of the two methods above. We use a controlled thermoelectric module to successively generate a single linear temperature elevation and a low frequency saw tooth temperature variation. Theory shows that the time derivative of the current induced from a linear temperature increase corresponds to a positive regular thermal step measurement. So a thermoelectric element can achieve thermal step measurements in a different manner. By producing slow periodic heating-cooling sequence, it may work in frequency domain as LIMM experiments does.

## Theory and results

We have demonstrated in a previous work how to set up a temporal scanning function which retrieves an approximated electric field E coming from a thermal step measurement [3]. Applying simple mathematic operations to the current i(t) from a linear temperature increase measurement, the time parametric curve below draws the electric field (k denotes the thermal diffusivity).

$$\begin{cases} X = x_s(t) = \sqrt{\pi k t} \\ Y = \sqrt{t}\,\dfrac{\partial}{\partial t} i(t) \propto E\left(x_s(t)\right) \end{cases}$$

Subtracting the real and imaginary parts from each LIMM frequencies measurements leads to an equivalent procedure to plot point by point an approximated electric field profile at each abscissa $x_r$ (ω denotes the thermal circular frequency) [4]:

$$\begin{cases} X = x_r(\omega) = \sqrt{2k/\omega} \\ Y = \Re\left(i(\omega)\right) - \Im\left(i(\omega)\right) \propto E\left(x_r(\omega)\right) \end{cases}$$

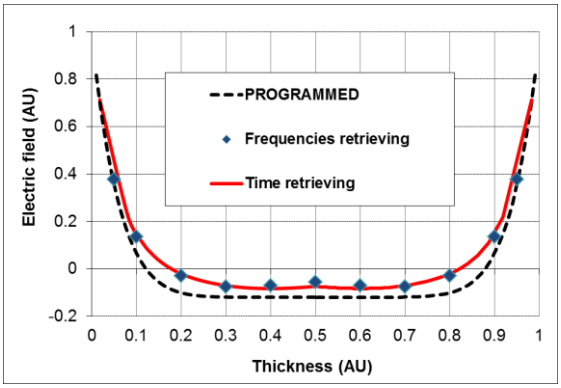


*Figure 1: Comparison of time and frequencies procedures for retrieving a programmed electric field from resp. linear heating and sine temperature measurements.*

## Conclusions

Theory and simulations confirm the equivalence of both mathematic procedures for the electric field recovery. Experimental measurements are in progress and would confirm these results.

## References

[1] A. Toureille, J.P. Reboul, P. Merle, J. Phys. III **1991**, 1, 111- 123.
[2] S. B. Lang and D. K. Das-Gupta, Ferroelectrics **1981**, 39, 1249-1252.
[3] J.-M. Reboul, Proc. of Inter. Conf. Diel. **2016**, 1, 131-134.
[4] B. Ploss, R. Emmerich, S. Bauer, J. App. Phys. **1992**, 72, 5363-5370.

# Thin functional dielectric elastomers: synthesis and applications

Dorina M. Opris[1], Simon J. Dünki[1,2], Yee Song Ko[1,2], Elena Perju[1,3], Philip Caspari[1,2], Dragan Damjanovic[2], Yauhen Sheima[1], Frank A. Nüesch[1,2]

dorina.opris@empa.ch

[1]Swiss Federal Laboratories for Materials Science and Technology Empa, Laboratory for Functional Polymers, Überlandstr. 129, CH-8600, Dübendorf, Switzerland

[2]École Polytechnique Fédérale de Lausanne (EPFL), Institut des matériaux, Station 12, CH 1015, Lausanne, Switzerland

[3]"Petru Poni" Institute of Macromolecular Chemistry of Romanian Academy, Aleea Gr. Ghica Voda, 41A, 700487, Iasi, Romania

**Abstract:** This presentation gives an overview of novel materials with high dielectric permittivity (ε ') which allow construction of actuators operated at unprecedentedly low voltages. They were prepared by a thiol-ene post-polymerization modification of polysiloxanes with polar thiols. Additionally, this presentation introduces novel piezoelectric elastomers that generate an electric signal when mechanically stressed. They were prepared by poling specially designed composites under an electric field.

**Keywords:** high dielectric permittivity, dielectric elastomer actuators, piezoelectric elastomers, sensors

## Introduction

Dielectric elastomer transducers (DETs) are elastic capacitors which can function as actuators, generators, or sensors.[1] The commercialization of this technology will significantly improve if dielectric elastomer materials with better performance were available. Of the various requirements that have to be met are an increased ε ', while maintaining all of the other dielectric and mechanical properties. Chemical modification with polar groups turned out to be an efficient way to increase the electromechanical response in DETs. It needs to be considered though that the glass transition temperature ($T_g$) of the elastomer is increased by the modification, which reduces the window in which the material can be used.[2] Piezoelectric materials respond to a mechanical stress by generating an electric signal. Unfortunately, most piezoelectric elastomers lack stretchability. Piezoelectric elastomers would greatly expand the range of possible applications.

## Results and Discussion

Chemical modification of polysiloxanes allows formation of materials with increased ε ' and low $T_g$. We modified the polysiloxanes with polar groups such as CN, $CF_3$, sulfone, and sulfolane (Figure 1).

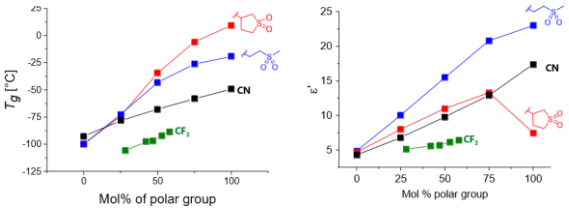


*Figure 1. The $T_g$ (left) and the ε ' (right) of some polysiloxane modified with polar groups.*

The highest permittivity value of ε ' = 22.7 (at $10^4$ Hz and room temperature) was achieved with a polysiloxane that carries a sulfone group at every repeat unit. Actuators constructed with one of the best materials show about 20.5% lateral strain at an electric field as low as 10.8 V/μm.[2]

Novel elastomeric composites of specially designed polymer nanoparticles with high $T_g$ and side groups with large permanent dipoles embedded in chemically crosslinked polydimethylsiloxane matrices were prepared. The initially randomly oriented polar groups in the nanoparticles are poled in a strong electric field while the film is heated above the $T_g$ of the nanoparticles. The polar groups orient in the direction of the electric field and the achieved orientation is subsequently frozen-in by cooling the material back to room temperature. Hence, a permanent polarization responsible for the piezoelectricity is induced in the elastomers.[3]

## Conclusions

Materials with predictable properties can be generated with molecular design and suitable synthetic chemistry and will bring DETs a significant step forward towards industrial implementation.

## References

[1] R. E. Pelrine et al., *Sens. Actuators A*, **1998**, *64*, 77.
[2] S. J. Dünki, et al., *Adv. Funct. Mater.*, **2015**, *25*, 2467.
[3] Y. S. Ko, et al., *Adv. Mater.*, **2017**, *29*, 1603813.

## Acknowledgements

We gratefully acknowledge SNF 142215, SNF 140577 and Empa, Dübendorf for financial support.

# A new wearable sensor in the shape of a braided cord (Kumihimo)

Y. Tajitsu

kenji_imoto@imonet.jp (Corresponding e-mail address)

[1] Department of Electrical Engineering, School of Science Engineering, Kansai University
3-3-35 Yamate, Suita, 564-8680 Osaka, Japan

**Abstract:** A new piezoelectric sensor was developed in the shape of a Japanese traditional braided cord known as a "Kumihimo", by weaving piezoelectric poly-*l*-lactic acid (PLLA) fibers (piezoelectric braided cord). We realized that the piezoelectric braided cord tied in various decorative knots, which can be worn as an accessory such as a choker or necklace, could detect pulse waves, swallowing, and coughing in a systematic order in one's daily life. For the demostartion, we developed a system for measuring pulse waves with a Wi-Fi communication system using a piezoelectric braided cord with decorative knots

**Keywords:** poly-*l*-lactic acid, piezoelectricity, braided cord, decorative knot, Kumihimo, fiber

## Introduction

Functional glasses and wristwatches have already been commercialized as wearable devices are already out in the market. However, the wearers feel unnatural when these devices are used. This unnatural feeling has contributed to the stagnant wearable device market. The ideal wearable device must be worn comfortably and stably. To achieve this, we attempted to realize a functional apparel [1,2]. In this study, we have developed a wearable sensor in the shape of a Japanese traditional braided cord, known as a Kumihimo, by weaving piezoelectric poly-*l*-lactic acid (PLLA) fibers.

## Piezoelectric braided cord

Using the Japanese traditional braided cord technique, the piezoelectric braided code which has a core yarn of conducting yarn covering PLLA and polyethylene terephthalate (PET) yarns, was developed by our cooperative research company Teijin Co. Ltd. The piezoelectric braided code can detect user motions such as elongation and contraction, bending and extension, and twisting. Figure 1 shows the piezoelectric response signal from the piezoelectric braided cord attached to a metallic ruler corresponding to damping oscillation of the metallic ruler. The accelerometer data and the result for the piezoelectric braided cord show good agreement.

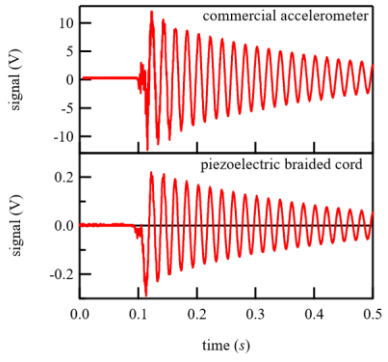


*Figure 1. Signal from piezoelectric braided cord*

## Pulse sensing by piezoelectric braided cord tied in decorative knot

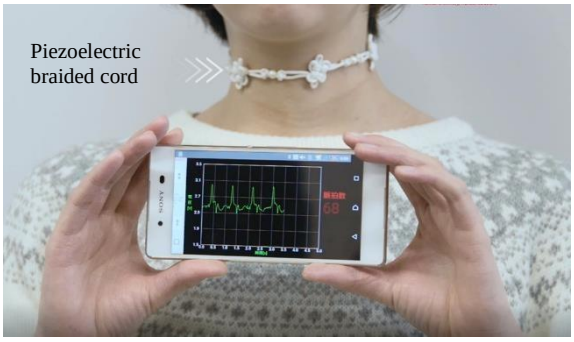


*Figure 2. Pulse wave signal*

As a demonstration, we developed the following system for detecting pulse waves. The Kicyo decorative knot of the piezoelectric braided code, which reacts only to the small motion of the human pulse without reacting to the direction of the large motion of the shoulder and neck, was used as a choker worn around the neck, as shown in Fig. 2. Figure 2 shows a demonstration of detecting a pulse wave by a choker braided by a piezoelectric braided cord. The signal due to the pulse wave detected by the choker sensor is sent to a smart phone through a Wi-Fi communication system.

## Conclusions

A braided-cord-shaped piezoelectric PLLA sensor has been developed using the technology of Japanese conventional weaving.

## References

[1] Carpi, F; Biomedical Applications of Electroactive Polymer Actuators; Wiley, London, 2009.
[2] Tajitsu, Y; *Ferroelectrics.* **2016**, 499, 36–46.

## Acknowledgements

We thank Teijin Co. Ltd., Japan, for kindly supplying the piezoelectric braided cords. This work was also supported in part by Grants-in-Aid for Scientific Research (Nos. 24655108 and 15K13714) from the Ministry of Education, Culture, Sports, Science and Technology of Japan.

# Influence of photoexcitation on the ferroelectric behaviour of ferroelectric-semiconductor-composites

**Sebastian Engel[1], David Smykalla,[2] Bernd Ploss[2], Stephan Gräf[1], Frank A. Müller[1]**

Sebastian.Engel@uni-jena.de

*[1]Friedrich Schiller University of Jena, Otto Schott Institute of Materials Research, Löbdergraben 32, 07743 Jena, Germany*
*[2]University of Applied Sciences Jena, Department of SciTec, Carl-Zeiss-Promenade 2, 07745 Jena, Germany*

**Abstract:** Ferroelectrics-semiconductor-composites combining piezo-, pyro- and photoconductive properties are investigated. These materials are of particular interest for future applications in the field of small and flexible sensors and actuators.

**Keywords:** ferroelectrics, semiconductor, polymer, photoconductivity, pyroelectric

## Introduction

Our future life will be significantly influenced by e.g. Industry 4.0 and autonomous driving. In this context suitable sensors and actuators have to become smaller and more flexible. For this purpose, ferroelectrics represent an ideal basic material, because of their intrinsic pyro- and piezoelectric properties. However, their simultaneous occurrence prohibits the discrimination between temperature and pressure changes without keeping one parameter constant. This problem can be solved by using a flexible active-matrix cell with a selective poled bifunctional polymer-ceramic composite based on the different curie temperatures of the matrix and the ceramic particles as well as on their different signs of the piezoelectric coefficient [1]. An additional doping of such ferroelectric composites with photoconductive materials like semiconductors enables to expand the sensor properties not only to photosensitivity but also to optimized extraction of the pyroelectric signal power by adjusting its conductivity [2].

## Results and Discussion

The present study investigates for the first time the interaction of photoexcitation, polarization and piezoelectricity in composite materials consisting of a non-ferroelectric semiconductor ($TiO_2$, rutile, $E_g \approx 3.03$ eV) dispersed in both a ferroelectric Poly(vinylidene fluoride trifluoroethylene) [P(VDF-TrFE)] polymer matrix and a composite matrix consisting of polyurethan [PU] and $BaTiO_3$-particles. For both composites, an influence of the photoexcitation on the I-V characteristics was obtained, that depends on its intensity and on the wavelength (Fig. 1a). The occurrence of a maximum conductivity at an excitation wavelength in the range of 415 nm can be explained by a required minimal photon energy combined with an optical penetration depth to generate a charge carrier channel. Furthermore, its remarkable influence on the ferroelectric behavior of both composites is reflected in the hysteresis loops depending on optical excitation. While the measured voltage at the reference capacitor in the case of the P(VDF-TrFE)-$TiO_2$-composite is not only influenced by the displacement current but also a result of the photo generated current. The photo generated carriers in the PU-$BaTiO_3$-$TiO_2$-composite enhance the polarization behavior of the $BaTiO_3$particles by saturating the surface charges in the usually insulating matrix [3]. A further influence of the photoexcitation on the ferroelectric behavior of the PU-$BaTiO_3$-$TiO_2$-composite is illustrated in Fig. 1b. Here, an optical excitation at $\lambda$ = 415nm leads to an improved coupling of the pyroelectric signal due to the introduction of a tunable direct conductivity (dc) of the matrix $\sigma_m$, which increases the imaginary part of the matrix permittivity $\varepsilon_m$ [2]:

$$\varepsilon_m = \varepsilon'_m - i\varepsilon''_m - {}^{i}/_{\omega\varepsilon_0}\,\sigma_m$$

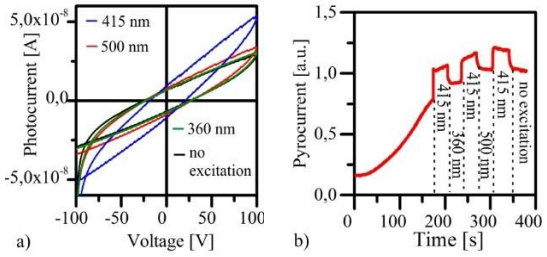


*Fig. 1: Properties of the PU-$BaTiO_3$-$TiO_2$-composite: a) I-V curves at different excitation wavelength and b) the time dependent pyrocurrent (ΔT=25K) under different photo excitation conditions (0,04 mW/mm² for each excitation wavelength).*

## Conclusions

Beyond the simple combination of piezo-, pyro- and photoconductive properties in one composite our results also demonstrate their mutual interaction. Thus, it is not only possible to optimize pyroelectric sensors by adjusting their conductivity via photo excitation but also to obtain novel actuator designs based on "laser-assisted direct polarization writing" due to optical induced charge carrier transport for surface charge saturation in a normal insulating matrix.

## References

[1] I. Graz, M. Krause, S. Bauer-Gogonea, S. Bauer, S. P. Lacour, B. Ploss, M. Zirkl, B. Stadlober, S. Wagner, *J. Appl. Phys.* **2009**, doi: 10.1063/1.3191677
[2] B. Ploss, S. Kopf, *Ferroelectrics* **2006,** 338, 145-151.
[3] B. Ploss, B. Ploss, F.G. Shin, H.L.W. Chan, C.L. Choy, IEEE Trans. on Diel. and El. Ins. **2000**, 7, 517522.

## Acknowledgements

DFG is thankfully acknowledged for financial support (MU1803/14-1.)

# pMUT device compatible with large-area display technology

Yongbin Jeong[1,2], Chih-Hsien Huang[1], David Cheyns[1], Guilherme Brondani Torri[1],
Xavier Rottenberg[1], Paul Heremans[1,2]

yongbin.jeong@imec.be (Corresponding e-mail address)

[1]IMEC, Large Area Electronics, Kapeldreef 75, Leuven B-3001, Belgium.
[2]KU Leuven, Department of Electrical Engineering, Kasteelpark Arenberg 10, Leuven B-3001, Belgium.

**Abstract:** Piezoelectric micromachined ultrasound transducers (pMUT) are promising in many technological areas. However, the classical process approach of pMUT fabrication is incompatible with the flat panel display industry because most of the process steps do not fit with large substrates, e.g. glass. In this paper, we demonstrate pMUT devices using process steps available in the display industry, with a maximum temperature budget of 200ºC. The device frequency response follows the expectation from simulations. We show that the obtained output pressure enables application in several display related use cases.

**Keywords:** PMUT, Large Area Electronics, piezoelectricity

## Introduction

Large area electronics is an emerging technology, starting from display devices and reaching out to other devices including RFID tags, photodetectors, batteries, energy generators and sensors[1]. Micromachined ultrasound transducers (MUTs) are an example of widely used sensors, currently limited to processing on top of silicon[2], with research aiming for large area processing. There are two main challenges: 1. The process temperature for conventional piezoelectric materials such as PZT or AlN is too high for glass based process flows[3], 2. micromachined structures rely heavily on crystalline materials[3]. We propose an effective process and material combination to fabricate pMUTs on glass substrates with a limited process window.

## Results and Discussion

A circular cavity is created by a bonding process on top of a glass substrate. On top of this, a piezoelectric polymer sandwiched between two metal layers is fabricated using photo-lithography based technology.

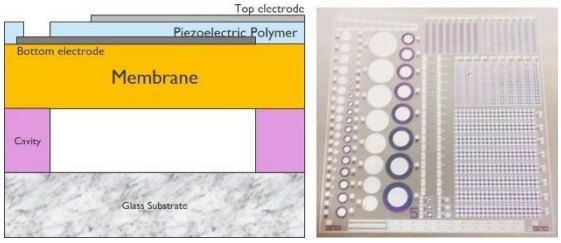


*Figure 1: Cross-sectional diagram of device structure (left) and picture of test device on glass substrate (right).*

The fabricated pMUT devices are subsequently annealed and electrically poled to reach a maximum remnant polarization. The polarization – electric field loop is measured using a Keithley 4200 and representative remnant polarization values are ~7μC/cm$^2$.

The deflection of the membrane of the devices with different radius of cavity size is measured with a laser Doppler vibrometer (Polytech MSA-500). The measured resonance frequency of the device follows the simulation results, with a clear dependence on the cavity size.

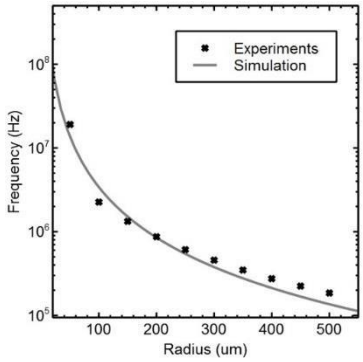


*Figure 2: Resonant frequency vs. radius of the cavity*

## Conclusions

Our pMUT devices fabricated on a glass substrate show a resonant frequency that can be controlled by the device geometry, and it can be tuned in the range of 100kHz – 2MHz. Both frequency and output power shows promising expectation for a variety of large area based applications.

## References

[1] Arias, A. C.; MacKenzie, J. D.; McCulloch, I.; Rivnay, J.; Salleo, A. *Chem. Rev.* **2010**, 110, 3 – 24.

[2] J.J. Bernstein, S.L. Finberg, K. Houston, L.C. Niles, H.D. Chen, L.E.Cross, K.K. Li, K. Udayakumar, *IEEE Trans. Ultrason. Ferroelectr. Freq. Control.* **1997**, *44*, 960–969.

[3] F. Akasheh, T. Myers, J.D. Fraser, S. Bose, A. Bandyopadhyay, *Sens. Actuators A.* **2004**, *111*, 275–287.

# Miniaturized Elastomer-Based Actuators: enabling complex smart soft machines

Herbert Shea herbert.shea@epfl.ch

LMTS, Ecole Polytechnique Fédérale de Lausanne (EPFL), rue Maladière 71b, CH-2000 Neuchâtel, Switzerland

**Abstract:** Picking up a raw egg, a half-filled water balloon, or a playing card is trivial for a child, but a major challenge for a conventional robotic gripper. As an illustration of what can be accomplished with elastomer-based actuators, we present a compliant gripper capable of all those tasks, combining electro-adhesion with Dielectric Elastomer Actuators. We then give an overview our lab's activities in µm- to cm-scale silicone-based DEAs for optics, haptics, and biology, including the integration of flexible 1 kV transistors with DEAs, an approach that enables smart soft machines with low-voltage addressing.

**Keywords:** Dielectric Elastomer Actuator (DEA), compliant electrodes, flexible TFTs

## Introduction

Dielectric Elastomer Actuators (DEA) are compliant transducers with many appealing features, in particular actuation strains in excess of 100%. The field has blossomed since the work of Pelrine *at al.* [1] in the late 1990s. DEAs are operated at electric fields near breakdown of the dielectric in order to obtain the best actuation performance.

## Results and Discussion

Our lab's research is centered on µm- to cm-scale DEAs, made from silicone elastomers, with printed stretchable silicone-based electrodes [2]. We present several examples of our devices for a wide range of applications, including: grippers, fast (200 µs) tunable lenses, transparent bioreactors to apply mechanical strain to biological cells, and haptic interfaces (Fig 1).

Reliability and lifetime are essential considerations for DEAs. The failure modes of DEAs are a complex interplay between mechanical and electrical phenomena. Avoiding mechanical failure is a major reason why we use silicone elastomers rather than the more widely used acrylics. For strain of 5%, we obtain lifetimes in excess of 400 million cycles at electric fields of order 100 V/µm.

Electrodes play an important role in thin DEAs. We will discuss several fabrication methods, and their impact on performance, manufacturability and lifetime.

## Conclusions

DEAs can be used as capacitive strain sensors to enable self-sensing. We present recent progress towards incorporating flexible high-voltage logic with DEAs, paving the way for intelligent soft actuators.

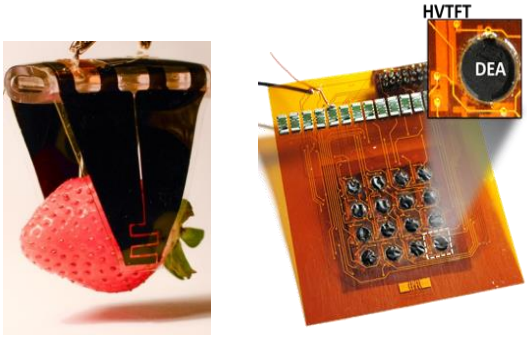


*Figure 1: Left: compliant DEA gripper capable of holding 60x its weight [3]. Right. Array of 16 DEAs with 16 integrated flexible thin film transistors, allowing independent control of the 16 DEA using only a single high-voltage power supply.[4]*

## References

[1] Pelrine, R., Kornbluh, R. D., Pei, Q., & Joseph, J. (**2000**). High-Speed Electrically Actuated Elastomers with Strain Greater Than 100%. *Science*, *287*(5454), 836–839.

[2] Rosset, S., & Shea, H. R. (**2016**). Small, fast, and tough: Shrinking down integrated elastomer transducers. *Applied Physics Reviews*, *3*(3), 31105.

[3] Shintake, J., Rosset, S., Schubert, B., Floreano, D., & Shea, H. R. (**2016**). Versatile Soft Grippers with Intrinsic Electroadhesion Based on Multifunctional Polymer Actuators. *Advanced Materials*, *28*(2), 231– 238.

[4] Marette, A., Poulin, A., Beese, N., Rosset, S., Briand, D & Shea, H. R. (**2017**). Flexible Zinc-Tin Oxide Thin Film Transistors Operating at 1 kV for Integrated Switching of Dielectric Elastomer Actuators Arrays**,** *Advanced Materials*, *in press*

## Acknowledgements

We thank the Swiss National Science Foundation, NCCR robotics, the European Space Agency, and the European Commission via FP7 and H2020 for financial support.

# Ambient Processing of P(VDF-TrFE) Ferroelectric Thin-Films for Application in non-Volatile Memory Devices

Hamed Sharifi Dehsari[1], Amr Saad[1], Jasper J. Michels[1], Kamal Asadi[1*]

asadi@mpip-mainz.mpg.de

[1]Max-Planck Institute for Polymer Research, Ackermannweg 10, Mainz, Germany

**Abstract:** It has been suggested that addition of nanoparticles enhances remanent polarization in ferroelectric P(VDF-TrFE). Here we first show a combined experimental and theoretical study on P(VDF-TrFE) film processing, and then leveraging from the knowledge gained, we show that addition of nanoparticles (NPs) actually reduces the remanent polarization.

**Keywords:** Ferroelectric polymer, Non-volatile memory, Vapor-induced phase separation, Metal-oxide NPs.

## Introduction

The most commonly used ferroelectric polymer for memory applications is the random copolymer of vinylidenedifluoride with trifluoroethylene (P(VDF-TrFE)). It has been recently suggested that addition of nanoparticles in the polymer matrix induces higher degree of remanent polarization. In this contribution we have revisited this observation. To achieve reliable result we have first developed a solid understanding of the film formation in solution processed P(VDF-TrFE) at ambient condition (room temperature and relative humidity of 45%). Using a combination of experiments and modelling we show that rough and unpacked films are produced due to the presence of water and vapor-induced phase separation (VIPS).[1,2] Using the insight gained, we fabricate ferroelectric capacitors under ambient conditions, *i.e.* 20 °C and 50% relative humidity (RH), to establish how the scattering in coercive voltage and device yield relates to the hydrophilicity of the solvent and also how the addition of nanoparticle affects the remanent polarization.

## Results and Discussion

Here, we have calculated approximate ternary phase diagrams for P(VDF-TrFE)/water/solvent systems, involving solvent evaporation, water condensation, and phase dynamics (Figure 1). We show that the hydrophilicity of the organic solvent is a deciding factor that determines the final film morphology. We show that (Figure 1), VIPS is effectively hindered by using a solvent that is immiscible with water, and also develop an ambient compatible processing recipe for P(VDFTrFE) with a large processing window that yields transparent, closely packed smooth thin-films. The yield of functional ferroelectric capacitors with sub-10V coercive voltages was close to unity (>95%).

In the second step, monodispersed nanoparticles with sub-20 nm diameters were added to the P(VDF-TrFE) matrix with different loading ratios. Homogeneous dispersion of nanoparticles in the matrix was obtained. We obtained highly reproducible capacitors that function at sub-10V regime, with a high yield of functional devices. We show that remanent polarization does not significantly change for loadings below 10wt%, whereas for 15% loading there is 50% drop in remanent polarization.

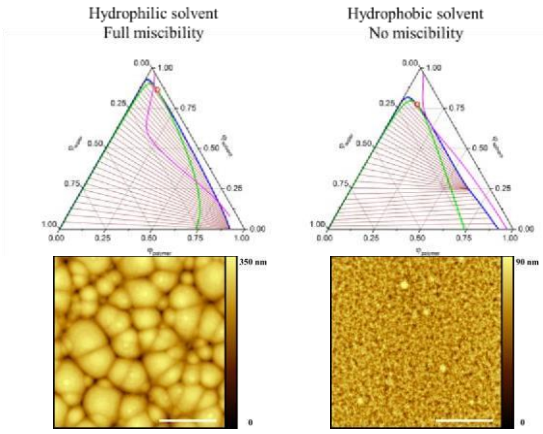


*Figure 1: Calculated ternary phase diagrams for P(VDF-TrFE) : water : solvent systems for both hydrophilic and hydrophobic solvents (top), and the corresponding morphologies experimentally obtained (bottom). Scale bar is 10 µm.*

## Conclusions

Here we presented a reliable process for fabrication of P(VDF-TrFE) thin-films using a solvent with low water miscibility. The yield of functional capacitors was >90%. We further showed that loading the ferroelectric polymer with nanoparticles leads to inferior ferroelectric properties.

## References

[1] M. Li, et al, *J. Mater. Chem. C*, **2013**, 1, 7695-7702.
[2] Benz, M. et al, *Langmuir*, 2001, 17, 239-243.

## Acknowledgements

We thank Alexander von Humboldt Foundation for the financial support via Sofja Kovalevskaja Award.

# Polymer Electrets with quadratic Nonlinear-optical activity

M.Yu. Balakina, A.A. Kalinin, M.Sharipova, T.A. Vakhonina, O.D. Fominykh, A.I. Levitskaya,

M.A. Smirnov, A.Sh. Mukhtarov

mbalakina@yandex.ru

A.E. Arbuzov Institute of Organic and Physical Chemistry, Kazan Scientific center, Russian Academy of Sciences, Arbuzov str., 8, 420088, Kazan, Russia

**Abstract:** Epoxy amine and methacrylic (co)polymers with covalently attached azochromophores and composite materials on the base of PMMA, containing novel effective chromophores with divinylquinoxaline π-electron bridge as guests, are developed and nonlinear-optical characteristics are determined.

**Keywords:** chromophores, local mobility, nonlinear-optical activity

## Introduction

Polymers exhibiting quadratic nonlinear-optical (NLO) response to the applied electric field are developed for use in photonics and optoelectronics. Organic chromophores, incorporated into the material either as guest molecules or as fragments of the main/side chains, are the molecular sources of the effect. However, to exhibit quadratic NLO activity the material should be transferred into the electret state with macroscopic polarization, what is achieved by the orientation of chromophores in the polymer matrix. Thus poling is one of the key stages in the development of such materials, optimization of time-temperature protocols with the account of data obtained by dielectric spectroscopy (DS), thermostimulated depolarization current (TSD) technique, and molecular modelling provides NLO characteristics improvement.

## Results and Discussion

Here we present the study of NLO characteristics and their relaxation stability for two types of polymer NLO electrets: first, on the basis of epoxyamine and methacrylic (co)polymers with azochromophores in the side chain (OAB-DR1 [1] and MMA-MAZ [2], correspondingly), and second – composite materials on the basis of PMMA and original chromophores with heterocyclic fragments in the end groups and in π-electron bridge – PMMA/DBA-VQV-TCF [3]. The electret state of the materials is formed as a result of either contact poling, or in the corona discharge field. The chromophores orientational order is controlled by the UV/vis spectroscopy. According to the Second Harmonic Generation measurements (λ =1064 nm), the PMMA/DBA-VQV-TCF material is characterized by rather high NLO coefficient, $d_{33}$ (see Fig.1). However, the relaxation stability of NLO activity is known to be low for composites. As for OAB-DR1 and MMA-MAZ, 90% and 70% of NLO activity was shown to remain after seven months. The poling protocols were optimized on the basis of the information about local mobility of chromophores and fragments of the bearing chain obtained by DS and TSD, molecular modeling data being accounted to assign the mobility of certain kinetic units to the detected relaxation processes [4]. The relaxation parameters were evaluated from the best fit to experimental data.

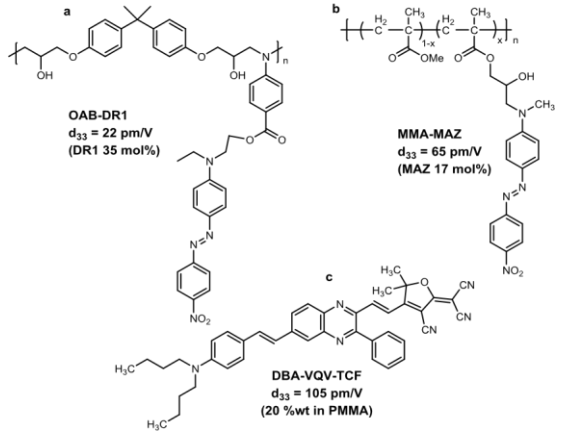


*Figure 1: Monomer units of polymers with azochromophore in the side chain (a,b); guest chromophore for composite material (c).*

## Conclusions

Polymer electrets with quadratic NLO activity are developed, the ways for achieving optimal NLO characteristics are considered.

## References

[1] G.N. Nazmieva, T.A. Vakhonina, et al. *Eur. Polym. J.* **2015**, *63*, 207–216.

[2] T.A. Vakhonina, N.V. Ivanova, et al. *Mendeleev Commun.* **2014**, *24*, 138-139.

[3] A.I. Levitskaya, A.A. Kalinin, O.D. Fominykh, M.Yu. Balakina, *Comp. Theor. Chem.* **2015**, *1074*, 91-100.

[4] N.A. Nikonorova, M.Yu. Balakina, *et al. Mater. Chem. Physics* **2016**, *181*, 217-226.

## Acknowledgements

The financial support of Russian Scientific Foundation (grant number 16-13-10215) is gratefully acknowledged.

# Record performance of organic ferroelectric liquid crystal BTA

Indre Urbanaviciute[1], Xiao Meng[2], Tim D. Cornelissen[1], Andrey V. Gorbunov[3], Subham Bhattacharjee[2], Rint P. Sijbesma[2], Martijn Kemerink[1]

indre.urbanaviciute@liu.se

[1]Department of Physics, Chemistry and Biology (IFM), Linköping University, 58183 Linköping, Sweden
[2]Laboratory of Macromolecular and Organic Chemistry, Eindhoven University of Technology, P.O. Box 513, 5600 MB Eindhoven, The Netherlands
[3]Department of Applied Physics, Eindhoven University of Technology, PO Box 513, 5600 MB Eindhoven, The Netherlands

**Abstract:** We demonstrate how simple structural modification of a prototypical organic ferroelectric molecule trialkylbenzene-1,3,5-tricarboxamide (BTA) can be used to tune its key ferroelectric properties. In particular, we find that shortening of the peripheral tail causes an increase in remnant polarization resulting in $P_r$ > 60 mC/m$^2$, and augments the depolarization activation energy and the coercive field. The combination of these characteristics leads to a record polarization retention time of close to 3 months at room temperature for capacitor devices of the BTA material with the shortest - $C_6H_{13}$ - alkyl chain.

**Keywords:** benzene-1,3,5-tricarboxamide, organic ferroelectrics, polarization retention, ferroelectric memories

## Introduction

Being non-toxic, lightweight, transparent, flexible, easily processable and potentially cheap, organic ferroelectric materials appear very favourable from the application point of view. However, besides the successfully commercialized ferroelectric polymer P(VDF:TrFE), not many of the reported alternatives have properties required for the actual devices. Here, we show how simple molecular engineering on the prototypical molecular ferroelectric BTA leads to a record material with a performance that is comparable to that of P(VDF:TrFE).

## Results and Discussion

The BTA molecule consists of a π-stacking benzene core, three hydrogen-bonding dipolar amide groups, and peripheral flexible alkyl chains (Figure 1). Due to this unique structure, BTA is able to form a helical network of hydrogen bonds in tightly packed columnar systems, which results in true ferroelectric switching.[1] We show that the ferroelectric properties of BTA can be tuned by changing the length of peripheral alkyl chains. These flexible tails influence molecular packing by determining the intercolumnar distance in a columnar hexagonal liquid crystalline phase. Therefore, shorter tails not only increase the dipole density, but also result in stronger interaction among columnar macro-dipoles. This augments the remnant polarization (to >60 mC m$^{-2}$), and the depolarization activation energy (to ~1.6 eV) as well as the coercive field (~100 V/µm, 23 °C, 5 Hz). As a result, the polarization retention for BTA-C6 becomes close to three months at room temperature, which is one of the best results reported for organic ferroelectrics so far. The observed trends can be rationalized using the thermally activated nucleation limited switching model, which also discloses an improvement in layer order for shorter-substituted molecules. In addition, sub-millisecond polarization switching time and electrical fatigue resistance over $10^5$ cycles further demonstrate the application potential of BTA-C6 devices.

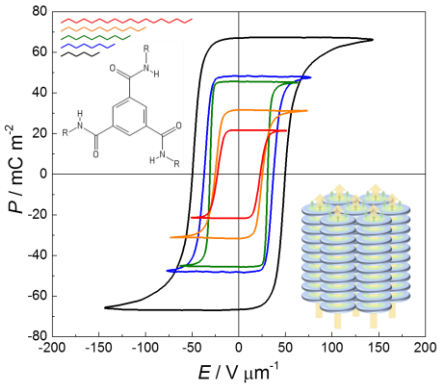


*Figure 1: Polarization hysteresis loops of all examined BTA homologues BTA-C6, C8, C10, C12 and C18 (corresponding to the alkyl chain $C_nH_{n+1}$). Inset: chemical structure of BTA with different alkyl chains -R and columnar hexagonal packing resulting in a molecular macro-dipole and ferroelectric behaviour in a full device.*

## Conclusions

Temperature stability, long retention and a remnant polarization that is as high as that of P(VDF:TrFE) distinguish the BTA-C6 material from other small molecular organic ferroelectrics and makes it a perspective choice for applications that require cheap, flexible and lightweight ferroelectrics.

## References

[1] A. V. Gorbunov, T. Putzeys, I. Urbanavičiūtė, R. A. J. Janssen, M. Wübbenhorst, R. P. Sijbesma, M. Kemerink, *Phys. Chem. Chem. Phys.* **2016**, *18*, *23663*.

# Piezoelectricity in screen-printed hydroxyapatite

Sarah Markham[1,2], Aimee Stapleton[1,2], Tofail Syed [1,2], Ehtsham U. Haq[1,2], Katarzyna Kowal[1,2]

sarah.markham@ul.ie

[1]Bernal Institute, University of Limerick, Castletroy, Limerick, Ireland.
[2]Department of Physics, University of Limerick, Limerick, Ireland

**Abstract:** Synthetic apatites including hydroxyapatite and a mixture of hydroxyapatite and tricalcium phosphates are extensively used in bone graft substitute and cement-less implant coating. The study of piezoelectricity in these apatites is of particular interest to understand the role of electricity in facilitating in vivo bone growth, bone growth stimulation and potential energy harvesting to run spinal or neuro stimulators.

**Keywords:** piezoelectricity, apatites, screen-printed, energy harvesting

## Introduction

Apatites are a family of calcium phosphates, $Ca_{10}(PO_4)_6(X)_2$, which are categorised by the presence of specific ions such as $OH^-$, $Cl^-$ or $F^-$. Apatites form the primary mineral component of the musculoskeletal system, and synthetic apatites are used extensively in orthopaedics and dentistry. [1,2] Since the prediction of piezoelectricity in hydroxyapatite in 2005 [3], calcined thin films and poled hydroxyapatite (HAp) ceramics have shown much higher piezoelectricity (1-16 pC/N) [4-6] than the originally measured weak piezoelectricity in unpoled HAp ceramics [7]. One of the pressing needs in obtaining quantifiable piezoelectricity in un-poled HAp is texturing and crystallisation control.

Screen printing can be a method of convenience to align particles for piezoelectricity. This work explores the piezoelectric potential of screen printed HAp and doped HAp to be used as a flexible energy generator and as substrates for physiological investigations.

## Results and Discussion

Spherical particles were observed in the single and triple-layer films indicating low levels of anisotropy in the precursor material. Despite this, piezo-electricity was observed in the triple-layer film.

Six identical samples, labelled A-F, of triple-layer films were tested with the piezometer. Each sample was measured six times and corresponding d33 coefficient values were recorded in both the upright and inverted state. The electrode connections were switched to simulate physically flipping the sample. Figure 1 shows the average positive (green) and negative (blue) d33 values measured for each sample with the associated error for each indicated.

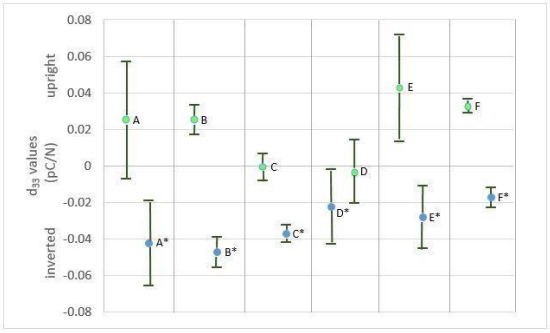


*Figure 1: Piezoelectric d33 coefficient measured for three-layer hydroxyapatite screen-printed films in the upright (green) and inverted (blue) configuration.*

## Conclusions

The values obtained are an order higher than that measured in PLD deposited hydroxyapatite and encourage further investigation in improving the particle size and anisotropy so that physiologically relevant level of potentials can be generated.

## References

[1] Oonishi H, Yamamoto M, Ishimaru H, Tsuji E, Kushitani S, Aono M, et al. Bone Joint J. **1989**;71(2):213-6.
[2] Ong JL, Chan DC. Crit Rev Biomed Eng. **2000**;28(5&6).
[3] Haverty D, Tofail SA, Stanton KT, McMonagle JB. Phys Rev B. **2005**;71(9):094103.
[4] Lang S, Tofail S, Gandhi A, Gregor M, WolfBrandstetter C, Kost J, et al. Appl Phys Lett. **2011**;98(12):123703.
[5] Gandhi AA, Wojtas M, Lang S, Kholkin AL, Tofail SA. J Am Ceram Soc. **2014**.
[6] Lang S, Tofail S, Kholkin A, Wojtaś M, Gregor M, Gandhi A, et al. Sci Rep. **2013**; 3: 22151
[7] Tofail S, Haverty D, Cox F, Erhart J, Hána P, Ryzhenko V. J Appl Phys**. 2009**;105(6):064103.

## Acknowledgements

Bernal Institute and the University of Limerick.

# Toward comprehensive understanding of piezoelectricity and its relaxation in VDF-based ferroelectric polymers

Takeo Furukawa, Hidekazu Kodama

furukawa@kobayasi-riken.or.jp

Kobayasi Institute of Physical Research, 3-20-41, Higashimotomachi, Kokubunji, Tokyo 185-0022, Japan

**Abstract:** By means of accurate measurements of piezoelectric resonance spectra, we evaluated true $e_{31}$, $e_{32}$ and $e_{33}$ constants of uniaxially-drawn and poled polyvinylidene fluoride and its copolymer. We identified three fundamental mechanisms of polarization changes induced by trans-chain elongation ($e_{31}$>0), interchain expansion ($e_{32}$, $e_{33}$<0) and dipole density reduction (dimensional effect, $e_{33}$<0). Discussion will be extended to correlations of these mechanisms with relaxational chain dynamics and electrostrictive coupling inherent to ferroelectric polymers.

**Keywords:** piezoelectricity, relaxation, polyvinylidene fluoride, ferroelectric polymer

## Introduction

It is generally accepted that piezoelectricity of polyvinylidene fluoride (PVDF) and its copolymer with trifluoroethylene (TrFE) originates in poling-induced dipole orientation in ferroelectric form I crystals[1]. However, uncertainties still remain in basic mechanisms due to structural complexity and relaxational nature inherent to polymers. Toward comprehensive understanding, we intended to evaluate the true *e*-constants that express the charge responses induced by a single strain and are essential for quantitative analysis.

## Results and Discussion

Figure 1 shows the temperature dependence of various *e*'s obtained from piezoelectric resonance spectra. Here 1 refers to draw direction, 3 to poling direction and 2 orthogonal to them. Thickness-mode resonance yields true $e_{33}$ whereas length mode yields apparent $e_{31}^a$, $e_{32}^a$ that are related to true *e* via. Poisson's ratio $\nu_{ij}=-s_{ij}/s_{jj}$.

$$e_{31a} = d_{31}/s_{11} = e_{31} - e_{32}\nu_{21} - e_{33}\nu_{31} \quad (1)$$

$$e_{32a} = d_{32}/s_{22} = -e_{31}\nu_{12} + e_{32} - e_{33}\nu_{32} \quad (2)$$

Width-mode provides information about ν.

As seen in *Figure 1*, $e_{33}$ is a major component with a value 60-80% larger than remanent polarization $P_r$ of 60mC/m$^2$ for PVDF and 100mC/m$^2$ for VDF/TrFE. The dimensional effect [1] is known to results in $e_{33} = -P_r$. Additional contributions come from a decrease in dipole moment due to interchain expansion that is predicted by recent first principle calculations (classical local field) [2].

VDF-based polymers exhibit segmental-mode relaxation near -10℃ where $e_{31}^a$ shows a marked increase. Analyses using eqs.(1) and (2) with elastically-uniaxial assumption revealed that such increase in $e_{31}^a$ was associated with positive $e_{31}$ generated by segmental motion. True $e_{32}$ was shown to be negative and attributable to interchain expansion similar in $e_{33}$.

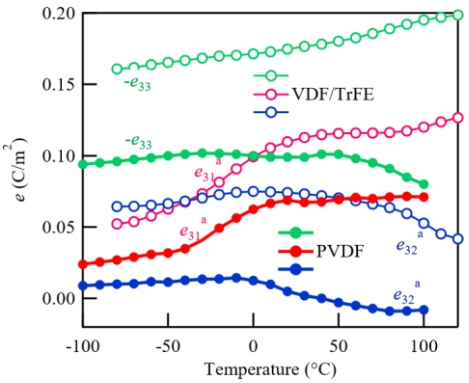


*Figure 1: Temperature dependence of $e_{33}$, $e_{31}^a$ and $e_{32}^a$ for uniaxially-drawn and poled PVDF and VDF/TrFE.*

Basic mechanisms of piezoelectricity associated with chain elongation, interchain expansion and dimensional effect are summarized in figure 2.

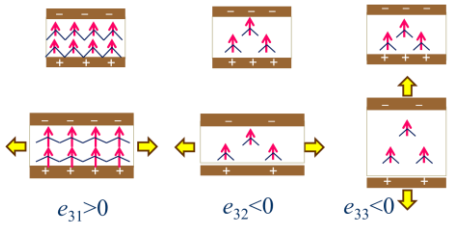


*Figure 2: Basic mechanisms governing $e_{31}$, $e_{32}$ and $e_{33}$.in VDF-based ferroelectric polymers.*

## Conclusions

Piezoelectric response resulting in true $e_{31}$ suggests that segmental motion can occur in ferroelectric crystalline regions. Three basic mechanisms must be related to ferroelectric electrostrictive coupling observed as the strain-dependent permittivity and the strain proportional to square of polarization.

## References

[1] Furukawa, T. *IEEE Trans. Electr. Insul.*, **1989,** *24*(3), 375-394.

[2] Nakhmanson, S. M.; Buongiorno Nardelli, M. ; Bernholc, J. Nardelli, *Phys Rev.* , **2005**, *B72*, 115210.

# Ferroelectric properties and detection of charge injection/trapping in liquid crystals via Laser Intensity Modulation Method (LIMM) and Dielectric Relaxation Spectroscopy (DRS)

Tristan Putzeys [1,2], Xiao Meng[1], Rint Sijbesma[1], Dick Broer[1], Michael Wübbenhorst[2]

Tristan.putzeys@kuleuven.be

[1] TU/e, Eindhoven University of Technology, The Netherlands
[2] KU Leuven, The catholic university of Leuven, Belgium

**Abstract:** Newly synthesized liquid crystals are analyzed for ferroelectric properties using the well-established LIMM setup, which allows polarization profiling with nanometer resolution, and broadband DRS method, which identifies molecular relaxations. The peculiar ferroelectric properties of certain liquid crystals are rationalized via and compared to the charge injection and trapping mechanism found in PVDF[1]. Charge injection and trapping play an important role in polarization retention.

**Keywords:** Pyroelectric, relaxation spectroscopy, ferroelectrets, LIMM, DRS, memory devices

## Introduction

Recent years have seen an increased interest in organic ferroelectrics, with the PVDF polymer and PVDF-TrFE copolymers seen as a 'golden' reference. PVDF is characterized by a strong coercive field and a good polarization retention, rationalized by the charge-polarization coupling and injection of charges via the electrodes during poling[1,2].

Based on the ferroelectric, discotic BTA's[3] (N,N´,N´´-trialkylbenzene-1,3,5-tricarboxamides), new liquid crystals are synthesized and characterized for ferroelectric properties.

Two promising candidates with coercive field similar to PVDF and retention times in the order of days to weeks are TPyA (6, 6', 6''-nitrilotris(N-(3,7-dimethyloctyl)nicotinamide)) **Fig. 1** and BPTA (N3,N3',N5,N5'-tetraoctyl-[1,1'-biphenyl]-3,3',5,5'-tetracarboxamide).

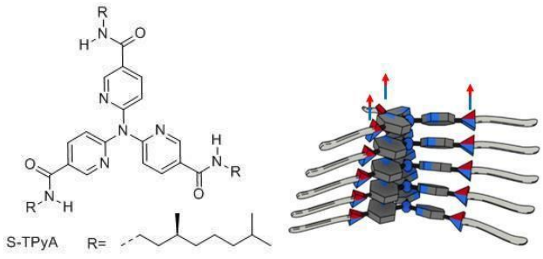


*Figure 1: Structural formula and visualisation of the S-TpyA molecule. In the ferroelectric phase, the discotic molecules form polar columns. The polarity of the columns arises from the amide dipole moments and can be switched along the column.*

## Results and Discussion

The combination of dielectric spectroscopy (DRS) with pyroelectric response measurements (LIMM) during different bias field conditions reveals the ferroelectric nature of the liquid crystals. For TpyA, **Fig. 2**, the LIMM measurement reveals a dead layer at the first 70 nm of the electrode interface, an intermediate layer strongly influenced by trapped injected charges in the range of 70 to 150 nm from the electrode and bulk behavior at further depth.

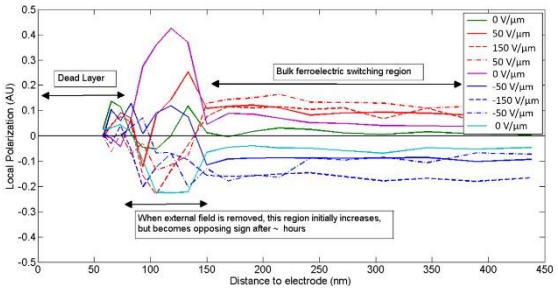


*Figure 2: Polarization profile of TpyA, obtained via LIMM. Three regions can be identified.*

Further measurements using DRS and Tower-Saywer techniques reveal that more than 50% of the polarization can be attributed to charges injected and trapped in the ferroelectric material.

## Conclusions

These organic ferroelectrics are susceptible to charge injection and trapping, which plays a crucial role in lowering the coercive field and stabilizing the polarization. Quite similar to the well known PVDF.

## References

[1] Womes M., Bihler E., Eisemenger W. (**1989**), IEEE Trans. Electr. Insul. 24, 461
[2] Putzeys T., Wübbenhorst M. (**2015**). Phys Chem Chem Phys (17), art.nr. 10.1039/C4CP06033D, 7767-7774
[3] Gorbunov A., Putzeys T., Urbanaviciute I., Janssen R., Wübbenhorst M., Sijbesma R., Kemerink M. (**2016**). Phys Chem Chem Phys, 18 (34), 2366323672.

# Change in the ferroelectric to paraelectric phase transition order in P(VDF-TrFE) copolymer ultra-thin films

Danny von Nordheim, Bernd Ploss

bernd.ploss@eah-jena.de

Department of SciTec, University of Applied Sciences Jena, Carl-Zeiss-Promenade 2, 07745 Jena, Germany

**Abstract:** Dielectric non-linearities in P(VDF-TrFE) ferroelectric thin films were measured in order to prove a thickness dependent change in the ferroelectric to paraelectric phase transition order. The relation between the second order non-linear permittivity $\varepsilon_3$ and the second Landau parameter $\gamma$ was used to derive the type of transition present in the thin films. It has been found, that the change in the sign of $\varepsilon_3$ for a 30 nm thin film possibly indicates a change in the Curie transition from 2nd to 1st order.

**Keywords:** Ferroelectrics, Phase Transition, P(VDF-TrFE), Thin Films

## Introduction

Due to their unique properties, thin films of ferroelectric materials have drawn increasing attention during the last years. They can be used in numerous applications, e.g. in thin film ferroelectric field effect transistors for non-volatile memory storage. It is well known, that the minimisation of thickness below a certain limit leads to a change in properties, i.e. in ultra-thin films. One of the key properties of a ferroelectric material is the order of Curie transition it undergoes.

## Results and Discussion

As published earlier [1], the higher order non-linear permittivities in the paraelectric phase can be related to the Landau parameters. By using the equations for the free energy $F$ and the dielectric displacement $D$:

$$F = F_0 + \frac{\alpha}{2} D^2 + \frac{\gamma}{4} D^4 + \frac{\delta}{6} D^6 - ED$$

$$D = P_S + \varepsilon_0 \varepsilon_1 E + \varepsilon_0 \varepsilon_2 E^2 + \cdots$$

it can be derived, that in the paraelectric phase the Landau parameter $\gamma$ and the permittivity $\varepsilon_3$ are related in the following way:

$$\varepsilon_0 \varepsilon_3 = -\gamma/\alpha^4.$$

Furthermore, the type of phase transition is determined by the sign of the second Landau parameter $\gamma$. While a negative sign indicates a first order phase transition, a positive sign will be assigned to a second order phase transition. As can be seen from the relation above, for $\varepsilon_3$ the opposite is true. *Qu* et al. [2] have suggested a change of the transition order for thin films, while *Ong* et al. [3] have concluded otherwise.

While our approach is of different nature, Figure 1 clearly indicates an alternation of the sign of $\varepsilon_3$ in the paraelectric phase if decreasing the thicknesses of the film. In the paraelectric phase we generally observe a negative $\varepsilon_3$ for films thicker than 100 nm indicating a second order transition. If the thickness is decreased to 30 nm, $\varepsilon_3$ stays positive after the ferroelectric to paraelectric phase transition.

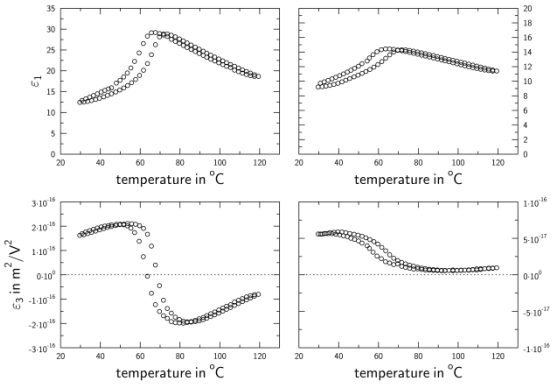


*Figure 1: Permittivities $\varepsilon_1$ and $\varepsilon_3$ for a 130 nm thick (left) and a 30 nm (right) thick P(VDF-TrFE) thin film.*

## Conclusions

It has been shown, that reducing the thickness of P(VDF-TrFE) ferroelectric thin films with molar ratio 56/44 causes a change in the sign of the second order non-linear permittivity $\varepsilon_3$. Using the equations derived earlier, this alternation indicates a change in the ferroelectric to paraelectric phase transition from second to first order.

## References

[1] D. von Nordheim, S. Hahne, B. Ploss, *Ferroelectrics* **2013**, *453*, 122-126.

[2] Bao-Dong Qu, Wei-Lie Zhong, Pei-Lin Zhang, *J. Phys.: Condens. Matter* **1994**, *6*, 1207-1212.

[3] Lye-Hock Ong, Junaidah Osman, D. R. Tilley, *Physical Review B* **2001**, *63*, 144109-1-10.

# Soft-X-ray-charged Piezoelectret with Embedded Electrodes

Jia Lu [1], Yuji Suzuki[1]

Email: jlu@mesl.t.u-tokyo.ac.jp

[1]Dept. of Mechanical Eng., The University of Tokyo, Hongo, Bunkyo-ku, 113-8656 Tokyo, Japan

**Abstract:** A flexible piezoelectret energy harvester with embedded electrodes is proposed. With the aid of soft X-ray charging and high-performance electret CYTOP-M, output power of 2.8 μJ has been obtained for 0.6 mm displacement in 0.4 s, with the max applied mechanical force as low as 0.9 N and piezoelectric coefficient $d_{33}$ as high as 16000 pC/N.

**Keywords:** piezoelectret energy harvesting, soft X-ray charging, flexible structure

## Introduction

Piezoelectret attracts much attention in energy harvesting due to its high piezoelectric coefficient [1] and its softness. Multi-layered piezoelectret structures are often built [2]. However, the effective bias voltage per layer for a multi-layered structure is much lower than the grid voltage during corona charging. To address this issue, we have proposed a multi-layered structure with embedded electrode [3] that can be efficiently poled with the soft X-ray charging [4]. In this paper, we devise a much softer piezoelectret by using MEMS technique and high-performance electret material CYTOP CTL-M [5].

## Device Design and Fabrication Process

As shown in Fig. 1, thin-film electrodes are integrated into the multi-layered structure, so that the bias voltage is directly applied to each layer during the soft X-ray charging. The electromechanical model with an electrostatic model [1] and a non-linear beam deflection model is used for the device design. 20 μm-thick parylene-C layers with a Cr/Au/Cr electrode are used as the membrane. 200 μm-high SU-8 pillars are patterned on the parylene-C layer by photolithography. After detachment from the wafer, chips shown in Fig. 2a are dip-coated with high-performance electret CYTOP-107M (Asahi Glass), with the coating thickness of 7 μm on each surface. Finally, stacked 4layered structure is formed and charged with soft X-ray charging.

## Experiments, Results and Discussion

Power generation experiment is made using a setup shown in Figure 2b and 2c. The 4-layered structure is poled using soft X-ray charging with bias voltage of 600 V for 30 min. Fig. 3 shows the deformation applied to the piezoelectret and the output voltage with different external loads. Up to 100 V is obtained for 0.6 mm displacement in 0.4 s, which corresponds to 2.8 μJ output energy. The effective Young's modulus is as slow as 15 kPa, so that the maximum applied force is as low as 0.9 N. This leads to extremely-large $d_{33}$ of 16000 pC/N, which is even higher than recent cellular PDMS ($d_{33}$ ~ 1148 pC/N) [2].

## Conclusions

In this research, we have proposed a flexible soft-Xray-charged 4-layered piezoelectret energy harvester. It generated 2.8 μJ output energy with max force applied 0.9 N and $d_{33}$ ~ 16000 pC/N.

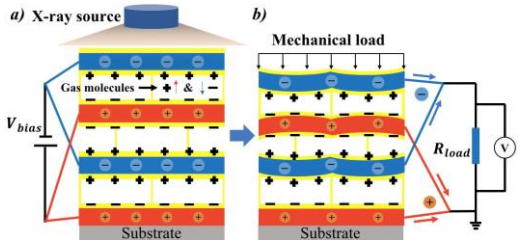


*Figure 1. Multi-layered piezoelectret structures with embedded electrodes. a) Charging, b) Operation.*

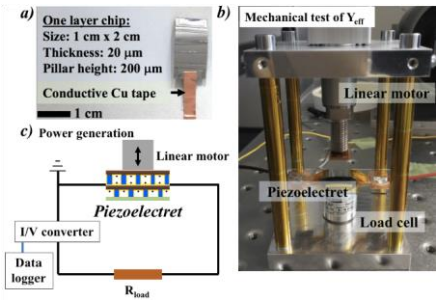


*Figure 2. a) single layer chip dip-coated by CYTOP. b) measurement of effective Young's modulus using a load cell. c) schematic of power generation experiment.*

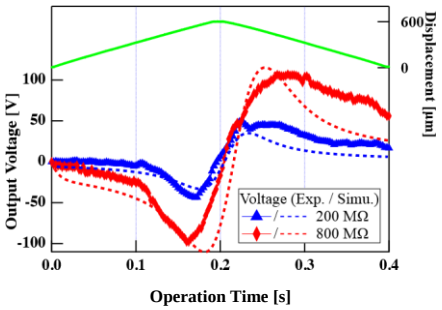


*Figure 3. Results of power generation experiment versus modelling using a 4-layered soft X-ray charged piezoelectret.*

## References

[1] G.M. Sessler et al., *Appl. Phys. Lett.*, 75, 3405 (1999).
[2] J.-J. Wang et al., *J. Micromech. Microeng.*, 22, 015013 (2012).
[3] J. Lu et al., *J. Phys.: Conf. Ser.*, 773 (2016).
[4] K. Hagiwara et al., *IEEE Trans. DEI.*, 19, 1291 (2012).
[5] Y. Sakane et al., *J. Micromech. Microeng.*, 18, 104011 (2008).

# On the generation of polarity:
# A property being not allowed for a stationary state

Jürg Hulliger[1]

juerg.hulliger@iac.unibe.ch

[1]Department of Chemistry and Biochemistry, University of Berne, Freiestr. 3,
3012 Berne, Switzerland

**Abstract:** The polar state of macroscopic objects is investigated by Monte Carlo methods, calculations of the inner electrical field and by experimental methods to study surface charge effects and the inhomogeneous spatial distribution of polarity in various materials (pyroelectric and phase-sensitive second harmonic microscopy).

**Keywords:** stochastic polarity formation, bi-polar state, reversal transition

## Introduction

In recent years the reinvestigation of the polar state of condensed molecular matter has led to a number of discoveries. Fundamental inside was gained by theoretical methods using Monte Carlo simulations and application of scanning pyroelectric and phase-sensitive second harmonic microscopy. A consistent view emerged covering phenomena found for molecular crystals, bio-mimetic inorganic-organic composite materials and biological tissues [1].

## Results and Discussion

Materials showing a polar symmetry feature surfaces carrying a charge density. At ambient conditions this charge gets compensated by charge carriers from the environment. Presently, we know only little about such processes. Calculations of the inner and outer electrical field of polar molecular crystals show that even in the surface charge compensated state a crystal can keep a net dipole moment. Further on, calculations demonstrate that the direction of the inner field depends on the relative size of a crystal (e.g. needle vs plate). This has a strong impact on the enhancement or reduction of the strength of electrical properties of molecular matter described by tensors. Present experimental work is thus focussing on a demonstration of surface charge effects by cutting crystals in the high vacuum or in air.

Further work is directed to understand how polar order in e.g. molecular crystals can emerge during the process of growth. This involves also theoretical investigations on nm sized seed crystals. Here, Monte Carlo simulations revealed a *bi-polar state* for seeds where building blocks can undergo 180° orientational disorder [2]. In the case of growth, Monte Carlo simulations have found a *reversal transition* when growth starts upon a polar seed [3]. This means, along one direction of the polar axis, suddenly dipolar entities start to invert their direction leading to a complete reversal of almost all dipoles of a growing sector. The resulting growth state is also a bi-polar state [4].

Scanning pyroelectric and phase-sensitive second harmonic microscopy have confirmed both the *bipolar state* and the *reversal transition* for some molecular crystals. Further evidence for such processes was gained by investigating solid solutions of molecular crystals built of dipolar entities grown in the presence of symmetrical entities. Here, the polarity in the bi-polar state got inverted, being in agreement with corresponding Monte Carlo simulations.

Expanding the experimental work to bio-mimetic inorganic-organic composite materials and natural tissues we find also bi-polar states for minerals grown in various long chain bio-genic gels [5]. In the case of natural tissues the analysis of bones and cementum of teeth has led to similar results [6].

## Conclusions

The stationary state of condensed molecular matter made of dipolar entities undergoing 180° orientational disorder (near the surface in the bulk or during growth) is represented by a bi-polar and in principle zero net polarity object. This is in agreement with a quantum statistical statement saying that the stationary state of a system does not carry an electrical dipole moment [7].

## References

[1] J. Hulliger et al. *New J. Chem.* **2013**, *37*, 2229-2235.
[2] J. Hulliger et al. *Z. Kristallogr.* **2013**, *228*, 607-610.
[3] T. Wüst et al. *Phil. Mag.* **2007**, *87*, 1683-1703.
[4] J. Hulliger et al. *Cryst. Growth Des.* **2012**, *12*, 52115218.
[5] M. Burgener et al. *Biomacromol.* **2015**, *16*, 28142819.
[6] H. Aboulfadl et al. *J. Struc. Biol.* **2015**, *192*, 67-75.
[7] P.W. Anderson, *Science* **1972**, *177*, 393-396.

## Acknowledgements

Funded by the Swiss SNF (200020_159231).

# Screen printed PVDF-TrFE-*co*-$PbTiO_3$ nanocomposite for selective piezo- or pyroelectric sensing

Jonas Groten [1], Martin Zirkl[1], Daniela Collin[2], Gerhard Domann[2], Barbara Stadlober[1]

jonas.groten@joanneum.at

[1]Joanneum Research Forschungsgesellschaft mbH, MATERIALS Institute, Leonhardstr. 59, A-8010 Graz, Austria

[2]Fraunhofer Institut für Silicatforschung, Neunerplatz 2, D-97082 Würzburg, Germany

**Abstract:** Piezo- and pyroelectricity are intrinsically combined material properties within ferroelectric materials. While the pyroelectric coefficients of PVDF-TrFE and $PbTiO_3$ have the same sign, their piezoelectric coefficients have opposing signs. This property can be used to create a composite material where either the piezo- or pyroelectric effect is cancelled out by a selective poling of the single constituents. We have formulated a screen-printable nanocomposite paste and successfully produced sensors that are either piezo- or pyroelectric on flexible substrates suitable for low-cost and large area applications.

**Keywords:** ferroelectric composites, screen-printing, PVDF-TrFE, $PbTiO_3$

## Introduction

Fully screen-printed ferroelectric polymer sensors based on PVDF-TrFE have been developed to a ready to market technology within the last decade [1]. The intrinsic combination of pyroelectric and piezoelectric activity of ferroelectric materials is, however, unsatisfactory for a wide range of applications, especially where quantitative measurements of temperature or pressure changes are required. Ploss *et al.* [2] and Graz *et al.* [3] addressed this problem already in the late 1990s and showed that a composite from PVDF-TrFE and $PbTiO_3$ nanoparticles allows to generate a selectively temperature or pressure responsive material. These results, however, remained an academic curiosity as the materials involved could not been easily processed.

We successfully paved the way for low-cost and large area applications of these nanocomposites by formulating a screen-printable paste and identifying a successful poling routine to the entirely screen-printed sensors.

## Results and Discussion

Since $PbTiO_3$ has a much higher Curie temperature than PVDF-TrFE a separate poling of the two constituents within the composite is possible. In a first step the inorganic particles are poled by applying an electric field above the Curie temperature of the polymer and in a second step an alternating electric field at room temperature can be used to pole the polymer matrix not affecting the orientation of the inorganic particles. Stopping this process either after a positive or negative half-wave results in a parallel or antiparallel orientation of the spontaneous polarization of the two ferroelectrics. The applied field strength in the poling process can be tuned to achieve a full suppression of the pyro- or piezoelectric response in a material with a proper $PbTiO_3$ to PVDF-TrFE ratio.

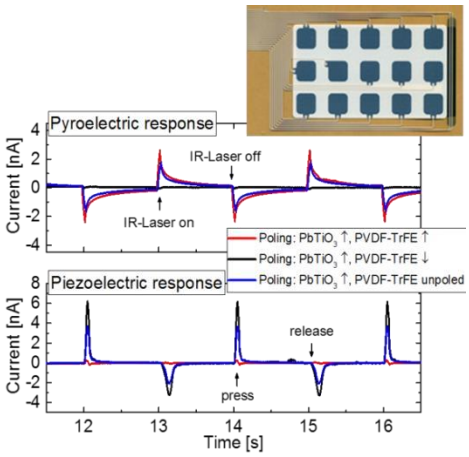


*Figure 1: Pyroelectric and Piezoelectric response of differently poled and entirely screen printed nanocomposite sensors selectively supressing the pyro- or piezoelectric signals.*

## Conclusions

The presented all-screen-printed nanocomposite sensors allow for the suppression of the crosstalk between piezo- and pyroelectricity and are hence robust against thermal drift or unwanted pressure signals arising e.g. from sensor movement in flexible or wearable applications.

## References

[1] Rendl, C.; Kim, D.; Fanello, S.; Parzer, P.; Rhemann, C.; Taylor, J.; Zirkl, M.; Scheipl, G.; Rothländer, T.; Haller, M.; Izadi, S. UIST '14 (ACM, NY, USA) **2014**, doi:10.1145/2642918.2647405

[2] Ploss, B.; Ploss, B.; Shin, F. G.; Chan, H.L.W.; Choy, C. L. APL 76(19) **2000**, doi:10.1063/1.126472

[3] Krause, M.; Graz, I.; Bauer-Gogonea, S.; Bauer, S.; Ploss, B.; Zirkl, M.; Stadlober, B.; Helbig, U. Ferroelectrics **2011**, doi:10.1080/00150193.2011.594412

## Acknowledgements

The research leading to these results has received funding from the EU, FP7/2007-2013 under grant agreement No 611104 with the project title FLASHED.

# First Principles Design of Organic Piezoelectric Devices

Sarah Guerin[1], Dr. Syed A. M. Tofail[1], and Dr. Damien Thompson[1]

sarah.guerin@ul.ie

[1]Department of Physics, Bernal Institute, University of Limerick, Ireland

**Abstract:** Piezoelectric materials exhibit the unique characteristic of becoming electrically charged when strained and conversely, becoming deformed in the presence of an electric field. Inorganic piezoelectric materials have been exploited for decades as nanogenerators, biosensors, resonators, acoustics, and in scanning probe microscopy (SPM). Here we present organic crystals as a basis for such applications, based on experimentally validated quantum mechanical models. Our models can quantify the piezoelectric response of small biomolecular crystals, and uncover significant electromechanical coupling along hidden crystallographic planes of up to 200 pm/V. In this project we present both our theoretical and experimental data on amino acid crystals, highlighting their low permittivity and high flexibility. Amino acids are the building blocks of proteins and other biological structures and in their uncrystallised form regulate a number of our bodies' functions.

**Keywords:** Piezoelectricity, biomolecules, molecular modelling, energy harvesting

## Introduction

Many hierarchal biological structures have been found to be piezoelectric[1-5]. This means that these materials are able to produce electricity proportional to an applied mechanical strain, and conversely, deform linearly in the presence of an applied electric field. Fibrous proteins such as collagen[2] and elastin,[3] bone[1] (calcified collagen), and some viruses[5] have, to date, exhibited relatively modest piezoelectricity, of the order of 0.1 pm/V to 10 pm/V. Deoxyribonucleic acid (DNA) has been known to be piezoelectric[6] for a long time, but the origin of piezoelectricity in DNA remains unclear and its quantitative value is uncertain. This contrasts with a variety of inorganic materials such as barium titanate ($BaTiO_3$)[7], polyvinylidene fluoride (PVDF)[8] and lead zirconate titanate (PZT)[9]. These materials exhibit relatively high piezoelectricity (20-800 pm/V) which is well understood, successfully engineered, and exploited

## Results and Discussion

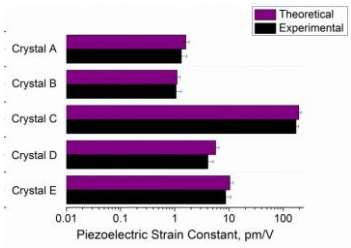


*Figure 1: An extremely high predictability can be seen between our quantum mechanical predictions and our experimental results for crystallised, undoped amino acids.*

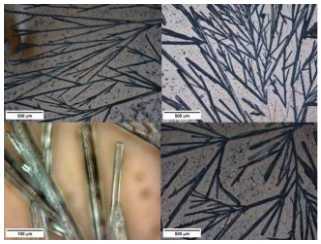

*Figure 2: Optical images of monoclinic amino acid crystals grown on a flexible substrate for sensing and energy harvesting applications*

- Density Functional Theory accurately predicts the piezoelectric behaviour of inorganic and organic materials.
- Amino acid crystals exhibit large and technologically significant piezoelectric constants
- Our research has validated piezoelectric strain constants of up to 178 pm/V in undoped amino acids, as well as amino acid energy harvesting voltages of 400 mV along longitudinal crystal planes
- Our calculations predict that the shear planes of amino acid crystals have unexploited electromechanical coupling potential an order of magnitude higher than conventional piezoelectric ceramics

## Conclusions

- Studying the electronic structure of crystallised biomolecules using quantum mechanics can aid understanding of biological macromolecules and assemblies
- Biomolecules with large and programmable piezoelectricity have huge potential in areas from improved energy harvesting technologies to deeper understanding of the role of electrical properties in evolutionary biology

## References

[1] Fukada, E.; Yasuda, I., Journal of the Physical Society of Japan 1957, 12 (10), 1158-1162.
[2] Fukada, E.; Yasuda, I.,. Japanese Journal of Applied Physics 1964, 3 (2), 117.
[3] Liu, Y.; Cai, H.-L.; Zelisko, M.; Wang, Y.; Sun, J.; Yan, F.; Ma, F.; Wang, P.; Chen, Q. N.; Zheng, H., Proceedings of the National Academy of Sciences 2014, 111 (27), E2780-E2786.
[4] Gandhi, A. A.; Wojtas, M.; Lang, S.; Kholkin, A. L.; Tofail, S. A., Journal of the American Ceramic Society 2014, 97 (9), 2867-2872.
[5] Lee, B. Y.; Zhang, J.; Zueger, C.; Chung, W.-J.; Yoo, S. Y.; Wang, E.; Meyer, J.; Ramesh, R.; Lee, S.-W.,. Nature nanotechnology 2012, 7 (6), 351-356.
[6] Ando, Y.; Fukada, E., Journal of Polymer Science: Polymer Physics Edition 1976, 14 (1), 63-79.
[7] Berlincourt, D.; Jaffe, H., Physical Review 1958, 111 (1), 143.
[8] Fukada, E., Ultrasonics, Ferroelectrics, and Frequency Control, IEEE Transactions on 2000, 47 (6), 1277-1290.
[9] Damjanovic, D., Reports on Progress in Physics 1998, 61 (9), 1267.

## Acknowledgements

Science Foundation Ireland Research for Medical Devices (CÚRAM) and the SFI Irish Center for High-End Computing
(ICHEC)

# Influence of elevated temperature and humidity on the electrical-insulation behaviour of cellular polypropylene (PP) foams

Xunlin Qiu, Frederick Groth, Werner Wirges, and Reimund Gerhard
Corresponding e-mail addresses: xunlin.qiu@hotmail.com or reimund@ieee.org
Applied Condensed-Matter Physics, Faculty of Science, University of Potsdam
Karl-Liebknecht-Strasse 24-25, 14476 Potsdam-Golm, Germany

**Abstract:** The influence of severe storage environment (elevated temperature and humidity) on the electrical insulation behaviour of cellular polypropylene is studied in comparison to their piezoelectret properties. The breakdown strength of the sample slightly increases with storage time up to 1000 h at 70 and 90 °C, while the piezoelectric $d_{33}$ coefficients decreases rapidly. At a rather high relative humidity of 95%, the breakdown strength perceptibly increases with storage time, and the $d_{33}$ coefficient slightly decreases.

**Keywords:** cellular polypropylene foams, electrical insulation, piezoelectricity, ferro- and piezoelectrets

## Introduction

Ferroelectrets are internally charged polymer foams that show high piezoelectricity [1]. In recent years, the piezo- and ferroelectricity of ferroelectrets has been investigated extensively. Dielectric polymers are more often used for electrical insulation e.g. in electronic devices or in signal and power cables. However, the electrical-insulation properties of the ferroelectret polymer-foam materials have not yet been studied in sufficient detail [2]. Here, we explore the influence of elevated temperature and humidity on the electrical-insulation behaviour of cellular polypropylene (PP) foams in comparison to their charging-induced piezoelectric properties.

## Results and Discussion

Cellular PP foam films with an initial thickness of 40 µm and an initial density of 620 kg/m$^3$ have been provided by Treofan, Germany (tradename VHD40). For breakdown tests, circular samples (diameter 3 mm) are mounted between a spherical top electrode and a plate as bottom electrode. A linearly increasing voltage ramp (HV power supply FUG HCP35-35000) was applied to the spherical top electrode at a rate of 100 V/s till breakdown. For assessing piezoelectric properties, the samples were inflated via gas-diffusion expansion, followed by corona charging for 15 s with a tip voltage of 20 kV. After charging, the samples were metallized on both surfaces with aluminium electrodes.

In order to study the influence of elevated temperatures, the samples were stored in an oven at 70 and at 90 °C. After selected time periods of storage, breakdown strength and piezoelectric $d_{33}$ coefficient were determined. Seven samples were used for each breakdown test, and the average of the breakdown strength was calculated. The $d_{33}$ coefficient was determined dielectric resonance spectroscopy (DRS) [3] on another sample that could be used again. The $d_{33}$ coefficient decays relatively fast already at 70°C, consistent with previous studies. The breakdown strength slightly increases with storage time up to 1000 h at 70 and 90 °C, which might be attributed to thermally induced changes in the microstructure of the molecules and to a reduction of free volume inside the polymer matrix.

The influence of high humidity is shown in Fig. 1. During storage under a relative humidity of 95%, the $d_{33}$ coefficient decays only slightly, while the breakdown strength increases noticeably. To achieve higher breakdown strength in the polymer foams, dielectric barrier discharges inside the cavities should be avoided (Otherwise, the electric field in the cavities will be partially or completely cancelled, and the electric field in the polymer layers will thus significantly increase.). Our results indicate that storage in very humid environments reduces the chargeability of the foam cavities.

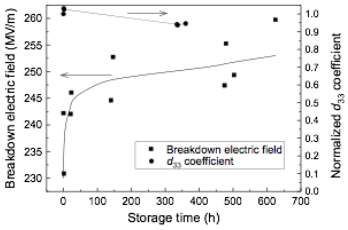


*Figure 1: Breakdown field (squares, left ordinate) and piezoelectric $d_{33}$ coefficient (circles, right axis) versus time of storage under 95% relative humidity.*

## Conclusions

The influence of a high-humidity and elevated-temperature environment on the breakdown strength and the piezoelectricity of cellular PP foam has been studied. $d_{33}$ decays rapidly already at 70 °C, while the breakdown strength increases slightly over time at 70 and 90 °C. At a relative humidity of 95%, the breakdown strength increases with time, and the $d_{33}$ coefficient slightly decreases.

## References

1. S. Bauer, R. Gerhard(-Multhaupt), and G. M. Sessler, *Phys. Today* **57**(2), 37 (2004), doi: 10.1063/1.1688068.
2. X. Qiu, et al., *IEEE Int. Conf. High Voltage Eng. Appl. (ICHVE)* **2016**, doi: 10.1109/ICHVE.2016.7800761.
3. Mellinger, IEEE Trans. Dielectr. Electr. Insul., 10, 842-861 (2003), doi: 10.1109/TDEI.2003.1237333.

# Structure and piezoelectric properties of self-polarized ferroelectric polymer thin film

Takashi Nakajima [1,2], Masanari Miyamoto [1], Yuuta Nakagawa [1], Yoichiro Hashizume [1], and Soichiro Okamura [1] nakajima@rs.tus.ac.jp

[1]Department of Applied Physics, Faculty of Science, Tokyo University of Science, 6-3-1 Niijuku, Katsushika, Tokyo 125-8585, Japan

[2] PRESTO, Japan Science and Technology Agency, 4-8-1 Honcho, Kawaguchi-shi, Saitama 332-0012, Japan

**Abstract:** We report on the self-polarization phenomenon observed in melt-crystallization process of ferroelectric polymer thin film. Ferroelectric polarization from top to bottom electrode was spontaneously formed when Pt was used as the bottom electrode. The driving force of the self-polarization remained after the fabrication and the effect of inhomogeneous film structure on the self-polarization was suggested.

**Keywords:** self-polarization, ferroelectric polymer, PFM

## Introduction

Controlling the ferroelectric polarization without electric poling is one of the key technological requirements for printable electronics using piezoelectric polymers. In this talk, we shall focus on the self-polarization alignment of ferroelectric polymer thin films by thermal annealing process. The mechanism of forming the polarization will be discussed on the basis of the interfacial effects and the crystallization process analysed by piezoelectric force microscope (PFM).

## Results and Discussion

We prepared VDF/TrFE and VDF/TeFE copolymer thin films on Pt- or Au-suputtered Si substrate by spin coating. The average thickness of the ferroelectric layers before thermal treatment is approximately 300 nm. To crystallize the thin films, we applied a melt crystallization process.[1] Figure 1 shows PFM image of VDF/TeFE copolymer thin film crystalized at 383 K on Pt electrode. To evaluate the polarization direction, electric poling was done on the center position using the AFM tip. Based on the phase image, polarization direction from top to bottom electrode ($P\downarrow$) is spontaneously formed in the as-grown thin film. The remanent polarization was evaluated to be 40 mC/m$^2$, which showed good agreement with the poled sample.[2] To evaluate the stability of the polarization, we compared domain growth under electric field pulse. As shown in Fig.2, polarization reversal toward $P\downarrow$ is easier, indicating the driving force of the self-polarization remains after the fabrication. Cross-sectional TEM image have revealed that the thin film is composed of two layers. The formation of the inhomogeneous layer at the interface of the bottom electrode could play an important role for the self-polarization. The mechanism will be discussed based on the quantitative structural analyse.

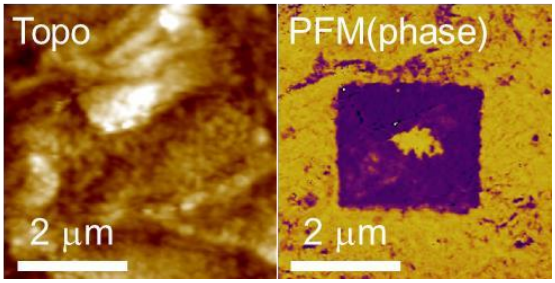


*Figure 1: Topographic and PFM images of VDF/TeFE copolymer thin film.*

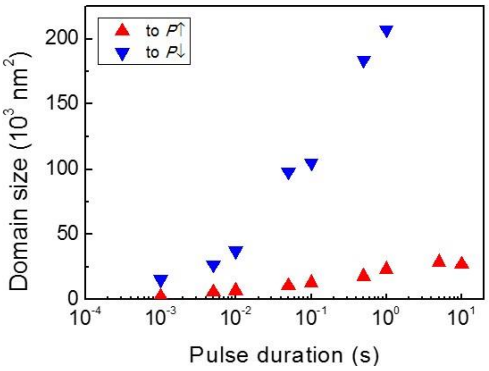


*Figure 2: Plots of grown domain size vs pulse duration for the VDF/TeFE copolymer.*

## References

[1] Y. Nakagawa, Y. Hashizume, T. Nakajima, and S. Okamura. *Jpn. J. Appl. Phys.* **2016**, doi: 10.7567/JJAP.55.051601.

[2] Y. Nakagawa, Y. Hashizume, T. Nakajima, A. Gruverman and S. Okamura. *Jpn. J. Appl. Phys.* **2016**, doi: 10.7567/JJAP.55.10TA12.

## Acknowledgements

This work was supported by JST PRESTO grant number JPMJPR16R4 and JSPS KAKENHI grant number 17H04814.

# Dielectric relaxations and ferroelectric behaviour of thin films of trialkylbenzene-1,3,5-tricarboxamide (BTA)

Michael Wübbenhorst[1], Andrey V. Gorbunov[2], Tristan Putzeys[1], Indre Urbanavičiūtė[3], Rene A.J. Janssen[4], Rint P. Sijbesma[4], Martijn Kemerink[3]

wubbenhorst@kuleuven.be

[1]Department of Physics and Astronomy, KU Leuven, Celestijnenlaan 200D, 3001 Heverlee, Belgium
[2]Department of Applied Physics, Eindhoven University of Technology, 5600 MB Eindhoven, The Netherlands
[3]Department of Physics, Chemistry and Biology (IFM), Linköping University, 58183 Linköping, Sweden
[4]Laboratory of Macromolecular and Organic Chemistry, Eindhoven University of Technology, 5600 MB Eindhoven, The Netherlands

**Abstract:** We have studied the dielectric relaxations and the ferroelectric switching behaviour of hydrogenated and deuterated BTA's at different temperatures and under the influence of (high) dc-bias fields. From all results, a consistent physical picture emerges that rationalizes the strength (easy self-assembly of macrodipoles) and drawbacks (columnar inversion by local mechanisms) of the supramolecular approach towards polar organic ferroelectric materials.

**Keywords:** dielectric relaxation spectroscopy, organic ferroelectrics, Curie-Weiss law, macrodipoles

## Introduction

Trialkylbenzene-1,3,5 tricarboxamides (BTAs) [1] represent a novel class of organic ferroelectric materials, the ferroelectric properties of which rely on a liquid crystalline columnar hexagonal arrangement of H-bonded, stacked polar disc-shaped building blocks. In this work the nature of the polar switching process is investigated by a combination of dielectric relaxation spectroscopy, depth-resolved pyroelectric response measurements, as well as classical frequency- and time-dependent electrical switching experiments.

## Results and Discussion

Dielectric spectroscopy revealed several molecular relaxation processes that can be assigned to short columnar reorientation (α-process), collective polarisation inversion in long columns (R-process) as well as a fast, third relaxation mode related to pre-transitional effects [2]. In addition, Curie-Weiss behaviour was found supporting the true ferroelectric nature of the $Col_{hex}$-phase.

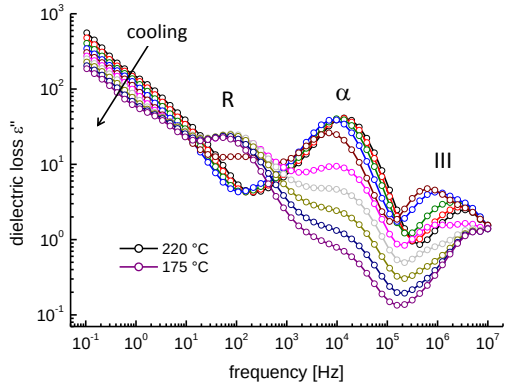


*Figure 1: Dielectric loss spectrum op BTA-C18 at temperatures around the ferroelectric/paraelectric phase transition showing the characteristic α- and R-relaxation as well as process III associated with the Curie-Weiss behaviour.*

Further experiments were devoted to understanding the limited temporal stability of the remnant polarisation at elevated temperatures; here, dielectric measurements under high electric dc-fields confirmed the role of collective H-bonding dynamics in conjunction with amide-flips, which manifests in both a field-dependent dc-conductivity and relaxation strength of the R-process.

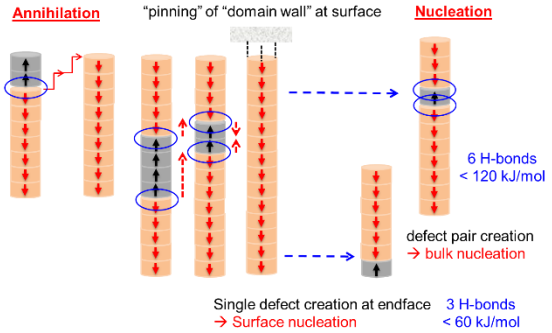


*Figure 2: Various proposed mechanisms for the nucleation, pinning and annihilation of columnar inversion defects as deduced from dielectric spectroscopy measurements under dc-bias fields.*

## Conclusions

Based on linear and nonlinear dielectric spectroscopy we have developed microscopic models that rationalize the ferroelectric behaviour of BTA's, the limited retention time as well as the temperature dependence of all relaxation processes.

## References

[1] C.F.C. Fitié, W.S.C. Roelofs, P.C.M.M. Magusin, M. Wübbenhorst, M. Kemerink, R.P. Sijbesma, *J. Phys. Chem. B* **2012**, *116*, *3928*.

[2] A. V. Gorbunov, T. Putzeys, I. Urbanavičiūtė, R. A. J. Janssen, M. Wübbenhorst, R. P. Sijbesma, M. Kemerink, *Phys. Chem. Chem. Phys.* **2016**, *18*, *23663*

# Revisiting Ferroelectricity in Nylons

Saleem Anwar [1], Kamal Asadi [1]

asadi@mpip-mainz.mpg.de

[1] Max Planck Institute for Polymer Research, Ackermannweg 10, 55128, Mainz, Germany

**Abstract:** Melt quenching of nylon films induces polar but highly defective crystalline structure. The dipoles in these weekly hydrogen bonded chains can be switched under applied electric field; resulting ferroelectricity in odd nylons. We have processed both odd and even nylons. Contrary to the common knowledge, we show that ferroelectricity is a common attribute of the nylon family.

**Keywords:** Ferroelectric crystalline phase, Ferroelectricity, Nylons

## Introduction

Among ferroelectric polymers, poly(vinylidene fluoride-trifluoroethylene) (P(VDF-TrFE)) has the highest piezoelectric and ferroelectric response at room temperature. However, low thermal stability of the polarization and high cost limit application of P(VDF-TrFE)[1]. While the research on alternative ferroelectric polymers is mainly focused on PVDF homo-polymer, other ferroelectric polymers such as nylons are overlooked. Nylons are inexpensive commodities. Piezoelectricity and ferroelectricity in odd nylons have been demonstrated. The question is whether ferro-electricity is limited to only odd nylons?

## Results and Discussion

Ferroelectric crystalline phase is obtained by uniaxial stretching of melt-quenched films with a drawing ratio of 3:1. Grazing incident wide angle X-ray scattering was performed to study the molecular organization of the films. We show that stretching induces a pronounced molecular organization along the polymer chain whereas non-stretched films showed lack of preferential order. In-situ high temperature XRD measurements have shown that the ferroelectric $\delta'$-phase does not change upon heating the films at higher temperature, whereas upon cooling, the films transform to the paraelectric $\alpha'$-phase. Parallel-plate capacitors were fabricated to study electromechanical response of nylons. Remanent polarization for melt-quenched-stretched films amounted to 5.6 ($\mu C/cm^2$); which is comparable to that of PVDF and its copolymer.

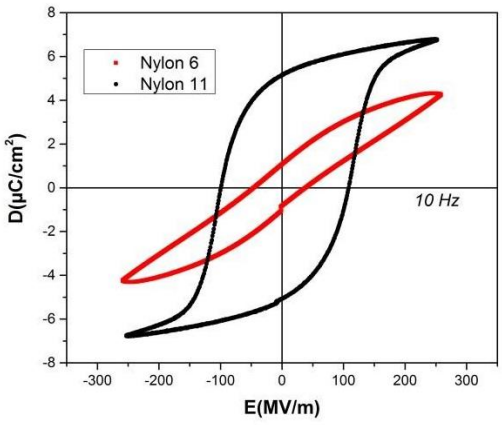


*Figure 1:* Room temperature ferroelectric hysteresis loop of nylon 6 and nylon 11

## Conclusions

Ferroelectric crystalline phase can be achieved by stretching the melt-quenched films. Observation of ferroelectricity in both odd and even nylons opens doors to unlimited numbers of commodity ferroelectric polymers.

## References

[1] Li, M., Wondergem, H. J., Spijkman, M. J., Asadi, K., Katsouras, I., Blom, P. W., & De Leeuw, D. M. (2013). Nature materials, 12(5), 433-438.

## Acknowledgements

We would like to acknowledge Wojciech Zajaczkowski for GWAX measurements and Alexander von Humboldt Foundation for the financial support.

# Polarized tubular fluoropolymer arrays with high piezoelectric response

Sergey Zhukov, Dagmar Eder-Goy, Bai-Xiang Xu and Heinz von Seggern

seggern@e-mat.tu-darmstadt.de

Institut für Materialwissenschaft, Technische Universität Darmstadt, Alarich-Weiss-Straße 2, 64287 Darmstadt, Germany

**Abstract:** A new approach for production of polymer piezoelectret arrays with open-tubular channels from commercial FEP tubes has been developed. By fusion bonding, flat arrays from regular tubular air cavities were produced and their piezoelectric properties were explored experimentally and theoretically. In addition, issues concerning temporal stability, optimal charging conditions and stability of the piezoelectric characteristics at different pressures and frequencies were experimentally investigated.

**Keywords:** ferroelectrets, piezoelectrets, piezoelectric response

## Introduction

A new kind of soft voided polymer materials with very high $d_{33}$ piezoelectric coefficients named ferroelectrets attracted considerable attention of researchers during the last years [1-3]. Since the initially very promising cellular polypropylene was not stable enough at temperatures above $+60^0$C, the search for novel suitable materials continues. Here, a new approach for fabrication of arrays with tubular channels from FEP tubes will be presented.

## Results and Discussion

Figures 1(a) and 1(b) display schematically the preparation procedure of a tubular array from a set of FEP tubes. In the first stage, about 25-30 tubes were regularly mounted on the bottom metal plate. Then the whole assembly was compressed so that the tubes took the form of an oval stadium. After that the assembly was heated up to $+260^0$C.

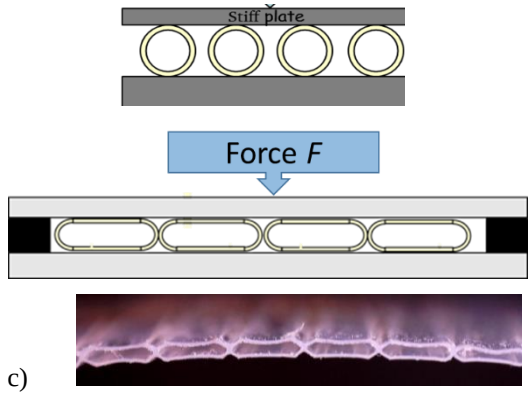


c)

*Figure 1. Schematic view of the preparation of a tubular array: (a) initial arrangement of FEP tubes, (b) FEP tubes compressed between two heated metal plates and (c) a photograph of the cross-section of array.*

This treatment provides an effective fusion bonding between individual tubes and results in an assembly with regular air voids shaped to nearly stadium form. As an example, Fig. 1(c) shows a typical micrograph of the cross-section of an array fabricated from tubes of 1 mm in diameter with 50 µm thick walls. By this approach a large number of flat arrays with regular tubular air cavities were produced from different FEP tubes. Best devices after the introduction of two metal electrodes and adequate poling show stable and high $d_{33}$ coefficients up to 1000 pC/N with a flat frequency response at 0.1 Hz-10 kHz. These structures exhibit a high ratio between piezo-electrically active and non-active (bonding) areas, which is improved by more than three times compared to earlier reports. To get a deeper understanding of the influence of material and geometric parameters on the piezoelectric performance of the tubular structure an analytical model as well as an electro-mechanical coupled continuum model was employed [2,3].

## Conclusions

The $d_{33}$ coefficient of fabricated devices sufficiently exceeds those made from classical ferroelectric polymers such as polyvinylidenefluoride and its copolymers. Moreover, the arrays with 25 µm thick walls exhibit high piezoelectric responses comparable with PZT ceramics. The obtained theoretical and experimental results are an excellent base for further optimizing the tubular array design and can serve for interesting new sensors.

## References

[1] S. Bauer, R. Gerhard-Multhaupt and G. M. Sessler, *Physics Today* **2004**, *57*, 37-43.

[2] S. Zhukov, S. Fedosov and H. von Seggern, *J. Phys. D. Appl. Phys.* 2011, *44*, 105501.

[3] B.-X. Xu, H. von Seggern, S. Zhukov, and D. Gross, *J. Appl. Phys.* **2013**, *114*, 094103.

## Acknowledgements

This work was supported by the Deutsche Forschungs-gemeinschaft (DFG) Grant Nos. SE 941/19-1, XU 121/51 and SE 941/17-1.

# Polarization switching dynamics in ferroelectric polymers by Inhomogeneous Field Mechanism

Sergey Zhukov, Yuri Genenko and Heinz von Seggern

zhukov.tud@gmail.com

Institut für Materialwissenschaft, Technische Universität Darmstadt, Alarich-Weiss-Straße 2, 64287 Darmstadt, Germany

**Abstract:** It is shown that the global polarization reversal of polymer ferroelectrics is predominantly controlled by the statistical characteristics of the disorder, and not by the specific law of local switching of the polarization. Thus, independent of certain microscopic mechanisms describing local polarization switching the overall polarization response appears to be determined by a statistical distribution of the local electric field values which originates from the intrinsic inhomogeneity of the material and hence, is directly related to internal disorder.

**Keywords:** polymer ferroelectrics, polarization switching dynamics

## Introduction

The understanding of polarization switching dynamics of ferroelectrics is of great importance for practical applications and has been steadily advanced for ferroelectric ceramics and polymers for more than half a century. The temporal behaviour of polarization reversal in ferroelectric copolymers like P(VDF-TrFE) cannot be satisfactory explained by simple models such as classical Kolmogorov-Avrami-Ishibashi nucleation and growth theory [1] but needs more sophisticated models.

## Results and Discussion

In the present contribution, the Inhomogeneous Field Mechanism (IFM) model recently proposed for PZT ceramics has been applied to polymer ferroelectrics such as PVDF and its copolymer P(VDF-TrFE) [2,3]. Similar to the Nucleation Limited Switching (NLS) model [4], the IFM approach is based on the assumption that the switching volume is divided into many spatial regions with independent dynamics. Unlike the NLS model, the reversal of the polarization in each region is mainly due to local electric fields that are randomly distributed over the ensemble of regions due to intrinsic material inhomogeneity. Therefore, an inhomogeneous switching behaviour is induced by the varying local fields of each region. Moreover, the statistical distribution of local field values can be directly extracted from the experimental data by the IFM approach. Figure 1 compares the experimental results with IFM model calculations for P(VDFTrFE) sample at room temperature. It is clearly seen from Fig. 1 that the model satisfactorily describes the switching response of P(VDF-TrFE) over a broad time-field domain covering eight orders of magnitude of poling time and electric field values from 60 kV/mm up to 140 kV/mm.

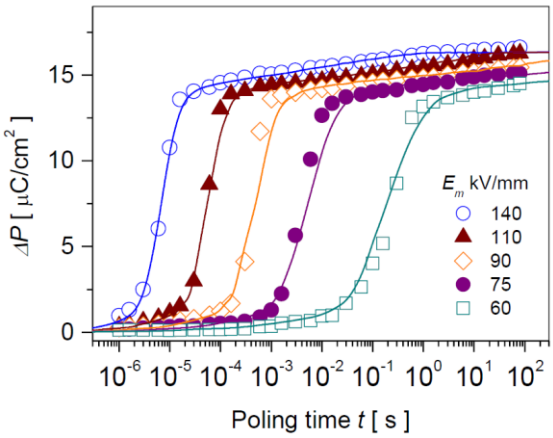


*Figure 1. Experimental data sets (symbols) together with theoretical IFM curves (solid lines) covering eight orders of magnitude in time and electric fields ranging from 60 to140 kV/mm.*

## Conclusions

It was demonstrated that the IFM model is a capable tool to describe the polarization switching response in ferroelectric polymers allowing direct extraction the local field distribution from experiment data.

## References

[1] Y. Ishibashi, *Ferroelectrics* **1989**, *98*, 193.

[2] Y.A. Genenko, S. Zhukov, S.V. Yampolskii, J. Schütrumpf, R. Dittmer, W. Jo, H. Kungl, M.J. Hoffmann and H. von Seggern, *Adv. Funct. Mater.* **2012**, *22*, 2058.

[3] J. Schütrumpf, S. Zhukov, Y.A. Genenko and H. von Seggern, *J. Phys. D: Appl. Phys.* **2012**, *45*, 165301.

[4] A.K. Tagantsev, I. Stolichnov, N. Setter, J.S. Cross, and M. Tsukada, *Physical Review B* **2002**, *66*, 214109.

## Acknowledgements

This work was supported by the Deutsche Forschungs-gemeinschaft (DFG) Grant No. SE 941/19-1.

# PVDF: a strong candidate for pressure gauge for blast loading measurements. Changes in shape of the hysteresis loop of a relaxor terpolymer with CFE under uniaxial stress.

Francois Bauer[1], Michel Arrigoni[2]

Francois.bauer@wanadoo.fr (Corresponding e-mail address)

[1]AIFP, 8 rue Oberlin 68300 Saint-Louis, France [2]ENSTA Bretagne, IRDL FRE CNRS n°3743, rue François Verny 2, 29806 Brest Cedex 09 France

**Abstract:** Early work, which explored the behavior of polyvinylidene fluoride (PVDF) for high pressure applications, led to recognition of the need for highly reproducible properties for PVDF. Enhance precise poled 9 mm² PVDF sensor has been tested in shock tube and has been calibrated in stress compression and release waves with respect to calibrated PCB sensors, and according to the shock tube theory. The reflected pressure obtained is around 4 bar (rel.) in a reproducible way for an initial loading pressure of 6.2 Bar ± 0.1. Additional results of the observed Relaxor → Ferroelectric transition under uniaxial pressure and electric field is presented.

**Keywords:** shock tube, blast, numerical simulation, PVDF, pressure, shock sensor, Relaxor → Ferroelectric transition under uniaxial stress

## Introduction

Nowadays, occidental nations live under the fear of the risk of explosions. The present work tackled in this study deals with the lab-design of an easy-to-use blast sensor for the pressure time resolved measurement of the blast reflected overpressure on a rigid wall. The goal is to investigate the development of a sensor for blast waves pressure measurement. The sensor relies on a Bauer shock gauge based on a 25 µm thin PolyVinyliDene Fluoride (PVDF) film. The gauge has been tested in laboratory conditions in a shock tube at ENSTA Bretagne. PVDF calibration in respect to the calibrated PCB sensor, according **new different methods (in compression, release, recompression modes...)** are presented. In the same time, measurements of hysteresis curves of relaxor terpolymer under uni-axial compression are shown.

## Results and Discussion

*Precise poled PVDF Sensor:*

The shock tube at ENSTA Bretagne is a 92 cm long driver section and 3.72 m driven section, having a 8 cm * 8 cm cross section. Two PVDF gauges were stuck next to the PCB® 113B21 SN # 28293 so that they can measure the reflected pressure [1].

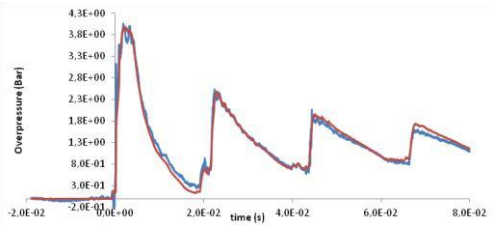


*Figure 1: Pressure versus time for the PVDF transducer in blue and plotted in red for the piezoelectric PCB 29293*

First observations show that all sensors exhibit the same rising front at the trigger time. They detect the arrival of the shock front at the end of the tube. The overpressure of the shock reflected is around 4 bar, with respect to a zero baseline (relative), which is conform to the 5 bar absolute, what predicted by the analytical approach in reference [2].

*Relaxor polymer under pressure*:

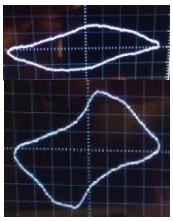

Under uni-axial pressure compression, measurements of hysteresis curves of relaxor terpolymer (PVDF/TrFE/CFE 64.3/27.6 /8.1 mol%) have been done. At zero pressure the electrical displacement (y axis) versus electrical field (X axis) has the shape of a relaxor one, as we can see in the upper picture. In the lower picture, the electrical displacement versus electrical field obtained at 500-700 bar pressure is a typical one of a ferroelectric polymer.

## Conclusions

The PVDF sensor has been calibrated in stress compression as well as in release mode with respect to the calibrated PCB sensor, according to three different methods that lead to comparable results. The electric displacement data confirms the reversible pressure-induced crossover form the relaxor (R) state to a ferroelectric (FE) state for (PVDF/TrFE/CFE 64.3/27.6/8.1 mol%).

## *References*

[1] F. Bauer, Shock Compression of Condensed Matter, 2003 (M.D. Furnish, Y.M. Gupta, J.W. Forbes, eds.), part II, pp. 1121-1124.

[2] M. Arrigoni, Proceeding of ICSMESP, Bucarest , to be published, 2017.

# Electrical polarization of chitosan and hydroxyapatite for tissue engineering

A.F. Esteves[1], E.M. Ribeiro[1], B.D. Marques[1], A.F. Correia[1], A.C. Videira[1], J. E. Pereira[1], C.F.C. João[1], E.R. Neagu[1], M.P.F. Graça[2], L.F.V. Pinto[3], J.C. Silva[1], J.P. Borges[1] and M.C. Lança[1]

mcl@fct.unl.pt

[1]Cenimat (I3N)/Dep. de Ciências dos Materiais, Faculdade de Ciências e Tecnologia, Universidade Nova de Lisboa, Campus da Caparica, 2829-516 Caparica, Portugal
[2]Dep. de Física e I3N, Universidade de Aveiro, Campus Santiago, 3810-193 Aveiro, Portugal
[3]Altakitin S.A., Rua J. Gomes Ferreira, 1-Arm. D 2660 – 360 São Julião do Tojal – Portugal

**Abstract:** The increase of bone diseases and fractures has evoked great interest in the development of biomaterials for use in bone replacement and regeneration. Recently has increased the interest in combining chitosan, a natural polymer, with hydroxyapatite, a bioactive bioceramic. Simultaneously, several studies have shown that electrical polarization of hydroxyapatite, enhances osteointegration and therefore bone regeneration. The influence of the electric polarization in the bioactivity of chitosan and chitosan/hydroxyapatite films and 3D scaffolds was studied.

**Keywords:** biomaterials, electrical polarization, bioactivity

## Introduction

Chitosan (CS) and hydroxyapatite (HAp) are biomaterials used in tissue engineering. HAp a ceramic similar to the natural apatite in hard tissue has been widely used in bone regeneration [1]. CS is a biopolymer with many biomedical applications [1]. On the other hand, studies started in 1990s show that electrical polarization of the surfaces of HAp increases its ability for osteointegration and bone regeneration [2].

## Results and Discussion

*Materials:* Porous scaffolds were developed to mimic the trabecular bone. Nanorods powders of HAp were used in the scaffolds (produced from commercial powders-Altakitin®). Films were produced by preparing homogeneous solutions that were poured into Petri dishes and subsequently dried. Samples were characterized by FTIR, XRD and DSC-TGA.

*Electrical polarization and thermally-stimulated discharge currents (TSDC) measurements:* Some samples were polarized by contact at 130ºC for 1h by applying a 4.5 kV/cm constant electric field. Other samples were thermally treated, i.e., kept at 130ºC for 1h (non-polarized). In this way it was possible to differentiate between the effect of temperature and the combined effect of temperature and field.

TSDC was used to investigate the polarization. Results show that non-polarized samples of CS already exhibit same electrical charge. Positive polarization enhances the charge deposited in the surface while the opposite effect is visible with negative polarization. CS has higher deposition of electrical charges compared to CS/HAp samples.

*Bioactivity assays*: were conducted by immersing samples in simulated body fluid solution at 37°C. Positive, negative and non-polarized surfaces were characterized by SEM-EDS, to evaluate the deposition of apatites. For the films, comparing CS with CS/HAp, bioactivity is significantly higher in the composite. For the scaffolds the non-polarized CS has higher bioactivity than the polarized CS but for the CS/HAp composite the higher deposition is observed on the negative surfaces.

## Conclusions

In the films, results indicate better bioactivity for the negative charged surfaces, followed by positive ones and finally by non-polarized. In the scaffolds also negative surfaces have higher bioactivity but no enhancement of apatite formation is observed on positive surfaces compared to non-polarized.

In conclusion the negatively surfaces of CS/HAp porous scaffolds and films show the highest bioactivity.

## References

[1] Buddy D. . Ratner, A. S. Hoffman, F. J. Schoen, and J. E. Lemons, Biomaterials science : an introduction to materials in medicine, Academic Press, 2013.

[2] F. Baxter, C. Bowen, I. Turner, and A. Dent, "Electrically active bioceramics: a review of interfacial responses," Ann. Biomed., vol. 38, pp. 2079–2092, Jun. 2010

## Acknowledgements

This work was funded by FEDER-QREN-COMPETE Programme-project POLARBONE and by National Funds throught FCT - Portuguese Foundation for Science and Technology, UID/CTM/50025/2013 and FEDER-COMPETE 2020 Programme-POCI-01-0145-FEDER-007688.

# Influence of corona charging on transformer-oil filtration of fluorinated nonwoven polypropylene films

Feipeng Wang, Fan Fan, Chunxiang Wan, Zhengyong Huang, Jian Li

fpwang@cqu.edu.cn

State key lab of power transmission & system security and new technology,
School of electrical engineering, Chongqing University, China

**Abstract:** Nonwoven polypropylene (PP) films were fluorinated and corona charged for transformer oil filtration. For comparison, different needle voltages were took to vary charge density. The surface morphology of PP fibres during fluorination and corona charging was characterized by scanning electron microscopy. The dielectric permittivity and loss, breakdown voltages at lightning and AC for the oil samples before and after filtration were measured and compared. It is found that fluorination brought fibres with increased surface roughness. Corona charging generated certain increase of porosity on the fluorinated samples. After filtration, the dielectric loss as well the conductivity of transformer oil obviously decreased. The breakdown strength got much improved for oils filtered by corona charged and fluorinated nonwoven PP films.

**Keywords:** Nonwoven polypropylene, Fluorination, Oil filtration, Dielectric loss, Breakdown strength.

## Introduction

Transformer oil is widely utilized in power system. The role is to remain insulation but also to be a cooling media. Due to various reasons, transformer oil maybe seriously polluted by metal particles, polar components with relatively high viscosity (condensed depositions). The filtration of transformer oil is showing increasing importance especially for ultrahigh voltage (UHV) transmission systems because they request higher grade of cleanness [1].

## Results and Discussion

The nonwoven PP films were fluorinated at 25°C for 60 min by mixed $F_2$ and $N_2$ with ratio $F_2$%=1% at the pressure of 1 atm. Corona charging was performed at ambient condition with point voltage of -10 kV and grid voltage of -2 kV by duration of 2 min. Lightly contaminated transformer oils were took from a 110 kV power transformer. The filtration was conducted with a sand core funnel.

The fluorination on PP films produced increased surface roughness of the PP fibres (*cf.* Figure 1). This is probably caused by the chemical reaction of fluorination which is typically exothermic. The much sized fluorine atoms and the shorter C-F bonds should significantly lead to the deformation of molecular chains during fluorination.

Corona charging on fluorinated PP films resulted in higher surface potential comparing with the nonfluorinated sample films. The filtered oils by fluorinated and corona charged PP films shown lowest tan delta values at low frequency range, which agree to the observed low conductivity (*cf.* Figure 2).

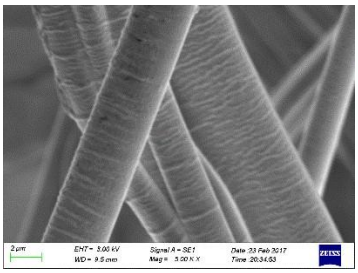

*Figure 1: SEM figure of the fluorinated PP fibres that show increased surface roughness.*

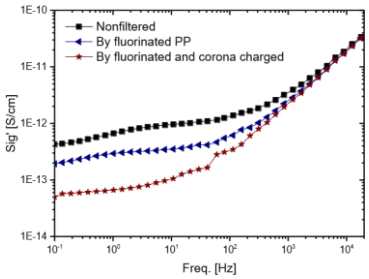


*Figure 2: Dielectric conductivity of transformer oils before or after filtration by fluorinated PP films.*

## Conclusions

Corona charging endows the fluorinated nonwoven polypropylene films significantly improved filtration efficiency, which paves a way for application of electret filters in transformer-oil purification.

## References

[1] Dervos, C. T.; Paraskevas, C. D.; Skafidas, P. D.; and Vassiliou, P. C. *Sensors* 2005, 5, 302-316.

## Acknowledgements

The authors acknowledge financial support from China 973 program (2015CB251003), State Key Program of NSFC (U1537211) and funding from Chongqing (CXTDX201601001).

# Abstracts

# Tutorial lectures

# Screen Printing as a powerful tool to add multiple functionality to flexible substrates

Dr. Barbara Stadlober [1], J. Groten[1], P. Hütter[1], A. Petritz[1], G. Scheipl[1], H. Gold[1], M. Zirkl[1], D. Collin[2], and G. Domann[2]

Barbara.stadlober@joanneum.at (Corresponding e-mail address)

[1] Institute for Surface Technologies and Photonics, Joanneum Research Forschungsgesellschaft mbH, Weiz, Austria

[2] The Fraunhofer Institute for Silicate Research, Würzburg, Germany

**Abstract:** We report about the screen-printing of multifunctional ferroelectric sensors and of organic electrochemical transistors on flexible substrates enabling a multitude of applications such as novel 3D user interfaces, force and proximity sensing surfaces and large-area digital circuits.

**Keywords:** PVDF-TrFE, poling, human-machine interfaces, organic circuits

## Introduction

Screen printing is one of the most common techniques used in printed electronics for the fabrication of large-area flexible components and multifunctional devices. It is highly tolerant to the type and form factor of substrates, the rheology of ink materials, provides sufficient alignment accuracy for multilayer printing and can be done in a sheet-to-sheet or roll-to-roll scheme. Here we present the usage of this well-known method for the large-area fabrication of two kinds of flexible devices: ferroelectric sensors and organic electrochemical transistors (OECT) and combinations thereof.

## Results and Discussion

The sensors are based on the ferroelectric material PVDF:TrFE which supports both the pyro- and the piezoelectric effect for sensing pressure, impact forces and bending interaction and for detecting IR radiation and the proximity of human beings [1]. The sensors have a sandwich structure of four layers that are printed onto any flexible and bendable substrate (e. g. plastic foils, paper, and textiles) over large areas (up to A3) and response accurately, fast and reproducibly to pressure and temperature changes with a large dynamic range. By optimizing the design, the printing and the annealing process as well as the poling conditions, functional sensors with a soft yield of more than 98% and less than ± 5% deviation in the remnant polarization were demonstrated. It is also interesting to note that extended aging tests under definite climate and shock conditions revealed more than 98% preservation of the remnant polarization for high molecular weight PVDF-TrFE polymers. Moreover, a novel printable nanocomposite material, which allows reducing the cross-sensitivity between the pyro- and piezoelectric sensing modes, will be presented.

This material is composed of inorganic ferroelectric nanoparticles blended in a ferroelectric polymer matrix [2].

OECTs in a lateral architecture are screen printed on A4 plastic substrates and investigated in view of a correlation between the electrical charge consumed during switching and the volume of PEDOT:PSS in the transistor channel. An understanding of the relation between charge consumption and the amount of electro-chemically active PEDOT is essential for the design of high performance transistors and for providing a deeper insight into the fundamentals of the electrochemical switching process in OECTs. It turned out that a precise control of the width of the PEDOT:PSS source-drain line is imperative for maximizing both the on current and the on/off current ratio of lateral OECTs [3]. In combination with screen-printed resistors, the printed transistors were also used as the building blocks for integrated logic circuits such as inverters, NAND gates, flip-flops, and a 2-bit shift register that operate at 1.5V. Only five different inks are needed to realize these circuits. Dynamic characterizations and comparison of 8 flip-flops (380 OECTs and PEDOT:PSS resistors in total, see Fig. 1) reveal a remarkably high reproducibility of the measured devices' output signals, which is traced back to the high uniformity and stability of the basic building blocks. In this way, the suitability of PEDOT:PSS-based devices for integrated logic circuitry on flexible substrates by means of a low-cost printing technique is clearly shown [4].

## Conclusions

Based on these building blocks applications such as flexible 3D user interfaces [5] (Fig. 1) and large-area force, impact and proximity sensors as well as medical patches will be presented either in a passive-matrix or an active-matrix ferroelectric sensor configuration with OTFT- or OECT-backplane.

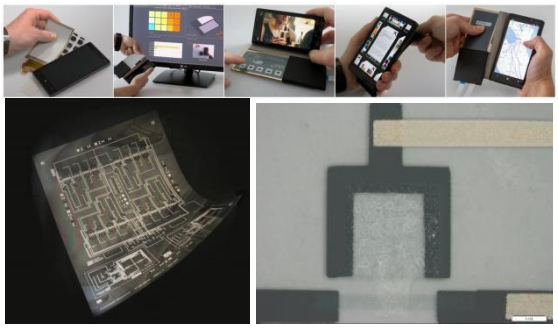

*Figure 1: (upper row) A flexible sensing and display cover based on the PyzoFlex technology supporting paper-like interaction in Laptop, book mode and backside mode (bottom row) Printed logic circuits on an A4 plastic film containing several hundred OECT devices.*

## References


[1] M. Zirkl, A. Sawatdee, U. Helbig, M. Krause, P. Bodö, P. Andersson Ersman, D. Platt, S. Bauer, G. Domann, and B. Stadlober, Adv. Mat. 23, 2069 (2011)

[2] I. Graz, M. Krause, S. Bauer-Gogonea, S. Bauer, S. P. Lacour, B. Ploss, M. Zirkl, B. Stadlober, and S. Wagner, J. Appl. Phys. 106, p. 034503 (2009)

[3] Philipp C. Hütter, Alexander Fian, Karl Gatterer, and Barbara Stadlober, ACS Appl. Mater. Interfaces 2016, 8, 14071−14076 (2016)

[4] Philipp C. Hütter, Thomas Rothländer, Gregor Scheipl, and Barbara Stadlober, IEEE Trans. Electron. Dev. 62, 4231 (2015)

[5] C. Rendl, D. Kim, P. Parzer, S. Fanello, M. Zirkl, G. Scheipl, M. Haller, S. Izadi, FlexCase: Enhancing Mobile Interaction with a Flexible Sensing and Display Cover, Proceedings of the 2016 CHI Conference on Human Factors in Computing Systems, San Jose, California, USA, pp. 5138-5150, doi: 10.1145/2858036.2858314


## Acknowledgements


This work was supported by the European Commission via FP7-project FLASHED (No: 611104) and This work was supported by the Austrian Research Promotion Agency through the NILaustria Project Cluster.

# Beyond PVDF-Based Normal Ferroelectric Polymers Advances, Opportunities, and Outlooks

Q. M. Zhang, Tian Zhang, and Xin Chen

Qxz1@psu.edu

School of Electrical Engineering and Computer Science, Materials Research Institute,
The Pennsylvania State University, University Park, PA 16802, USA

**Abstract:** PVDF-based normal ferroelectric polymers have been investigated for many decades and have found applications in sensors, actuators, and transducers. Advances in the last two decades reveals that there still exist broad rooms for re-designing PVDF-based polymers to induce responses beyond normal ferroelectricity. Recent works show that these newly developed PVDF-based polymers exhibit properties and responses far beyond what achievable in the normal ferroelectric phases of PVDF-based polymers and hence open up great opportunities for applications in energy storage and conversions, which will be presented in this talk.

**Keywords:** energy storage, relaxor ferroelectric, dielectric, polymer thin film devices, and electrocaloric cooling

PVDF-based normal ferroelectric polymers have been investigated since the end of 1970s and have found broad applications in sensors, actuators, and transducers. On the other hand, works since later 1990s show that PVDF-based polymers can also be modified and re-designed to exhibit properties and responses beyond the normal ferroelectric polymers. This talk will highlight major progresses made through these efforts and their impacts on important applications. Potential new materials, opportunities, and outlooks will be presented. Some examples of this talk include:

(i) Modified PVDF-polymers and nanocomposites for energy storage [1][2][3]:

Energy density of a dielectric material is in general proportional to the polarization change P and applied electric field E. To achieve a high energy density, a dielectric polymer should possess a large and reversible electric field induced polarization changes and high dielectric strength. Practical dielectric energy storage applications also require low energy loss (i.e., the charge/discharge efficiency) and high operating temperature. Past efforts in modifying PVDF-polymers to meet these challenges will be presented.

(ii) PVDF-relaxor ferroelectric polymers [4][5]: large electromechanical response and high dielectric constant (> 50) at room temperature.

The talk will review methods to modify PVDF based polymers into relaxor ferroelectric polymers, the difference in polarization responses between differently modified relaxor PVDFs, as well as applications of high room temperature dielectric response of PVDF based polymers [6].

Basic molecular mechanism responsible for achieving large electromechanical response will be presented and several application examples will be discussed [4].

(iii) PVDF-based polymers and nanocomposites: large electrocaloric (EC) effect and advanced cooling devices enabled by the polymers with large ECE [7][8][9].

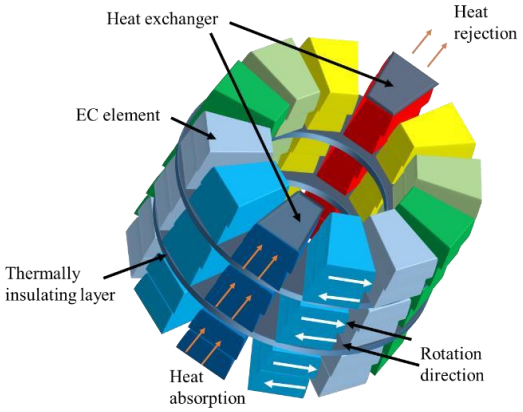


*Figure 1: An example of a compact EC cooling device.*

## References

[1] Chu, B, et al. *Science* **2006**, 313, 334-337.
[2] Zhou, X, et al. *Appl. Phys. Lett.* **2009**, 94, 162901162904.
[3] Zhang, S., et al. *IEEE Trans. DEIS* **2012**, 19, 1158.
[4] Zhang, Q. M., et al. *Science* **1998**, 280, 2101 2104.
[5] Xia, F. et al. *Adv. Mater* **2002**, 14, 1574-1578;
[6] Wu, S., et al. *Appl. Phys. Lett.*, **2013**, 102, 013301.
[7] Neese, B. *Science* **2008**, 321, 821-823.
[8] Lu, S.G. & Zhang, Q.M. *Adv. Mater.***2009**, 21, 1983.
[9] Gu, H.M. *Appl. Phys. Lett*. **2014**, 105, 162905.

## Acknowledgements

The works have been supported by US DARPA, DOE, ONR, and NIH.

# Soft Electronics and Machines with Tough Hydrogels

Daniela Wirthl[1], Robert Pichler[1], Michael Drack[1], Siegfried Bauer[2], Martin Kaltenbrunner [1]
martin.kaltenbrunner@jku.at

[1] Linz Institute of Technology, Johannes Kepler University Linz, Altenbergerstr. 69, 4040 Linz, Austria
[2] Soft Matter Physics, Johannes Kepler University Linz, Altenbergerstr. 69, 4040 Linz, Austria

**Abstract:** Introducing methods for instant tough bonding between hydrogels and antagonistic materials – from soft to hard – allows us to demonstrate elastic, yet tough biomimetic devices and machines with a high level of complexity. Tough hydrogels strongly attach, within seconds, to plastics, elastomers, leather, bone and metals reaching unprecedented interfacial toughness exceeding 2000 J/m$^2$. Soft, transparent multi-layered hybrids of elastomers and ionic hydrogels endure biaxial strain with more than 2000 % increase in area, facilitating soft transducers, generators and adaptive lenses. We demonstrate soft electronic devices, from stretchable batteries, self-powered compliant circuits and autonomous electronic skin for triggered drug delivery.

**Keywords:** dielectric elastomers, electro-electrets, hydrogels, soft actuators, soft electronics

## Introduction

Hydrogels are versatile building blocks of life – living beings are in essence gel-embodied soft machines. The intricacy and vast diversity found in nature, from entirely soft cnidaria or molluscs to hybrid vertebrates, relies on insightful merging of a wide variety of biological materials forming gels, tissues, fibres, muscles, tendons and skeletal structures. The unique properties of engineered, tough hydrogels advance soft machines and electronics. A high level of functionality in the artificial counterparts is achievable through hybrid combinations of hydrogels and soft-to-solid materials, from elastomers to polymers, metals or mineralized tissue.

## Results and Discussion

Robust interfaces between the individual layers prevent delamination and are essential for mechanically tough yet soft, highly functional and compliant systems. By mixing synthetic adhesives that rapidly polymerize in the presence of hydroxyl ions with suitable non-solvents, we achieve easy-to-use dispersions. Our adhesive dispersion is applied to form tough, instant bonds between i) separate hydrogels, ii) hydrogels and elastomers and iii) hydrogels and solid surfaces. We demonstrate the versatility of our approach on fully swollen hydrogels, including PAAm, PHEMA, PVA and double network PAAm/Alginate with internal dissipation. We employ our methods in demonstrating tough, stretchable adaptive optics, soft machines and generators. Our approach utilizes transparent PAAm hydrogel sheets as ionic conductors, bonded to a convex lens formed from acrylic elastomer filled with NaCl solution. Applying a DC voltage causes the whole lens to thin, thereby changing the focal length by up to 110 % at a voltage of 6.5 kV. We further demonstrate soft hydrogel generators, and transform approximately 500 mJ of mechanical into 54 mJ electrically usable energy per cycle, yielding an overall conversion efficiency of 11 %. We demonstrate untethered hydrogel-based electronic patches including power supply, control/readout electronics, wireless communication and stretchable actuators and sensors (Figure 1).

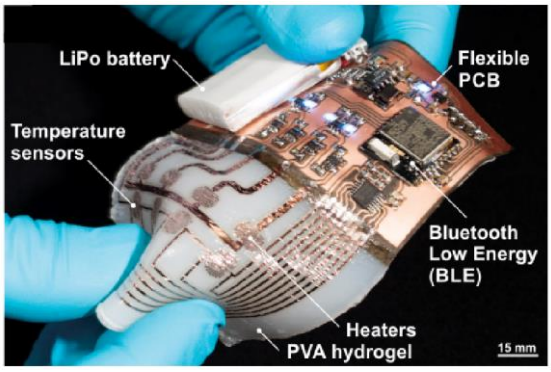


*Figure 1: Photograph of an untethered electronic hydrogel with four stretchable heating elements and adjoined temperature sensors strongly bonded to a PVA hydrogel. Battery, control, readout and Bluetooth Low Energy communication electronics are hosted on a flexible circuit board.*

## Conclusions

In summary, we here introduce a facile, universally applicable method for instant tough bonding of hydrogels to a wide variety of materials – from soft to hard – with unprecedented interfacial toughness exceeding the intrinsic fracture strength of the gels. We apply our approach to create a new set of soft machines and electronics, demonstrate instant healing, adaptive optics, soft actuators and generators, tough batteries and hydrogel electronic skins. Applications range from robotics, energy harvesting from renewable sources, consumer electronics and wearables to a new class of medical tools and health monitors.

## Acknowledgements

Work supported by the ERC Advanced Investigators Grant SoftMap and the European Unions Horizon 2020 WETFEET project (Grant agreement No. 641334). Funding through the LIT startup Grant LIT013144001SEL is acknowledged.

# Polymeric ferroelectric diodes for non-volatile memory applications in flexible electronics

Kamal Asadi[1]

asadi@mpip-mainz.mpg.de (Corresponding e-mail address)

[1]Max-Planck Institute for Polymer Research, Ackermannweg 10, 55128, Mainz, Germany, [2]University of

**Abstract:** Organic ferroelectric memory diodes based on the blends of ferroelectric copolymer of vinylidenefluoride with trifluoroethylene and organic semiconductors are promising candidates for non-volatile memories. In this contribution we discuss state-of-the-art developments and understanding of the device physics of the ferroelectric memory diodes and confer the limits for the upscaling.

**Keywords:** Organic non-volatile memory, ferroelectric diode, organic semiconductor, polymer blend

## Introduction

Organic electronics has emerged as a promising technology for large-area micro-electronic applications, such as foldable displays, electronic papers, contactless identification transponders, and smart labels. Storing information is a key factor in many of the envisioned applications. A memory element is needed that retains its data in the absence of external power, hence non-volatile, and that further can be programmed, erased, and readout electrically. Organic ferroelectric memory diodes are promising candidates. A microstructure is needed that consists of bicontinuous columns of a semiconducting polymer embedded in the matrix of a ferroelectric copolymer of vinylidenefluoride with trifluoroethylene (P(VDF-TrFE)). We have shown that such microstructure can be realized either using a phase separated blends of a semiconducting polymer and P(VDF-TrFE) or using imprint patterning. Memory diode is realized by deliberately choosing an injection limited contact. Depending on the ferroelectric polarization, the current density is high and the diode is in the on-state or the current density is low and the diode is in the off-state.

## Results and Discussion

Key to high current density and current modulation is the areal density of well-defined interfaces. We have developed a morphology relevant device model and elucidate on the operation mechanism of the ferroelectric diode and show that the operation is based on the modulation of the injection barrier. Since the dependence of polarization on electric field is explicitly taken into account, the current-voltage characteristics of the diodes can be quantitatively described. The model provides design rules for the implementation of organic ferroelectric memory diodes, and predicts an ultimate theoretical memory density in the order of Tbit/cm$^2$ for a polymeric ferroelectric diode arrays.

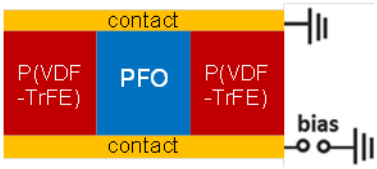


*Figure 1: (Top) An schematic of the polymeric ferro-electric diode wherein a column of semiconducting polymer is surrounded in a ferroelectric matrix.*

## Conclusions

We have developed the technology for two terminal information storage based on rectifying diodes. We have further developed a model that reproduces the current-voltage characteristics by taking the dynamics of the polarization with the applied field into account. We predict limit of Tbit/cm$^2$ for the storage capacity of the organic memories.

## Acknowledgements

Alexander von Humboldt is acknowledged for the funding provided through the Sofja Kovalevskaja Award.

# Abstracts

# Poster presentations

# Influence of foreign chemical structures from nitric acid treatment on electret and electrical-insulation properties of polypropylene

Jingwen Wang [1], Dmitry Rychkov and Reimund Gerhard

jingwen.wang@uni-potsdam.de

[1]Applied Condensed-Matter Physics, Institute of Physics and Astronomy, Faculty of Science, University of Potsdam, Karl-Liebknecht-Strasse 24-25, 14476 Potsdam, Germany

**Abstract:** Usually, chemical defects such as additives, broken chains and bonded foreign chemical structures can serve as deeper charge trapping centres in polymer dielectrics than physical defects. However, nitrogen- and oxygen-containing structures introduced by the treatment of polypropylene (PP) with nitric acid ($HNO_3$) can form shallower traps and accelerate the surface charge decay on PP. The treatment may serve as an efficient method to modify and improve the relevant properties of PP for electret and electrical-insulation applications.

**Keywords:** polypropylene, nitric acid, electrets, insulator, trap model, surface charge and charge retention

## Introduction

It is commonly believed that, in the trap-controlled hopping model of non-polar polymeric dielectrics, the traps originated from chemical-structure defects and from foreign chemicals in particular, are generally deeper than those from certain molecular configurations and from crystalline-amorphous structures, *i.e.* physical defects, as indicated by theoretical calculations [1, 2] and experimental results [3]. However, our experimental results from $HNO_3$ treatment may suggest the opposite in this particular case.

## Results and Discussion

After immersion in $HNO_3$ (68%) at 75 °C for 24 h, the PP films (50 µm) were metallized on one side and charged in a point-to-plane corona setup to an initial surface potential of ca. ±1 kV. Normalized thermally stimulated discharge (TSD) curves of **nitric**-acid-treated films with either polarity are plotted in figure 1 together with the as-received PP for comparison. The surface-charge decay process is obviously accelerated by the treatment and the half-value temperatures of positively and negatively charged samples are decreased by 18 °C to 79 °C and 77 °C, respectively, although the similar **phosphoric** acid treatment considerably increases the surface charge stability on PP [4].

Fourier-Transform InfraRed spectroscopy (FTIR) of treated and as-received PP samples shows that some nitrogen- and oxygen-containing chemical structures are covalently bonded to PP molecules. In addition, contact-angle measurement indicates that PP, a non-polar polymer, acquired a polar surface during the $HNO_3$ treatment. The foreign chemicals introduced by the treatment may form traps that are shallower than the intrinsic ones and these shallow traps might constitute new routes for charge transport in PP, leading to charge decay at lower temperature, as observed during the TSD measurements [5]. Nanofillers can also generate shallow traps in PP and positively affect its insulating performance [5].

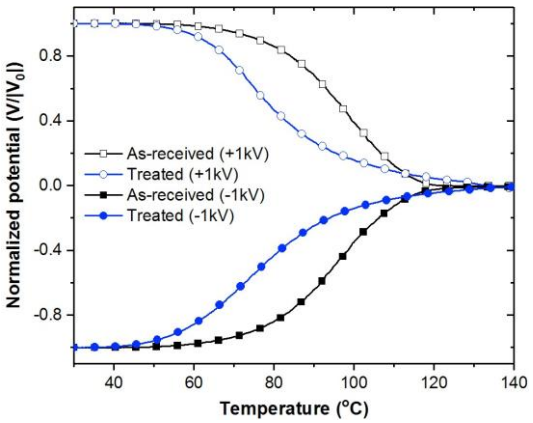


*Figure 1: TSD curves of $HNO_3$-treated and non-treated PP normalized by the absolute value of the initial surface potentials.*

## Conclusions

$HNO_3$ treatment of PP may thus lead to the formation of shallower traps through covalently bonded foreign chemical structures, which can accelerate the charge decay process by (partially) replacing the original deeper traps (defects) or by creating alternative pathways for charges to hop across the film more easily [1, 5].

## References

[1] Sessler, G. M., Electrets, 2nd ed.; Springer: Berlin Heidelberg, 1987.

[2] Meunier, M., Quirke, N., Aslanides, A., *IEEE CEIDP* **2000**, doi: 10.1109/CEIDP.2000.885218.

[3] D. Rychkov, R. A. P. Altafim, X. Qiu, R. Gerhard, *J. Appl. Phys.* **2012**, *111*, 124105.

[4] Wang, J., Rychkov, D., Gerhard, R., *IEEE CEIDP* **2016**, doi: 10.1109/CEIDP.2016.7785496.

[5] G. C. Montanari, R. Mulhaupt, et al., *IEEE Trans. Dielectr. Electr. Insul.* **2004**, *11*, 754-762.

# Comparative study on charge storage capacity of mesomorphic and α crystalline polypropylene melt-blown electret fabric

Xi Chen, Gangjin Chen*, Huiming Xiao, Xumin Chen, Hua Huang, Chunping Xiao

Lab. of Electret and Its Application, Hangzhou Dianzi University, China, 310018
*Author to whom correspondence should be addressed, Email: cgjin@hdu.edu.cn

**Abstract:** The charge storage capacity of α and mesomorphic crystal form melt-blown polypropylene fabric electret, charged by means of corona charging method, was investigated by measuring the filtration efficiency stability and thermally stimulated discharge spectrum. The results show that the charge storage stability of α crystal polypropylene is better than that of the mesomorphic crystal polypropylene. The higher crystallinity and larger grain size of α crystal polypropylene is responsible for the better performance stability of α crystal polypropylene.

**Key words:** electret, melt-blown PP non-woven fabric, charge storage capacity, crystal structure

## Introduction

Used as air filter materials, the melt-blown polypropylene (PP) non-woven electret fabric is highly concerned for its multiple functions of low flow resistance, high filtration efficiency and super sterilization[1,2]. The capacity of its charge storage is the key to determine whether it can be widely applied or not. It was known that the charge storage density and stability of PP are expected to have connection with its crystalline features such as crystal form, amorphous-to-crystalline ratio and crystal grain size [3,4].

It was reported in this paper that the charge storage capacity of α and mesomorphic crystal form melt-blown PP electret fabric, charged by means of corona charging method, was investigated by measuring the filtration efficiency stability and thermally stimulated discharge spectrum. The mesomorphic crystal form melt-blown PP fabric was made by custom-designed micro melt-blown apparatus. The α-crystal form melt-blown PP fabric was obtained by thermally treating for 10 minutes at the temperature of 120℃. The crystalline features were determined by an X-ray diffraction meter from Philips of Netherlands with Cu Kα irradiation.

## Results and Discussion

From Figure 1, there are five diffraction peaks in the XRD spectrum of thermal treated sample, and only two diffraction peaks in the XRD spectrum of the sample before heat-treated. The results are in accordance with α crystal and mesomorphic crystalline feature of PP respectively, which is exactly the same as reported in the literatures[5,6]. The crystal parameters calculated from the XRD patterns of Fig.1 are shown in Table 1. Crystallinity is calculated using Hinrichsen's method [7] and Grain size by the Scherrer equation [8]. Both the crystallinity and the grain size of α crystal PP fabric are larger than mesomorphic crystal PP fabrics.

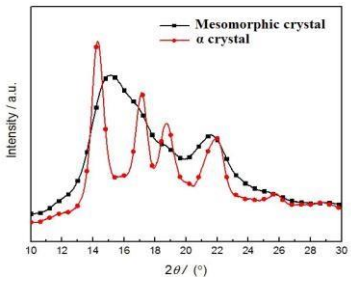


*Fig.1 .XRD spectra of α and mesomorphic crystal melt-blown PP fabrics*

Table 1 Crystallinity and grain size of α and mesomorphic crystal melt-blown PP fabrics

| Crystal form | Crystallinity / % | Grain size / nm |
|---|---|---|
| Mesomorphic | 35.50 | 4.13 |
| α | 41.44 | 4.77 |

From Figure 2 The TSD current peak appears at 85℃ for mesomorphic crystal PP, and 125℃ for α crystal PP, respectively. The peak temperature for α crystal PP is 40℃higher than mesomorphic crystal PP. This result is related to the batter charge storage stability for α crystal PP than mesomorphic crystal PP. The reason may originate from the higher crystallinity and larger grain size of α crystal PP fabric than that of mesomorphic crystal PP fabrics.

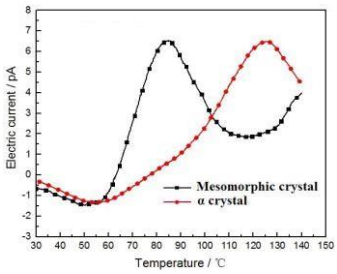


*Fig.2 TSD spectra of α and mesomorphic crystal for melt-blown PP electret fabrics*

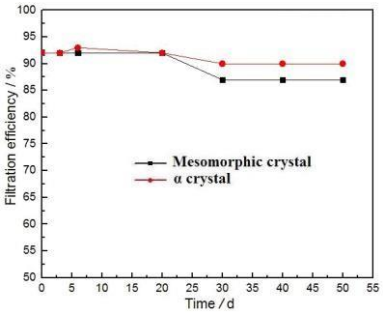


*Fig.3 Filtration efficiency as a function of storage time under ambient condition for α and mesomorphic crystal melt-blown PP electret fabrics*

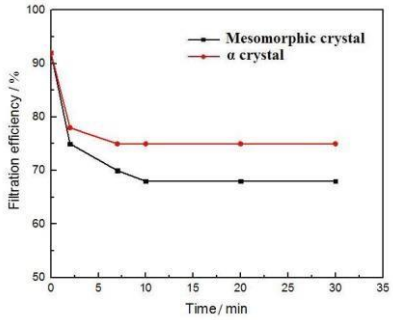


*Fig.4 Filtration efficiency as a function of storage time under 90℃for α and mesomorphic crystal melt-blown PP electret fabrics*

α crystal PP fabrics also display the better stability of filtration efficiency than mesomorphic crystal PP fabrics. From Figure 3, the filtration efficiency for α crystal and mesomorphic crystal PP electret fabrics both decay a little after storing 50 days at room temperature. The stable filtration efficiency of α crystal PP fabric is 90% of its initial value, and that of mesomorphic crystal PP fabrics is 87% of its initial value. From Figure 4, when two kinds of crystal PP fabrics are thermally treated under 90℃, their filtration efficiency drops fast in the first few minutes and then achieves a constant. The declining amplitude of mesomorphic crystal PP fabrics is larger than that of α-crystal PP fabrics. The stabilized constant filtration efficiency for α crystal PP fabric is 75%, whereas that of mesomorphic crystal PP fabrics is 68%. These results indicate that α crystal melt-blown PP electret air filter material shows better filtration performance stability than the mesomorphic crystal PP.

## Conclusions

The α-crystal melt-blown PP electret air filter material shows better filtration performance stability than the mesomorphic crystal PP. This result is attributed to the batter charge storage stability for α-crystal PP than mesomorphic crystal PP. The higher crystallinity and larger grain size of α-crystal PP fabrics than that of mesomorphic crystal PP fabrics is responsible for this results.

## References

[1] Kestelman V.; Pinchuk L.; Goldade V. Electrets in Engineering. Kluwer Academic Publishers, Boston: **2000**, p.186.

[2] Baumgartner H. P.; and Loffler F. *J. Aerosol Science* **1986**, 17, 438-445.

[3] Thyssen A, Almdal K, Thomsen E V. Electret stability related to the crystallinity in polypropylene[C]// Sensors. IEEE, 2015:1-4.

[4] Xiao H. M.; Gui,J. Y.; Chen G. J.; Xiao C. P.; J. Appl. Polym. Sci., **2015**, 132: 42807(1-5)

[5] Rosa C. D.; Auriemma F.; Galotto N. G.; Girolamo R. D. *Polymer* **2012**, 53(12), 2422 - 2428.

[6] Wang J. B.; Dou Q. J. *Macromolecular Science: Physics* **2007**; 46: 987–1001.

[7] Hinrichsen G. *Journal of Polymer Scienece Part C: Polymer Symposia* **1972**, 38(1), 303-314.

[8] Gupta A. K.; Singhal R. P. *Journal of polymer science: polymer physics edition* **1983**, 21(11), 2243-2262.

## Acknowledgements

This research was sponsored by the National Natural Science Foundation of China (No.51177032)

# Piezoelectrically generated Pressure Steps (PPS) for studying charge distributions on corona-charged Polypropylene (PP) films

Q. D. Nguyen[1], J. Wang[1], D. Rychkov[1], and R. Gerhard[1]

doanguyen@uni-potsdam.de (Corresponding e-mail address)

[1]Applied Condensed-Matter Physics, Institute of Physics and Astronomy, Faculty of Science, University of Potsdam, Karl-Liebknecht-Strasse 24-25, 14476 Potsdam, Germany

**Abstract:** Charge distributions on thin corona-charged polypropylene (PP) films have been probed by means of non-destructive piezoelectrically generated pressure steps (PPS). For higher charging levels which lead to higher electric fields between the corona-deposited charges and the charges on the aluminium/chromium (Al/Cr) electrodes, there are some indications of charge injection into the PP films. Additional results will be presented and analyzed with respect to charge injection and other possible influences on the observed charge profiles.

**Keywords:** Electro-acoustical probing of charge profiles, Piezoelectrically generated Pressure Steps (PPS), Polypropylene (PP), Corona charging, Charge storage and transport

## Introduction

We investigate charge profiles on one-side Al/Crmetallized PP films (OPP-TSS from Puetz-Folien) (thickness approx. 50µm) after corona charging at room temperature for ca. 15 s at several different corona voltages. Different surface potentials result in average electric fields between 19 and 90 MV/m. Charge profiles were obtained by means of the PPS method [1]. Overviews of the PPS and other charge-probing methods are found in [2]. In order to preserve the surface charge on the PP sample, a second uncharged, but otherwise identical PP film was inserted between the PPS-generating quartz crystal and the conducting-rubber electrode.

## Results

Charge profiles for positively and negatively charged samples are shown in Figures 1 and 2, respectively. It is obvious that the corona-deposited charges are approximately twice as large as the image charges in the front electrode because the other image charges are at the rear electrode on the second uncharged PP film. It also seems that there is some charge injection at higher electric fields.

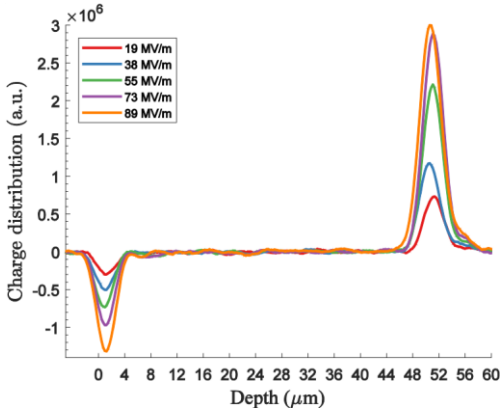


*Figure 1: Charge profiles in positively corona-charged PP films. Left: Surface with Al/Cr electrode. Right: Corona-charged film surface.*

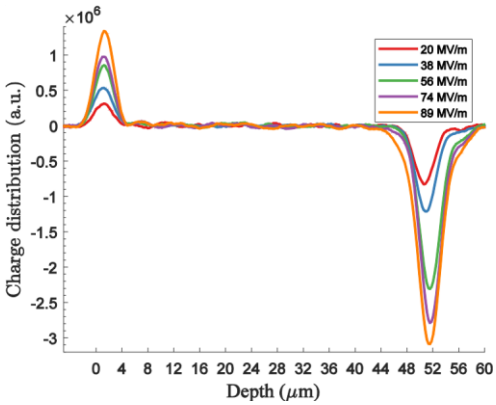


*Figure 2: Charge profiles in negatively corona-charged PP films. Left: Surface with Al/Cr electrode. Right: Corona-charged film surface.*

## Conclusions

During the relatively short charging time at room temperature, there may already be some charge injection from the corona-charged surface into the bulk of the film for both polarities, while there seems no injection from the electrode. Further details and possible artefacts will be discussed.

## References

[1] W. Eisenmenger and M. Haardt, *Solid State Communications*, Vol. 41, pp. 917–920, **1982**, doi: 10.1016/0038-1098(82)91235-2; R. Gerhard, M. Haardt, W. Eisenmenger and G. M. Sessler, *J. Phys. D: Appl. Phys.*, Vol. 16, pp. 2247-2256, **1983**, doi: 10.1088/0022-3727/16/11/027.

[2] R. Gerhard, *Phys. Rev. B*, Vol. 27, pp. 2494-2503, **1983**, doi: 10.1103(PhysRevB.27.2494; G. F. Leal Ferreira and R. Gerhard, *ibid.*, vol. 42, no. 12, pp. 7317–7321, **1990**, doi: 10.1103/PhysRevB.42.7317.

## Acknowledgements

Q. D. Nguyen gratefully acknowledges funding for his Ph.D. project in Germany from the Vietnamese Ministry of Education and Training (MOET/VIED).

# Space Charge Measurement System for High Hydrostatic Pressure Based on PIPWP Method

Tao Li[1], Yewen Zhang[1*], Stéphane Holé[1, 2], Penghao Zhang[1], Feihu Zheng[1] and Zhenlian An[1]

[*]E-mail: yewen.zhang@tongji.edu.cn ; [']E-mail: stephane.hole@tongji.edu.cn

[1]Tongji University, Shanghai, 201804, China

[2] ESPCI-ParisTech, Paris 75005, France

**Abstract:** Polyethylene is widely used as insulation in submarine DC cables due to its excellent dielectric property and mechanical performance. However, space charge may cause the degradation and even premature breakdown of insulators. Considering the extremely harsh undersea environment such as the very high pressure, it is significant to study the space charge behavior on this condition. Thus, in this paper, based on Piezoelectric Induced Pressure Wave Propagation (PIPWP) method, a pressure device and measurement system were designed and improved which could detect the space charge distribution in the dielectric materials.

**Keywords:** space charge, Piezo-electric Induced Pressure Wave Propagation method, high hydrostatic pressure

## Introduction

Nowadays, with the wide use of polyethylene in electrical insulators, especially in power cables, the problems caused by space charge have focused much attention[1]. Accordingly, the research of space charge distribution has been continuously widened and deepened[2]. With the growing demand for transportation of marine renewable energy, submarine DC cable technology continues to move forward. Considering the extremely harsh undersea environment such as the very high pressure, it is significant to study the space charge behavior on this condition. Thus, in this paper, a pressure device and measurement system were designed and improved which could detect the space charge distribution in the dielectric materials.

## Results and Discussion

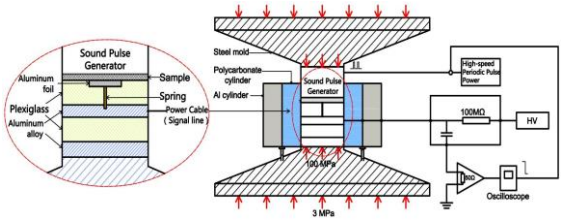


*Figure 1: Principle of the hydrostatic pressure device and measurement system*

The principle of the whole experimental setup is illustrated in Figure 1. In this device, the piezoelectric ceramic is used as the core part of the sound pulse generator. The measurement system consists of hydrostatic pressure generating device, high speed periodic pulse power, sound pulse generator, sample bin and measuring circuit. With this system, LLDPE planar samples are subjected to a high hydrostatic pressure which is up to 100MPa. Figure 2 shows the typical PIPWP results after calibration from the LLDPE samples under the application of 17 kV DC voltage at 20°C with different pressure levels.

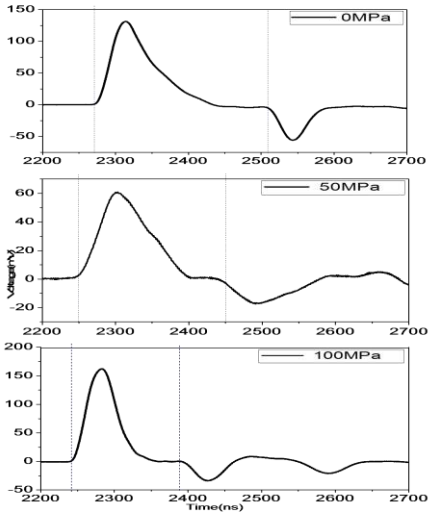


*Figure 2: Typical results of space charge distribution in LLDPE samples at DC 17 kV voltage under different pressure levels*

## Conclusions

This paper introduced a space charge measurement system under high hydrostatic pressure. Charge distribution signals under different pressure levels were showed. Typical experimental results revealed that the system is suitable and reliable to monitor the internal charge distribution. With this system, further research about space charge behavior under high pressure will be carried on in the future.

## References

[1] C. Laurent, G. Teyssedre, S. Le Roy, and F. Baudoin, IEEE Trans. Dielectr. Electr. Insul., vol. 20, pp. 357381, 2013.

[2] Y. Zhang, J. Lewiner, C. Alquie, and N. Hanpton, IEEE Trans. Electr. Insul., vol. 3, pp. 778-783, 1996.

## Acknowledgements

This work was supported by the National Natural Science Foundation of China (Grant Nos. 51477118).

# Swift optimization and prediction of the beneficial effect of physical aging on electrets

J. van Turnhout
j.vanturnhout@tudelft.nl
Dept. Materials Science and Engineering, Delft University of Technology,

Mekelweg 2, 2628CD Delft, The Netherlands

**Abstract:** A quick appraisal of the benefit of PA is proposed. It is based on analysing the TSD of a corona-charged polymer. The clue is to let the polymer pre-age for at least 2 periods before charge injection. By running the TSD at 2 speeds not only the PA kinetics, but also that of the thermal activation can be found. With this information we worked out the prediction of the loss in charge vs. time and optimize the gain in stability by PA.

**Keywords:** physical aging kinetics, long term prediction decay, all-in-1fitting, variable embedding

## Introduction

Physical aging, a phenomenon typical of polymers, is due to the gradual decline in free volume. It restricts the molecular motions and thus retards the charge decay. PA has been studied mainly mechanically [1]. This showed that the relaxation times increase with a power law:

$$\tau(T, t_a) = \tau_T (1 + t_a/t_s)^a$$

where $t_a$ is the aging and $t_s$ a scaling time, while $\tau_T$ represents the T-dependent part. Knowledge of $t_s$ and $a$ is crucial in order to predict the gain in stability. Fig.1 shows a fast route to find their values. It is based on running TSD twice right after the corona charging for at least two isothermal pre-agings. PA proceeds the faster, the closer the aging temperature comes to the glass transition. The boost in stability be pre-aging can thus be optimized.

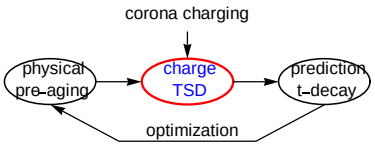


*Fig.1: The role of PA can be assessed quickly using TSD and corona charging after pre-aging.*

## Results and Discussion

Fig.2 shows the effect of pre-aging on the charge TSD spectra. The thermal stability clearly improves due to the increase in the relaxation times. We could calculate $t_s$ and $a$ from the shift upwards using all-in-1 fitting [2].

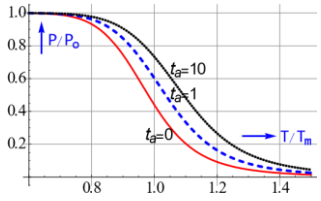


*Fig.2: TSD spectra demonstrating that electrets become more stable by pre-aging.*

Fig. 3 shows the charge vs time for a stretched exponential or KWW decay (taking b=0.5) without PA and backed up by PA. We can further see that pre-aging during $t_{oa}/\tau_m$ before the corona charging leads to an extra slowing down in the decay.

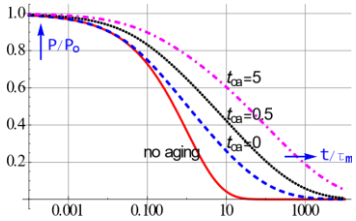


*Fig.3: Charge decay vs time showing that PA increases the stability.*

With the help of $t_s$ ,$a$ and the activation energy we could predict from Fig.2 the long term time decay. Fig.4 shows the results, the lower curves hold for a decay not supported by PA, while in the upper curves we have assumed that PA goes along with the decay.

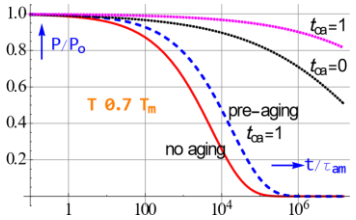


*Fig.4 Long lasting prediction of the drop in charge at $T=0.7T_m$ with time from TSD spectra.*

## Conclusions

Assuming an Arrhenius activated decay we have converted TSD spectra by means of variable embedding to the time domain. A reliable prediction could thus be made about the life time of electrets. We have further quantified the stabilizing effect of PA. This was made possible after assessing the kinetic parameters of aging by analysing TSD spectra after a few pre-agings.

## References

[1] L.C.E. Struik: Physical aging in amorphous polymers and other materials, Elsevier: Amsterdam 1978.
[2] J. van Turnhout, *Front. Chem.* 2016, doi: 10.3389/Fchem.2016.00022.

## Acknowledgements

The author thanks Profs. J. Sietsma and I.M. Richardson of the Dept. Materials Science and Engineering of the TU Delft for their hospitality.

# Air-stable reconfigurable memory diodes based on ferroelectric:semiconductor blends

Manasvi Kumar[1], Hamed Sharifi Dehsari[1], Kamal Asadi[1]

[1]Max-Planck Institute for Polymer Research, Ackermannweg 10, Mainz, Germany

*Corresponding Author: asadi@mpip-mainz.mpg.de

**Abstract** Organic non-volatile resistive bistable diodes based on phase-separated blends of ferroelectric and semiconducting polymers are promising candidates for storing information for low-cost solution processable electronics. One of the key issues impeding upscaling if the reconfigurable array is air-stability, which has been addressed in this contribution.

**Keywords:** Non-volatile memory diodes, polymer-semiconductor blend, air stability, ferroelectric polarization.

## Introduction

Ferroelectric diodes have attracted much attention for their potential use in the field of non-volatile memories owing to their advantageous features like low voltage operation, long retention time and short switching times.[1] Bistable rectifying diodes have been realized using ferroelectric semiconductor blends which can be integrated into functional cross-bar memory arrays.[2],[3] The switchable diode effect in such memory devices is due to the modulation of the charge injection into organic semiconductor due to the polarization switching of the ferroelectric polymer. One of bottlenecks deterring upscaling is air stability of the semiconducting polymers. In this contribution we present a polymer blend system wherein an air– stable amine-based polymer is used as the semiconductor.

## Results and Discussion

Random copolymer poly(vinylidenefluoridetrifluoro-ethylene (P(VDF-TrFE)) (65%–35% molar ratio) was used as the ferroelectric polymer. The thin-film processing was optimized to obtain high yield of functional memory diodes. Electrical characterization of the memory diodes was performed in normal ambient condition (23 C and 45% relative humidity). The memory diodes showed on/off ratios larger than 100 (Figure 1), and further exhibited robust and stable performance upon continuous write-read-erase-read cycles over time of typically 30 days.

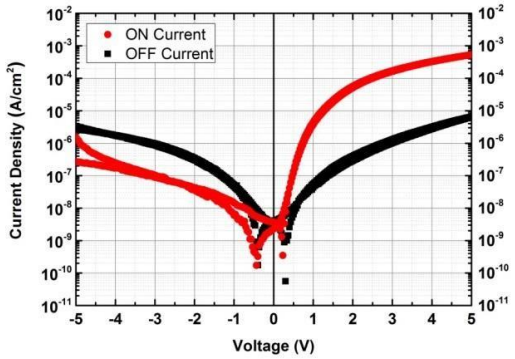


*Figure 1. Current-voltage characteristics of the memory diode after positive and negative polarization.*

## Conclusions

We have demonstrated air-stable reconfigurable ferroelectric:semiconductor blend. The thin-film formation was optimized for ambient processing. Due to high reproducibility and high yield of functional devices a cross-talk free 4-bit reconfigurable array could be demonstrated.

## References

[1] J. C. Scott, L. D. Bozano, Adv. Mater. 2007, 19, 1451.
[2] Asadi, K., De Leeuw, D. M., De Boer, B. & Blom, P. W. Nat Mater 7(7), 547–550 (2008).
[3] Asadi, K., Li, M., Stingelin, N., Blom, P. W. & de Leeuw, D. M. Appl Phys Lett. 97(19), 193308 (2010).

## Acknowledgements

We acknowledge financial support from Alexander von Humboldt Foundation.

# Capacitive-electret sensor for measuring high-voltage discharges

Falconi D.R.[1], Sousa F.S.I.[1], Altafim R.A.C.[1], Altafim R.A.P.[2]

ruy@ci.ufpb.br

[1] Department of Electrical and Computer Engineering, EESC, University of São Paulo, São Carlos-Brazil
[2]Department of Computer Systems, CI, Federal University of Paraíba, João Pessoa-Brazil

**Abstract:** A description of a capacitive-electret sensor for detecting high-voltage peaks is presented. The electret sensor consisting in two electrodes, with an electret film in between allows determine the magnitude of the applied voltage through the discharge pattern formed on the electret surface. The pattern results from the distinct design of one the electrodes and the voltage amplitude. By correlating the pattern with the amplitude voltage is possible to visually identify the discharge magnitude.

**Keywords:** capacitive-sensor, electret films, high-voltage, discharge pattern.

## Introduction

Determine the amount and location of electrical charges trapped on an electret surface, has always inspired researchers from the electret field. Another source of motivation that is not fully related to electrets is the measurement of overvoltage discharges in distribution lines. These two unusual phenomena were here combined to create a capacitive-electret sensor through which one could monitor high-voltage discharges in power lines. The sensor was developed based on the discharge patterns that can be formed on an electret film after they have being exposure to high electrical field [1]. These patterns, which are directly related to the electrode shape and the voltage amplitude, can be visualized if proper treatment is applied [2]. Here we present a brief description of the electret sensor and some partial results, which was obtained during characterization.

## Experimental Details

The capacitive-electret sensor is composed of two parts: a sensing device and a capacitive divider. The later will not be discussed here since its purpose is the sensor installation in distribution lines. The electret-sensor, named (PES) consisted in two circular electrodes, arranged in parallel and an electret film, made of fluorinated ethylene propylene (Teflon® FEP), in between.

It is known that if an impulse voltage is applied to the electrodes terminals, electrical charges are injected on the film surface and depending on the voltage amplitude, circular patterns with different diameters can be observed if toner ink is applied [2]. Base on this principle the PES top electrode was designed with 12 small circles, separated by gaps with different distances ($d_1 \ldots d_{11}$), as schematically shown in Fig. 1a. When the potential between the top and bottom electrodes is high enough, a barrier discharge between two circles will occur, equalizing the potential and injecting charge at these places. Increasing the voltage on the electrodes will lead to charge more circles. Thus, by designing the gaps with increasing distances it was possible to correlate the voltage amplitude with a specific number of charged circles.

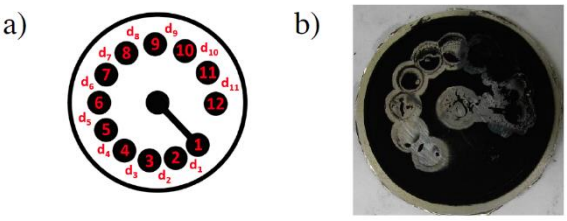


*Figure 1: a) Shows a representation of the grounded electrode with several gaps ($d_1 \ldots d_{11}$) and the how it was implemented on a circuit board. b) Shows an image of the electret films after it was exposed to an impulsive voltage of 4.9 kV.*

## Results and Discussion

After the films has been charged and exposed to the toner ink, a pattern with several circles is formed as shown in Fig. 1b. From a preliminary characterization 2, 6, 8, 10 and 12 circles were obtained with voltage amplitude of 1.1, 2.1, 3.2, 5.1 and 5.9 kV, respectively.

## Conclusions

It was demonstrated here how dielectric barrier discharge can be combined with electret polling to determine the voltage magnitude applied on two electrodes. This effect is for instance relevant for monitoring systems on distribution lines that is commonly affected by lightning overvoltage.

## Acknowledge

Thanks to CNPq for the financial support.

## References

[1] Altafim, R.A.C.; Giacometti, J.A.; Janiszewski, J.M., *IEEE Trans. Indus. Appl.* **1992**. v. 28 n. 5, pp. 1217.
[2] Falconi, D.R., Altafim, R.A.P and Altafim, R.A.C, 13th Spanish-Portuguese Conf. Elec. Eng., Valencia, **2013**, p. 230.

# Studying the electrical polarization of coatings of hydroxyapatite and bioglass deposited by plasma-spray and CoBlast techniques

I. Dias[1], D.J. Ramos[1], M.P.F. Graça[2], E. Pires[3], J.P. Borges[1] and M.C. Lança[1]

mcl@fct.unl.pt

[1]Cenimat (I3N)/Dep. de Ciências dos Materiais, Faculdade de Ciências e Tecnologia, Universidade Nova de Lisboa, Campus da Caparica, 2829-516 Caparica, Portugal
[2]Dep. de Física e I3N, Universidade de Aveiro, Campus Santiago, 3810-193 Aveiro, Portugal
[3]Altakitin S.A., Rua J. Gomes Ferreira, 1-Arm. D 2660 – 360 São Julião do Tojal – Portugal

**Abstract:** Several studies have shown that electrical polarization of hydroxyapatite enhances osseointegration. Films of hydroxyapatite and hydroxyapatite/bioglass, deposited on Ti plates by the new technique of CoBlast, were polarized by DC contact and surface charged by corona. Thermally stimulated discharge currents (TSDC) method was used to investigate polarization and for corona charging, surface potential technique was used to measure the charge decay. Results were compared with films of hydroxyapatite obtained by plasma spraying.

**Keywords:** biomaterials, electrical polarization

## Introduction

Hydroxyapatite is widely used in the coating of bone implants because of its biocompatibility and similarity to the bone mineral. On the other hand, it is known that the bioglass 45S5, has anti-microbial and anti-inflammatory properties and presents an ability to osseointegration [1].

To obtain hydroxyapatite coatings in titanium and its alloys, the most common is to use plasma spray deposition, which, requires high temperatures [3]. As for bioglass there are few studies of its use as a coating [2]. A recent coating technique, CoBlast, was developed and consists of a mechanical micro-shot blasting process, in which granules are accelerated and deposited on the substrate. Films can be obtained at room temperature [3]. On the other hand, studies started in 1990s show that electrical polarization of the surfaces of HAp increases its ability for osseointegration and bone regeneration [4].

## Results and Discussion

*Materials:* The substrate used for all depositions were plates of commercial Titanium. The hydroxy-apatite used was commercial micropowders (Altakitin). 45S5 bioglass micropowders were produced by the sol-gel method. The Ti plates were coated with hydroxyapatite by plasma-spraying and by CoBlasting. A composite of hydroxyapatite and bioglass was coblasted. Average coating thickness by plasma spray is 13 □m and by CoBlast 5 µm.

*Electrical polarization and measurements:* Some samples were polarized by contact at 200 ºC. Other were corona charged at 250 ºC, by applying a negative voltage. TSDC was used to investigate the contact polarization. Surface potential measurements were made for corona charged samples. The thermosgrams showed that plasma sprayed coatings were polarized. The CoBlasted samples had results very difficult to reproduce. Similar results were obtained for the corona charged samples. The reproducibility issues found in CoBlasted samples appear to be related to the thinner coated film (4-5 µm). The coating roughness gives rise to small localized regions were the coating is much thinner, which can act as higher electrical conduction channels and result in very fast decay of the deposited charges.

## Conclusions

The plasma-sprayed samples show promising results either by contact polarization or corona charging. The CoBlasted coatings need a better control of roughness in order to increase the decay time.

## References

[1] Buddy D. . Ratner, A. S. Hoffman, F. J. Schoen, and J. E. Lemons, Biomaterials science : an introduction to materials in medicine, Academic Press, 2013.

[2] J. N. Barry, B. Twomey, A. Cowley, L. O'Neill, P. J. McNally, and D. P. Dowling, "Evaluation and comparison of hydroxyapatite coatings deposited using both thermal and non-thermal techniques," Surf. Coatings Technol., vol. 226, pp. 82–91, 2013.

[3] F. Baxter, C. Bowen, I. Turner, and A. Dent, "Electrically active bioceramics: a review of interfacial responses," Ann. Biomed., vol. 38, pp. 2079–2092, Jun. 2010

## Acknowledgements

This work was funded by PT2020-FEDER-QREN-COMPETE Programme-project DENTALBLAST and by National Funds throught FCT - Portuguese Foundation for Science and Technology, UID/CTM/50025/2013 and FEDER-COMPETE 2020 Programme-POCI-01-0145-FEDER-007688.

# Influence of surface fluorination on space charge characteristics of oil-impregnated Nomex paper

Feipeng Wang, Tao Zhang, Khan Muhammad Zeeshan, Jian Li, Muhammad Sohaib Bhutta

fpwang@cqu.edu.cn

State Key Lab of Power Transmission Equipment & System Security and New Technology, School of Electrical Engineering, Chongqing University, Chongqing 400044, China

**Abstract:** Accumulated space charges in insulation paper will distort the electric field distribution, accelerate the degradation of insulation paper and generate great influence on electrical performance of oil-paper insulation system. In this paper, Nomex paper was fluorinated with fluorine/nitrogen gas to suppress space charge accumulation. The space charge distribution was profiled using Pulsed Electroacoustic (PEA) measurements. The results shown that the density of negative charge was obviously reduced and the injection of positive charge was significantly inhibited by surface fluorination.

**Keywords:** surface fluorination; Nomex paper; space charge; oil-paper insulation

## Introduction

Insulation paper is preferred as insulation material in high voltage power transformer due to its good overall electrical and mechanical properties. Space charge accumulation in insulation paper was believed to have great influence on its electrical performance of oil-paper insulation system. Surface fluorination is an effective approach to modify the surface of dielectric without changing the matrix's property [1]. In this work, the DuPont T410 Nomex paper was fluorinated at 25°C for 30 min using $F_2/N_2$ mixture with 10% $F_2$ in volume at 0.1 MPa. After 48 h drying in vacuum at 90 °C, the untreated (F0) and fluorinated (F30) samples were impregnated in mineral oil in vacuum at 40 °C for 24 h [2]. Space charge distribution under DC stress was measured using the system described in reference [3].

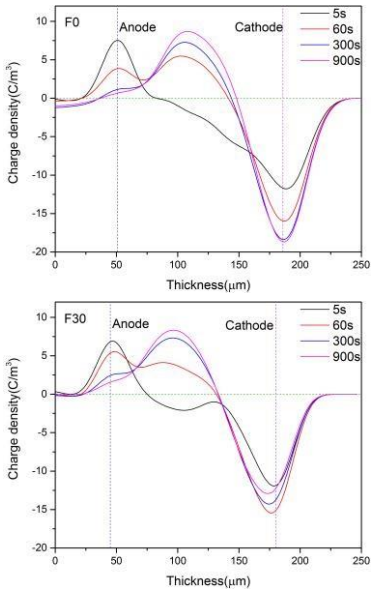


*Figure 1: space charge distribution of untreated (F0) and fluorinated (F30) samples.*

## Results and Discussion

Figure 1 shows the space charge distribution of sample F0 and F30. It's seen that positive and negative charges accumulate on sample surface respectively close to anode and cathode quickly. With electric field application, positive charges gradually shift to bulk while negative charges remain on sample surface. Higher density and less injection of positive charges close to the anode were observed in sample F30 comparing to F0. Obviously, the accumulation of positive and negative charges was inhibited after fluorination. With the increasing of poling time, the negative charge density of F0 increased first and then kept almost unchanged, yet the negative charge density of F30 was much lower than F0 and increased first and then decreased.

## Conclusion

Space charge accumulation of oil-impregnated Nomex paper was inhibited by surface fluorination. The introduced fluorinated layer may reduce the surface resistivity and shallow surface traps due to chain scission during fluorination, thus reduce the accumulation of space charge.

## References

[1] Kharitonov A P. *Progress in Organic Coatings*. 2008, 61(2–4):192-204.

[2] Liao R, Lv C, Yang L, et al. *Journal of Nanomaterials*. 2013, 2013: 1.

[3] Wang Y, Xiao K, Wang C, et al, *Journal of Nanomaterials*. 2016, 2016(28):1-10.

## Acknowledgements

The authors gratefully acknowledge the National Key Basic Research Program of China (973 program) (No. 2015CB251003), China National Science Fund for Distinguished Young Scholars (No. 51425702).

# Numerical model for calculating the space charge around defects inside polymer films

A. Mulla [1], S.J.Dodd, N.Chalashkanov, L.A.Dissado

aamm3@le.ac.uk

[1]Department of Engineering, University of Leicester, University Road, LE1 7RH Leicester, U.K

**Abstract:** Space charge is a very important feature of insulting polymers used in DC applications. Here we consider the impact the presence of a conducting defect has upon space charge and the consequent field distribution. Almost invariably this problem is tackled through a field-dependent approach. Here we include the temperature gradients produced by Joule heating and show that at high fields they introduce effects that modify the space charge outcome considerably.

**Keywords:** space charge, polymeric films, conducting defects

## Introduction

Continued application of DC voltages increases space charge accumulation within insulating polymers [1], and results in electric field enhancement that will contribute to premature breakdown in the worst case. Such accumulation is partly the consequence of the dependency of insulation conductivity on both the electric field and temperature [2]. Defects give rise to local electric field enhancement, producing current density gradients and hence temperature gradients, both of which will influence the generation of space charge. Here we use a numerical model to simulation these effects in a two dimensional 30x30 matrix with the overall size in each direction being 500 µm. A conducting defect is simulated by making the potential of four vertical bonds the same. An empirical field and temperature dependent expression was used for the polymer conductivity.

## Results and Discussion

When the polymer conductivity was considered to be temperature independent and only dependent upon the local electric field a significant amount of space charge accumulated around the defect, This had the effect of decreasing the electric field enhancement surrounding the defect and increasing it near the electrodes. When the conductivity was taken to be both field and temperature dependent, the result depended upon the magnitude of applied field. At fields $E \leq 40$ kV/mm the Joule heating was small and did not have a significant effect on the accumulated space charge. However, applied fields above 40 kV/mm led to an increase in the local Joule heating surrounding the defect, with the consequent temperature gradient resulting in a reduction of the accumulated space charge around the defects as demonstrated in figure 1.

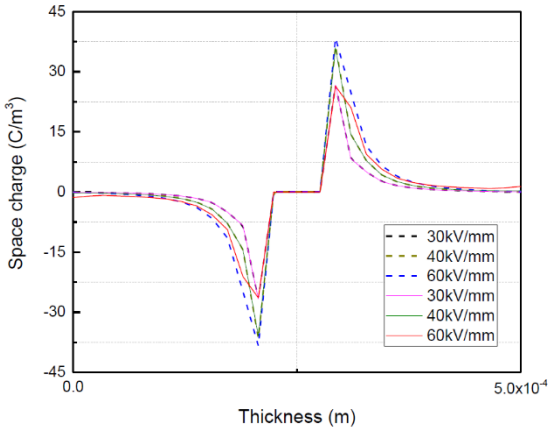


*Figure 1: Space charge profile around the defect at different applied voltage. The dotted line represent the space charge accumulation due to field dependent conductivity, while the solid lines represent the results of space charge accumulation due to the field and temperature dependent conductivity.*

## Conclusions

For the parameters used in this simulation, the field below 40 kV/mm the field enhancement due to the presence of conducting defects in insulating polymers is to some extent transferred to the electrodes as a result of space charge accumulation at fields below 40 kV/mm. This is an apparently unexpected movement of the risk of breakdown to a more dangerous location. At higher fields the defect again becomes the location of higher risk as its space charge shielding is reduced.

## References

[1] Z. Huang, "Rating methodology of high voltage mass impregnated DC cable circuits," University of Southampton, 2014.

[2] J. Hjerrild, S. Boggs, J. Holboll, and M. Henriksen, "DC-field in solid dielectric cables under transient thermal conditions," in *Solid Dielectrics, 2001. ICSD'01. Proceedings of the 2001 IEEE 7th International Conference on*, 2001, pp. 58-61

# Molecular mobility studies on the amorphous part of poly(vinylidene fluoride) (PVDF)/silica nanocomposites

Kyritsis A.[1], Klonos P.[1], Bolbukh Yu.[2], Tertykh V.A.[2], Gun'ko V.M.[2], Pissis P. [1]

akyrits@central.ntua.gr (Corresponding e-mail address)

[1]Department of Physics, National Technical University of Athens, Zografou Campus, 15780, Athens, Greece
[2]Chuiko Institute of Surface Chemistry, National Academy of Sciences of Ukraine, 17 General Naumov Street, 03164, Kiev, Ukraine

**Abstract:** Morphology, thermal transitions and molecular mobility of poly(vinylidene fluoride) (PVDF) were investigated in PVDF/silica nanocomposites (NCs). The interplay between segmental motions in the amorphous regions ($\alpha_a$-relaxation) and local motions of the main chain (β-relaxation) is thoroughly studied in both, semi crystalline PVDF matrix with embedded silica nanoparticles and in highly amorphous PVDF physically adsorbed onto spherical-like silica nanoparticles (core-shell type of NCs).

**Keywords:** PVDF, segmental relaxation, silica nanocomposites, dielectric technique

## Introduction

Semi-crystalline PVDF is favourably positioned among electroactive polymers [1]. Its polymorphism, the morphology of crystalline and amorphous regions and their interfaces as well, define significantly the properties and the processability of PVDF. The dielectric behavior of neat PVDF is determined mainly by three relaxation processes: the β-relaxation and $\alpha_a$relaxation, which are related to the local and segmental motion of the main chain, respectively, and the $\alpha_c$-relaxation, which is associated with VDF segments mobility within the crystalline phase. Investigation of changes in those dielectric relaxation processes in PVDF based NCs, where fumed silica nanoparticles are dispersed within PVDF matrix or PVDF is physically adsorbed onto spherical-like silica ($SiO_2$) nanoparticles [2], may provide insight to crystal transformations and/or to constraints to the amorphous part of PVDF chains.

## Results and Discussion

PVDF/silica NCs were studied employing morphology (SEM, WAXS), calorimetry (DSC) and dielectric (BDS, TSDC) techniques. Silica nanoparticles [2] were dispersed in semi-crystalline PVDF matrix in concentrations of 0.2, 2 and 20% w/w whereas in core-shell type NCs the silica concentration was 67 and 77% w/w.

In NCs with low silica concentrations the degree of crystallinity is slightly reduced, compared to neat PVDF, while the $\Delta C_p$ increment at $T_g$ decreases with increasing silica content indicating prominent interfacial effects on the amorphous part of PVDF. In core-shell NCs the PVDF crystallinity is highly suppressed and no calorimetric $T_g$ is observed. TSDC measurements show only the secondary β-relaxation peak, whereas, in agreement with DSC, the main relaxation peak does not appear. On the contrary, BDS reveals molecular mobility at temperatures around $T_g$ of PVDF providing evidence on the interplay between β- and $\alpha_a$-relaxation processes in the amorphous regions of PVDF.

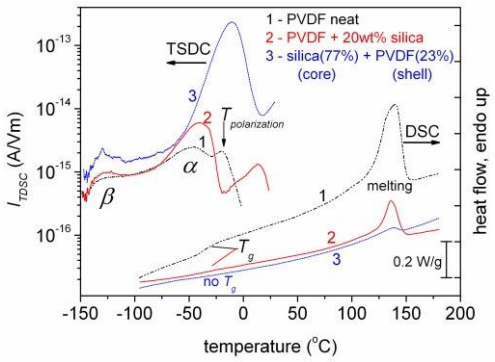


*Figure 1: comparative TSDC and DSC thermos-grams, for the samples described on the plot.*

## Conclusions

PVDF/silica NCs with strong interfacial effects exhibit highly suppressed crystallinity and allow for the investigation of molecular mobility in amorphous PVDF regions. It seems that segmental and local motions of the main chain are activated selectively depending on the constraints imposed by the silica nanoparticles.

## References

[1] S. Kripotou, S. Sovatzoglou, C. Pandis, J. Kuliček, M. Mičušík, M. Omastova, A. Kyritsis , A. Konsta, P. Pissis, Phase Transitions **2016**, 89, 717 – 730

[2] Klonos, P.; Kulyk, K.; Borysenko, M.; Gun'ko, V.M.; Kyritsis, A.; Pissis, P. *Macromolecules* **2016**, 49, 9457 – 9473.

## Acknowledgements

This research was partially supported by FP7 – PIRSES–GA–2013–612484 NANOBIOMAT.

# Ferroelectret Behavior in De-Lignified Wood

Iain Kierzewski[1], Chao Jia[3], Brendan Hanrahan[2], Sarah Bedair[2], Liangbing Hu[3], Nathan Lazarus[2]

imkanine@gmail.com , jiachao0806@gmail.com , brendan.m.hanrahan.civ@mail.mil , sarah.s.bedair.civ@mail.mil , binghu@umd.edu , nathan.lazarus2.civ@mail.mil

[1]General Technical Services, Wall Township NJ
[2]Army Research Lab, Adelphi MD
[3]University of Maryland, College Park MD

**Abstract:** This paper presents the first demonstration of ferroelectret behaviour in wood de-lignified for higher porosity. De-lignified wood contains a high density of eye-shaped pores ideal for ferroelectrets, and when a 940 µm-thick sample is charged past a coercive field of 2.9 MV/m, the de-lignified wood is shown to retain a large remnant polarization of 73.8 mC/m$^2$.

**Keywords:** wood, cellulose, ferroelectrets

## Introduction

By taking advantage of structures available in nature, we can obtain very good ferroelectret behaviour without the need for specialized fabrication processes, with a notable example the giant electret behaviour recently noted in nacre [1]. Wood is a highly porous hierarchical material consisting of a large number of aligned cellulose pores filled with the biopolymer lignin, and is known to experience thermally stimulated discharge suggesting electret behaviour [2]. Here for the first time we investigate the possibility of improving wood-based electret performance by removing the biopolymer for higher pore density using standard de-lignification process common in the pulp processing industry [1].

## Results and Discussion

Natural and de-lignified basswood samples approximately 1 cm$^2$ were prepared with thicknesses of 350 and 940µm, respectively. The high porosity is evident in an SEM cross-section of de-lignified wood taken against the grain, Figure 1a. Using sputtered electrodes approximately 50 mm$^2$ in area, sample capacitances of 1.5pF and 7.7pF were measured for de-lignified and natural wood respectively, after a dehydration bake for 10 minutes at 160° C. The samples were characterized in a voltage-voltage mode modified Sawyer Tower setup similar to that in [4]. Polarization was extracted from the stored charge by subtracting the charge due to the sample capacitance and dividing by the electrode area.

De-lignifying the wood results in a large improvement in ferroelectret charging behaviour, with a 45% percent lower threshold for pore breakdown as well as an 18% larger remnant polarization. The remnant polarization of 73.8 mC/m$^2$ for this un-optimized sample is competitive with the low hundreds of mC/m$^2$ seen in modern engineered electrets based on polymers such as PVDF [5], and we believe further improvements are possible with careful selection of wood species for pore control.

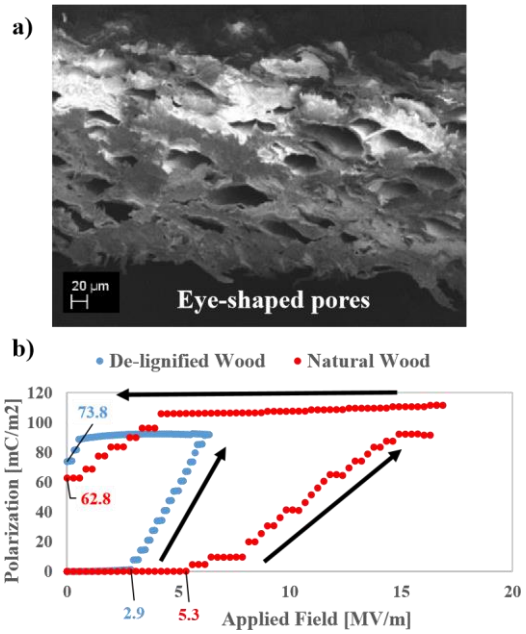


*Figure 1: (a) SEM cross-section of de-lignified wood and (b) polarization curves for wood samples.*

## Conclusions

De-lignified wood demonstrates a substantial improvement in remnant polarization. In addition to the partial hysteresis loop presented here, we plan on presenting a more complete hysteresis loop and characterizing the resulting thermally-stimulated discharge at the conference.

## References

[1] Yao, Y et al., *Advanced Materials 2012*, doi: 10.1002/adma.201202079
[2] Fushitani, M, *Mokuzai Gakkaishi, 1981, vol. 27, no. 4, p.263-269*
[3] Zhu, M et al., *Adv. Mat., 2016*, doi:10.1002/ adma.201600427.
[4] Qiu, X; Wirges, W.; Gerhard, R., *Ferroelectrics 2014, 472, 100 – 109*, doi: 10.1080/00150193.2014.964603.
[5] Ghosh, S et al., *Nano Energy 2016*, doi: 10.1016/j.nanoen.2016.10.042

# In situ measurement of electrical field distribution in thin films from double sides by thermal pulse method

Minghui LIANG, Feihu ZHENG[1], Shanzhao PAN, Zhenlian AN, Yewen ZHANG

feihuzheng@tongji.edu.cn (Corresponding e-mail address)

[1]Department of Electrical Engineering, Tongji University, 4800 Cao'an HWY, Shanghai, China

**Abstract:** A double-side thermal pulse apparatus is developed. With this apparatus, thermal pulse measurements can be taken in-situ on both sides of the sample under an applied voltage. A complete set of measurements are accomplished in the original position without reversing the sample. Therefore, the measuring procedure is simplified and the risk of injuring the very thin sample during reversing the sample is reduced. The sample is heated by a short laser pulse from both sides and the responding signal is recorded, respectively.

**Keywords:** thermal pulse method, space charge, electric field

## Introduction

A continuously applied DC voltage usually leads to space charge accumulation in polymer films, which results in distortion of internal electric field. Monitoring the internal electric field distribution under an applied voltage is an effective way to understand the space charge behavior in polymer films. Thermal pulse method is a powerful tool to conduct the measurements. However, due to the rapid thermal attenuation and dispersion through the sample, high spatial resolution is only achieved near the heated surface of the sample.

## Results and Discussion

The thermal response current is amplified by a homemade current preamplifier with a bandwidth of 300 kHz and recorded with a digital storage oscilloscope at a rate of 50MS/s after averaging 100 laser pulses. The tested samples are polypropylene films with thickness 9.8μm. Opaque aluminum electrodes with 5mm diameter are deposited on both sides of the films by means of evaporation to act as the pulse target and provide electrical contact. The electric field distribution of the sample is reconstructed from the Fourier-transformed response current with scale transformation method in frequency domain. The result obtained from a pristine film under an applied electric field of 10kV/mm is used for calibration. It is considered that no space charge accumulates in the bulk of the sample under the circumstances and the electric field distribution is uniform. The measured data should be calibrated on both sides respectively. It is noted that the configuration of experiment for the calibration procedure must be identical to the subsequent measurements. The result of the calibration test (Figure 1) shows a uniform electric field distribution in the bulk of the sample as expected, despite a distortion near the sample surface due to the bandwidth limitation of the measuring system. With calibration, surveillance of electric field evolution in the sample can be realized by taking a series of measurements at intervals. The results indicate that the internal electric field of the films becomes increasingly non-uniform with time. It can be inferred that space charge accumulates gradually in the samples under the applied DC voltage and distorts the original electric field. The electric field and space charge distribution of the samples without applied voltage is measured in addition. The effect of temperature on electric field and space charge evolution is also investigated. As the temperature increase, the electric field distortion becomes more obvious and the build-up of space charge faster as well.

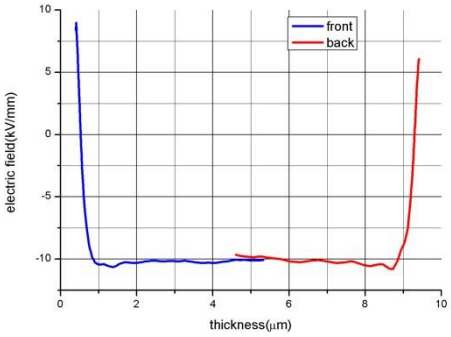


*Figure 1: Electric field distribution of a polypropylene film with thickness 9.8μm under an applied 100V DC voltage*

## References

[1] A. Mellinger, R. Singh, and R. Gerhard-Multhaupt, Rev Sci Instrum, 2005, 76 (013903).

[2] F. Zheng, C. Liu, C. Lin, Z. An, Q. Lei, and Y. Zhang, Measurement Sci. Technology, 2013, 24(065603)

## Acknowledgements

Financial support from the National Natural Science Foundation of China (NSFC Nos. 51477119 and 51477118).

# Lifetime estimation for electrical breakdown on PVC sheath

A. Laifaoui[1], J.M. Reboul[2], H. Ait Said[1] et Y. Zebboudj[1]

abdelkrim.laifaoui@univ-bejaia.dz

[1]Laboratoire de Génie Electrique, Université Abderrahmane Mira, Bejaia, Algérie
[2]Laboratoire Universitaire des Sciences Appliquées Cherbourg, Université de Caen Normandie, France

**Abstract:** We present the study of electrical breakdown of polyvinyl chloride sheaths (inner diameter 4mm and thickness 1.5mm.) which is evaluated from the lifetime curve. The tests were carried out with the following AC voltage levels: 40, 37.5, 35, 32.5, 30, 27.5, 25, 22.5, 20, 17.5, 16.5 and 15.5 kV. For each voltage level, 50 samples have been tested so a total of 600 measurements have been obtained. And the values obtained are treated by the Weibull method, and then validated by the khi-2 test, with 90% confidence intervals. The results show three behaviours in life time predictions.

**Keywords:** electrical breakdown, long-term aging, Weibull model, lifetime, inverse power law.

## Introduction

Polymer insulation, such as polyvinyl chloride (PVC), is the basis for medium voltage application. However these materials are subject to aging; which may lead to electrical breakdown and damage the equipment where they are used. Thus, a better knowledge of lifetime is of good interest.

The dielectric failure tests need experiments on a large number of samples and use a statistical approach. The most used model is the Weibull method [1, 2]. It leads to a mean time-to-breakdown value for a known voltage.

## Experiments

The tests were carried out with the following voltage: 40, 37.5, 35, 32.5, 30, 27.5, 25, 22.5, 20, 17.5, 16.5 and 15.5 kV. For each voltage level, 50 samples (PVC sheath, length 80 cm, in-diameter 4 mm and thickness 1.5 mm) have been tested with cylindrical aluminium electrodes. The time-to-breakdown occurring for the first to the last sample of the series is measured and recorded with a programmable counter for a total recording of 600 single values of time-to-breakdown. The quickest time measured under the highest voltages is of tens of seconds and the longest value of the last sample under the lowest voltage is greater than 3 years. All these experiments have been realized in Bejaia's high voltage laboratory and lasted 5 years. All the results have been treated with the Weibull model and the likelihood algorithm [2]. The extracted data have been certified with the khi-2 test using 90% confidence intervals.

## Results and Discussion

The figure 1 shows the mean time-to-breakdown for the all tested voltages. The double logarithmic scale discloses three zones with regular straight line corresponding to the following power law each [3]:

$$t = kU^{-n}$$

where t denotes the mean time-to-breakdown, U the applied voltage, k an experimental coefficient and n the electrical endurance coefficient.

The electrical endurance coefficients n are respectively 4.950, 16.949 and 7.194 for the zones I, II and III. There are two transition times at 6.01 h and at 524.13 h reflecting changes in the behavior aging of the material studied.

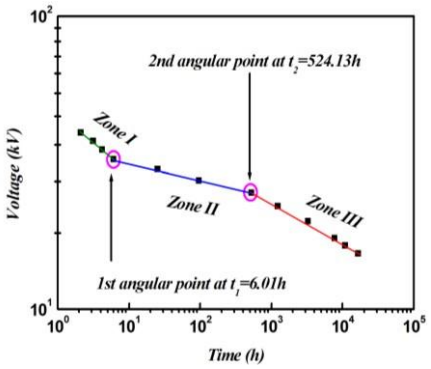


*Figure 1: PVC life time for the all tested voltages.*

## Conclusions

The lifetime curve of the PVC sheaths obeys the inverse power model [3]. It is composed of three zones. Zone I is attributed to the insulation defects of the insulation relating these extrinsic defects. Zone II characterizes the random dispersion of intrinsic defects in the material and, lastly, zone III reflects the real aging of the material. As an example, the 30-years-reliability of PVC sheath deduced from zone III is for a maximum AC voltage of 10 kV.

## References

[1] W. Weibull, J. Appl. Mechanics, **1951**, 18, 293-297.
[2] V. Englund, R. Huuva, S.M. Gubanski and T. Hjertberg, Poly Degra. and Stab. **2009**, 94, 823–833.
[3] C. Dang, J.L. Parpal, J.P. Crine, Trans. Diel. Electr. Ins, **1996**, 3, 2, 237- 247.

# Study of electret state in epoxyamine polymers by dielectric spectroscopy

Eduard Galikhanov[1], Ekaterina Mochalova[2], Ivan Lounev[1], Mansur Galikhanov[2],

Ildar Gabdrakhmanov[2], Roza Fatikhova[1], Yurii Gusev[1]

mgalikhanov@yandex.ru

[1]Kazan (Volga region) Federal University, Kremlevskaya, 18. Kazan, 420008, Russia
[2]Kazan National Research Technological University. K. Marx, 68. Kazan, 420015, Russia

**Abstract:** Electret and dielectric properties of polymer materials based on epoxide oligomer and polyamine amide. Via dielectric spectroscopy method it is proved that dipole groups orientation of epoxide polymer macromolecules fixed by third-dimensional grid and are carriers of thermoelectret charge occurs under polymer transition into electret state. Electret state of polymer matrix is characterized by a free state of epoxyamine macromolecules.

**Keywords:** epoxy oligomer, diethylene triamine, macromolecules free state, thermoelectret, dielectric permittivity

## Introduction

Combining processes of epoxy polymers synthesis and polarization, thermoelectrets with controllable structure and properties could be obtained. In this case, there are orientation of oligomer molecular dipoles (polar groups, segments of oligomer molecules) in electric field and their fixation by forming third-dimensional grid of polymer [1]. For studying different materials structure and properties, including polymeric, dielectric spectroscopy method is widely used [2, 3].

Purpose of paper is epoxy polymers dielectric properties study to describe their electret state.

## Results and Discussion

For thermoelectrets based on epoxy resin with curing agent at 60$^{th}$ day after charging $V_e$ = 0,64 kV, $\sigma_{ef}$ = 0,35 μC/m$^2$ и $E$ = 34,7 kV/m. Study of epoxy polymers with dielectric spectroscopy method (fig. 1) showed the presence of two relaxation processes. Experimental data handling by Havriliak-Negami method allowed to reveal quantitively relaxation energies of these processes. First relaxation process with activation energy $E_{a1}$ = 243,2 kJ/mole is correlated with polymer transition from glassy to highly-elastic state. Second one with $E_{a2}$ = 170,4 kJ/mole is correlated with postcure reactions behavior which accelerates with temperature raise.

During the study of thermoelectrets based on epoxy polymers similar picture were discovered. However, values of epoxy material dielectric permittivity increase with its transit to electret state, that indicates about dipole macromolecular groups orientation. Activation energy calculation data of thermoelectret dielectric relaxation process looks interesting: $E_{a1}$ = 188,3 kJ/mole, $E_{a2}$ = 149,6 kJ/mole, so there is a small decrease in comparison with nonpolarized materials values. It is quite explainable, taking into consideration the fact that electret state of polymeric matrix, forming in curing process and being fixed by chemical bounds third-dimensional grid, becomes a free state of epoxyamine macromolecules.

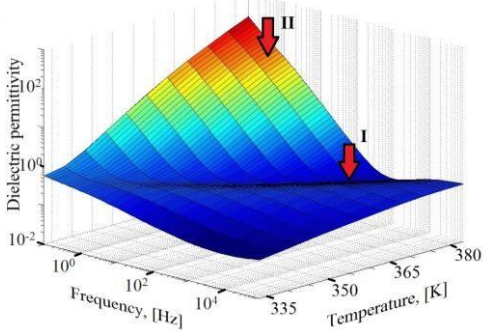


*Figure 1: Frequency and temperature dependences of dielectric losses for nonpolarized epoxy polymer*

Thus charge carriers (dipoles), mostly oriented in one direction, are "frozen" in curing product net structure. They are playing the role of thermoelectret charge carriers.

## Conclusions

Hereby using dielectric spectroscopy method dipole macromolecular groups orientation of epoxy polymer material, typical for polymer dielectrics electret state, is proved. Polymeric matrix electret state, forming in curing process and being fixed by chemical bounds third-dimensional grid, is a free state of epoxyamine macromolecules.

## References

[1] Mochalova E.N. et al. // Polymer Science, Series D. 2016. Vol.9. No.4. P.396-401.
[2] Mazur K. // J. Phys. D: Appl. Phys. 1997. Vol.30. P.1383-1398.
[3] Galikhanov E. et al. // AIP Conference Proceedings. 2016. Vol.1722. 290002.

# Cell detection by surface imprinting polymers (SIPs) – a study of the sensor surface by optical and dielectric relaxation spectroscopy

Alessia Gennaro[1], Derick Yongabi[1], Olivier Deschaume[1], Patrick Wagner[1], Michael Wübbenhorst[1]

alessia.gennaro@kuleuven.be

[1]Department of Physics and Astronomy, Laboratory for Soft matter and Biophysics, KU Leuven, Celestijnenlaan 200d, 3000 Leuven, Belgium

**Abstract:** Previous studies on cell detection have demonstrated that cell imprinting on polymer layers produces synthetic receptors which are effective for specific and selective cellular recognition [1]. Despite the potential use of these receptors, their binding mechanisms remain unexplored. Therefore, in this study, the molecular dynamics of cell-imprinted and non-imprinted polyurethane (NIP) layers were studied by dielectric spectroscopy.

**Keywords:** polyurethane, cell detection, dielectric relaxation spectroscopy, surface-imprinted polymers, IDEs, phospholipids, membrane proteins

## Introduction

In this study, we explore the factors influencing the recognition of cells by their corresponding SIPs using different spectroscopic techniques.

Earlier we hypothesized that membrane proteins, lipids and hydrogen bonds are transferred from the cell membrane to the imprinted cavities during imprinting. Therefore, we explored the dynamic and temperature-dependent dielectric relaxation signatures of proteins and lipids on the imprinted polyurethane layers.

## Results and Discussion

Baker's yeast cells (*Saccharomyces cerevisiae*) were used to create SIPs.

SIPs and NIPs were characterized by Atomic Force Microscope (AFM) by scanning the surface topology and by dielectric spectroscopy in the frequency range from $10^{-1}$ to $10^{7}$ Hz, to examine the transfer of geometrical and chemical information to the imprints. The results show a clear distinction between the spectra acquired from a layer of cells, otherwise referred to SIP with cells, a SIP and a NIP. As shown in Figure 1, within the 370K–256K temperature range, the temperature-dependent relaxation time is characteristic of lipids [2] with an activation energy of 67 kJ/mol, calculated according to the Arrhenius equation. This characteristic relaxation process was not observed for the NIP, thus, leading to the conclusion that imprinting transfers lipid molecules from the cell membrane to the polymer layer, which likely play a role in the mechanisms by which cells bind to SIPs.

These results are consistent with Fourier Transformed Infrared Spectroscopy (FTIR) and X-ray Photoelectron Spectroscopy analysis of the cells, SIP, and NIP layers, which both reveal lipid residuals on the SIP layer.

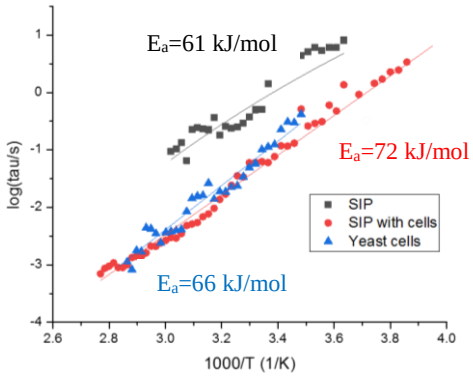


*Figure 1: Relaxation time vs temperature*

## Conclusions

We have shown that besides the transfer of geometric information of the cells to the imprinted layers, lipids are the main chemical moieties being transferred during cell imprinting. While we strongly belief that transferred lipids play a major role in the SIP recognition mechanism, the correlation between the DRS, FTIR and XPS results indicate that DRS is a reliable technique to analyse the chemical information transferred to the SIP layer during imprinting.

## References

[1] K. Eersels et al., ACS Applied Materials and Interfaces **5**, 7258 (2013).

[2] Physiology of membrane disorders, T. Andreoli, F. Hoffmann, S. Schultz.

## Acknowledgements

This study was financed by the KULeuven project C14/15/066 ''Smart Cellular Scaffolds''.

# New interdigitated comb electrode (IDE) design for detecting cells

Alessia Gennaro[1], Patrick Wagner[1], Michael Wübbenhorst[1]

alessia.gennaro@kuleuven.be

[1]Department of Physics and Astronomy, Laboratory for Soft matter and Biophysics, KU Leuven, Celestijnenlaan 200D, 3001 Heverlee, Belgium

**Abstract:** Previous studies on cell detection have demonstrated that cell imprinting on polymer layers produces synthetic receptors, which are effective for specific and selective cellular recognition [1]. Despite the successful use of these receptors, their binding mechanisms are not yet fully understood. Therefore, in this study, the dielectric properties of cell-imprinted and non-imprinted polyurethane (NIP) layers were studied by dielectric spectroscopy using a patterned thin film electrode structures.

**Keywords:** IDE, dielectric relaxation spectroscopy, surface-imprinted polymers, cell detection, phospholipids, membrane proteins

## Introduction

It has already been shown that cells bind to imprint surface due to the matching between template cells (*Saccharomyces cerevisiae*) and imprinted cavities on the surface imprinted polymer (SIP) layer and a chemical binding, since the geometry and cell residues are transferred from the cell membrane to the imprinted cavities.

Therefore, dielectric relaxation spectroscopy has been used to study the dynamic and the temperature-dependent relaxation signatures of proteins and lipids on the imprinted polyurethane layers.

In this study, an alternative detection scheme for electrical properties of the imprinted polymer layer have been explored. The new idea is to modify the electrode configuration to explore the electrical properties of the polymer/cell interface.

## Results and Discussion

The results**,** obtained using the classical parallel plate configuration show a clear distinction between the spectra acquired from a layer of cells, otherwise referred to SIP with cells, a SIP and a NIP. Unfortunately, a parallel plate configuration is a closed structure and has no specific sensitivity for relaxation phenomena originating from proteins located at thin interfacial regions. Another drawback is that the Al- evaporated top electrode, following the SIP profile with cavities, seals the structure and causes undesired variations in the local sample thickness and thus the local dielectric sensitivity.

By using an IDE structure, it is possible to measure the dynamics of an open and evolving system. Taking advantage of the open configuration, it will be possible to deposit cells and observe in real-time the kinetics of cells binding or cell release.

Moreover, by placing this patterned thin film electrode structure close to the cell recognition layer, we can obtain local information on a length scale comparable to the IDE-gap distance. For this reason, we have designed various IDE with finger spacings of 1.5, 3 and 6 µm. The sensitivity of 3 µm spacing IDE has been tested with glycerol according to what has been demonstrated in previous studies on glycerol [2].

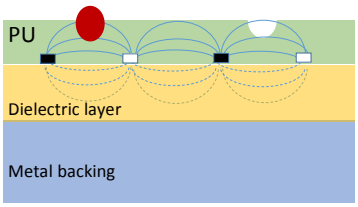


*Figure 1: Proposed measurement configuration for cell recognition detection by embedded IDE*

## Conclusions

To push the detection limit for bound cells via optimized, highly sensitive dielectric sensing structures, variably spaced IDEs have been realized and tested. The new configuration, over the classical parallel plates configuration, allows to tune the sensitive volume around the sensor surface and helps to explore the binding mechanisms between cells and SIP measuring a cell specific dielectric response.

## References

[3] K. Eersels et al., ACS Applied Materials and Interfaces **5**, 7258, 2013.

[4] S. Capponi et al. 'Supercooled liquid with enhanced orientational order.' Nat. Commun., vol.3, p.1233, Jan. 2012.

## Acknowledgements

This study was financed by the KULeuven project C14/15/066 "Smart Cellular Scaffolds". We gratefully appreciate Dr.Frederik Ceyssens of the MICAS KULeuven, for his support in the Nanocentre cleanroom.

# Study of Dielectric Parameters of γ-irradiated atactic Polymethylmethacrylate (PMMA) by the Thermostimulated Depolarisation Currents (TSDC) Method

Derbil Samia[1], Khemici Mohammed Wafik[1,2], Doulache Naima[1], Azeddine Gourari[1]

khemici@gmail.com

[1]University of Sciences and Technology Houari Boumediene (USTHB) BP 32, El-Alia, Bab Ezzouar 16111, Algeria

[2]Department of Physics, Faculty of Sciences, University of M'Hamed Bougara, Boumerdes, 35000, Algeria

**Abstract:** The aim of this work, is to study the effect of γ-irradiation on the dielectric parameters of PMMA by the use the thermally stimulated depolarization currents method (TSDC). TSDC spectrum shows two peaks appearing respectively at -30°C and 113°C. A particular interest was reserved to the α-relaxation appearing around 113°C. Study of the individual modes of the relaxation processes allows us to deduce the dielectric parameters of the material at $10^{-3}$Hz. When the radiation dose increases, the dielectric losses of PMMA increases and its dielectric behavior changes from a typical Cole-Cole behavior towards a rare behavior of Davidson.

**Keywords:** TSDC technique, PMMA, γ-irradiation, dielectric parameters

## Introduction

The impact of ionizing radiation have been widely used in order to modify the structure of macro-molecular chains and change the macroscopic, chemical and physical properties of polymeric materials [1]. In this work, a particular interest was reserved to the study of the dielectric behavior of irradiated PMMA in the Jonscher equation [2,3].

## Results and Discussion

The samples of PMMA in the form of thin films were irradiated, using a Cobalt $^{60}$Co source, at ambient air with an average dose rate of 22.35 Gy/min. Different doses were then obtained according to the sample exposure time to radiation The recording of the different experimental spectra of TSDC revealed a change in the peak shape and it shift towards lower temperatures. Also, an increase in the polarization of the irradiated PMMA is observed. The thermal windowing method allows us to resolved experimentally the obtained peaks into a set of elementary peaks with a temperature that ranges by 5°C. Using Debye hypothesis (4), we were able to compute the dielectric dispersion for each elementary peak. The real and the imaginary parts of the dielectric permittivity (Δε′ and ε" ) were then deduced. The evolution of ε" versus the temperature for all radiation doses of PMMA is illustrated on figure 1. This latter reveals an increase of ε" when the radiation dose increases. This result implies the augmentation of the energy dissipation which is directly related to ε".

Using the equation of Jonsher, we have been able to represent the evolutions of the dielectric losses as a function of the dielectric dispersion (see the upper light corner of the inset of figure 1).

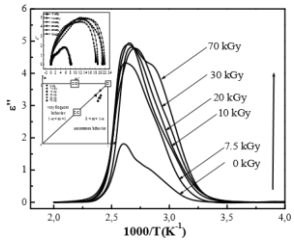


*Figure 1: Evolution of dielectric losses versus radiation dose (insets: evolutions of ε" versus Δε' and m versus n-1).*

The obtained graphs allowed us to deduce, for each sample, the m and n-1 parameters of the Jonsher equation. The representation of m versus n-1 revealed that the non-irradiated PMMA exhibited a Cole and Cole behavior. On the other hand, when the dose of radiation increases, the behavior of the material tends towards a Davidson behavior which is described as uncommon or rare.

## Conclusions

We have been able to highlight the effect of γ-radiations on the dielectric behavior at low frequency, of atactic PMMA by the TSDC technique. This study shows a decrease in the dielectric losses. The dielectric behavior of irradiated PMMA is uncommon (Davidson type).

## References

[1] Sinha, D; 2013. Adv. Appl. Sci. Res., 4:225-236.
[2] Khemici, M.W; Rahmani, B; Doulache, N; Gourari. A; 2013. Inter. Conf.Sol. Dielec (ICSD), 354-357.
[3] Coelho, R; 1979. Physics of dielectrics for the engineer, Elsevier

# Study of thermally stimulated discharge current and optical bandgap of ZnO filled polysulfone polymer nanocomposites

Pramod Kumar Singh[1] , Mulayam Singh Gaur

drpksinghsengar@gmail.com (Corresponding e-mail address)

[1]Interdisciplinary Research laboratory, Hindustan College of Science and Technology, Farah, Mathura, UP 281122, India Affiliated to Dr. A. P. J. Abdul Kalam Technical University, Lucknow ( U P ), India

**Abstract:** Polymer nanocomposite thin film of polysulfone (PSF) with different wt. % were prepared by solution grown technique. In this paper we have discussed thermal and optical property of PSF and ZnO nanoparticle filled nanocomposite. The thermally stimulated discharge current (TSDC) of PSF and PSF/ZnO nanocomposites samples were characterized by single peak and significant enhancement of different TSDC parameters. UV-vis spectroscopy reflect the significant improvement in optical band gap, which may useful for electronic and optoelectronic applications.

**Keywords:** TSDC, optical band gap, polysulfone, ZnO

## Introduction

The principle concern of TSDC research is to study the charge decay and storage, relaxation processes by heating the charged polymer samples at a constant heating rate [1]. Recent years have shown a considerable interest in electret state of amorphous polymer. Polysulfone (PSF) is an amorphous thermoplastic polymer, which is frequently used in the electrical, electronic, and other industrial applications [2] because of the excellent mechanical, thermo-oxidative and flame retardancy properties. It is superior replacement of Polycarbonate. ZnO is one of the multifunctional inorganic nanoparticles which has significant physical, chemical stability as well as wide band gap which is very useful for different electronic and optoelectronic applications [3]. Therefore, in this study ZnO nanofillers filled Polysulfone (PSF) were used to investigate the charge storage and transportation mechanism and investigation of the optical properties of polymer nanocomposites.

## Results and Discussion

TSDC spectra as shown in figure 1, have been recorded at 30 $^0$C and 60 $^0$C poling temperature with different polarizing field (30, 90 kV cm$^{-1}$), and it is evident from all the observed TSDC thermograms, initially the current starts at higher order and gradually it decays up to a certain temperature and after that with the increase in polarizing field or temperature it increases. TSDC thermograms show the magnitude of the TSD current decreases with ZnO nanofillers in PSF matrix. This may be attributed by the formation of interface between polymer and nanofillers. Mostly, all the TSDC parameter such as peak current, activation energy and charge released are increasing with increasing the poling field of pristine sample as well as of nanocomposite with polarizing field at polarizing temperature and polarizing fields. The observed higher value of activation energies can be associated with the trapping of charge carries. The magnitude of the charge released of all nanocomposite samples is lower than the pristine PSF sample but continuously increases with polarizing fields at 30 $^0$C and 60 $^0$C. The TSDC peak in pristine and all nanocomposite sample cases are most likely to be a function of distribution in relaxation times, because the peak occurs near the glass transition (Tg) of the polymer, where the side groups moves in unison with the main chain because the distribution of diploes in the amorphous phase is most likely to be random, it may be expected that this is the complex process involving both distributions of the activation energy and relaxation times. The UV-Vis spectroscopy observations this indicates the decrease in optical band gap by 2.43 eV from pristine to 10 wt. %.

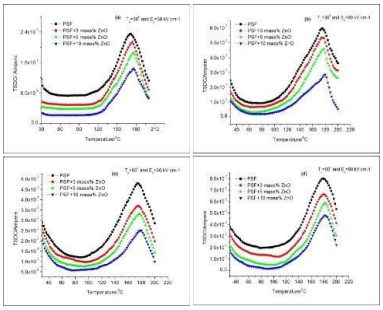

## Conclusion

TSDC results shows the significant improvement in different TDSC parameters such as activation energy, relaxation time and charge released. Whereas, UV-vis spectroscopy shows the enhancement of optical band by 56.77 % after incorporation of 10 wt. % of ZnO nanoparticles, which directly reflect the significant enhancement of refractive index

## References

[1] Lee K.Y.; Lee K. W.; Choi Y. S.; Park D. H.; Lim K. J.; *IEEE Dielectr. Electr. Insul.* 2005, 12, 566-572

[2] Gaur, M.S.; Singh P.K.; Chauhan R.S. *Journal of Thermal Analysis and Calorimetry*. 2014; 117:1407-1417.

[3] Tachikawa S, Noguchi A, Tsuge T, Hara M, Odawara O, Wada H.. *Materials*. 2011, 4:1132-1143

# New ways of TSD sampling for a high resolution activation energy analysis

J. van Turnhout

j.vanturnhout@tudelft.nl

Dept. Materials Science and Engineering, Delft University of Technology,

Mekelweg 2, 2628CD Delft, The Netherlands

**Abstract:** We present 3 methods to probe TSD spectra locally. Our approach relies on running a few TSD's at different speeds, in order to ensure that both the temperature and heating rate can act as variable. The highest resolution is obtained with bivariate differential sampling.

**Keywords:** differential sampling, equal level sampling, activation barriers, trap depth mapping

## Introduction

The dipoles and charges in electrets are usually stored at different energies. Often thermal windowing and BFG plots are used to gain insight in the height of the energies. This repetitive procedure takes time and lacks reliability and resolution.

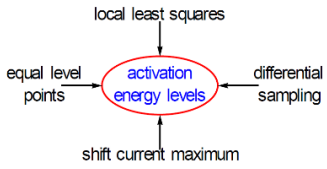


*Fig.1: The energy levels at work in charge storage can be assessed in 4 ways.*

Fig 1 depicts quicker and more accurate ways to determine the energy levels. They require that the TSD is redone at least twice, at different heating rates. The ensuing spectra are scanned together at multiple levels. One of the methods, the familiar shift of the current maximum, scans at only one level. It gives the mean of the energies.

## Results and Discussion

Fig.2 gives charge decay curves for 3 different inverse heating rates s. On top we show the combined pointwise equal level sampling, followed by equal level sampling using local l.s.q. This joined local fitting was done with all-in-1 modelling [1]. Next we have sketched the discrete differential sampling vs. 1/T and vs. lns. The ratio of these derivatives R gives the "local" activation energy: $A/kT_m=R-1.915T/T_m$.

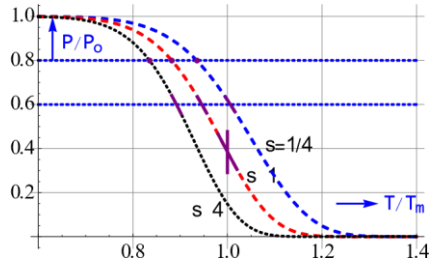


*Fig.2: Stepwise sampling of charge spectra at equal level points and by local l.s.q. and bivariate differential sampling.*

Fig 3 illustrates the pointwise equal level sampling of current spectra from the front to the rear side of the peaks. The use of the shift of the maxima is also indicated. Note that we should analyse $sjT^2$.

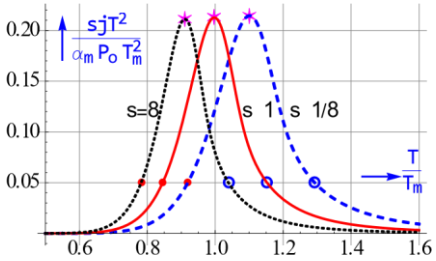


*Fig. 3: Pointwise probing of current spectra at equal levels and by the shift of their maxima.*

Fig.4 shows the almost constant energy profile of a KWW relaxation with *one* activation energy found by sifting 3 current spectra with differential sampling. We calculated the ratio of the discrete derivatives for $sjT^2$.

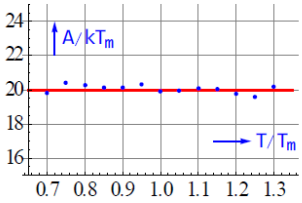


*Fig.4 Energy profile obtained by DS of current spectra.*

## Conclusions

The HR-analysis can be done model free and thus has general applicability. The methods proposed can also be applied to other TS phenomena, such as thermoluminescence. Pointwise sampling has been proposed earlier in e.g. [2], but these isoconversion analyses have been restricted to just one spectrum.

## References

[1] J. van Turnhout, *Front. Chem.* 2016, doi: 10.3389/ fchem.2016.00022.

[2] S. Vyazovkin: Isoconversional kinetics of TS processes, Springer: Heidelberg 2015.

## Acknowledgements

The author likes to thank Prof. J. Sietsma and Prof. I.M. Richardson for allowing him a stay in the Dept. of Materials Science and Engineering at the TU-Delft.

# TSDC study of polyvinyl chloride/polymethyl methacrylate (PVC/PMMA) blends

M'Zir Tawous[1], Doulacha Naima[1], Khemici Mohammed Wafik[1,2]

nkhemicidoulache@gmail.com
[1]University of Sciences and Technology Houari Boumediene (USTHB)
BP 32, El-Alia, Bab Ezzouar 16111, Algeria
[2]Department of Physics, Faculty of Sciences,
University of M'Hamed Bougara, Boumerdes, 35000, Algeria

**Abstract:** The present work focus on the study of PMMA / PVC blends. After preparing our samples in different concentrations, we carried out their characterization using the thermally stimulated currents (TSDC) technique. The obtained results revealed miscibility of the two materials (PVC and PMMA) for concentration of PMMA less than or equal to 60%. The TSDC spectra of the blends present single peak whose position is intermediate between the one of its constituents as well as the activation energy and the compensation parameters deduced by the fractional polarization technique.

**Keywords:** PMMA/PVC blends, TSDC, miscibility.

## Introduction

Research on new materials focuses on the study of blends of already existing and well known materials. Among the latter appears the PMMA / PVC blend which is the material of the present study. The study of these blends has been the subject of several previous works using various characterization methods [1-2]. Nevertheless, their studies using the TSDC techniques are not as abundant.

## Results and Discussion

Films of (PMMA/PVC) blends were prepared by using solution cast technique. Pure PMMA and PVC were dissolved separately in tetra chlorure(THF) at room temperature. The solutions of the two homopolymers were then mixed with different concentrations during 24hours. Then, we sub-sequently cast ontoglass dishes and let in an oven at 50°C for 5 hours to eliminate all residual solvent and moisture traces. The concentrations of the prepared (PMMA/PVC) blends are (0/100, 10/90, 20/80, 30/70, 40/60, 50/50, 60/40, 90/10, 80/20, 100/0)

After preparing our blends in the form of films, and before proceeding to the measurements of the TSDC currents, we analyzed our samples by several methods. In particular, observations by a polarization optical microscope revealed homogeneity of the films for PMMA rate less than 60%. This observation was then confirmed by the differential scanning calorimetry. Indeed, a single glass transition temperature was observed for PMMA rates less than 60%. In order to explain this behavior, FTIR spectra in ATR mode were recorded. The latter revealed a shift of the peak relative to the C = O bond of the carbonyl ester group of PMMA. This shift reflects an interaction between PVC and PMMA, mainly due to the presence of a hydrogen bond between the two materials.

After establishing the miscibility domain of our blens, TSDC spectra were recorded (see Figure 1).

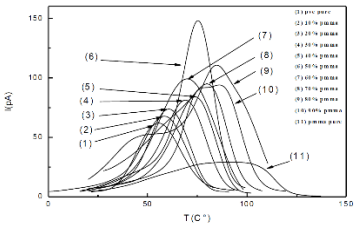


*Figure 1: Thermally stimulated depolarization currents (TSDC) spectra.*

This figure shows the appearance of a single TSDC peak for miscible blends. On the other hand, from 60% of PMMA, a second peak appears in the form of a shoulder: this result confirms one again, the miscibility domain previously established.

The thermal sampling technique allows us to determine the activation energy, fragility index, compensation temperature and the dielectric parameters at equivalent frequency of $10^{-4}$ Hz. of our blends.

## Conclusions

The TSDC technique enabled us to confirm the miscibility domain of the PMMA / PVC blends. The analysis of the obtained spectra shows that the structural parameters of the blends (activation energy, fragility index ...) are between those of the basic constituents.

## References

**[1]** K. Aouachria, Phd diss, 2011, Farhat Abass university, Setif, Algeria.

**[2]** Belhaneche-Bensemra, B. Bel l.aabed, A. Bedda, Annales de Chimie - Science des Matériaux, 2003, 28, 77.

# Refined conversion of TSD data to ultralow frequency ε′, ε″ and dε′/dlnω spectra

J. van Turnhout
j.vanturnhout@tudelft.nl
Dept. Materials Science and Engineering, Delft University of Technology,
Mekelweg 2, 2628CD Delft, The Netherlands

**Abstract:** Three options will be discussed. The easy to use first one involves the modification of the isothermal t to ω conversion based on kernel matching. Fitting TSD directly to a model of which ε′ and ε″ are known, offers a second choice. In the third the dielectric quantities ε′ and ε″ are found by evaluating the appropriate Laplace and Fourier transform in a fast way.

**Keywords:** isothermal and non-isothermal conversion, kernel matching, fast Laplace and Fourier transform

## Introduction

TSD measurements take a few hours, so they provide information about the relaxation behaviour at extremely low frequencies. This makes it appealing to convert the non-isothermal data to ε′ and ε″ spectra, which are often more easily modelled. The conversion of TSD to ε′ and ε″ has been discussed in [1]. This conversion was restricted to the T-domain. We have found a way to extend the conversion to the ω-domain by using variable embedding. We could also improve the accuracy. We explored 3 routes, cf. Fig.1. The most attractive is the one based on kernel matching. This method is well established for isothermal conversions [2]. It provides ε′ and ε″ from a sum of p and/or j values. In addition, dε′/dlnω and Δε′, which have a resolution higher than ε″, can be computed as well.

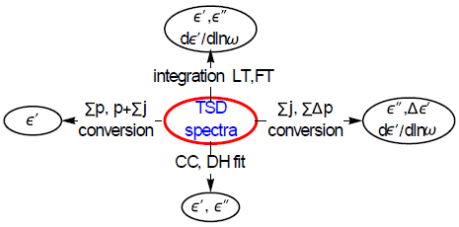


*Fig.1: Three routes to convert TSD data of p and j to dielectric data of ε′,ε″, dε′/dlnω and Δε′ in the T and/or ω domain.*

## Results and Discussion

Fig.1 shows ε′-spectra vs. T by transforming TSD p-data of KWW. Such spectra are interesting because neither ε′ nor ε″ is known analytically for KWW. The ε′ values were obtained by summing a few p-values.

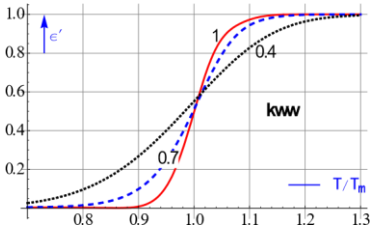


*Fig.2: ε′ spectra vs. T obtained from TSD polarization-data for KWW.*

Fig.3 shows the ε″ spectra vs ω for KWW and CC, that of KWW is clearly asymmetric due to a lower spectral density at small ω's.

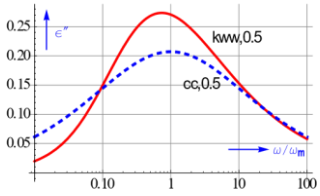


*Fig.3: Difference between the ε″-spectra from KWW and CC current data.*

Fig.4 gives dε′/dlnω for KWW for 3 shape factors b. The spectra are clearly asymmetric with a spectral density that is less at high τ .

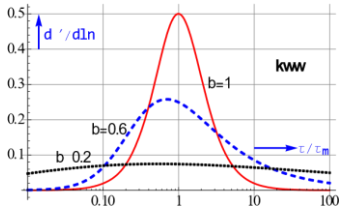


*Fig.4: dε′/dlnω spectra of KWW found by converting TSD current spectra.*

## Conclusions

Conversion of TSD via kernel matching can be implemented rather easily. Fitting with e.g. Dissado and Hill's model of which ε′ and ε″ are known should be done with all-in-1 fitting using TSD data for 2 heating rates. This also provides the activation energy, which is required to convert to time data by variable embedding. The conversion via fast integration of the Laplace or Fourier transform is less versatile.

## References

[1] J. van Turnhout: Thermally stimulated discharge of polymer electrets, Elsevier: Amsterdam 1975.
[2] N.W. Tschoegl: The phenomenological theory of linear viscoelastic behavior, Springer: Berlin 1989.

## Acknowledgements

Many thanks to Prof. J. Sietsma and Prof. I. M. Richardson for a stay in the Dept. of Materials Science and Engineering.

# New avenues for calculating the distribution function from TSD spectra

J. van Turnhout

j.vanturnhout@tudelft.nl

Dept. Materials Science and Engineering, Delft University of Technology,
Mekelweg 2, 2628CD Delft, The Netherlands

**Abstract:** Four methods will be discussed. An obvious one is to fit TSD curves to models with a known distribution function. Another option is to modify existing LTI-algorithms to TSD by variable embedding. Stieltjes inversion offers a third way after the TSD spectra have been converted to ε′ or ε″ spectra. At last we revised the old inversion to a line spectrum using non-negative l.s.q. and all-in-1fitting.

**Keywords:** distribution function, Laplace and Stieltjes inversion, line spectra, all-in-one fitting, variable embedding

## Introduction

The high resolution of TSD can be enhanced even further by calculating the underlying distribution. Early attempts to unravel the distribution were made in e.g. [1,2]. Fig.1 depicts the 4 routes we have pursued recently. A trivial one is fitting the TSD data to a model of which the distribution is known. An attractive alternative is to fit the TSD curves with a rational approximation and next use LTI. A less obvious way is to apply Stieltjes complex inversion. This can be accomplished by turning the TSD spectra into ε′ or ε″ ones. We finally revisited the calculation of the discrete line spectra established long ago. We gave it a new impetus by recruiting all-in-1 fitting. The latter was done for a combination of 3 current spectra recorded at 3 different heating rates.

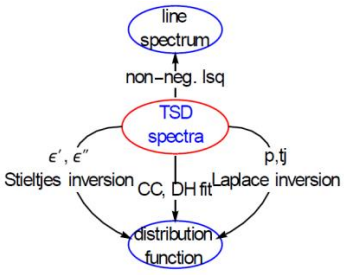


*Fig.1: Four routes to find the distribution function from TSD data. The LTI can be done with oneliners.*

## Results and Discussion

Fig. 2 shows distributions of KWW extracted from TSD by LTI. They were found by adding variable embedding to the easy to use Gaver-Stehfest inversion, based on the activation energy present.

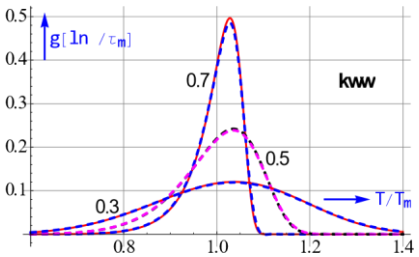


*Fig.2: Recovery of three KWW distributions vs. T obtained from TSD by LTI.*

Fig.3 depicts distributions vs. τ . KWW's one is seen to lack spectral states at high τ 's. These distributions were found by converting the TSD data to ε′ spectra, which can easily be transformed to distributions by Stieltjes inversion.

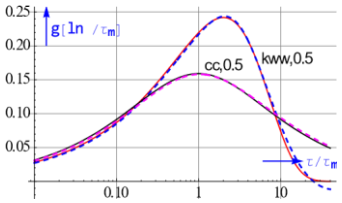


*Fig.3: The recovered distributions for KWW and CC differ markedly for the same shape factor.*

Fig.4 gives the weird spiky DH distributions found by fitting the TSD data to the DH model the distribution of which is known analytically.

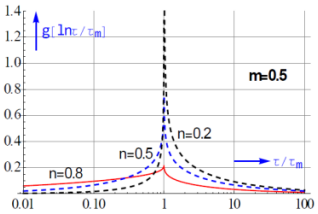


*Fig.4: These curious sharply peaked Dissado-Hill distributions can only be obtained by a direct DH-fit to the TSD results..*

## Conclusions

The results gathered are quite reliable. Cumulative distributions though not been given, can be uncovered as well. In the poster we will also present distributions in activation energy, they have to be found via the line spectrum route.

## References

[1] J. van Turnhout: Thermally stimulated discharge of polymer electrets, Elsevier: Amsterdam 1975.

[2] J. van Turnhout: "TSD of electrets", in Electrets ed. by G.M. Sessler, 2nd ed., Springer: Berlin 1989.

## Acknowledgements

Many thanks to Prof. J. Sietsma and Prof. I. M. Richardson for a stay in the Dept. of Materials Science and Engineering at the TU-Delft.

# Low cost electrostatic energy harvester based on negatively charged polypropylene cellular films with a folded structure

Xingchen Ma *, Xiaoqing Zhang maxingchen@tongji.edu.cn

Shanghai Key Laboratory of Special Artificial Microstructure Materials and Technology, School of Physics science and Engineering, Tongji University, Siping Road 1239, Shanghai 200092, China

**Abstract:** Stripes of electrostatic vibration energy harvesters based on negatively-charged polypropylene cellular films with a folded structure were exposed to mechanical stress in the length direction by a seismic mass excited to vibrations. A current in a terminating resistor was generated due to the capacitance variation of the samples. For a typical double-periodic folded-structure electrostatic vibration energy harvester sample whose effective length and width were 30 mm and 20 mm, respectively, the harvested power across a matching resistor at a resonance frequency of 36 Hz amounts to 0.3 mW for a seismic mass of 4 g and an acceleration of 1 *g* (*g* is the gravity of the earth).

**Keywords:** energy harvesting, electrets, polypropylene cellular films, negatively charged, folded structure

## Introduction

The rapid development of miniaturization, integration and low power consumption of electronics has opened up a research field of energy harvesting. [1] Ambient vibration as potential inexhaustible source is popular in energy harvesting and the transduction mechanism is mainly based on piezoelectric, electromagnetic and electrostatic. For the electrostatic energy harvesting, a bias voltage is needed. Electret is a dielectric material with a quasi-permanent charge, so it can serve as a practical self-sustaining bias source for an electrostatic energy harvester. In this study, we focused on low cost electrostatic energy harvester based on PP cellular electret films. Their structure design allowed for a high output power at a low resonance frequency with a pony-size sample even for a small seismic mass.

## Results and Discussion

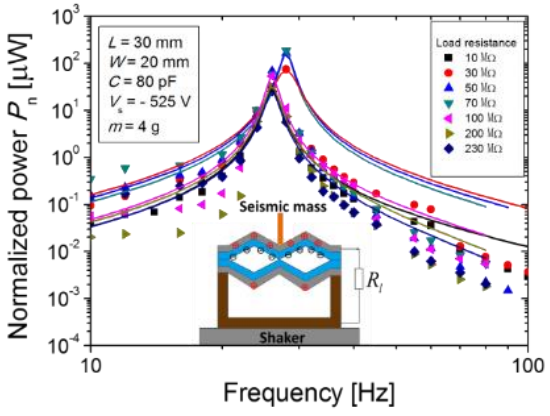


*Figure 1: Frequency response of normalized powers generated at various load resistances. The inset is the schematic setup for energy harvesting.*

Figure 1 presents the results on the normalized output power of an electrostatic energy harvester as a function of vibration frequency at various load resistances. Experimental data was compared to the theoretical calculations. The output power of an electrostatic energy harvester is given by [2]

$$P_{out} = \frac{m^2 M^2 a^2 R_l \omega^2}{[(\frac{\omega^2}{\omega_0^2} - 1)^2 + 4\zeta_m^2 (\frac{\omega}{\omega_0})^2][1 + (\frac{R_l}{R_c})^2]}$$

Where $\zeta_m$ is the mechanical damping ratio, $M$ is the charge sensitivity, and $R_c = 1/\omega C$ with $C$ the sum of the sample and parasitic capacitances. Here, the electrostatic energy harvester is seen as a "black box" with a piezoelectric coefficient $d_{33}=M$. The maximum power may be harvested at the resonance frequency $\omega_0$ if a terminating resistance of $R_l=R_c$ $1/\omega_0 C$ is chosen.

## Conclusions

The suggested harvester is an innovative device with a relatively simple design, which is capable of delivering a relatively large amount of power (presently up to about 0.3 mW). It appears that upon further development, this harvester will significantly advance the field since it exceeds in performance other electrostatic devices.

## References

[1] P. D. Mitcheson, E. M. Yeatman, G. K. Rao, A. S. Holmes, T. C. Green, *Proc. IEEE.* **2008**, *96*, 14571486.
[2] X. Zhang, P. Pondrom, L. Wu, G. M. Sessler, *Appl. Phys. Lett.* **2016**, *108*, 193903.

## Acknowledgements

The authors gratefully acknowledge financial support from the Natural Science Foundation of China (NSFC, 51173137 and 11374234) and the Fundamental Research Fund for the Central Universities (Tongji University 2014).

# Polarisation profiles in VDF-TrFE copolymer bilayers of molar ratio 70/30 and 56/44

David Smykalla, Sowmya Karnati, and Bernd Ploss

bernd.ploss@eah-jena.de

Department of SciTec, University of Applied Sciences Jena

Carl-Zeiss-Promenade 2, 07745 Jena, Germany

**Abstract:** Ferroelectric bilayers have been fabricated by hot-pressing vinylidene fluoride-trifluoroethylene (VDF-TrFE) copolymer films of molar ratios 70/30 and 56/44 and polarized by electrode poling. The laser-intensity-modulation method (LIMM) has been used to investigate profiles of the pyroelectric activity. After poling a quite homogeneous polarisation is observed in the bilayer. Annealing at 80° C essentially depolarizes the layer of molar ratio 56/44. The layer of molar ratio 70/30 stays polarized, but polarization is declining smoothly through the thickness of the bilayer.

**Keywords:** ferroelectric polymers, bilayers, polarization profiles, LIMM

## Introduction

The formation of bilayers of ferroelectric materials is an attractive way to fabricate systems with modified dielectric and polarisation properties [1]. In a recent study the effective properties of bilayers of VDF-TrFE ferroelectric copolymer thin films of molar ratios 56/44 and 70/30 have been characterized in terms of polarisation behaviour and dielectric nonlinearities [2].

## Results and Discussion

To investigate the polarization in more detail ferroelectric VDF-TrFE copolymer bilayers have been fabricated by hot-pressing and polarized with electrodes. The laser intensity modulation method (LIMM) [3,4] has been applied to measure profiles of the pyroelectric activity. Figure 1 shows a relative homogeneous polarisation in the bilayer after poling. After annealing the bilayer at temperature 80° C, i.e. above the Curie temperature of the copolymer with 56/44 molar ratio, the polarization in the 56/44 layer is drastically reduced but essentially maintained in the 70/30 layer as shown in figure 2.

## Conclusions

Annealing an initially homogeneously polarised bilayer of VDF-TrFE copolymer films with molar ratios 70/30 and 56/44 above the Curie temperature of the 56/44 material essentially depolarizes this layer. The resulting profile is not a step function, however, but shows a smooth decline of the polarization through the bilayer. This may be caused by electric fields arising when the 56/44 material is being depolarised. (This decline is significant and not an effect of the limited resolution of the thermal scanning technique only.)

## References

[1] K.-G. Lim, K.-H. Chew1, L.-H. Ong, M. Iwata, *EPL (Europhysics Letters)* **2012**, *99*, 46004-p1-p6.

[2] D. von Nordheim, A. Austin, B. Ploss, K.-H. Chew, *IEEE Trans. on Diel. and El. Ins.* **2016**, *23*, 129-133.

[3] S.B. Lang, D.K. Das Gupta, *J. Appl. Phys.* **1986**, *59*, 2151-2160.

[4] B. Ploss, R. Emmerich, S. Bauer, *J. Appl. Phys.* **1992**, *72*, 5363-5370.

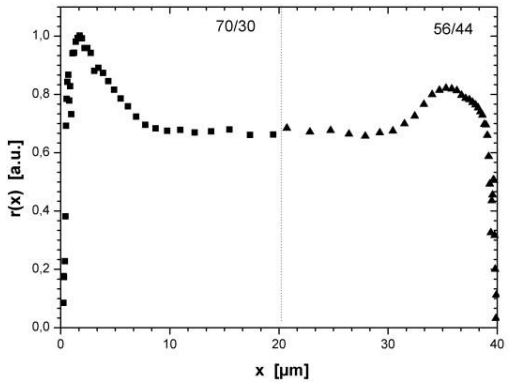


*Figure 1: The spatial distribution of the pyroelectric coefficient r(x) of a 40 µm thick VDF-TrFE bilayer of molar ratios 70/30 and 56/44 after electrode poling.*

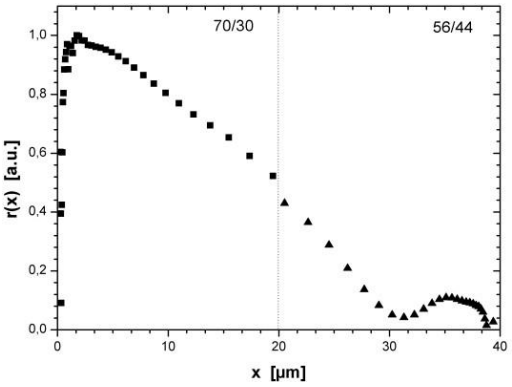


*Figure 2: The spatial distribution of the pyroelectric coefficient r(x) of the sample of Fig. 1 after annealing at temperature 80° C.*

# Acoustic energy harvesting using ferroelectret film attached Helmholtz resonators

Yuan Xue, Xiaoqing Zhang

1410569@tongji.edu.cn

School of Physics Science and Engineering, Tongji University, 1239 Siping Road, Shanghai 200092, China

**Abstract:** In this paper, acoustic energy harvesting with cross-linked polypropylene (IXPP) ferroelectret films, attached on a Helmholtz resonator, is reported. The results show that the output power of 9.7 nW is achieved at a sound pressure level (SPL) of 100 dB, an optimum load resistance of 1.5MΩ and a resonance frequency of 940 Hz.

**Keywords:** acoustic energy harvesting, ferroelectrets, Helmholtz resonator

## Introduction

Recently, the technologies of energy harvesting have been generating great interests of researchers. Among these alternative technologies, acoustic energy harvesting (AEH), which converts acoustic energy available in the environment into electrical energy, is a viable one [1].

Ferroelectrets, a new kind of polymer piezoelectric material, was applied in several harvesters for vibration-based energy harvesting [2]. In this study, IXPP ferroeletret films were integrated with a Helmholtz resonator to scavenge acoustic energy.

## Results and Discussion

A Helmholtz resonator was fabricated by acrylic, and has the effective length of neck $L_{eq}$ of 11 mm, the round cross sectional area $A$ of neck of 314 mm$^2$ and the volume of cavity $V_0$ of 64,000 mm$^3$. The resonance frequency of around 1140Hz of this resonator is given by

$$f = \frac{c}{2\pi}\sqrt{\frac{A}{V_0 L_{eq}}} \quad (1)$$

where $c$ is speed of sound in air.

An IXPP piezoelectret film was attached to the Helmholtz resonator by tapes replacing the back plate. In order to match the resonance frequency of the designed Helmholtz resonator, a seismic mass was attached on the bottom of ferroelectret film. The schematic of the acoustic energy harvester based on ferroelectret film is depicted in Figure 1.

The fabricated harvester was used to scavenge energy from acoustic waves produced by speaker. The output charge in short circuit is recorded by the computer, and actual sound pressure in the cavity is monitored by using a calibrated microphone (KW4420) placed on the wall of Helmholtz resonator.

The output power of such harvester is given by

$$P_{out} = R_l I^2 = R_l \omega^2 Q_{\mathrm{rms}}^2 \quad (2)$$

where $R_l$ is the load resistance, $I$ is the current through the load resistor, $\omega$ is the angular frequency of acoustic waves, and $Q_{\mathrm{rms}}$ is the root mean square (RMS) value of charge.

Figure 1 also shows the frequency dependence of the output power at a SPL of 100 dB. The measured resonance frequency of the harvester is around 940Hz. The optimal load resistance of 1.5MΩ of this harvester for obtaining maximum power harvested is calculated. This IXPP ferroelectret acoustic energy harvester produced a maximum output power of 9.7 nW at frequency of resonant. The deviation of experimental and designed resonance frequency is still under investigation.

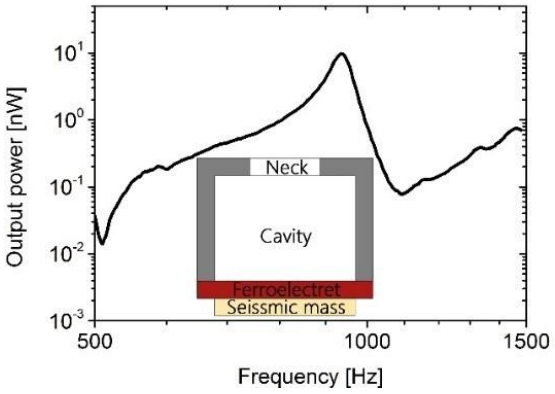


*Figure 1: Frequency dependence of output power and schematic of acoustic energy harvester based on ferroelectret film.*

## Conclusions

A ferroelectret acoustic energy harvester with maximum output power of 9.7nW at a SPL of 100 dB and 940 Hz resonant frequency is reported. The performance of this harvester can be further improved.

## References

[1] M. A. Pillai, E. Deenadayalan, *International Journal of Precision Engineering and Manufacturing*, **2014**, 15(5), 949-965.

[2] P. Pondrom, J. Hillenbrand, G. M. Sessler, J. Bös, and T. Melz, *Appl. Phys. Lett*. **2014**, 104, 172901.

## Acknowledgements

The authors gratefully acknowledge financial support from Natural Science Foundation of China (NSFC, No.11374232).

# Piezoelectric resonance and electro-mechanical relaxation in uniaxially-drawn and poled of polyvinylidene fluoride

Hidekazu Kodama [1], Hajime Ishii [1], Wee Chen Gan [2], T.S. Velayutham [2], W.H. Abd Majid [2] and Takeo Furukawa [1]

kodama@kobayasi-riken.or.jp

[1]Piezoelectric Physics and Devices Laboratory, Kobayasi Institute of Physical Research, 3-20-41 Higashimotomachi, Kokubunji, Tokyo 185-0022, Japan
[2]Low Dimensional Materials Research Centre, Physics Department, University of Malaya, 50603 Kuala Lumpur, Malaysia

**Abstract:** Electro-mechanical properties of uniaxially-drawn and poled Polyvinylidene fluoride (PVDF) were studied by piezoelectric resonances. Frequency spectra of complex permittivity were measured in a broad frequency band from 10mHz to 1GHz. The poison ratio and the piezoelectric constant $e_{31}$ and $e_{32}$ are estimated below and above mechanical relaxation temperature. A mechanism of piezoelectricity in PVDF is discussed.

**Keywords:** polyvinylidene fluoride, piezoelectric resonance, electro-mechanical properties

## Introduction

Piezoelectric responses depend on product of the piezoelectric *e* constant and the strain generated in length, width and thickness directions through poison ratios. Values of $e_{31}$ and $e_{32}$ are required to well understanding of piezoelectricity in PVDF.
We have estimated poison ratio, $e_{31}$ and $e_{32}$ above and below mechanical relaxation temperature by detail analysis of piezoelectric resonance.

## Results and Discussion

Figure 1 shows frequency spectra of complex permittivity $\varepsilon'/\varepsilon_0$ and $\varepsilon''/\varepsilon_0$ from -50°C to 60°C. Piezoelectric resonances due to length extension (LE), width extension (WE) and thickness extension (TE) were observed at 100kHz, 1MHz, and 30MHz respectively. We have calculated the piezoelectric *e* constant and the elastic compliance *s* by fitting method.
Figure 2 shows temperature dependences tensile components of the piezoelectric *e* constant and the elasic compliance *s*. The coordinate axis, the 1st axis parralel to the stretch direction, the 3rd axis parralel to the poling direciton and the 2nd axis parpendicular to those axes, is applied to the sample. The apparatus values $e_{ij}^{a}$ and $s_{jj}^{a}$ are given by $d_{ij}/s_{jj}$ and $1/c_{jj}$. $e_{ij}^{w}$ and $s_{jj}^{w}$ given by WE mode are the value in the case of length direction is clamped.
We have calculated poison ratios $\nu_{12}$ ($=s_{12}/s_{22}$) and $\nu_{21}$ ($=s_{12}/s_{11}$) by using equations $s_{11}^{w}/s_{11}=1-\nu_{21}\nu_{12}$ and $s_{22}/s_{11}=\nu_{21}/\nu_{12}$. The experimental results show that $\nu_{21}$ $\nu_{12}$ was almost constant 0.1 to 0.15 and $\nu_{21}/\nu_{12}$ became 1 above the relaxation temperature. Also we have estimated that $e_{31}$=-25 to -35mC/m$^2$ and $e_{32}$=-35 to -45 mC/m$^2$ at -60 °C and $e_{31}$=20 to 30mC/m$^2$ and $e_{32}$=-25 to -35 mC/m$^2$ at 50 °C by assuming $\nu_{12}=\nu_{13}$.

## Conclusions

The experimental results suggest that $e_{31}$ depends on temperature between -60 °C and 50°C. However, $e_{32}$ is negative and almost constant in the temperature range. It means that temperature dependences of piezoelectricity in PVDF are mainly caused by temperature dependence of $e_{31}$.

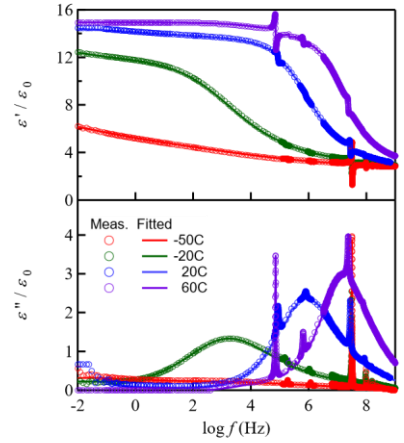


*Figure 1: Frequency spectra of permittivity in PVDF*

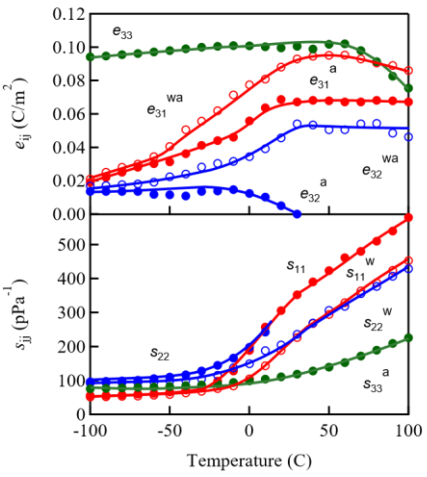


*Figure 2: Temperature dependence of $e_{ij}$ and $s_{jj}$*

# Effect of rare-earth ions on the properties of modified $Sr_{0.47}Ba_{0.53}Nb_2O_6$ ceramics

T.S. Velayutham [1*], W.C. Gan[1], W.H. Abd. Majid[1]

* t_selvi@um.edu.my

[1] Low Dimensional Materials Research Centre, Department of Physics, Faculty of Science, University of Malaya, 50603 Kuala Lumpur, Malaysia

**Abstract:** Effects of 1 mol% rare-earth (RE) dopants ($La^{3+}$, $Ce^{3+}$, $Dy^{3+}$ and $Gd^{3+}$) on the dielectric, ferroelectric, and pyroelectric properties of strontium barium niobate, $Sr_{0.53}Ba_{0.47}Nb_2O_6$ (SBN) ceramics was investigated. Doping SBN with RE strongly lowers the $T_c$ and increase the diffuseness of the phase transition. As a result, RE doping provides a tool for an enhancement of many important parameters in SBN. We demonstrate a significant increase in the dielectric permittivity, pyro- and ferroelectric properties of the samples. The effects of non-equilibrium charge carriers on polarization are discussed.

**Keywords:** ferroelectric, pyroelectric, ceramics, relaxor

## Introduction

Relaxor ferroelectrics are disorder crystals with extraordinary dielectric, piezoelectric and electrooptic properties. Disorder is crucial in the physics of relaxor and many models were developed to explain its behavior [1]. Strontium barium niobate, $Sr_xBa_{1x}Nb_2O_6$ (SBN) is a group of disordered uniaxial ferroelectrics belongs to unfilled tetragonal tungsten bronze structure. The phase transition of SBN is altered by the relative amount of Sr/Ba ions or by means of doping with rare-earth ions. Previously, the Sr/Ba ratio was studied for the SBN ceramic and we found that the optimal ferroelectric and pyroelectric properties were observed for $Sr_{0.53}Ba_{0.47}Nb_2O_6$ [2]. Moreover, doping SBN with a minute concentration of $La^{3+}$, $Ce^{3+}$, and $Gd^{3+}$ ions strongly affect the ferroelectric phase transition [3]. The anomaly in the dielectric permittivity broadens and its frequency dispersion becomes significant. In addition, the macroscopic properties of rare-earth doped SBN ceramics have much in common with relaxor. We report here the modifications of the macroscopic properties induced by doping rare-earth ions on SBN ceramics.

## Results and Discussion

The general formula of the solid solutions is $R_{0.03}Sr_{0.53}Ba_{0.47}Nb_2O_6$ where R = $Ce^{3+}$, $La^{3+}$, $Dy^{3+}$ and $Gd^{3+}$. The ionic radius for $Ce^{3+}$> $La^{3+}$> $Dy^{3+}$> $Gd^{3+}$. SBN consist of a three-dimensional network of distorted Nb/O octahedral connected to form pentagonal, tetragonal and trigonal tunnels. $Sr^{2+}$and $Ba^{2+}$ ions occupy the pentagonal and tetragonal sites while the trigonal sites are empty. In pure SBN, the $Sr^{2+}$and $Ba^{2+}$ions have the same charge and thus there are no strong electrostatic forces related to the distribution of the ions while the charge irregularity was due to the presence of unfilled trigonal sites. However, in the doped-SBN, extra charge disorder is introduced when the trivalent rare earth ions, $R^{3+}$ replace the $Sr^{2+}$ sites which likely to cause simultaneous charge and chemical randomness. Figure 1 shows the summary of results obtained such as the tetragonality, c/a, phase transition temperature, $T_m$, remnant polarization, $P_r$ and pyro-coefficient, $p$ of the modified SBN.

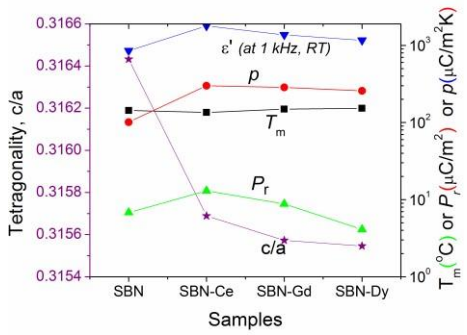


*Fig 1: Summary of modified SBN.*

## Conclusions

The dielectric, ferro- and pyroelectric properties of the RE (Ce, La, Dy and Gd) doped SBN53 ceramic were studied. All samples show similar grain size and pure TTB phase. Among the dopants, the Cedoped samples show much larger $P_r$, ε'and $p$. We found that the functional properties of the SBN are enhanced when it is doped with larger ionic radius impurities (almost similar radius with $Sr^{2+}$).

## References

[1] Peláiz-Barranco, A.., et.al., *Relaxor Behaviour in Ferroelectric Ceramics*, in *Advances in Ferroelectrics*, A.P. Barranco, Editor. 2012, InTech: Rijeka. p. Ch. 5

[2] Said, M.; Velayutham, T.S., et. al., *Ceram. Int.* **2015**, *41*, 7119 –7124.

[3] Velayutham, T.S.; et. al, *J. Alloys Comp*. **2016**, *666*, 334 – 340.

## Acknowledgements

This work is supported by the University of Malaya through UMRG grant: RP026D-15AFR.

# Pyroelectric Properties of hybrid nanocomposites sytem

Mulayam Singh Gaur[1], Rohan Sagar

mulayamgaur@rediffmail.com (Corresponding e-mail address)

[1]Interdisciplinary Research laboratory, Hindustan College of Science and Technology, Farah, Mathura, UP 281122, India Affiliated to Dr. A. P. J. Abdul Kalam Technical University, Lucknow ( U P ), India

**Abstract:** Polyviyleidine fluoride / polyvinyl chaloride / barium titanate (PVDF/PVC/ BaTiO3) system have been fabricated by solution mixing method. The pyroelectric properties of the hybrid nanocomposite films were examined for their use in infrared detectors. The heating rate dependent pyroelectric coefficients have illustrated in pure PVDF, PVDF-PVC system and PVDF/PVC/$BaTiO_3$ hybride nanocomposites. The results indicated Figures-of-merit of hybrid nanocomposites film were higher than pristine polyvinylidene fluoride films. The pyroelectric coefficient for nanocomposite at 190°C is about 351μC/$m^2K^1$ which is higher than that of PVDF/PVC/ $BaZrO_3$ (153.04 μC/$m^2K^1$).

**Keywords:** Pyroelectric coefficient, PVDF, PVC, Blending nanocomposites

## Introduction

The hybrid nanocompoite of PVDF with ferroelectric ceramics have attracted much attention from scientific communities because of their exceptional pyroelectric and ferroelectric properties. The $BaTiO_3$ (ferroelectric) nanoparticles inclusions play an important role in providing functional effects to hybrid thin film, but have poor mechanical properties. On the other hand, the polymer has a high degree of mechanical flexibility, but low piezoelectric and pyroelectric properties. By combining these two effects, composite thin films offer promising potential in term of functional electronic applications for use in sensors and transducers. Their specifications can be tailored by appropriate selections of constituent components and also by varying their volume fraction. Present study shows an alternative approach to improve the pyroelectric property of PVDF compared with the current conventional studies by using ferroelectric inclusion in composite thin film with a high volume fraction[1].

## Results and Discussion

The PVDF/PVC and PVDF/PVC/$BaTiO_3$ composites with 4% $BaTiO_3$ were prepared. The pyroelectric current was recorded at different heating rate (i.e., 1, 2 and 3°C $min^{-1}$) by electrometer (Keithley 6514). For pure PVC, the measured value of p is 26.62 μC/$m^2K^1$.The pyroelectric coefficient of PVDF/PVC/$BaZrO_3$ reaches about 88.58, 153.04 μC/$m^2K^{1,}$ respectively. The measured pyroelectrioelectric coefficient increases to enhancement of β phase by inclusion of $BaTiO_3$ in hybrid matrix [2]. In hybrid nanocomposites consist of large number of interface. The role of interface to change the pyroelectric properties of PVDF. As far as our knowledge this drastic change in properties has been observed first time. Series of concentration of $BaTiO_3$ have been considered but 4% BaTiO3 have best result. It may be due to uniform distribution of nanoparticle in polymer matrix [3].

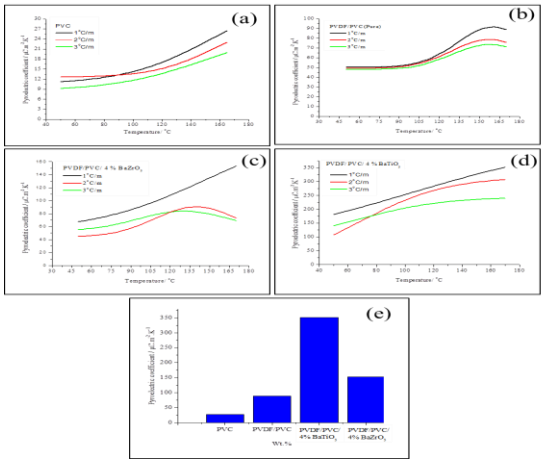


Figure1: Pyroelectric coefficient of hybrid nano-composite system at different heating rate

## Conclusions

It I concluded that the pyroelectric coefficient of the hybrid thin film increases significantly due to enhancement of β phase.

## References

[1] Baorang, Li.; Wei, S.; Delong, Z.; Mingjun, H.; *J. of Nanoscience and Nanotechnology* 2016,16, 7225–7233

[2] Lang, B.S.; Muensit, S.; *Appl Phys A.* 2006 ,85,125– 34

[3] Sakamoto, W.K.; Kanada, D.H.F.; *Res. Innovat.* 2002, 5, 257.

# Pressure dependence of the piezoelectric $d_{33}$ coefficient and the cellular-foam structure in polypropylene ferro- and piezoelectrets

Werner Wirges, Xunlin Qiu, Dmitry Rychkov, and Reimund Gerhard
Corresponding e-mail addresses: xunlin.qiu@hotmail.com http://hotmail.com/or reimund@ieee.org
Applied Condensed-Matter Physics, Faculty of Science, University of Potsdam
Karl-Liebknecht-Strasse 24-25, 14476 Potsdam-Golm, Germany

**Abstract:** For many applications of piezoelectric materials, the pressure dependence of the piezoelectricity is very important. Here, we study the dependence of the piezoelectric $d_{33}$ coefficient of cellular polypropylene (PP) ferroelectrets on applied static pressures up to 2000 kPa, a pressure range much broader than that covered in previous studies. The $d_{33}$ coefficient first increases with static pressure, and then sharply decreases above 380 kPa. However, a very high pressure up to 2000 kPa does not destroy the PP films. Indeed, $d_{33}$ coefficients much higher than those of freshly prepared samples are observed when the pressure is reduced back to lower values.

**Keywords:** Piezoelectricity, pressure dependence, ferro- and piezoelectrets, cellular polypropylene (PP)

## Introduction

Ferroelectrets are internally charged polymer foams that exhibit high piezoelectricity [1]. Due to their special cavity-containing material structure, ferroelectrets are quite soft at least in the thickness direction. Therefore, the pressure dependence of the $d_{33}$ coefficient is of particular importance for applications of ferroelectrets. So far, the dependence of $d_{33}$ on pressure up to one hundred kPa has been studied. However, much higher pressures may be present in many applications e.g. in pressure sensors, underground or deep-sea exploration, etc. Here, we study the pressure dependence of the $d_{33}$ coefficient of cellular polypropylene (PP) ferroelectrets up to 2000 kPa.

## Results and Discussion

The dynamic piezoelectric $d_{33}$ coefficient of a cellular PP ferroelectret is shown as a function of the applied static pressure in Figure 1. The cellular PP film was provided by VTT Processes in Finland. After being inflated by means of a gas-diffusion expansion technique [2], the film was corona charged with a tip voltage of –17 kV for 15 s. The sample was then metallized on both surfaces with circular aluminium electrodes 50 mm in diameter. Measurements were preformed with a Zwick Z005 (Zwick GmbH & Co KG, Germany) tensile testing machine. In order to determine the dynamic $d_{33}$ coefficient, a triangular force with an amplitude of 5 N and a frequency of 0.2 Hz was superimposed onto the applied static force. The piezoelectric $d_{33}$ coefficient was calculated from the dynamic force and the resulting electric response (recorded via a Brüel&Kjær model 2635 charge amplifier).

The $d_{33}$ coefficient of the PP sample first increases with increasing static pressure (black squares), probably indicating over-inflation of the sample. Cellular PP foams require a medium inflation in order to have the lowest Young's modulus. Too little or too much inflation results in stiffer material structures, leading to smaller $d_{33}$ coefficients. With applied static pressure, an over-inflated sample is compressed towards the optimal foam structure.

A pressure above about 380 kPa, however, seems to harden the PP-foam structure considerably, as indicated by the sharp decrease of the $d_{33}$ coefficient. Interestingly, the sample is able to withstand static pressures up to about 2000 kPa, corresponding to a static force of 3900 N in the present case. $d_{33}$ recovers when the static pressure decreases from its maximum (red circles). Much higher $d_{33}$ values are found when the static pressure is reduced back to values below about 380 kPa.

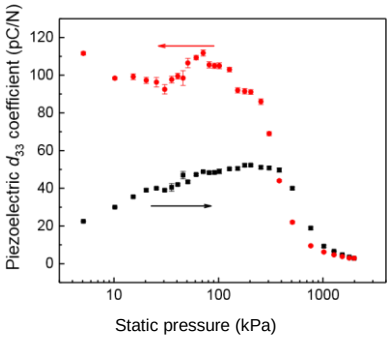


*Figure 1: Dynamic piezoelectric $d_{33}$ coefficient vs. applied static pressure. The static pressure was first increased from about 5 to 2000 kPa (black squares) and then reduced back to the initial value (red circles), as also indicated by the arrows.*

## Conclusions

The dependence of $d_{33}$ in cellular PP ferroelectrets on applied static pressure up to 2000 kPa is studied. Appropriate static pressures may lead to optimal sample structures and to quite high $d_{33}$ coefficients. Surprisingly, pressures up to 2000 kPa do not destroy the films, but much higher $d_{33}$ values than before are found after lowering the pressure again.

## References

[1] S. Bauer, R. Gerhard, and G. M. Sessler, *Phys. Today* **57**(2), 37 (2004), doi: 10.1063/1.1688068.

[2] M. Wegener, W. Wirges, J. Fohlmeister, B. Tiersch, and R. Gerhard(-Multhaupt), *J. Phys. D: Appl. Phys.* **37**, 623 (2004), doi: 10.1088/0022-3727/37/4/013.

# Nonlinear Capacitance Dilatometry in Laminated Ferroelectrets

Nathan Spink and Axel Mellinger

axel.mellinger@cmich.edu (Corresponding e-mail address)

Central Michigan University, Department of Physics, Mount Pleasant, MI 48859, USA

**Abstract:** Nonlinear capacitance dilatometry is an all-electrical technique for *in situ* measurements of the piezoelectric coefficient and Young's modulus in soft piezoelectric materials. In this work, we show that the accuracy of this technique can be improved by replacing the purely sinusoidal waveform applied to the sample with pre-distorted one, in order to compensate for non-linearities of the detection circuit.

**Keywords:** ferroelectrets, piezoelectrets, nonlinear capacitance dilatometry, piezoelectric coefficient

## Introduction

Laminated ferroelectrets have been extensively studied in recent years due to their large piezoelectric $d_{33}$ coefficients and their ease of manufacture. However, measuring their piezoelectric activity requires an *in situ* method, as mechanical access is often difficult during sample preparation and charging. For soft materials, nonlinear capacitance dilatometry [1] is a suitable, all-electric method. In brief, application of a sinusoidal high voltage leads to periodic changes in the sample thickness due to the converse piezoelectric effect and Maxwell stress. As a result, the capacitive current is no longer purely sinusoidal, but has 2nd and 3rd harmonic components that are related to $d_{33}$ and Young's modulus $Y$. In this work we demonstrate how elimination of parasitic nonlinearities of the data acquisition circuit can improve the accuracy of the measurement.

## Results and Discussion

For a driving voltage of $V = V_0 \sin(\omega t)$, theory [1] predicts a second harmonic component of the capacitive current proportional to $d_{33}\ V_0^2 \sin(2\omega t)$ and a third harmonic component proportional to $Y^{-1}V_0^3 \cos(3\omega t)$. However, in a practical setup, nonlinearities of the function generator and high voltage amplifier (in our case, an Agilent 33120A arbitrary waveform generator driving a Matsusada AMT-20B10 amplifier) may generate extra contributions to the higher harmonics that mask the electromechanical response of the sample.

To compensate for these instrumental artifacts, reference measurements were carried out where the ferroelectret was replaced by a capacitor with a capacitance similar to that of the sample. As the dielectric spacer in commercial capacitors is much more rigid than ferroelectrets, any 2nd and 3rd harmonic currents must be due to the detection circuit. Correction terms were recorded at 50 V intervals. From these, a "pre-distorted" waveform was generated, that was then applied to the actual ferroelectret. As shown in Fig. 1, this procedure leads to significantly cleaner signal with second and third harmonics proportional to $V_0^2$ and $V_0^3$, as expected.

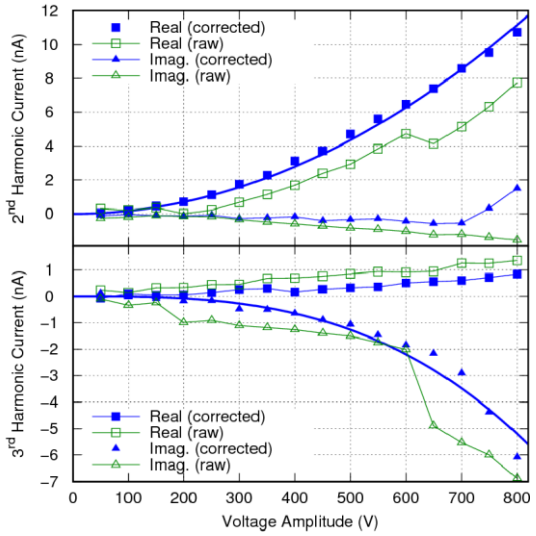


*Figure 1: Second (top) and third (bottom) harmonic response of a ferroelectret upon application of a sinusoidal high voltage with a given amplitude. The open symbols indicate the response without correction for high-voltage amplifier nonlinearities; the solid symbols show the current with the amplifier nonlinearities corrected.*

## Conclusions

Applying a pre-distorted waveform to soft ferroelectric samples is a viable way of correcting instrumental artifacts in capacitance dilatometry measurements of $d_{33}$ and $Y$. This technique will play in important role of upcoming studies on the charging process in laminated ferroelectrets.

## References

[1] S. Bauer-Gogonea, F. Camacho-González, R. Schwödiauer; B. Ploss and S. Bauer, Appl. Phys. Lett. **91**, 122901 (2007).

# Synthesis and Study of Bone like hydroxyapatite from cuttlefish bones and its piezoelectric properties

Abin Abraham Sebastian[1,2], Sarah Markham[1,2], Dr. Karrina McNamara[1,2], Prof. Tofail Syed[1,2]

sarah.markham@ul.ie / tofail.syed@ul.ie

[1]Bernal Institute, University of Limerick, Castletroy, Limerick, Ireland. [2]Department of Physics, University of Limerick, Limerick, Ireland

**Abstract:** Synthesis of Hydroxyapatite (Hap) from cuttle fish bones using a wet chemical method. The cuttle fish bones are powdered and mixed with phosphoric acid (H3PO4) in the wet chemical process. The result was characterized by Atomic Force Microscopy (AFM), Fourier Transform Infrared Spectroscopy (FTIR) and Scanning Electron Microscopy (SEM). Fine and crystallized HAp was obtained. The piezoelectric effect of the synthesized hydrozyapatite is studied.

**Keywords:** Hydroxyapatite, cuttle fish, phosphoric acid, piezoelectric effect

## Introduction

Hydroxyapatite (HAp) is carbonate apatite which is similar to apatite present in natural bone, based on its chemical composition (Ca5(PO4)3(OH)) and structure. Bone is an arrangement of carbonate hydroxyapatite in a matrix with the collagen. It has excellent biocompatibility, bioactivity and osteo-conductivity so reduces the risk of rejection in medical applications like dental, orthopaedics, coatings etc [1,2,3,4].

HA has been synthesized and used to manufacture various forms of implants (solid and porous) and as a coating on other implants. Pure HAp is a stoichiometric apatite phase with a Ca/P molar ratio of 1.67 which is the most stable calcium phosphate salt at normal temperatures and between pH 4 and 12 [5].

Piezoelectric, pyroelectric and ferroelectric[6,7] properties have been observed in synthetic hydroxyapatite. This work explores the production of naturally derived HAp from cuttlefish bones, and the piezoelectric potential of the manufactured material.

## Results and Discussion

An average particle size of approximately 20-25µm was determined using AFM. The HAp nanoparticles produce a relatively smooth surface, confirmed via AFM and SEM.

The FTIR characterisation identifies the functional groups associated with hydroxyapatite. The carbonate ions are present in between the range of 1500- 2000 and the phosphate ions are present in the range of 1000-1500.

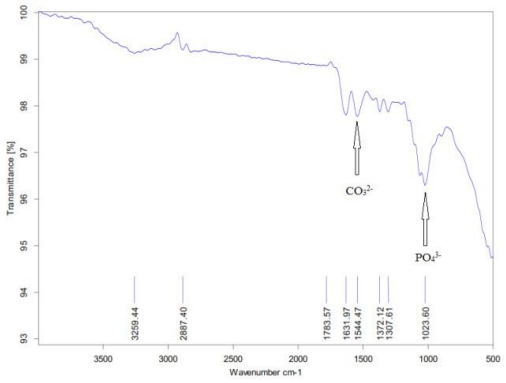


Figure 1: FTIR for Synthesized Hydroxyapatite

## Conclusions

Naturally derived HAp can be obtained from cuttlefish bones. The particle size obtained provides potential for the production of HAp thin films. Studies of the piezoelectric properties of this naturally derived Hap are underway.

## References

[1] Hong, Y., Fan, H., Li, B., Guo, B., Liu, M. and Zhang, X. (2010). *Materials Science and Engineering: R: Reports*, 70(3-6), pp.225-242.

[2] Aktug, S., Kutbay, I. and Usta, M. (2017). *Journal of Alloys and Compounds*, 695, pp.998-1004.

[3] Valletregi, M. (2004). *Progress in Solid State Chemistry*, 32(1-2), pp.1-31.

[4] McConell D. (1973). *Berlin: Springer.*

[5] Curie, Jacques and Curie, Pierre (1880). *Bulletin de la Societe de Minerologique de France*, 3: 90-93.

[6] Lang, S. B., Tofail, S. A. M., Gandhi, A. A., Gregor, M., Wolf-Brandstetter, C., Kost, J., & Krause, M. (2011).. Applied Physics Letters, 98(12), 123703.

[7] Lang, S. B., Tofail, S. A. M., Kholkin, A. L., Wojtaś, M., Gregor, M., Gandhi, A. A., & Plecenik, A.

[8] (2013). Scientific reports, 3, 2215.

## Acknowledgements

Bernal Institute and the University of Limerick.

# Pyroelectricity in Polycrystalline Aggregates of the Globular Protein Lysozyme

A. Stapleton[1,2], M.R. Noor[1,2], C. Silien[1,2], T. Soulimane[1,2], S.A.M. Tofail[1,2]

tofail.syed@ul.ie

[1]Department of Physics, University of Limerick, Limerick, V94 T9PX, Ireland
[2]Bermal Institute, University of Limerick, Limerick, V94 T9PX, Ireland

**Abstract:** Pyroelectricity is the ability of some materials to generate a current in response to a change in temperature. Pyroelectric materials are used in a range of applications from burglar alarms to thermal imaging. Some biological materials also exhibit pyroelectricity but examples of the effect are somewhat rare. Here, we examine the pyroelectric effect in lysozyme, a globular protein, using a conventional method. We find that crystalline aggregate films of lysozyme are pyroelectric consistent with the classical theory of pyroelectricity.

**Keywords:** e.g. pyroelectricity, proteins, lysozyme, Byer-Roundy method

## Introduction

Pyroelectricity is the ability of certain materials to generate a current in response to a changing temperature. Pyroelectric materials are a subset of piezoelectric materials; 10 of the 20 piezoelectric crystal classes are polar and thus, may demonstrate the pyroelectric effect. Examples of biological pyroelectricity are somewhat rare but include bone and tendon [1], plant leaves [2], insects [3] and amino acids [4]. Here, we investigate pyroelectricity in crystals of lysozyme, a globular protein. Crystallised in its monoclinic form, it belongs to a polar crystal class and should demonstrate pyroelectricity.

## Results and Discussion

Here, we use a modified Byer-Roundy method that is based on the principle that the pyroelectric current is proportional to the rate of change of temperature. Crystalline aggregate films of lysozyme were grown by drop casting the protein solution on to an electrode. As the protein drop dried, crystals grew forming an aggregate film. The type of electrode used was a silver inter-digitated electrode (IDE) printed on an alumina substrate. A Peltier heating stage and temperature controller (Linkam, Scientific Instruments) were used to heat/cool the sample while an electrometer (Keithley 6514) measured the current generated. The system was automated with LabVIEW, which facilitated data logging. Figure 1 shows the result of five temperature cycles applied to a monoclinic aggregate film of lysozyme Although the signal contains noise, there is a clear change in polarity of the current in each measurement cycle when the temperature ramp changes from heating to cooling and *vice versa*. The red annotated line in Figure 1 highlights this trend.

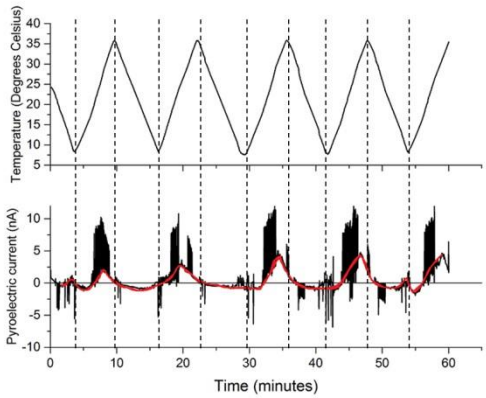


*Figure 1: Pyroelectric effect in a monoclinic aggregate film of lysozyme. The polarity of the pyroelectric current switches when the temperature cycle changes from heating to cooling.*

## Conclusions

We have used the Byer-Roundy method to observe the pyroelectric effect in crystalline aggregate films of lysozyme. During some temperature cycles, the current does not immediately switch polarity when the temperature ramp changes from heating to cooling which may indicate the contribution of thermally stimulated currents effects. Future studies might use other methods (e.g. Chynoweth method) to minimise these effects.

## References

[1] S.B. Lang, *Nature*, **1966**, 212, 704-705.
[2] S.B. Lang, H. Athenstaedt, Ferroelectrics, **1977**, 17, 511-519.
[3] H. Athenstaedt, H. Claussen, *Biophysical Journal*, **1981**, 35, 365-374.
[4] V. Lemanov, *Ferroelectrics*, **2000**, 238, 211-218.

## Acknowledgements

Funding from the Irish Research Council EMBARK Postgraduate Scholarship to A.S. is acknowledged.

# Calcite crystals show weak, measurable piezoelectricity

Sarah Guerin[1], Syed A. M. Tofail[1], and Damien Thompson[1]

sarah.guerin@ul.ie

[1]Department of Physics, Bernal Institute, University of Limerick, Ireland

**Abstract:** Here we report a preliminary quantitative investigation into calcite piezoelectricity using quantum mechanical modelling, as well as the characterisation of both naturally occurring and synthesised calcite crystals. The low symmetry of crystallised biomolecules – from amino acids and peptides to viruses and fibrous proteins – can result in useful electrical properties, including ferroelectricity, pyroelectricity, and piezoelectricity. Biominerals such as hydroxyapatite and calcites are generally not considered as piezoelectric. Our quantitative study will help to reconcile decades' old observation of second harmonics generation by calcite microcrystals occurring in the human pineal gland.

**Keywords:** Piezoelectricity, biominerals, molecular modelling, transduction, biology, crystal growth

## Introduction

Many biological structures have been found to be piezoelectric[1-5]. Fibrous proteins such as collagen[2] and elastin,[3] bone[1] (calcified collagen), and some viruses[5] have, to date, exhibited significant piezoelectricity, of the order of 0.1 pC/N to 10 pC/N**.** Calcite, one of three polymorphs of calcium carbonate, $CaCO_3$, is abundantly available in both biological and non-biological systems. Its trigonal symmetry suggests that it should exhibit a piezoelectric response although no quantitative study is available[6]. It is found naturally in areas rich with limestone or volcanic rock, and also in the shells of a number of marine creatures[7]. Geological calcite single crystals are well known as birefringent. Calcite microcrystals that occur in the pineal gland of the human brain have shown a rare hexagonal morphology and weak but measurable second harmonics generation[8] thus confirming the absence of a centre of symmetry.

## Results and Discussion

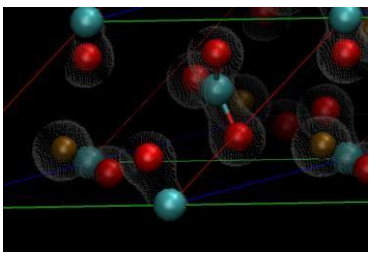

*Figure 1: Calculated Electron Density of a Mechanically Strained Calcite Unit Cell*

- We have predicted that calcite single crystals are very weakly piezoelectric, with a longitudinal $d_{33}$ value of 4 x $10^{-16}$ C/N. The highest predicted piezoelectric strain constant for calcite single crystals is a shear $d_{25}$ value of 4 x $10^{-15}$ C/N. Calcite's symmetry allows for thirteen non-zero piezoelectric coefficients.
- The mechanical response of the crystals are being measured using Scanning Probe Microscopy (SPM), including Piezoresponse Force Microscopy (PFM)
- The interaction between calcite microcrystals and macroscopic amino acid crystals is being characterised and studied using a combination of imaging, spectroscopic and piezoelectric characterisation tools
- Modelling of the interaction between calcite crystals and its amino acid based organic matrix[9] in the inner ear is also ongoing

## Conclusions

- Though weak in single crystal form, calcite crystals naturally stack along their longitudinal axis during growth[10], potentially amplifying its transduction signal in a way not normally possible in polycrystalline aggregates
- The electromechanical coupling found in this polymorphic biomineral has implications for our understanding of frequency detection in human and mammalian ears, as well as depth perception in aquatic animals[11]

## References

[1] Fukada, E.; Yasuda, I., Journal of the Physical Society of Japan 1957, 12, 1158.
[2] Fukada, E.; Yasuda, I, Japanese Journal of Applied Physics 1964, 3, 117.
[3] Liu, Y.; Cai, H.-L.; Zelisko, M.; Wang, Y.; Sun, J.; Yan, F.; Ma, F.; Wang, P.; Chen, Q. N.; Zheng, H., Proceedings of the National Academy of Sciences 2014, 111, E2780-E2786.
[4] Gandhi, A. A.; Wojtas, M.; Lang, S.; Kholkin, A. L.; Tofail, S. A., Journal of the American Ceramic Society 2014, 97, 2867.
[5] Lee, B. Y.; Zhang, J.; Zueger, C.; Chung, W.-J.; Yoo, S. Y.; Wang, E.; Meyer, J.; Ramesh, R.; Lee, S.-W., Nature Nanotechnology 2012, 7, 351.
[6] Nye, John Frederick. *Physical properties of crystals: their representation by tensors and matrices.* Oxford university press, 1985.
[7] Beniash, E., et al; Proceedings of the Royal Society of London B: Biological Sciences 1997, 264.1380, 461.
[8] Baconnier, S.; Lang, S.B., IEEE Transactions on Dielectrics and Electrical Insulation 2004, 11, 203.
[9] J. Aizenberg, M. Ilan, S. Weiner & L. Addadi; Connective Tissue Research Vol. 34, Iss. 4, 1996
[10] P. E. Hillner, A. J. Gratz, S. Manne, P. K. Hansma; Geology Apr 1992, 20 (4) 359-362
[11] Morris, Robert W., and L. R. Kittleman; Science 158.3799 (1967): 368-370.

## Acknowledgements

Science Foundation Ireland Research for Medical Devices (CÚRAM) and the SFI Irish Center for High-End Computing (ICHEC)

# Printed flexible sensors based on P(VDF:TrFE) for spatially resolved monitoring of impact forces

Philipp Schäffner[1], Gernot Pauer[2], Gregor Scheipl[1], Herbert Gold[1], Martin Zirkl[1]

philipp.schaeffner@joanneum.at (Corresponding e-mail address)

[1] Institute for Surface Technologies and Photonics, Joanneum Research Forschungsgesellschaft mbH, Franz-Pichler-Straße 30, 8160 Weiz, Austria

[2] Altran Concept Tech GmbH, Concept-Straße 1, 8101 Gratkorn, Austria

**Abstract:** All-screen printed piezoelectric sensors based on P(VDF:TrFE) were used to spatially resolve large forces (up to ~10kN) as created during impact tests. The used sensors are flexible, thin, lightweight and low-cost in production and can be scaled to enable high lateral resolution and large measuring areas. Modeling and finite element simulation were applied to support the reconstruction of force values from the piezoelectric response.

**Keywords:** piezoelectric polymers, printed sensors, simulation

## Introduction

There is a growing demand for flexible, thin, lightweight and fast pressure sensors in impact test applications like component testing. The ferroelectric polymer P(VDF:TrFE) is a perfect candidate to meet these demands as it can be formulated as printable paste and deposited on flexible foil substrates using screen-printing or R2R printing [1].

Within this work we present P(VDF:TrFE)-based piezoelectric sensors for measuring distributed impact forces. The sensor have a capacitive-like structure with the sensor material being sandwiched by PEDOT:PSS top and bottom electrodes, all screen printed on a flexible foil substrate. Evaluation of the sensor response is supported by modeling of the mechanic and piezoelectric behaviour of the sensor material upon large forces and simulation of the overall sensor unit.

## Results and Discussion

A drop tower setup was used to evaluate the force response of a 2x2 sensor array with an active sensor area of about 20x20mm² per sensor (figure 1). The array was placed under an impact attenuator which was deformed upon impact within about 20ms. Reference measurement of the total impact force was obtained by means of a commercially available, calibrated load cell at the bottom, and the total peak forces amounted to >10kN.

Local force diagrams were reproduced from the individual sensor responses and clearly reflect the non-uniform force distribution due to the unevenly shaped impact attenuator. Moreover, the total force calculated from the individual sensor responses is noticeably in good agreement with the reference measurement. Modeling and finite element simulations are used to accurately reconstruct impact forces as well as to optimize the sensor design and processing parameters.

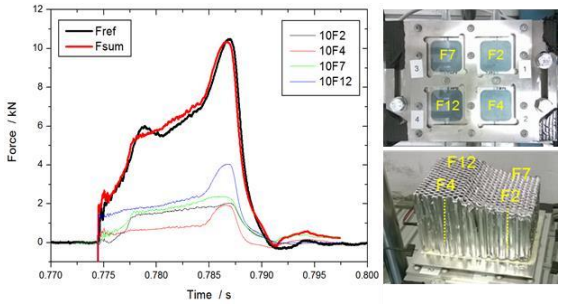


*Figure 1: Drop tower test using a 2x2 piezoelectric polymer sensor array to spatially resolve impact forces with high temporal resolution. Left: distributed force diagrams measured with individual sensors (10F2-12) and comparison of total sensor force response (red) with reference measurement (black). Right: drop tower test setup.*

## Conclusions

Our work shows that flexible, piezoelectric polymer sensors are suitable for spatially resolved measurement of high impact forces with high dynamic range. Based on physical modeling and simulation these lightweight, low-cost and robust sensors can be further tuned for increased spatial resolution and optimized response. Furthermore, we believe that these sensors have the potential to replace large, heavy and rigid load cells in many impact test applications.

## References

[1] Zirkl, M.; Sawatdee, A.; Helbig U.; Krause M.; Scheipl G.; Kraker, E.; Ersman, P.A.; Nilsson D.; Platt, D.; Bodö P.; Bauer S.; Domann G.; Stadlober B. *Adv. Mater.* **2011**, doi: 10.1002/adma.201100054.

## Acknowledgements

The presented work was performed in the frame of the project ATLASS that has received funding from the European Research Council (ERC) under the European Union's Horizon 2020 research and innovation programme (grant agreement n°636130)

# Intermediate polarization states in organic ferroelectrics

T. D. Cornelissen[1], I. Urbanavičiūtė, M. Kemerink

tim.cornelissen@liu.se

[1] Department of Physics, Chemistry and Biology, Linköping University, Linköping, Sweden

**Abstract:** Organic ferroelectrics are an attractive alternative for their inorganic counterparts. Here we investigate intermediate polarization states in a prototype small molecular ferroelectric. We characterize these states with the Preisach model. We also show the possibility to use the intermediate states for multibit memories, and show that these states have a greatly improved retention time.

**Keywords:** Organic Ferroelectrics, Preisach Model, Memory, Polarization Retention

## Introduction

Organic ferroelectrics are an attractive alternative for their inorganic counterparts. We investigate the possibility to create intermediate polarization states, which can be used for multibit memories, in various organic ferroelectrics using the Preisach model. This model assumes that a ferroelectric consists of a distribution of small perfect hysterons with varying positive and negative coercive fields *U*, *V* (see inset Figure 1(b)). Intermediate states are constructed by poling parts of this distribution.

## Results and Discussion

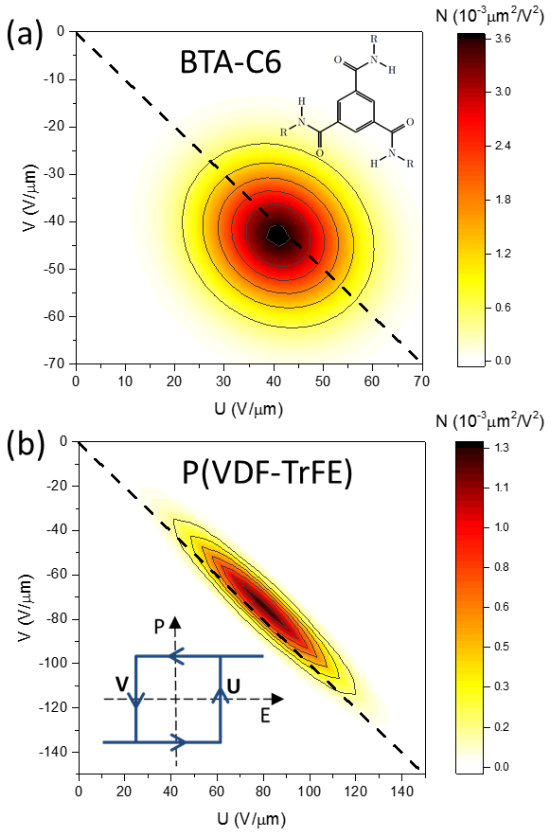


*Figure 1: The Preisach distribution for (a) a BTA with an alkyl chain length of 6, BTA-C6 and (b) P(VDFTrFE). Insets show (a) the general structure of BTA and (b) a hysteron with coercive fields* U *and* V.

We experimentally determine the Preisach distribution for several homologues of the prototypical small molecular liquid crystalline ferroelectric trialkylbenzene-1,3,5-tricarboxamides (BTA)[1] in thin film capacitor devices and contrast this to the distribution found for the ferroelectric polymer P(VDF-TrFE).For BTA's we find a symmetric two-dimensional Gaussian distribution, as shown in Figure 1, in marked contrast to the ellipsoid distribution found for P(VDF-TrFE). This difference is attributed to differences in structural disorder between the liquid crystalline BTA and (semi)crystalline P(VDF-TrFE).

By poling different parts of the Preisach distribution, it is possible to create intermediate polarization states that can be used for multibit memories. We investigate the switching kinetics and stability of these states. Whereas fully poled organic ferroelectrics often suffer from limited polarization retention times[2], we find that intermediate states have much longer retention times. This is attributed to the reduced depolarization field, which scales with the net polarization of the device.

## Conclusions

Our results thus give better insight into the switching behavior of ferroelectric liquid crystals, and provide a general way to construct multibit memories and improve retention times in organic ferroelectrics.

## References

[1] A. V. Gorbunov *et al*., *Phys. Chem. Chem. Phys.* 2016, DOI 10.1039/C6CP03835B.

[2] A. V. Gorbunov *et al*., *Phys. Chem. Chem. Phys.* 2017, DOI 10.1039/C6CP08015D.

## Acknowledgements

T.D.C. acknowledges financial support from the Swedish Government Strategic Research Area in Materials Science on Functional Materials at Linköping University (Faculty Grant SFO Mat LiU No 2009 00971). I.U. acknowledges funding by Vetenskapsrådet.

# Electrical polarization of chitosan and hydroxyapatite for tissue engineering

A.F. Esteves[1], E.M. Ribeiro[1], B.D. Marques[1], A.F. Correia[1], A.C. Videira[1], J. E. Pereira[1], C.F.C. João[1], E.R. Neagu[1], M.P.F. Graça[2], L.F.V. Pinto[3], J.C. Silva[1], J.P. Borges[1] and M.C. Lança[1]

mcl@fct.unl.pt

[1]Cenimat (I3N)/Dep. de Ciências dos Materiais, Faculdade de Ciências e Tecnologia, Universidade Nova de Lisboa, Campus da Caparica, 2829-516 Caparica, Portugal
[2]Dep. de Física e I3N, Universidade de Aveiro, Campus Santiago, 3810-193 Aveiro, Portugal
[3]Altakitin S.A., Rua J. Gomes Ferreira, 1-Arm. D 2660 – 360 São Julião do Tojal – Portugal

**Abstract:** The increase of bone diseases and fractures has evoked great interest in the development of biomaterials for use in bone replacement and regeneration. Recently has increased the interest in combining chitosan, a natural polymer, with hydroxyapatite, a bioactive bioceramic. Simultaneously, several studies have shown that electrical polarization of hydroxyapatite, enhances osteointegration and therefore bone regeneration. The influence of the electric polarization in the bioactivity of chitosan and chitosan/hydroxyapatite films and 3D scaffolds was studied.

**Keywords:** biomaterials, electrical polarization, bioactivity

## Introduction

Chitosan (CS) and hydroxyapatite (HAp) are biomaterials used in tissue engineering. HAp a ceramic similar to the natural apatite in hard tissue has been widely used in bone regeneration [1]. CS is a biopolymer with many biomedical applications [1]. On the other hand, studies started in 1990s show that electrical polarization of the surfaces of HAp increases its ability for osteointegration and bone regeneration [2].

## Results and Discussion

*Materials:* Porous scaffolds were developed to mimic the trabecular bone. Nanorods powders of HAp were used in the scaffolds (produced from commercial powders-Altakitin®). Films were produced by preparing homogeneous solutions that were poured into Petri dishes and subsequently dried. Samples were characterized by FTIR, XRD and DSC-TGA.

*Electrical polarization and thermally-stimulated discharge currents (TSDC) measurements:* Some samples were polarized by contact at 130ºC for 1h by applying a 4.5 kV/cm constant electric field. Other samples were thermally treated, i.e., kept at 130ºC for 1h (non-polarized). In this way it was possible to differentiate between the effect of temperature and the combined effect of temperature and field.

TSDC was used to investigate the polarization. Results show that non-polarized samples of CS already exhibit same electrical charge. Positive polarization enhances the charge deposited in the surface while the opposite effect is visible with negative polarization. CS has higher deposition of electrical charges compared to CS/HAp samples.

*Bioactivity assays*: were conducted by immersing samples in simulated body fluid solution at 37°C. Positive, negative and non-polarized surfaces were characterized by SEM-EDS, to evaluate the deposition of apatites. For the films, comparing CS with CS/HAp, bioactivity is significantly higher in the composite. For the scaffolds the non-polarized CS has higher bioactivity than the polarized CS but for the CS/HAp composite the higher deposition is observed on the negative surfaces.

## Conclusions

In the films, results indicate better bioactivity for the negative charged surfaces, followed by positive ones and finally by non-polarized. In the scaffolds also negative surfaces have higher bioactivity but no enhancement of apatite formation is observed on positive surfaces compared to non-polarized.

In conclusion the negatively surfaces of CS/HAp porous scaffolds and films show the highest bioactivity.

## References

[1] Buddy D. . Ratner, A. S. Hoffman, F. J. Schoen, and J. E. Lemons, Biomaterials science : an introduction to materials in medicine, Academic Press, 2013.

[2] F. Baxter, C. Bowen, I. Turner, and A. Dent, "Electrically active bioceramics: a review of interfacial responses," Ann. Biomed., vol. 38, pp. 2079–2092, Jun. 2010

## Acknowledgements

This work was funded by FEDER-QREN-COMPETE Programme-project POLARBONE and by National Funds throught FCT - Portuguese Foundation for Science and Technology, UID/CTM/50025/2013 and FEDER-COMPETE 2020 Programme-POCI-01-0145-FEDER-007688.

# Charge Stability of Water Submerged Dielectric Elastomers for Ocean Wave Energy Harvesting

Robert Pichler[1], Daniela Wirthl[1], Martin Kaltenbrunner[2], Reinhard Schwödiauer[1], Siegfried Bauer[1]

robert.pichler@jku.at

[1]Department of Soft Matter Physics, Johannes Kepler University Linz, Altenbergerstraße 69, 4040 Linz, Austria
[2]Linz Institute of Technology (LIT), Soft Electronics Laboratory, Johannes Kepler University Linz, Altenbergerstrasse 69, 4040 Linz, Austria

**Abstract:** Dielectric elastomer generators (DEGs) are lightweight and potentially low cost. Best suited for low frequency motions, they are promising for harvesting the mechanical energy of ocean waves. The choice and combination of elastomers as electroactive material with suitable stretchable electrodes is a key issue. We evaluate the suitability of electroactive membranes and various electrodes in direct contact with water by charge stability- and dielectric measurements. The presented work may open additional pathways for water-powered DEGs.

**Keywords:** energy harvesting, dielectric spectroscopy, charge storage stability

## Introduction

The acrylic elastomer VHB and natural rubber are two materials known to be highly appropriate for the fabrication of electroactive membranes of dielectric elastomer generators (DEGs) in dry environments. The suitability of these materials for water powered elastomer generators, where the membrane will be in direct contact with water, was unexplored and has been investigated.

## Results and Discussion

Comprehensive measurements of charge stability, dielectric strength, and dielectric impedance spectroscopy on water submerged elastomers showed a progressing degradation of the dielectric insulation properties. Impedance measurements indicate that water is being continuously absorbed by the elastomers. The adsorbed water causes an increase in mobility of ionic impurities and a decrease of the bulk resistance. Both effects reduce the charge storage stability of the elastomer membranes. Promising results however, were obtained with more elaborate compound multilayer systems. An improved charge storage stability, sufficiently high for energy harvesting, was found with a hydrogel/VHB compound (Fig. 1a). An energy harvesting experiment revealed a mechanical-to-electrical conversion efficiency of ca. 11.5% (Fig. 1b-d). This marks a substantial improvement in comparison to bare VHB membranes. The successful experiments with hydrogel and sandwich multilayer systems are setting the perspective for further developments. The water barrier properties of hydrogel layers will be discussed and their long term stability at various stretch ratios and different water pressures will be investigated. In addition, new fluoro- and silicone elastomer materials with improved water resistance will be examined for their applicability as electroactive membrane and as barrier layers.

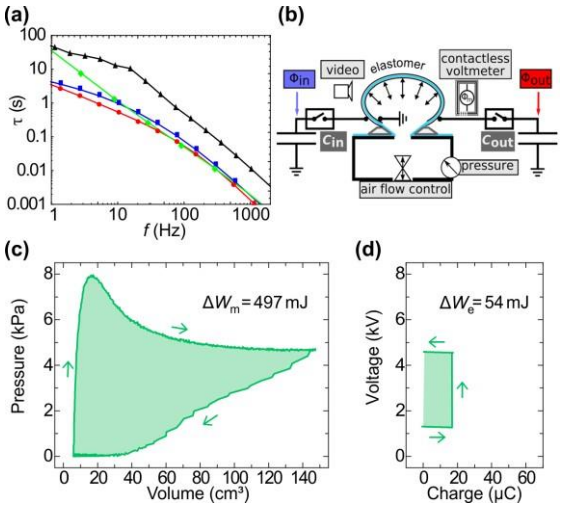


*Figure 1: Time constant, τ=RC, for natural rubber (circle, red), VHB (square, blue), hydrogel/VHB compound (diamond, green), and PTFE (triangle, black). (a) Schematic of the experimental test stage to measure the mechanical and electrical energy flow in a dielectric elastomer generator membrane. (b) Mechanical work conjugate pressure/volume graph measured with hydrogel electrodes, (c) and the corresponding electrical work conjugate voltage/charge graph. (d)*

## Conclusions

The characterization of dielectric elastomers in direct contact with water provides a basis for ocean wave energy harvesting with DEGs. We designed a proof of concept dielectric elastomer generator using hydrogel electrodes with a positive feedback between materials characterization, DEG design and optimization.

## Acknowledgements

Work supported by the European Union's Horizon 2020 research and innovation program under grant agreement No 641334, WETFEET

# Design of a combined-structural piezoelectret system for sensing force signals in both normal and tangential directions

Peng Fang [1], Xingchen Ma [2], Xiaoqing Zhang [2], Guanglin Li [1]

peng.fang@siat.ac.cn (Corresponding e-mail address)

[1]Chinese Academy of Sciences (CAS) Key Laboratory of Human-Machine Intelligence-Synergy Systems, Shenzhen Institutes of Advanced Technology, Shenzhen 518055, China
[2]Shanghai Key Laboratory of Special Artificial Microstructure Materials and Technology & School of Physics Science and Engineering, Tongji University, Shanghai 200092, China

**Abstract:** In this work, a piezoelectret-system based on a combined structure was proposed. The combined structure consisted of two substructures layers: the top layer had a rough surface which was sensitive to normal signals like pressure and tangential signals such as friction; the bottom layer was only sensitive to normal signals which were transferred through the top layer. The proposed piezoelectret system could be applied as a tactile sensor in intelligent artificial-skins for detecting pressure and slip signals.

**Keywords:** piezoelectret, combined structure, sensor

## Introduction

In intelligent robotics and artificial skins, tactile sensors are needed to detect the pressure and slip signals. In most of the current applications, pressure sensors (e.g. capacitive type) and slip sensors (e.g. piezoelectric type) are individually used to acquire the signals in different directions, which would increase the complexity of whole sensor system [1]. Piezoelectrets, also known as ferroelectrets, are polymer-based space-charge electrets with piezoelectric effects, which exhibit a number of advantages and very desirable for sensor applications [2]. In this work, a piezoelectret system based on combined structure was proposed on the aim of sensing force signals in both normal and tangential directions with the same sensor unit.

## Results and Discussion

The piezoelectret system consisted of two substructures *A* and *B*. As schematically shown in figure 1, the substructure *A* had a cellular structure with rough outer surface, and *B* had a cellular structure with smooth surface. In this work, PTFE layer structure prepared by template method [3] and PP foam structure by gas-expansion [4] were selected for the substructures *A* and *B*, respectively. The two substructures were separately fabricated, charged, and metalized with metal electrodes. Then, the substructures *A* (as top layer) and *B* (as bottom layer) were bounded with a selective binding agent, but individually connected to the electric circuit. In addition, the piezoelectric properties of both *A* and *B* were calibrated.

Usually, a force signal can be divided into two parts: the normal and tangential components. In force sensing with the proposed piezoelectret system, the top layer *A* was facing the measurand force. It could detect the normal signal (pressure) and also the tangential signal (sliding friction) due to its rough surface, with output named $Y_A$. The bottom layer *B* could only measure the normal signal which was transferred through the layer *A*, with output named $Y_B$. In signal processing, $Y_B$ was considered as the measurement result of pressure signal, and ($Y_A$ - $Y_B$) was the friction signal.

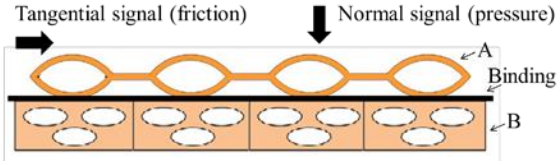


*Figure 1: Schematic illustration of the combined structure with substructures A and B.*

## Conclusions

The preliminary experiments demonstrated that the proposed piezoelectret system could detect both pressure and slip signals with the same sensor unit, which could be calculated from the outputs of two substructures. An improvement of the sample preparation and signal processing is suggested for future applications in the intelligent artificial-skins.

## References

[1] M. L. Hammock, A. Chortos, B. C. K. Tee, et al., *Adv. Materials* **2013**, 25, 5997 – 6038.
[2] S. Bauer, R. Gerhard-Multhaupt, and G. M. Sessler, *Phys. Today* **2004**, 57, 37 – 44.s
[3] R. A. P. Altafim, X. Qiu, W. Wirges, et al., *J. Appl. Phys.* **2009**, 106, 014106.
[4] M. Wegener, W. Wirges, R. Gerhard-Multhaupt, et al., *Appl. Phys. lett.* **2004**, 84, 392 – 394.

## Acknowledgements

This work was supported in part by the Natural Science Foundation for Distinguished Young Scholars of Guangdong Province, China (2014A030306029) and the Special Support Program for Eminent Professionals of Guangdong Province, China (2015TQ01C399).

# Preparation and electromechanical properties of P(VDF-TrFE-CFE) relaxor-ferroelectric terpolymer films

Thulasinath Raman Venkatesan[1], Anna A. Gulyakova[2], Peter Frübing[1], Reimund Gerhard[1]

thuraman@uni-potsdam.de

[1]Institute of Physics and Astronomy, Faculty of Science, University of Potsdam,
Karl-Liebknecht-Strasse 24/25, 14476 Potsdam, Germany
[2]Department of General and Experimental Physics, Herzen State Pedagogical University,
Moika River Embankment 48, 191186 St. Petersburg, Russia

**Abstract**: Polyvinylidenefluoride-co-trifluoroethylene-co-chlorofluoroethylene (P(VDF-TrFE-CFE)) terpolymer films were prepared by means of solvent casting. The influence of various processing conditions on film structure and dielectric properties were studied with Fourier Transform Infrared (FTIR) spectroscopy and Dielectric Relaxation Spectroscopy (DRS), respectively. On the basis of the results, samples prepared with acetone as solvent and annealed at 60°C during solvent evaporation were chosen for electromechanical tests. A maximum transverse electrostrictive strain of 2.6 % was observed at an electric field of 150 MV/m.

**Keywords:** Relaxor-ferroelectric polymer, P(VDF-TrFE-CFE) terpolymer , electromechanical properties

## Introduction

P(VDF-TrFE-CFE) based terpolymers form very small crystallites compared with PVDF and its copolymers, which show pronounced ferroelectric-hysteresis behavior. Therefore terpolymers may exhibit relaxor-ferroelectric properties like a vanishing hysteresis, but strong polarisation [1, 2]. They also have been found to exhibit high electrostrictive strain (up to 7% in the thickness direction) [1]. Therefore, this special class of ferroelectric terpolymers is particularly important for energy storage devices such as supercapacitors and electromechanical actuators.

In the present study, terpolymer films with a VDF/TrFE/CFE composition of 55.4/37.2/7.3 mol%, respectively, were prepared from solution, and their electrical and in particular their electromechanical properties were investigated and analyzed.

## Results and discussion

DRS on films obtained from a terpolymer solution in acetone and annealed at 60 °C for better solvent evaporation revealed the lowest DC conductivity in comparison to films prepared with other solvents. For voltage application, vacuum-evaporated 50nm thick aluminium electrodes were employed.

The electrostrictive strain in the transverse (lateral) direction of the terpolymer films from acetone solution was determined by measuring the change in film length upon application of a DC voltage by using a Keyence VHX-600 optical microscope and a Trek PD05031 high-voltage amplifier. The transverse strain [%] for an unstretched film (25µm thickness) plotted as a function of the applied electric field is shown in Figure 1. The plot shows the expected quadratic strain-*vs.*-field dependence at lower fields and a tendency to saturate at higher fields. A maximum transverse strain of 2.6% is obtained at 150 MV/m which is comparable to the value of 3% obtained by F. Bauer *et al.* [1] for an unstretched sample of P(VDF-TrFE-CFE) with a relative monomer composition of 65/35/8.6 mol%.

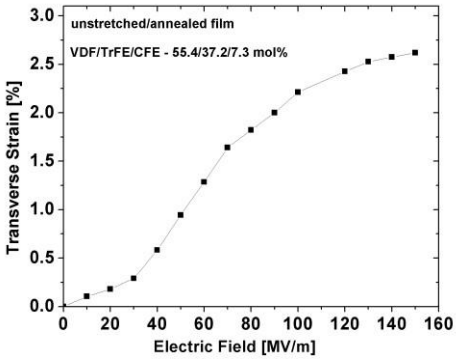


*Figure 1: Transverse strain in a terpolymer film vs. the electric field applied across its thickness.*

## Conclusions

Hysteresis measurements show that in order to increase the electromechanical response the crystalline structure of the terpolymer films, particularly the size of the crystallites still must be optimized. This might be achieved through a high-electric-field pre-treatment and/or via annealing and quenching procedures.

As another way to increase the electromechanical response, a combination of the electrostrictive strain with the Maxwell strain caused by Coulomb interaction of the oppositely charged electrodes upon application of a DC voltage should be taken into consideration.

## References

[1] F. Bauer *et al.*, IEEE Trans. Diel. Electr. Insul. **13**(5), 1149-1154 (2006)
[2] R. J. Klein *et al.*, J. Appl. Phys. **97**, 094105 (2005)

## Acknowledgements

The authors are indebted to Piezotech Arkema for providing the P(VDF-TrFE-CFE) terpolymer and to Xunlin Qiu, Werner Wirges and Manuel Schulze (U Potsdam) for stimulating discussions and generous support.

# Controling Dielectric Loss and Ionic Conductivity through Film Processing Optimization of Fluorinated Electrostrictive Polymers

Francesco PEDROLI[1]*, Mathieu TAUBAN[2], Pierre-Jean COTTINET[1], , Olivier SANSEAU[2], Jean-Fabien CAPSAL[1†]

[1] *Laboratoire de Génie Electrique et Ferroélectricité, Université de Lyon, Institut National des Sciences Appliquées de Lyon, F-69621, Villeurbanne, France*
[2]*Laboratoire Polymères et Matériaux Avancés, CNRS/Rhodia-Solvay, UMR 5268, 85 avenue des Frères Perret, F-69192 Saint Fons, France*

* francesco.pedroli@insa-lyon.fr † jean-fabien.capsal@insa-lyon.fr

**Abstract** The interesting and highly promising features of electro-active polymers in the field of sensors and actuators, such as P(VDF-TrFE-CTFE), are severely limited by their low dielectric strength driven by ionic conductivity. The quadratic dependence of Applied-Electric Field on Field-Induced Strain highlights the importance of improving electrical breakdown of electro-active polymers: increasing the electrical breakdown of 32%, by controlling processing parameters from polymer synthesis to film fabrication, we will enhance the ideal Maximum Field-Induced Strain of about 73%. Effect of polymer crystallinity, molecular weight, solvent purity and crystallization temperature were investigated showing direct relationship between dielectric losses at low-frequency and electrical breakdown.

**Keywords:** Electrical breakdown, Fluoropolymer, Dielectric Spectroscopy, Actuator, Electro-strictive.

## Introduction

The advantages of using EAPs for smart electrical devices are due to their low cost, elastic properties, low density and ability to be manufactured into various shapes and thicknesses. In earlier years, terpolymer P(VDF-TrFE-CTFE) attracted many researchers due to its relaxor ferroelectric property that exhibits high electrostriction phenomena [1].
In order to improve the electro-mechanical performances of electrostrictive polymers, the increase of maximum voltage at which the material can operate seems to be one of the most relevant parameters. Enhancing the electrical breakdown strength corresponds to both enlarging the range of operative voltages and to reducing the probability of material degradation at a given voltage.

$$S \propto M\, E^2$$

*Where S is the mechanical strain, M the electric-field-related electrostrictive coefficient [2]*

As shown in the above equation, the quadratic relation of applied voltage on the maximum electric field-induced strain highlights once again the relevance of material strength in withstanding large electric fields.
In this research, polymeric films via solution-casting of P(VDFTrFE-CTFE) having different molecular weights and different degrees of crystallinity are synthetized and their electrical properties in terms of Dielectric Loss, Conductivity and Breakdown Voltage are measured. Process parameters such as Crystallization Temperature and Purity of Polymeric dissolution are varied in order to investigate the extention of their influence on final electrical strength and to research the relationship between Low-Frequency Dielectric Losses and Breakdown Voltage.

## Results and discussion

Films of P(VDF-TrFE-CTFE) were prepeared via solution-casting of polymeric dissolution. Films undergo a thermal treatment aimed to control the crystallinity rate. Augmented crystallity reflects on electrical behavior reducing dielectric losses at low electric field and delaying the appearance of Mott's law beahviour at high electric field.
In order to further improve the electric breakdown, which is the main technical-lock, the effect of purity of polymeric dissolution is investigated: butanone solvents having different degrees of purity and filtering systems allowed us to investigate the effect of impurities at various scale. Controlling the extention of ionic conductivity and interfacial polarization allowed to increase the electrical strength of fluorinated terpolymer.
As already studied in literature[3], larger polymer molecular weights help to reduce dielectric losses. Characterization of terpolymers having different molecular masses shows direct relationship between the electrical behavior at low and high electric field, enabling to define low-field marker for predicting the behavior at high electric field such as electrical breakdown and Mott's law voltage.

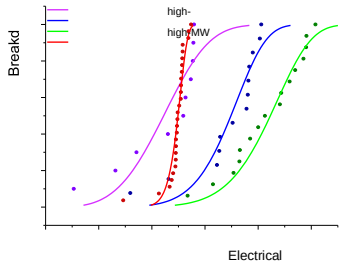


*Figure 1. Breakdown voltage distributions for various processed samples*

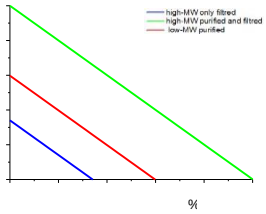


*Figure 2. Process dependence of Normilized Displacement vs. Force for unimorph actuators*

## Conclusion

Ionic Conductivity seems to be the most limiting factor for achieving high strains and high blocking forces for polymeric actuators. Leakage current promotes material degradation under electric field, limiting the maximum applicable voltage. So, ion mobility and charge density have been identified as the primary factors responsible for low breakdown voltage. Controlling synthesis and processing parameters allowed us to govern these two factors increasing the dielectric strength from 95V/µm to 125V/µm, corrensponding to an improvement in electric field-induced strain of about 73%.

## Acknowledgement

The author are grateful to support of THESE CIFRE from ANRT and SOLVAY.

## References

**[1] B. Chu, X. Zhou, K. Ren, B. Neese, M. Lin, Q. Wang, and Q.M. Zhang, *Science*, *vol. 313(5785), pp. 334-336 (2006)*.**
**[2] P. Brochu and Q. Pei, *Macromol. Rapid Commun.*, vol 31, 10–36 (2010).**
**[3] M. Watanabe *at all., Polymer J.*, vol 15, No. 1, pp 65-69 (1983).**

# CHITOSAN/CASEIN MULTILAYERS ON CORONA CHARGED POLYLACTIC ACID SUBSTRATES

T. Yovcheva[1], A. Viraneva[1], A. Marinova[1], B. Pilicheva[2], S. Sotirov, Y. Uzunova[2], I. Vlaeva[3], G. Exner[1], I. Bodurov[1], M. Marudova[1]

yovchevat@gmail.com

[1]University of Plovdiv "Paisii Hilendarski", Faculty of Physics, 24 Tzar Assen str., 4000 Plovdiv, Bulgaria
[2]Medical University Plovdiv, Faculty of Pharmacy, 15A Vassil Aprilov Blvd., 4002 Plovdiv, Bulgaria
[3]University of Food Technologies, Department of Mathematics and Physics, 26 Maritsa Blvd., 4002 Plovdiv, Bulgaria

**Abstract:** The aim of the present study was to investigate the influence of the structure and physico-chemical properties of chitosan/casein multilayer films on their potential use as drug delivery systems. In the present paper the effect of the substrate corona polarity was investigated.

**Keywords:** corona discharged, polyelectrolyte multilayers, drug delivery

## Introduction

In the last decades, the layer-by-layer self-assembly technique received extensively renewed interests as an attractive technique for the production of polyelectrolyte multilayer thin films. The multilayered structures have been widely used because of their fabrication easiness and great potential for application in drug delivery [1, 2], biomedicine [3], optics [4], food science [5], as biomembranes [6], etcIn the present study, the selfassembling process and the morphology of chitosan/casein polyelectrolyte films deposited onto charged poly(lactic) acid substrate is investigated by means FT-IR, AFM, SEM and XPS.

## Results and Discussion

The multilayer films were prepared using the layer-by-layer self-assembly method of chitosan and casein on polylactic acid substrates, preliminary treated in a positive or in a negative corona. The experimental corona discharge system was consist of a corona electrode, a grounded plate electrode and a grid placed between them. The dependences of the normalized surface potential on the storage time for positively and negatively charged PLA have been studied for 6 hours. After 2 hours the steady state values of the surface potential were established for all investigated samples. Time dependences of the normalized surface potential for all investigated samples are obtained. Each experimental point is a mean value from 5 samples. The standard deviation with confidence level 95% is indicated by an error bar. The final values of the normalized surface potential for the samples charged in a positive corona are higher than those for the samples charged in a negative corona.

The deposition process was studied by changes in the ATR FT-IR spectra and surface energy. ATR FT-IR spectra proved the formation of polyelectrolyte complexes between the chitosan and the casein. The increasing content of chitosan and casein with increasing the number of bilayers was further confirmed by XPS analysis. Surface topography was investigated by AFM and the average roughness was evaluated. A comparative analysis of the experimental results was presented and the most appropriate substrate type for the irreversible binding of the chitosan/casein polyelectrolytes was determined.

## Conclusions

It was shown in this paper that dipping layer-by-layer self-assembly methods are successfully applied for the deposition of chitosan and casein multilayers on PLA corona charged substrates. It was established that the positive charged substrates are more appropriate for the multilayered structures formation.

## References

[1] Gunjkar, V., Patwekar, S., Dhage, S. World J. Pharmacy and Pharmaceutical Scie. 2015, 4, 216238.
[2] Tian, F., Min, J., Kanka, J., Hammond PT and Du H 2015 Proc. SPIE, 2015, 9480 948005.
[3] Costa, R., Mano, J. Chem. Soc. Rev. 2014, 43, 34533479.
[4] Bharadwaj, R., Mukherji, S., Mukherji, S. OSA Technical Digest (online) paper SeM3C.5, 2014.
[5] Poverenov, E., Danino, S., Horev, B., Granit, R., Vinokur, Y., Rodov, V. Food Bioprocess. Technol. 2013, 7, 1424-1432.
[6] Pasco, E., Shi, H., Xagoraraki, I., Hashsham, S., Parent, K., Bruening, M., Tarabara, V. J. Membrane Scie. 2014, 469, 140-150.

## Acknowledgements

This study was funded by Bulgarian National Scientific Fund, Project No DFNI B-02/7.

## Author index